DEVELOPMENT OF HIGH-THROUGHPUT MEMBRANE FILTRATION TECHNIQUES

DEVELOPMENT OF HIGH-THROUGHPUT MEMBRANE FILTRATION TECHNIQUES FOR BIOLOGICAL AND ENVIRONMENTAL APPLICATIONS

By

AMIR SADEGH KAZEMI, B.Eng. M.A.Sc.

A Thesis Submitted to the School of Graduate Studies in Partial Fulfillment of the Requirements for the Degree Doctor of Philosophy

McMaster University Ph.D. of Engineering (2018) Hamilton, Ontario (Chemical Engineering)

DOCTOR OF PHILOSOPHY (2018) McMaster University

(Chemical Engineering) Hamilton, Ontario

TITLE: DEVELOPMENT OF HIGH-THROUGHPUT MEMBRANE FILTRATION TECHNIQUES FOR BIOLOGICAL AND ENVIRONMENTAL APPLICATIONS

AUTHOR: Amir S. Kazemi, B.Eng. (Amirkabir University of Technology),

M.A.Sc. (McMaster University)

SUPERVISOR: Dr. David R. Latulippe

NUMBER OF PAGES: xxx, 228

Lay Abstract

Membrane filtration is widely used as a key separation process in different industries. For example, microfiltration (MF) and ultrafiltration (UF) are used for sterilization and purification of bio-products. Furthermore, MF, UF and reverse-osmosis (RO) are used for drinking water and wastewater treatment. A common misconception is that membrane filtration is a process solely based on the pore size of the membrane whereas numerous factors can significantly affect the performance. Conventionally, a large number of lab- or full-scale experiments are performed to find the optimum operating conditions for each filtration process. High-throughput (HT) techniques are powerful methods to accelerate the pace of process optimization—they allow for multiple experiments to be run in parallel and require smaller amounts of sample. This thesis focuses on the development of different HT techniques that require a minimal amount of sample for parallel testing and optimization of membrane filtration processes with applications in environmental and biological separations. The introduced techniques can reduce the amount of sample used in each test between 10-50 times and accelerate process development and optimization by running parallel tests.

Abstract

Membrane filtration processes are widely utilized across different industrial sectors for biological and environmental separations. Examples of the former are sterile filtration and protein fractionation via microfiltration (MF) and ultrafiltration (UF) while drinking water treatment, tertiary treatment of wastewater, water reuse and desalination via MF, UF, nanofiltration (NF) and reverse-osmosis (RO) are examples of the latter. A common misconception is that the performance of membrane separation is solely dependent on the membrane pore size, whereas a multitude of parameters including solution conditions, solute concentration, presence of specific ions, hydrodynamic conditions, membrane structure and surface properties can significantly influence the separation performance and the membrane's fouling propensity. The conventional approach for studying filtration performance is to use a single lab- or pilot-scale module and perform numerous experiments in a sequential manner which is both time-consuming and requires large amounts of material. Alternatively, high-throughput (HT) techniques, defined as the miniaturized version of conventional unit operations which allow for multiple experiments to be run in parallel and require a small amount of sample, can be employed. There is a growing interest in the use of HT techniques to speed up the testing and optimization of membrane-based separations. In this work, different HT screening approaches are developed and utilized for the evaluation and optimization of filtration performance using flat-sheet and hollow-fiber (HF) membranes used in biological and environmental separations. The effects of various process factors were evaluated on the separation of different biomolecules by combining a HT filtration method using flat sheet

UF membranes and design-of-experiments methods. Additionally, a novel HT platform was introduced for multi-modal (constant transmembrane pressure vs. constant flux) testing of flat-sheet membranes used in bio-separations. Furthermore, the first-ever HT modules for parallel testing of HF membranes were developed for rapid fouling tests as well as extended filtration evaluation experiments. The usefulness of the modules was demonstrated by evaluating the filtration performance of different foulants under various operating conditions as well as running surface modification experiments. The techniques described herein can be employed for rapid determination of the optimal combination of conditions that result in the best filtration performance for different membrane separation applications and thus eliminate the need to perform numerous conventional lab-scale tests. Overall, more than 250 filtration tests and 350 hydraulic permeability measurements were performed and analyzed using the HT platforms developed in this thesis.

Acknowledgements

First of all, I would like to thank my supervisor, Dr. David Latulippe, for his continuous support, encouragement and patience throughout my studies at McMaster University. This work could not have been completed without your vision, insight, inspiration and most importantly your guidance and supervision. Thanks for trusting me as one of the first members of your lab. I would also like to thank my committee members, Dr. Carlos Filipe and Dr. Younggy Kim for their advice and positive attitude during our meetings. I would like to thank other professors in the department of Chemical Engineering, at McMaster University, for their valuable insight. I would like to express my gratitude to Dr. Raja Ghosh for his counsel during my master's and Ph.D. projects and aiding me acquire knowledge about membrane separations. I would also like to thank Dr. Kim Jones for trusting me to TA her courses during the past couple of years. I am also grateful to all my other instructors.

From the department of Chemical Engineering, I would like to acknowledge all the staff, especially: Kristina Trollip, Michelle Whalen, Linda Ellis, Justyna Derkach, Doug Keller, Mike Clarke, Tim Stephens, Kathy Goodram, Lynn Falkiner and Cathie Roberts. Thanks for the support and encouragement. Many thanks to Paul Gatt who aided me in fabricating my modules. Paul, you are definitely one of the most helpful people I have met at McMaster. Also, I owe a very special thanks to Dan Wright, who is unfortunately no longer with us, for his help in setting up my experimental system. We will all miss you Dan but your memory will live in our hearts. May you rest in peace and your family find strength and comfort in your memory.

I would also like to thank all my friends in Latulippe Lab for their support and friendship. Thanks to Shabnam, Jeff, Farhad, Salman, Ryan, Patrick, Caroline, Reza, Wael, Neil, Kurt, Mehdi, Evan, Damien, Devon and Eric. Special thanks to Kimia for her kindness, friendship and continuous love and support. It was a wonderful experience working with such a great group of co-workers and friends. I would also like to acknowledge the undergraduate students with whom I have worked including: Karina, Luke, Melissa, Blake and Panos. All the best of luck in your future endeavours! I would further like to thank all my friends and colleagues from other research groups who have assisted me during my time at McMaster. Special thanks to Roozbeh, Ali, Vida, Rahul, Pedram, Sana, Maria, Amin, and Hadi who were always there to offer their help and friendship both in my academic and personal life. I would particularly like to thank Roozbeh, for his very special friendship and constant support and for all the ping pong games that we played, Ali, for being my first squash-mate at McMaster and Vida for her friendship.

I would also like to acknowledge Dr. Henk Koops, Juliane Kagansky, and Dr. Nick Adams from SUEZ Water Technologies & Solutions for providing the hollow-fiber membranes, Dr. Nick Burke and Dr. Harald Stöver from Department of Chemistry for their assistance with the GPC analysis, Mr. Kevin Dunn from TU Delft for his helpful suggestions in improving the presentation of the filtration test results in the DOE format and Prof. Singh and Dr. Eric Seidlitz for allowing us to use their microplate reader at the beginning of our project. I would also like to thank the Biointerfaces Institute at McMaster for providing access to the microplate reader, contact angle measurement

instrument, Fourier-transform infrared spectroscopy and gel imaging systems, and Natural Sciences and Engineering Research Council of Canada (NSERC) for their financial support of my research.

I would like to take this opportunity to thank my professors during my undergraduate studies at Amirkabir University of Technology to whom I owe my foundation in Chemical Engineering and who encouraged me to pursue my graduate studies abroad. Special thanks to Dr. Babak Bonakdarpour, my undergraduate research project supervisor, for his guidance during my bachelor's degree. I consider myself extremely lucky to have worked under your supervision and I appreciate all the great lessons you taught me. Unfortunately, during my time at McMaster I learnt that three of my former professors, Dr. Manouchehr Nikazar, Dr. Morteza Sohrabi and Dr. Mohammad Edrisi, were no longer with us. May God bless your souls, your legacy is eternal.

Last but not least, I consider myself extremely fortunate to have such a wonderful family. To my first and best teachers, my mom and dad, I cannot thank you enough for all the endless love and support you have given me through the years. I love you so much. Thank you for all the video chats and phone conversations, which are the most relaxing and amazing thing ever! To my lovely sister, you have always been my best friend. Anyone who has a sister like you, would easily be able to make all their dreams come true. Thanks for being the best sister in the world! Special thanks to my grandparents, Madarjoon and Babajoon, who have made me extremely happy with their phone calls every weekend. I would also like to express my gratitude to my aunt and uncle (Minou &

Mahmoud) and my cousins (Rouzbeh, Delnavaz, Sara, and Ali) for making Toronto a pleasurable place for me during my visits and all my friends and relatives in Hamilton and Toronto who have been with me through thick and thin. I would particularly like to thank my cousin, Sara who was my inspiration in pursuing a career in Chemical Engineering and who introduced me to the subject and bought me my first books when I was barely ten years old. Likewise my cousin Rouzbeh for always being there for me, as the older brother I never had, and for all the football/soccer-related discussions.

I would like to dedicate this thesis to the memory of my grandmother, Malijoon, who unfortunately passed away as I was completing my Ph.D degree but whose encouragement played an important role in motivating me to complete this work. I miss you grandma. I have faith that you are watching over me as I complete my thesis. I know you valued higher education and I am certain that you are proud of me today. God bless you and may you rest in peace. Thanks God, for the health and strength that was given to me all these years, and for the ability and opportunity to complete my thesis and the chance to contribute an infinitesimal amount to science. I hope that this would be the beginning of a new journey of learning and discovering the fascinating world of science.

Table of Contents

List of Figures

.

List of Tables

List of Acronyms, Abbreviations and Symbols

A	Area
ATPS	Aqueous two-phase system
BAK	Bioartificial kidneys
BCA	Bicinchoninic acid
BSA	Bovine serum albumin
CA	Cellulose acetate
CAS	Conventional activated sludge
C_b	Bulk concentration
CFD	Computational fluid dynamics
CFUF	Crossflow ultrafiltration
CHES	2-(Cyclohexylamino)ethanesulfonic acid
$C_{i,b}$	Bulk concentration of solute 'i'
$C_{i,p}$	Permeate concentration of solute 'i'
$C_{i,w}$	Wall concentration of solute 'i'
cm	Centimeters
CN	Cellulose nitrate
CNT	Carbon nanotube
C_p	Permeate concentration
CV	Coefficient of variation
C_w	Wall concentration
Da	Daltons
DA-HCl	Dopamine hydrochloride
DAQ	Data acquisition
DEX	Dextran
D_{ji}	Diffusion coefficient
DNA	Deoxyribonucleic acid
DOE	Design-of-experiments

EDTA	Ethylenediamine tetraacetic acid
EfOM	Effluent organic matter
EOM	Extracellular organic matter
EPA	Environmental Protection Agency
EPS	Extracellular polymeric substances
FBS	Fetal bovine serum
FITC	Fluorescein isothiocyanate
FITC-DEX	Fluorescein isothiocyanate dextran
FTIR	Fourier transform infrared
GA	Genetic algorithm
GFD	gal/ft^2/day
GFP	Green fluorescent protein
GPC	Gel permeation chromatography
HA	Humic acid
HF	Hollow-fiber
HPLC	High performance liquid chromatography
HT	High-throughput
HT-HF	High-throughput hollow-fiber
HT-MBR	High-throughput membrane bioreactor
ID	Internal diameter
IF	Irreversible fouling
IgG	Immunoglobulin G
J	Flux
kDa	Kilodaltons
k or $k_{i,b}$	Mass transfer coefficient
LC-MS	liquid chromatography–mass spectrometry
LMH	L/m^2/h
L_p	Hydraulic permeability OR hydraulic permeability of fouled membrane

L_{p0}	Hydraulic permeability of native (i.e. unused) membrane
$L_{p\text{-}BW}$	Hydraulic permeability of backwashed membrane
M	Molar
mAbs	Monoclonal antibodies
MBR	Membrane bioreactor
MEC	Microbial electrolysis cell
MF	Microfiltration
MFT	Microscale flocculation test
MLSS	Mixed liquor suspended solids
mM	Millimolar
MMFC	Multi-channel microfluidic flow control
Mn	Number-average molecular weight
Mp	Peak molecular weight
MQ	Milli-Q
MS-PS-CFF	Microscale, parallel-structured, cross-flow filtration (MS-PS-CFF) system
MW	Molecular weight
Mw	Weight-average molecular weight
MWCO	Molecular weight cut-off
ND	Not disclosed
NF	Nanofiltration
NOM	Natural organic matter
OD	Outside diameter
PAC	Powdered activated carbon
PAN	Polyacrylonitrile
PB	Phosphate buffer
PBS	Phosphate buffer saline
PDA	Polydopamine
pDNA	Plasmid deoxyribonucleic acid

PEG	Polyethylene glycol
PEO	Polyethylene oxide
PES	Polyethersulfone
pI	Isoelectric point
ppm	Part per million
PS	Polysulfone
psi	lbf/in^2
PTFE	Polytetrafluoroethylene
PVDF	Polyvinylidene fluoride
r	Pore radius
R_a	Apparent rejection coefficient
RF	Reversible fouling
R_i	Intrinsic rejection coefficient
RI	Refractive index
RNA	Ribonucleic acid
RO	Reverse osmosis
RSM	Response surface modeling
SA	Sodium alginate
S_a	Apparent sieving coefficient
SD	Standard deviation
SEM	Scanning electron microscopy
S_i	Intrinsic sieving coefficient
SMP	Soluble microbial products
SPI	Sodium periodate
SRNF	Solvent resistant nanofiltration
SWF	Stirred well filtration
TE	Tris/EDTA
TF	Total fouling
TFF	Tangential flow filtration

TMP	Transmembrane pressure
TRITC	Tetramethylrhodamine isothiocyanate
UF	Ultrafiltration
UV	Ultraviolet
VIRADEL	Virus adsorption–elution
WHO	World Health Organization
WW	Wastewater
δ	Membrane thickness
ΔP	Pressure difference or transmembrane pressure
ε	Porosity
μ	Dynamic viscosity
τ	Tortuosity
Ψ	Selectivity

Preface – Declaration of Academic Achievement

This Ph.D. dissertation is prepared in a "sandwich style" based on the published, submitted and prepared for submission papers listed below:

- Chapter 2: A.S. Kazemi, K. Kawka, D.R. Latulippe, Optimization of Biomolecule Separation by Combining Microscale Filtration and Design-of-Experiment Methods, Biotechnology and Bioengineering, 113 (2016) 2131-2139.
- Chapter 3: A.S. Kazemi, M.J. Larocque, D.R. Latulippe, Microscale filtration via a multi-modal microfluidic flow control system, Separation Science and Technology, Accepted for publication: doi.org/10.1080/01496395.2018.1483949.
- Chapter 4: A.S. Kazemi, L. Boivin, S.M. Yoo, R. Ghosh, D.R. Latulippe, Elucidation of filtration performance of hollow-fiber membranes via a high- throughput screening platform, Journal of Membrane Science, 533 (2017) 241–249.
- Chapter 5: A.S. Kazemi, B. Patterson, R.J. LaRue, P. Papangelakis, S.M. Yoo, R. Ghosh, D.R. Latulippe, Microscale Parallel-structured, Cross-flow Filtration System for Evaluation and Optimization of the Filtration Performance of Hollow-fiber Membranes, Submitted to Separation and Purification Technology: June 2018.

For coherency, the abstract and the keywords of each paper are removed and replaced with a preface summarizing the work and highlighting the connection between different chapters. The majority of the papers listed above were planned, performed, analyzed and written by Amir Kazemi between September 2014-June 2018 under Dr. David Latulippe's supervision who also contributed to the project planning in addition to the

writing and revising of the papers. The following undergraduate students have contributed to different parts of this thesis as explained below:

- Karina Kawka assisted me with performing some of the experiments described in chapter 2 in summer 2015.
- Melissa Larocque helped with running the preliminary MMFC tests and troubleshooting of the system (described in chapter 3) as well as data analysis in summer 2016.
- Luke Boivin contributed to performing the filtration experiments described in chapter 4 as well as data analysis in summer 2016.
- Blake Patterson helped with performing the majority of the experiments described in chapter 5 and data analysis in summer 2017. Also, Panagiotis Papangelakis assisted with performing some of the experiments described in chapter 5 and sample analysis in summer 2017.

Paul Gatt, Dr. Seung Mi Yoo and Dr. Raja Ghosh provided helpful guidance on the sealing mechanism of the HF membrane modules introduced in chapters 4 and 5. Ryan LaRue contributed to editing the paper described in chapter 5. Ryan has also helped in some of the surface modification experiments described in chapter 5. Paul Gatt fabricated all of the modules used in this thesis based on the designs provided by the author. Dan Wright and Michael Clarke contributed to setting up and troubleshooting the pressure transducers used in chapters 2 and 4 for monitoring the TMP.

Chapter 1 - Introduction and Literature Review

1.1. Membrane Technology

Among different separation processes, membranes have obtained an important place in industrial applications during the past 50-60 years because of their reliability, efficiency, ease of operation and low energy consumption requirements. One of the key traits of a membrane is to control the permeation rate [1]. Membranes can be used as a contactor, a separation barrier, or a drug delivery tool. In terms of separation processes, a membrane is commonly defined as a very thin barrier (typically around 100 μm) by which materials can be selectively transported. Membrane processes have been used for different applications in pharmaceutical, paper, metals, food, textile and environmental industries [2]. At the early stages, the use of membranes was very limited because of being unselective, unreliable, slow and expensive. Improvements in membrane properties (e.g. chemical, mechanical and thermal properties) and the design of new process configurations that enhance the filtration performance and the economic efficiency of the process have led to increased use of membranes in industrial applications. Membranes are grouped based on pore size (microfiltration, ultrafiltration, nanofiltration or reverse osmosis), test format (flat sheet, spiral-wound, tubular or hollow-fiber), material (polymeric or inorganic), modes of operation (dead-end or cross-flow) and structure (isotropic/anisotropic, porous/dense and homogenous/heterogeneous).

In membrane filtration a driving force is applied across the membrane to separate the substances. Although membrane filtration is normally considered a size-based

separation, the filtration performance is quite complex and depends on multiple factors such as the feed solution conditions, pre-treatment conditions, membrane material properties, and hydrodynamic conditions. Filtration performance can be affected by solute accumulation adjacent to the membrane known as concentration polarization as well as by attachment and adsorption of the solutes known as membrane fouling.

1.2. Membrane Classifications

1.2.1. Filtration Spectrum

Membranes are classified based on average pore size. Different membrane filtration processes and their separation spectrum for biological and environmental separations are shown in Fig. 1.1.

Microfiltration (MF) membranes (0.1-10 μm) are typically used for purifying water, biological or food products by removing impurities such as particles, viruses and bacteria. One of the first applications of MF membranes was in testing drinking water samples by culturing microorganisms [1,3,4]. During the mid 1960s, MF had a very limited application either in laboratories or very small scale industrial applications [1,5]. The production of commercial membrane cartridges has led to more widespread application of such membranes in different industries such as pharmaceutical and electronics processes. MF membranes have also been used for sterilization (e.g. in food, dairy and pharmaceutical industries). Furthermore, MF membranes are used in drinking water and wastewater sectors following the cryptosporidium outbreak in the US [1–3,5] and as a pre-treatment step in reverse osmosis (RO) units to improve the RO efficiency.

Ultrafiltration (UF) membranes are finely porous membranes with the average pore diameter between 1-100 nm. In addition to pore size, UF membranes are characterized by molecular weight cut-off (MWCO), defined as the lowest molecular weight (MW) solute (usually reported in kilo Daltons) in which more than 90% of the solute is rejected by the membrane. Although MWCO is an arbitrary measure of membrane pore size, it has been widely agreed and employed by most of the membrane community because of the simplicity and ease of understanding for the users. In addition to MW, other factors such as the shape and charge of the molecule may affect the MWCO measurements of a UF membrane. For example, membranes behave differently when filtering a polysaccharide such as dextran against globular proteins of the same MWs. Also, the operating conditions such as transmembrane pressure (TMP) or permeate flux can affect the passage of the different molecules such as polydextrans or DNAs through the membrane. For example, previous studies have shown that transmission of large DNA molecules across UF membranes may occur due to elongation and deformation effects at the pore entrance [6,7]. Also, higher transmission of dextrans was observed in previous studies at higher fluxes presumably because of increased shear forces within membrane pores and molecular deformation of the coiled dextrans [8,9]. Although there is no direct correlation between the MWCO and average pore size of a membrane, Fig 1.1 shows a comparison chart for MWCO and average pore size. Fig 1.2 shows scanning electron microscopy (SEM) images of the skin-layer[1] of a polyvinylidene fluoride (PVDF) UF

[1] Skin side of a membrane is the very thin dense polymeric layer which consists of the smaller pores and plays the main role during the filtration/separation. The other structure is typically referred to as the microporous support.

membrane in hollow-fiber (HF) format used in the studies described in chapters 4 and 5. While Fig 1.2.a shows the relative size of the pores on the surface (40 nm as reported by the manufacturer), Fig 1.2.b shows that the membrane is an anisotropic membrane which consists of a thin barrier and a support layer. UF membranes are employed in different fields; for example, purification and separation of certain biomolecules of interest (e.g. proteins) for pharmaceutical applications can be performed using UF. Additionally, UF is used for removal of particulate matters and macromolecules in water treatment.

RO membranes are usually dense membranes that not only completely reject colloidal and particulate matter, but have also a very high rejection of salts. The membranes are usually rated on sodium chloride rejection or fractional decrease in the conductivity of the permeate which ranges from 90.0 to 99.8% of the feed solution [4,5]. From the early days, RO membranes have been used in plate-and-frame, tubular, HF and spiral-wound formats among which spiral-wound is the most commonly used configuration [1,10]. The RO process is very well-known for its application in desalination of sea water and for water reuse. During the past decades, RO has been regarded as one of the most economical methods for desalination which can be crucial in obtaining fresh water from seawater, brackish water and wastewater resources for industrial wastewater and drinking water applications [5]. The main trends in the development of new RO systems during the past years has been developing low-pressure membranes (i.e. membranes with improved hydraulic permeability) for energy saving as well as high-rejection membranes for a higher permeate quality and efficiency. Among other challenges related to development of RO membranes one can list inadequate boron

rejection [11], biofouling tendency [12] and chlorine tolerance [13]. World Health Organization (WHO) has indicated a maximum boron concentration of 2.4 mg/L in their provisional 2017 guideline for drinking water [14]. Because of the molecular size of the boric acid present in the seawater and the seawater's pH, the rejections obtained by RO membranes are typically between 88.0 to 93.0 % which is not sufficient in many cases. Biofouling has been considered as the most serious problem of RO operation. Development of low- or anti-fouling membranes as well as new cleaning methods can help to resolve this problem. In addition to biofouling, chemical fouling can occur by the adsorption of organic matter (e.g. humic acids) by hydrophobic or electrostatic interactions. Chlorine tolerance is also an important characteristic of the RO membranes since chlorine is commonly used as a disinfection for microorganisms.

Nanofiltration (NF) membranes were initially developed when attempts were made to develop RO membranes with higher permeabilities and lower operating costs. Development of membranes which require lower pressures (typically between 50-225 psi [15]) and have a lower rejection compared to RO units would be an improvement since in many cases the quality of the permeate in the RO systems is too high. Since NF's average pore size lies between RO and UF spectrums, it has always been difficult to define NF. In some cases, NF membranes with larger pore sizes can be considered tight UF membranes and tight NF membranes can be considered as RO membranes. NF membranes are usually expected to have a very high rejection for multivalent ions (90-98% [15]), a moderate rejection for monovalent ions (20-80% [15]) and a high rejection for organic compounds (70-97% [16–18]) with a MW smaller than the membrane's MWCO

(typically below 1000 Da). NF membranes have a wide range of applications including water softening, removal of organics from surface waters, removal of micro-pollutants, water reuse and removal of specific contaminants from water [5]. Research on NF has grown significantly during the past 10-20 years and new membranes such as solvent resistant nanofiltration (SRNF) membranes [19,20] and ceramic NF membranes [19,21] have been developed.

a

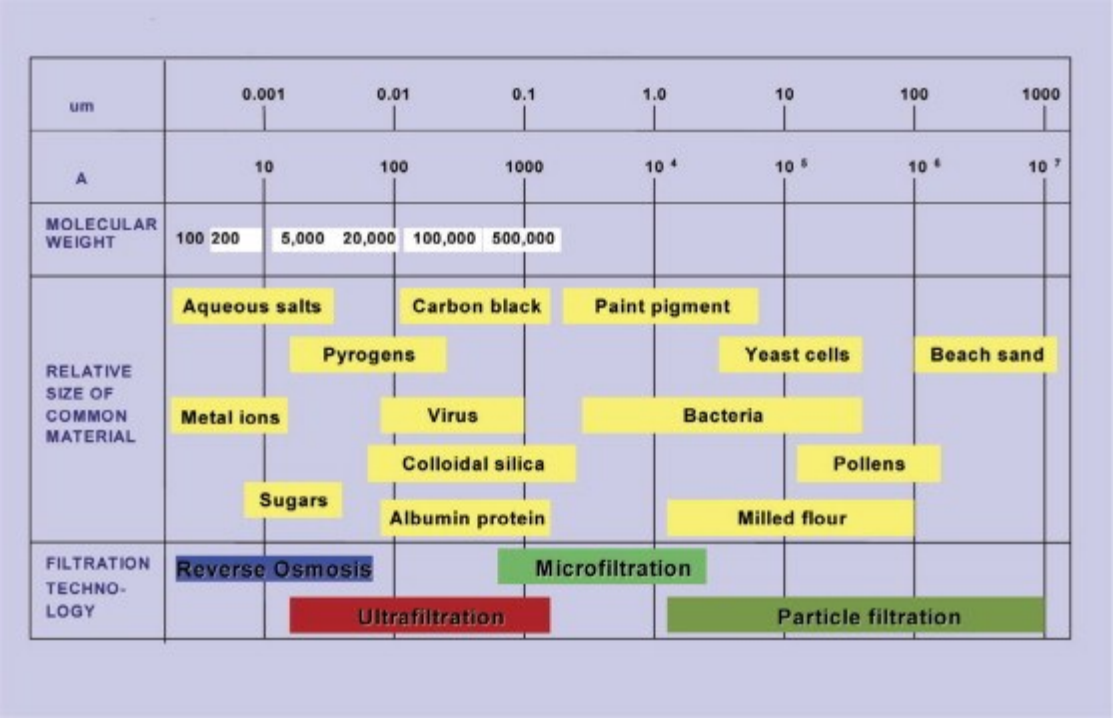

b

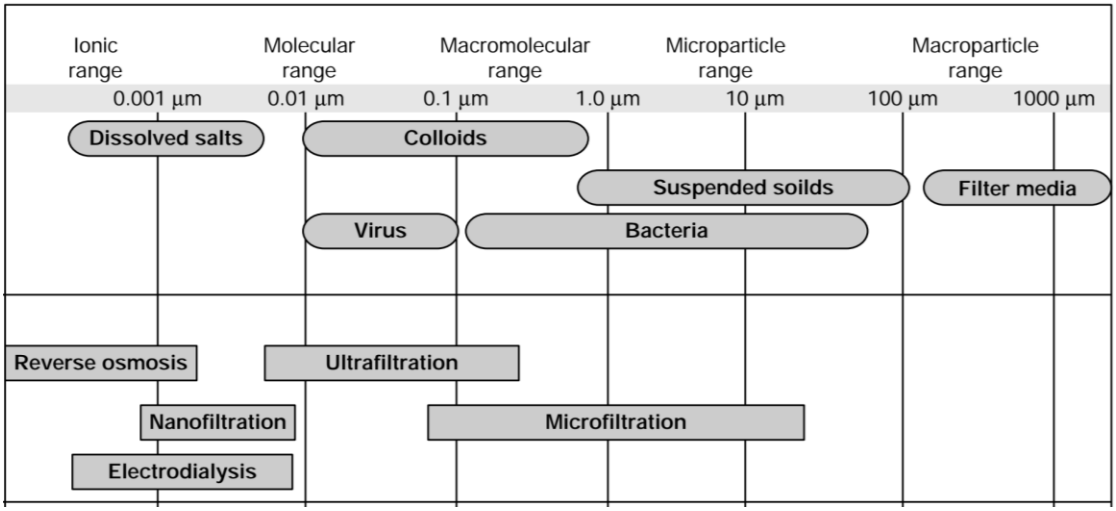

Fig 1.1. a. Pore size chart and filtration guideline for some of the common solutes (reprinted with permission [22]). b. Some of the typical contaminants present in different water sources with their sizes and their respective filtration processes (adapted from [4] reprinted with permission).

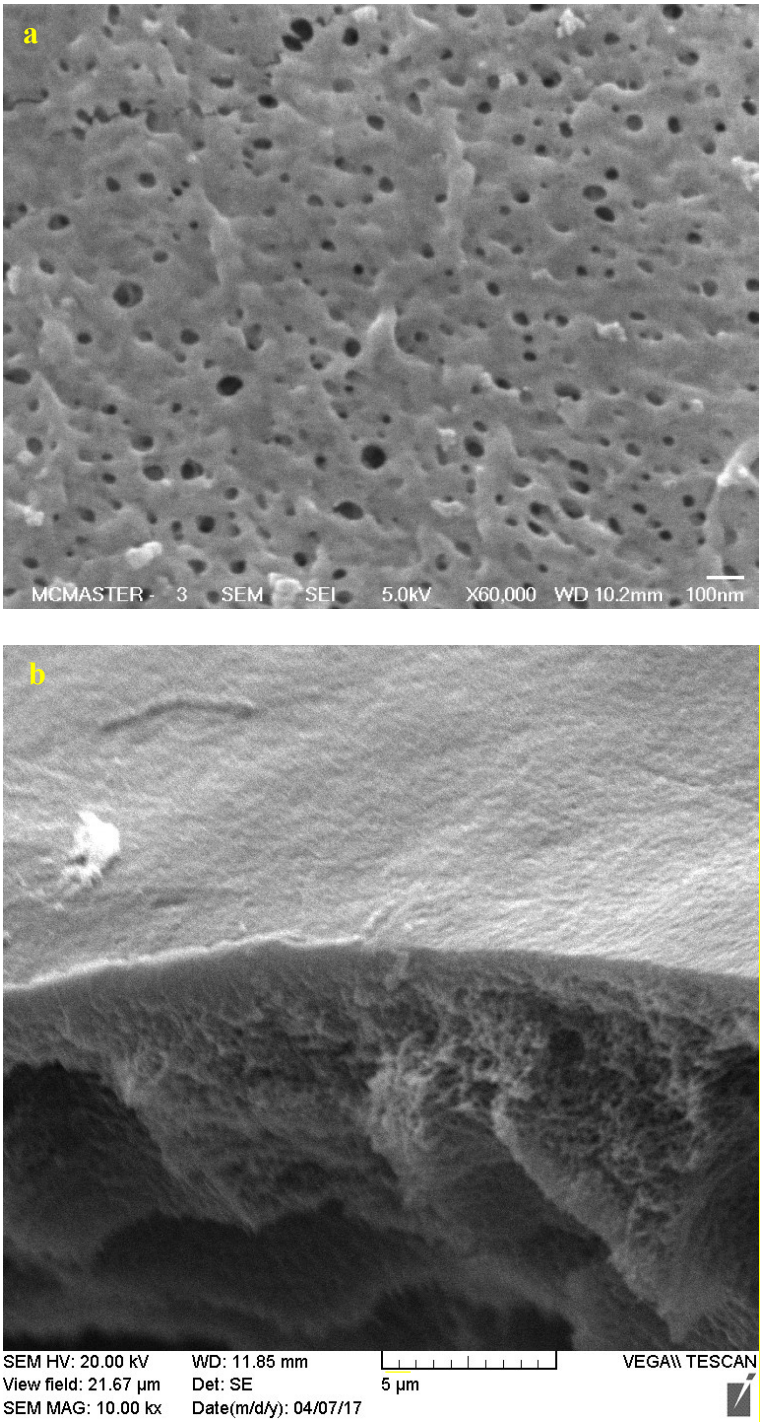

Fig 1.2. Scanning electron microscopy images of a. top surface and b. cross section of the skin-layer of a PVDF hollow-fiber membrane (average pore size 0.04 µm) used in ZeeWeed 500d module from SUEZ Water Technologies & Solutions (formerly GE Water and Process Technologies).

1.2.2. Membrane Geometry and Module Configurations

Typical laboratory scale filtration experiments are performed using flat-sheet membranes (Fig. 1.3a) either in a sealed stirred cell or using tangential flow filtration (TFF) modules. A stirred cell consists of a membrane disc that is placed at the bottom of a cylindrical cell and a magnetic stirrer is suspended above the membrane. The module is filled with the feed solution and a magnetic stir plate is used to induce the magnetic field required for stirring. In some cases, continuous feed can be supplied using a separate pressurized feed reservoir. These types of modules are used for initial membrane tests. However, solute build-up due to the dead-end (i.e. normal flow) regime adversely affects the permeate flux at constant TMPs. The solute transport in the boundary layer above the membrane surface of a stirred cell is generally explained using a stagnant-film model [23] due to the complex nature of its hydrodynamic conditions. These modules are typically available from different companies (e.g. Amicon Series from Millipore and UHP series from Advantec MFS) and in different capacities (3-2000 mL) [24]. Alternatively, TFF (also known as cross-flow filtration) can be performed where the feed flow is oriented parallel to the membrane face and the permeate portion passes through the membrane. Membrane filtration performance can be improved by using TFF since the adverse effects of concentration polarization can be minimized using the hydrodynamic conditions. Recirculation streams are typically used in cross-flow filtration by which the filtration performance can be enhanced. However, cross-flow filtration costs more energy and requires more complex equipment to operate. Flat sheet membranes in different formats are used in downstream bioprocessing laboratory experiments such as cell harvesting,

sterile filtration, buffer exchange, biomolecules separation, biomolecules concentration and biomolecules purification using MF/UF membranes.

HF filtration modules (Fig. 1.3b) consist of numerous long (typically between 1-2.5 m) porous filaments (i.e. fibers) sealed inside a shell. Each HF is very narrow and flexible, with typical inside and outside diameters (ID and OD) between 0.5-2.0 and 0.75-2.5 mm respectively, and can be either internally or externally skinned. Some of the HF membranes (e.g. ZeeWeed HF from SUEZ Water Technologies & Solutions) are manufactured with a 'supported' structure, where a relatively thick porous support layer is used beneath the membrane, to increase the mechanical strength of the fiber during the module assembly and the filtration process. While the SEM image of a HF membrane was shown earlier in Fig 1.2, Fig 1.4 demonstrates a number of ZeeWeed HF cassettes (SUEZ Water Technologies and Solutions) used in pilot- and full-scale filtration processes. HF membranes have been used for different MF, UF and RO applications but are most commonly used for MF and UF. HF membranes are usually considered as the ideal configuration for various membrane-based environmental separations including tertiary treatment[2] of wastewater, pre-treatment for RO processes and drinking water treatment. The high packing density, the inherent ability to backwash the membrane and the self-supporting design are the main advantages of HF membranes. By using HF membranes, the filtration can be performed in either inside-out or outside-in format for internally and externally skinned HF membranes and the opposite flow regime can be

[2] In wastewater treatment, the stage where the final treatment is performed to further improve the effluent quality (either for reuse or before its discharge to the environment) is referred to as tertiary treatment.

used for backwashing of the membranes with water or cleaning solutions for membrane reuse. For the externally skinned membranes, filtration is typically performed by application of vacuum inside the fiber or pressure outside the fiber. On other hand, the internally skinned HFs should be pressurized from inside the fiber when introducing the feed solution.

Spiral-wound modules (Fig. 1.3c) consist of flat-sheet membranes, feed and permeate spacers and a permeate tube. The membranes and spacers are sandwiched together and wrapped around a tube in a certain configuration. Feed travels through the flow channels tangentially across the length of the module. The feed spacers are used to provide uniform flowing space for the feed solution between the membrane sheets. The permeate is collected and directed into the permeate spacer where it is carried towards the permeate tube. Therefore, the feed gets more concentrated. Spiral-wound modules are mainly used for high-pressure filtration applications such as RO, UF or gas separations. Spiral-wound modules have a relatively smaller packing density compared to HF membranes and have a more limited range of scalability compared to HF modules or flat-sheet cassettes [25].

In tubular membrane modules (Fig. 1.3d), the tube consists of a porous support (typically made of fiber glass or paper) and the membrane is formed inside the tube (with inside diameters and lengths of 5-25 mm and 1-2 m respectively). Unlike the HF membranes, the tubular membranes have a low packing density and their application is usually limited to UF processes where the feed has a high solid content and the fluid hydrodynamics can have a favourable effect on the fouling behaviour of the membrane.

Plate-and-frame modules (Fig. 1.3e) were among the first configurations developed for commercial MF/UF applications. In these modules, multiple flat-sheet membranes are sandwiched with supporting plates and the channel spacers. The membranes can be glued or sealed using gaskets and clamped to form a tight fit. Permeates are directed separately from the feed stream and can be combined within or outside the module. Most of the plate-and-frame modules are built in rectangular configuration. Attempts for design improvements have been made within the past years to enhance the mass transfer properties by inducing turbulent flow. Although plate-and-frame membranes are favourable in terms of packing density and hold-up volume of the module, the cleaning of these modules is usually impractical considering the design of the module where the membrane is only supported on one side. Also, leakage potential through gaskets required for each plate is a serious problem which has increasingly limited the use of these modules since their introduction.

Fig 1.3 summarizes different module configurations used for membrane filtration processes.

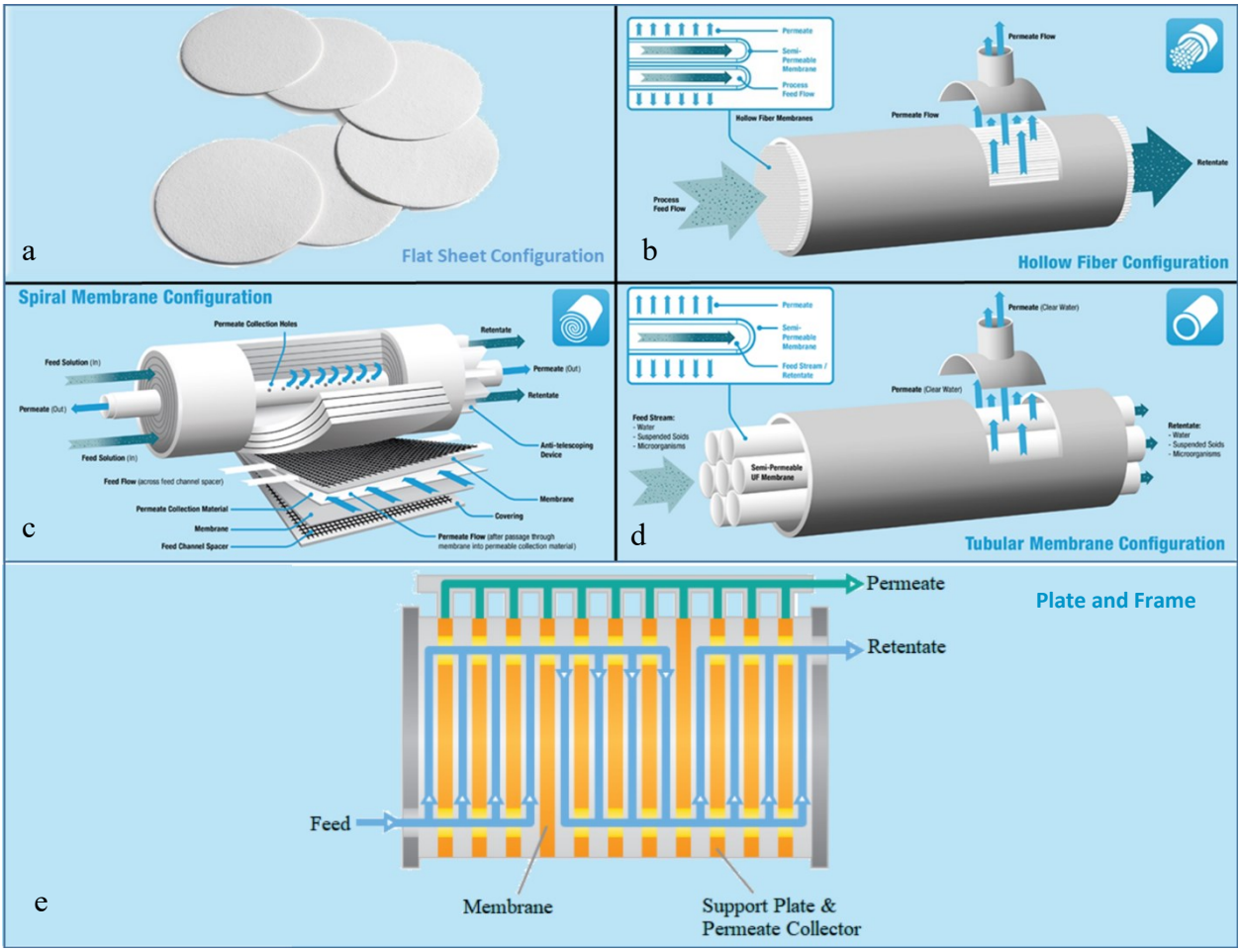

Fig 1.3. Module configurations: a. flat sheet; b. hollow-fiber; c. spiral wound; d. tubular; e. plate-and-frame. Panel a image adapted and reproduced with permission of Thermo Fisher Scientific Inc., copyright holder. Panels b, c and d Figures courtesy of Koch Membrane Systems, Inc (www.kochmembrane.com) and used by McMaster University with permission. Panel e Figure courtesy of Synder Filtration (www.synderfiltration.com) and used with permission.

Fig 1.4. Picture demonstration of different ZeeWeed hollow-fiber membrane cassettes (from SUEZ Water Technologies & Solutions) a. ZW150 with 12 modules per cassette (1995); b. ZW500A with 8 modules per cassette (1997); c. ZW500C with 22 modules per cassette (2000); d. ZW500D with 48 modules per cassette (introduced in 2003, improved design presented in 2010). For more information refer to Cote et al. [26] (figure reprinted with permission).

1.2.3. Membrane Materials

Membrane materials are mainly categorized into two groups: inorganic and polymeric. Inorganic membranes (e.g. ceramic or metal membranes) are usually employed for very specific applications (e.g. H_2 separation from coal-derived gas)

because of their higher price compared to polymeric membranes while polymeric membranes are widely used in different industries such as water and wastewater treatment, bioseparations and food processing. However, inorganic membranes are typically more tolerant against harsh process conditions. Verweij [27] have presented an excellent review on inorganic membranes. Although the range of available polymers is steadily expanding, not all of them are appropriate for membrane fabrication [3,28]. For example, according to Zeman and Zydney [3] there are around 17 polymers that are commonly used in manufacturing of MF and UF membranes. Of course the provided list does not include all the novel custom-made and modified polymeric membranes which are being continuously developed by researchers for enhanced physicochemical properties. The choice of a polymeric membrane material is usually based on the targeted application. For example, in bioseparations the membrane might be selected based on its protein-binding affinity or tolerance against sterilization (e.g. by γ-rays) while in other applications such as water and wastewater treatment the chemical and mechanical tolerance of the membrane might be of a great importance due to the repeated exposures to harsh chemicals and cleaning cycles. Furthermore, the polymer of choice has to be affordable, be available in reproducible quantities and be a good membrane former. For example, to be a good membrane former, the polymer needs the ability to form stable lacquer or melt. The polymer also has to be compatible with the targeted membrane formation technology. For instance, the solubility of the polymer in a safe solvent is important in immersion and air casting while low melting point of the polymer in the presence of solvents and additives is key in melt casting. Membrane surface chemistry

(e.g. hydrophobicity, charge, chemical resistance and binding affinity for specific particles and molecules) is another important factor to consider when picking a polymer for membrane formation. For example, membrane hydrophobicity, which is usually determined by water contact angle measurements, can significantly affect solute-membrane and solvent-membrane interactions and affect the filtration performance. Some of the most common polymers used in commercial membrane fabrication are cellulose, cellulose acetate (CA), cellulose nitrate (CN), polysulfone (PS), polyethersulfone (PES), PVDF and polytetrafluoroethylene (PTFE). A brief description including the key properties of some of these membrane materials are outlined below:

- Cellulose (Fig. 1.5.a) is a hydrophilic polysaccharide and cellulose-based membranes are mostly used for production of conventional low-fouling MF, UF and RO membranes. These membranes offer low-protein binding but have a poor biological and chemical resistance. Cellulose membranes can typically be used in a narrow operating range with no chemical cleaning of the membrane [3].
- PVDF (Fig. 1.5.b) is a semicrystalline thermoplastic polymer which is made of repeated $-(CH_2CF_2)_n-$ units [29]. In recent years, PVDF membranes have become popular for different processes such as membrane distillation, membrane contactors and membrane filtration for water and wastewater treatment and bioseparations. These membranes are usually prepared in flat sheet, HF or tubular formats [31]. PVDF can easily be dissolved in organic solvents used in membrane fabrication and hence porous PVDF membranes

can be formed using phase inversion by a simple immersion-precipitation process. PVDF membrane has a high thermal, chemical and aging resistance as well as a high mechanical strength [29–31]. Furthermore, PVDF contains low levels of extractables which is advantageous for bioseparation applications [31]. However, PVDF is considered quite hydrophobic compared to some of the other common membrane materials such as PS and PES which is often attributed to its lower critical surface tension [31]. Although in some cases such as membrane contactors and membrane distillation hydrophobicity is considered advantageous, it is well known that hydrophobicity can lead to more severe fouling in other applications such as water and wastewater treatment. Hence, there is a considerable interest in utilizing membrane modification techniques to enhance the surface properties of the PVDF membranes. PVDF has an excellent thermodynamic compatibility with other polymers over a wide range of blend compositions and thus membrane properties can be tailored to some extent by using other polymers depending on the desired application. PVDF can also be modified to have some specific functions and can be cross-linked by beam- or γ-radiation[31].

- PTFE (Fig. 1.5.c) is a hydrophobic semicrystalline thermoplastic polymer with repeated $–(F_2C–CF_2)_n–$ units. PTFE has a high resistance toward harsh solvents but it is easily degraded by γ -radiation (e.g. in sterilization). In addition to membrane filtration applications, PTFE is widely used in membrane distillation [32] and CO_2 capture [33] processes.

- PS and PES (Fig 1.5.d and 1.5.e) are both from polysulfone families and are among amorphous thermoplastic polymers. Both of these polymers exhibit excellent stability at high temperatures (glass transition temperatures of 185 and 220 °C for PS and PES respectively). However, PES exhibits better mechanical strength and chemical resistance properties. The main factor causing the membrane resistance is the presence of aromatic groups which limits the chain mobility [34]. Chlorine resistance is a key issue for water treatment applications. However, the main disadvantage of these membranes is their hydrophobicity and high protein-binding for bioseparation. Most researchers have attributed the fouling of PS and PES membranes to their hydrophobicity although the opposite has been reported in a few studies [34,35]. To enhance the filtration behaviour, these membranes are typically modified using either blending or surface modification techniques to improve the surface properties and reduce the fouling propensity [34–37].

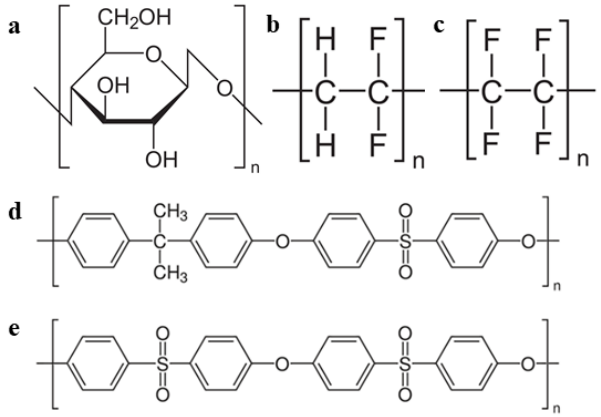

Fig 1.5. Some of the common polymers used in membrane fabrication: a. Cellulose b. PVDF; c. PTFE; d. PS; e. PES (chemical structures adapted from Wikipedia).

1.3. Membrane Filtration: Theory

1.3.1. Hydraulic Permeability

Derived from the Darcy's law, volumetric flow rate through a membrane of thickness δ is related to the driving pressure by equation 1.1:

$$J = \frac{\Delta P}{\mu} \times L_p \qquad (1.1)$$

where J, ΔP, μ and L_p are the volumetric flux, TMP, dynamic viscosity of the liquid and membrane permeability respectively. As a result, membrane permeability is proportional with the ratio of volumetric flux and the TMP. Although the form of permeability reported above is commonly used in the literature, some researchers –especially in the field of water and wastewater treatment– prefer to disregard the effect of viscosity for the measurement of hydraulic permeability of the membrane (i.e. permeability of the pure water) since such measurements are typically performed at identical temperatures and the change in viscosity is not going to significantly affect the permeability of the membrane. Therefore, a modified version of equation (1.1) is:

$$J = \Delta P \times L_p \qquad (1.2)$$

where L_p is the membrane permeability. It should be noted that L_p has different units in equations 1.1 and 1.2. In equation 1.1, L_p has units of length while in equation 1.2 L_p has units of length/time/pressure. In experimental setups, the membrane permeability is typically calculated from the slope of the linear portion of a volumetric flux-TMP graph. On the other hand, membrane resistance is defined as the reciprocal of membrane

permeability. Membrane filtration processes are operated either in constant flux or in constant TMP mode. In constant flux filtration, the permeate flux is typically controlled using a fluid delivery system (i.e. pump) and an increase in transport resistance due to buildup at membrane surface (concentration polarization), or physical blocking of membrane pores is identified via an increase in TMP. On the other hand, constant TMP filtration is performed by applying a positive pressure (typically via compressed gas feed) on the feed side and having permeate at atmospheric pressure or by using a vacuum unit to establish negative pressure on the permeate side and having feed at atmospheric pressure. In this case, increase in transport resistance is identified via decrease in flux.

The Hagen–Poiseuille equation can be used to relate the membrane structure with permeability measurements when using a feed free of any solutes, clean membrane (i.e. no fouling) with cylindrical pores and assuming a laminar flow:

$$J = \frac{\varepsilon r^2}{8\mu\tau}.\frac{\Delta P}{\delta} \qquad (1.3)$$

where ε, r and τ are the membrane porosity[3], pore radius in m and tortuosity factor respectively. For track etched membranes with capillary cylindrical pores the tortuosity equals unity. Furthermore, for flow through a porous media of packed spheres, the Kozeny-Carman equation can be used as shown below:

$$J = \frac{\varepsilon^3}{K\mu A^2(1-\varepsilon^2)}.\frac{\Delta P}{\delta} \qquad (1.4)$$

[3] $n\pi r^2$/surface area where n is the number of pores

where ε, K, and A are the bed porosity, the Kozeny-Carman constant and the specific area (i.e. surface area per unit of volume) respectively.

1.3.2. Concentration Polarization and Fouling

Concentration polarization refers to the accumulation of solutes or particles in a mass transfer boundary layer adjacent to the membrane surface and is a natural result of the selective transmission of different membranes. Concentration polarization can dramatically affect the filtration performance by causing flux decline, TMP rise and decrease in permeability.

Concentration polarization in normal flow filtration under steady state condition and in the absence of chemical reactions can simply be explained using the following equation by taking a number of assumptions into consideration:

- Back diffusion obeys Fick's law.
- Constant density and diffusion coefficients.
- Negligible concentration changes parallel to the membrane.

$$J.\,C_i = J.\,C_{i,P} - D_{ji}.\frac{dC_i}{dx} \qquad (1.5)$$

with the boundary layer conditions:

$$x = 0 \rightarrow C_B = C_{i,w} \qquad (1.6)$$

$$x = L \rightarrow C_B = C_{i,b} \qquad (1.7)$$

where $C_{i,p}$, $C_{i,b}$, $C_{i,w}$ are the permeate, bulk and wall concentrations of the solute respectively, L is the thickness of the boundary layer and D_{ji} is the diffusion coefficient. Using the boundary conditions, equation 1.5 can be simplified:

$$J=\frac{D_{ji}}{L}.\ln\left(\frac{C_{i,w}-C_{i,p}}{C_{i,b}-C_{i,p}}\right) \quad (1.8)$$

and for a fully rejected solute:

$$J=\frac{D_{ji}}{L}.\ln\left(\frac{C_{B,w}}{C_{B,b}}\right) \quad (1.9)$$

where term $\frac{D_{ji}}{L}$ is substituted for $k_{i,b}$ which is known as the mass transfer coefficient. The concept of concentration polarization is demonstrated in Fig 1.6 using a fully transmitted (A) and a partially rejected (B) solute.

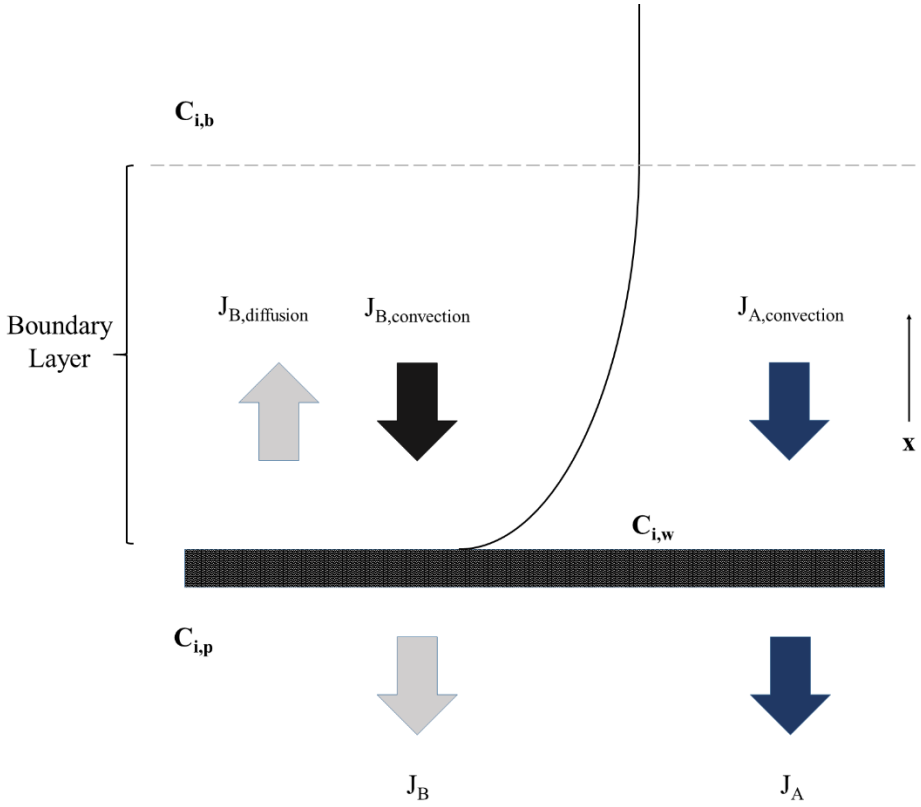

Fig 1.6. Schematic demonstration of concentration polarization phenomenon in the boundary layer above the membrane in normal flow filtration configuration using a fully transmitted (A) and a partially rejected (B) solute.

Fouling is described as deposition of material inside the membrane pores or on the membrane surface. There are different fouling mechanisms such as adsorption, pore blockage, deposition, gel formation and cake formation. Pore blockage significantly affects the permeate flux by partial or complete closure of membrane pores. Adsorption is caused by the specific membrane-solute interactions and other factors such as solute concentration and physicochemical conditions of the solution. Adsorption can adversely affect the filtration performance by causing an increased membrane resistance. The

increased resistance is commonly denoted as cake resistance (most commonly in multi-layer particle deposition) and/or gel resistance (in case of concentrated solutions of macromolecules such as proteins) [38]. Membrane fouling is generally categorized based on its reversibility. Hydraulically reversible fouling can be reversed by backwashing of the membrane. In some cases the fouling is chemically reversible, which means backwashing by water is not effective and chemical cleaning is required to reduce the adverse effects of fouling. Fouling can also change the quality of the membrane permanently which is usually denoted as chemically irreversible fouling [4]. Fig 1.7 shows an example of the difference between reversible and irreversible fouling during repeated UF of natural water samples and membrane cleaning cycles in constant TMP mode [39] and constant flux protein MF [40]. Fouling can negatively affect the filtration performance by decreasing the hydraulic permeability of the membrane and making its separation performance unpredictable. The extent of fouling depends on pore size of the membrane and its distribution, solute size, membrane material, surface characteristics of the membrane, solution conditions and hydrodynamic conditions of the module. Some of the most common foulants are proteins, polysaccharides, organic matters, particulates, colloids, microorganisms and inorganic precipitates which can adversely affect the filtration performance depending on the membrane pore size and properties.

a

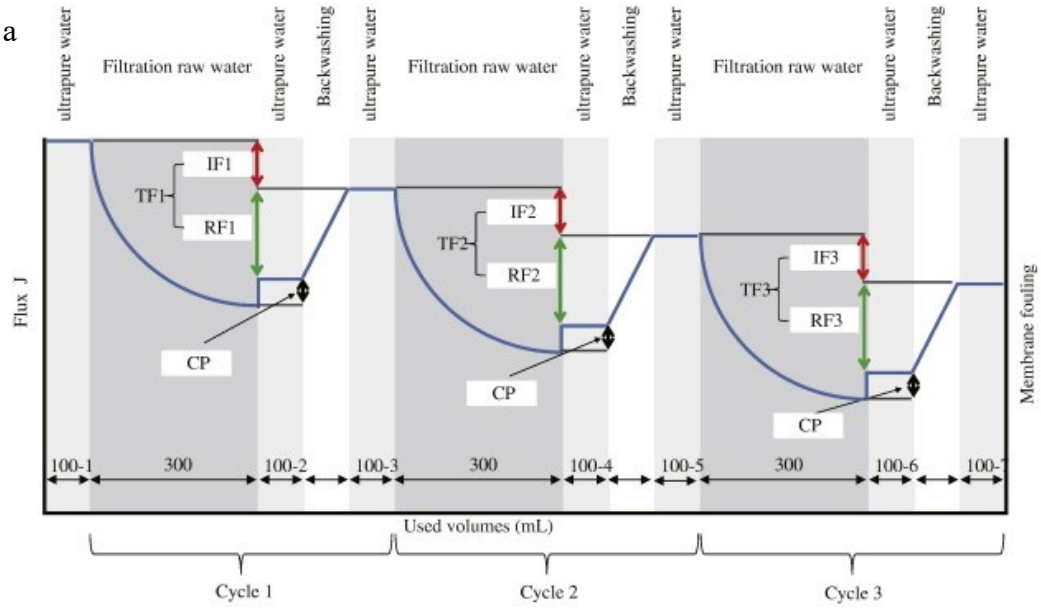

b

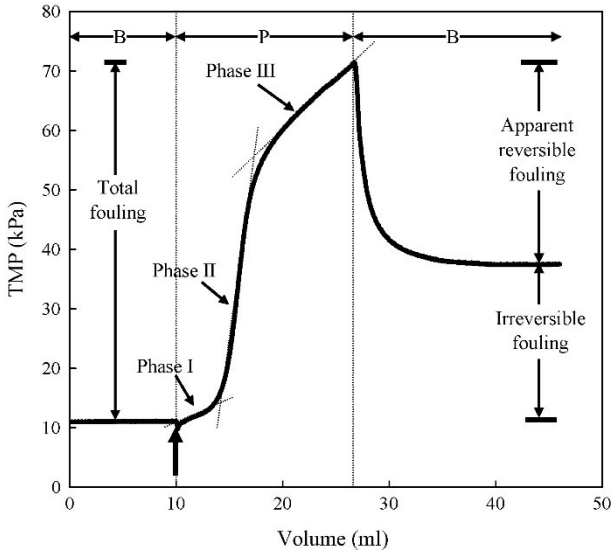

Fig 1.7. a. Demonstration of the reversible (RF), irreversible (IF) and total (TF) membrane fouling in: a. constant TMP UF by Sun et al. [39] and b. constant flux protein MF by Kanani et al. [40] (images reproduced with permission [39,40]).

A variety of methods have been employed to enhance membrane filtration performance by controlling fouling including the introduction of gas bubbles by sparging

[41–46], turbulence introduction by stirring near the membrane surface[47–52], using pulsatile flow [53,54] and turbulence promoters [55] , membrane surface modification [35,37,56–61], membrane cleaning by backwashing [62–66], applying electrical field [67,68], ultrasonic waves and membrane vibration [69–71]. Introduction of mixing near the membrane surface is one of the simplest and most common approaches to limit these effects in dead-end flat-sheet filtration modules [47–52,72,73]. One of the earliest practical uses of stirring was to study the transport of lipoproteins through a UF membrane [47]. Later Fane and colleagues [48,49] were among the first researchers to study concentration polarization and membrane fouling in a stirred UF cell. They showed an improved performance of constant TMP UF of a colloidal silica suspension, proteins and polysaccharides in the presence of stirring above the membrane.

1.3.3. Separation Performance and Optimization

The transmission of particles, solutes or ions through a membrane can be quantified in terms of the intrinsic sieving coefficient (S_i) or intrinsic rejection coefficient (R_i):

$$S_i = \frac{C_p}{C_w} \times 100 \qquad (1.10)$$

$$R_i = 100 - S_i \qquad (1.11)$$

where C_p and C_w are the permeate concentration (also known as C_f; filtrate concentration) and wall concentration above the membrane respectively. Since C_w is difficult to

determine, apparent sieving and rejection coefficients (S_a and R_a) are used instead of intrinsic coefficients:

$$S_a = \frac{C_p}{C_b} \times 100 \quad (1.12)$$

$$R_a = 100 - S_a \quad (1.13)$$

where C_b, the bulk concentration, is used instead of C_w. It should be noted that sieving and rejection coefficients are interchangeably used as a useful measure of transmission and removal respectively. Intrinsic sieving coefficient depends on the solute and membrane properties, physicochemical conditions of the solution and the permeate flux and it is usually quantified using diffusive-convective membrane transport theory as reported in the literature [47,74–76]. Apparent sieving coefficient depends on the hydrodynamic conditions as well as the other factors mentioned for intrinsic sieving coefficient [75,76]. Equation 1.8 can be used to derive a correlation between the apparent and intrinsic sieving coefficient by having the mass transfer coefficient, k (where term $\frac{D_{ji}}{L}$ is substituted for k), and the flux, J:

$$\ln\left(\frac{S_a}{1-S_a}\right) = \ln\left(\frac{S_i}{1-S_i}\right) + \left(\frac{J}{k}\right) \quad (1.14)$$

For a binary separation, the performance of a membrane is usually quantified using the selectivity (ψ) defined as:

$$\psi = \frac{S_{a,\text{smaller molecule}}}{S_{a,\text{larger molecule}}} \quad (1.15)$$

As mentioned earlier, a common misconception is that membrane filtration is a process solely based on the pore size of the membrane. However, this process is quite complicated and is affected by physicochemical, hydrodynamic and operating conditions of the process [76,77]. A summary of the effects of different factors on membrane filtration performance is presented in the next two sections.

1.3.3.1. Separation Performance in Biological Separations

It has been widely reported that changes in the physicochemical conditions can significantly affect the filtration performance by changing the concentration polarization, sieving coefficient and fouling behaviour of the membrane [76,78–83]. For example, in constant TMP protein filtration, the maximum sieving coefficient and the minimum permeate flux are observed at pH close to the protein isoelectric point (pI) where its net surface charge is zero. In fact, both protein and membrane charge are affected by pH. When the protein and the membrane have the same charge, presence of repulsive forces cause reduction in protein transmission. On the other hand, when the membrane and the protein carry the opposite charge, a layer of protein is formed on the membrane surface due to the charge adsorption which decreases the protein transmission due to particle-particle interactions. Also, it must be noted that at pHs other than the pI, an electrostatic double layer is formed around the protein which increases the size of the molecule and decreases the protein transmission. Changing ionic strength can significantly contribute to changes in the sieving behaviour of the protein when the molecule is charged.

Furthermore, very low and very high salt concentrations are known to cause severe membrane fouling [76,80–83]. To provide more details, some of the studies are summarized in what follows.

Fane et al. [80] have observed changes in bovine serum albumin (BSA) UF behaviour at different pHs using different salt concentrations. At pH 5 (close to the pI) flux increase was observed by changing the ionic strength from 0 M to 0.2 M. However, the flux did not change significantly while changing the ionic strength from 0.2 to 0.8 M at pH 5. Increasing the ionic strength had a different effect at pHs 2 and 10 and resulted in a decrease in the permeate flux. A minimum permeate flux was observed when filtering BSA at different pHs in the absence of salt while no minimum was observed in the presence of salt. Furthermore, the highest extent of BSA adsorption was observed at pH 5 which was increased by increasing the salt concentration. Kazemi and Latulippe [73] have observed higher TMPs when performing constant flux UF of BSA at pH 5 (close to the BSA pI of 4.9) compared to pH 7.

Feed solutions containing at least two proteins are commonly used to study the effect of different factors along with solute-solute interactions on the filtration performance. Protein-protein separation has been widely studied by different researchers. Saksena and Zydney [83] have studied the effect of pH and ionic strength on the separation of BSA and immunoglobulin G (IgG) using UF membranes where the extent of permeate flux, protein sieving coefficients, protein adsorption, bulk mass transfer coefficients and membrane transport properties were all functions of ionic strength and pH. It was shown that higher selectivities were achievable by using pH 4.8 where BSA

and IgG have their highest transmission and rejection respectively. Ghosh and Cui [42,81] have investigated the effect of pH on membrane selectivity using a UF process for lysozyme-BSA separation and observed selectivities ranging from 3.3 to 220 due to the changes in the proteins charge. Cheang and Zydney [84] have studied the separation of α-lactalbumin and β-lactoglobulin to determine the optimal pH, ionic strength, and filtration conditions. Selectivities over 55 were observed at pH 5.5 and 50 mM ionic strength with a 30 kDa MWCO cellulose membrane. The transmission of α-lactalbumin was lower at pH 7.2 since greater negative charge exists on the protein. Conversely, the β-lactoglobulin transmission was greater at pH 7.2 due to dimers dissociation above pH 6.5. van Eijndhoven et al. [85] used a similar approach for the separation of BSA and hemoglobin where selectivities of greater than 70 were observed by reducing the salt concentration and adjusting the pH to 7 (pI of hemoglobin). Baek et al. [86] have evaluated the UF performance of an Fc-fusion protein (MW=94 kDa and pI of 5.5–6.1) in different buffers and protein concentrations. They have later compared the UF behaviour of an Fc-fusion protein and two monoclonal antibodies (mAbs; mAb-1 with pI of 7.2-7.8 and MW of 144 kDa and mAb-2 with pI of 8.2-8.8 and MW of 149 kDa) in different buffers using different concentrations [87]. More detailed discussions regarding protein-protein separation can be found in the review papers published in the literature [88–90].

Some of the recent studies have investigated the filtration of biomolecules other than proteins. Manzano et al. [91] have studied the effect of membrane material, membrane pore size and flux on the UF of RNA. A significant increase in RNA transmission was observed by increasing the permeate flux when using Biomax® (PES)

membranes with 50 and 100 kDa MWCO. Hadidi et al. [92] have studied the filtration performance of UF of different bacterial polysaccharides by investigating the effects of permeate flux, membrane structure and the type of polysaccharide over a wide range of solute concentrations. It was reported that large polysaccharide molecules can be transmitted through UF membranes by controlling the operating conditions including flux and polysaccharide concentration. This phenomena was also observed by LaRue et al. [9] when performing UF experiments with different FITC- and TRITC-dextran solutions through UF membranes with reported MWCOs smaller than the MW of the solute. Similar effect of flux on the filtration performance has been reported in studies that investigated the filtration behaviour of large DNA molecules [6,7,93]. While the extent of polysaccharide transmission can be elucidated according to the convective transport at higher fluxes due to the concentration polarization effects, the DNA transmission was discovered to be due elongation/deformation effects at the pore entrance. Arkhangelsky et al. [94] and Li et al. [95] have also investigated the effect of ionic strength on the filtration behaviour of linear and supercoiled plasmid DNAs and found that while transmission of different DNA molecules increased at higher ionic strengths, a better membrane fouling control can be achieved by using higher salt concentrations.

1.3.3.2. Filtration Performance in Environmental Separations

The performance of environmental separations significantly depends on different factors. For example, natural organic matter (NOM) behaviour in filtration process is

believed to be highly dependent on pH, ionic strength, presence of divalent metal cations and chelating agents [96] as well as membrane pre-treatment and surface modification [60]. Lin et al. [97] have used a single HF UF membrane to study the effectiveness of humic acids (HA) removal with different MWs under different operating conditions including, constant concentration, constant TMP and with powdered activated carbon (PAC) addition. They have observed the optimum quality of the permeate for larger HAs (6.5-22.6 kDa); however, an extreme flux decline was observed in this process. The UF membrane was not effective in removal of smaller (< 650 Da) HAs. PAC addition was observed to have negative effect on membrane filtration performance in this case by causing more severe flux decline.

Kuhn and Oshima [98] have used a polyacrylonitrile (PAN) HF UF membrane to evaluate and optimize the removal and recovery of *Cryptosporidium parvum* oocysts from different water samples including deionized, tap, and natural waters. The authors observed that the optimum recovery can be obtained when using a 5% fetal bovine serum (FBS) to block the membrane and the addition of 0.05% FBS in the initial oocyst suspension. The same approach was successfully used by Morles-Morales et al. [99] for the optimization of enteric bacteria, protozoa, and viruses recovery from water.

Decarolis et al. [100] used a pilot scale inside-out HF membrane filtration unit to study the effect of different operating factors on tertiary wastewater. The module configuration allowed for simultaneous operation of six experiments in parallel using six identical modules, where each module contained around 2000 UF fibers (with approximate length of 50 cm and internal fiber diameter of 0.8 mm) with a total

membrane area of 1.9 m^2. The authors studied the effect of operating flux, membrane cleaning and coagulant addition on membrane fouling by running a total of fifteen pilot experiments. The results suggested that flux increase causes a higher extent of membrane fouling and lower runtime[4] without backwashing. Furthermore, it was observed that lower backwashing intervals and addition of $FeCl_3$ as a coagulant can significantly decrease the membrane fouling.

Lei [101] have employed different configurations to study UF PVDF membranes and investigated the effect of hydrodynamics on the fouling behaviour using natural water with low and high organic content. The results were modelled and compared with Hermia [102] and Field [103] models and the hydrodynamic conditions and the system configuration were found to have a significant impact on the permeate flux and the pseudo-steady-state permeate flux.

Katsoufidou et al. have evaluated the effect of different factors on UF performance with solutions of HAs [104], sodium alginate [50] and mixture of the two [105]. They observed that calcium ions concentration acts as an important factor in the membrane fouling since it promotes HA aggregation. The experimental and modelling results showed that a rapid irreversible fouling occurs due to adsorption while pore blockage and cake formation can be partially reversed by backwashing. In addition to HAs, extracellular polymeric substances (EPS) and especially polysaccharides are among the main fouling sources in membrane filtration processes. Sodium alginate was used as a

[4] Runtime is defined as the time at which the maximum TMP of the membrane is achieved (or in other words filtration time between the cleaning cycles).

model foulant to study the fouling mechanism in the HF module [50]. An increase in calcium concentration was shown to cause more cake formation and to eliminate adsorption phenomenon hence causing more reversible fouling of sodium alginate. Sodium alginate cake layer was found to be weak in the absence of calcium as well. For the binary solution of HA and sodium alginate [105], the flux recovery was more similar to the one observed when using a solution containing sodium alginate only. However, the fouling mechanism was found to be affected by the simultaneous action of the fouling mechanisms due to the presence of each molecule. As observed in previous studies, calcium ion concentration was found to intensify the cake formation.

Huang et al. [106] investigated the effect of NOM source (White river raw water, Twente Canal raw water, Tampa Bay raw water and Scottsdale secondary effluent) and hydrodynamic conditions (permeate and backwash flux) on reversible and irreversible fouling of HF UF membranes and found that HA source is of a great importance to filtration performance and membrane fouling. Kim and Dempsey [107] have tested the filtration behaviour of several commercially available HA, soluble microbial products (SMP) and sodium alginate as surrogates for NOM and effluent organic matter (EfOM). It was observed that SMP and HA were most similar to EfOM and Suwannee River NOM respectively while sodium alginate demonstrated a unique filtration behaviour not similar to the filtration behaviour of any of the other organic matters. Furthermore, calcium ion addition has resulted in a different behaviour (higher membrane resistance) in case of sodium alginate filtration compared to the other cases. Yamamura et al. [108] investigated the fouling propensity of MF and UF membranes against the hydrophilic and hydrophobic

fractions of NOM. It was reported that hydrophilic fraction of NOM, which mainly contains biopolymers, were the main source of irreversible fouling while the extent of fouling strongly depends on the membrane material and NOM characteristics. Qu et al. [109] studied the effects of membrane pore size and surface hydrophobicity on extracellular organic matter (EOM) from *Microcystis aeruginosa* fouling during UF; the flux decline caused by EOM was independent of pore size and the membrane hydrophobicity.

Overall, the studies summarized above show the importance of evaluation and optimization of membrane filtration performance for biological and environmental separations.

1.4. Membrane Filtration: Conventional Applications and Recent Trends

1.4.1. Biological Separations

Membrane filtration processes are widely used in bioprocessing industries including food, pharmaceutical and biotechnological sectors. MF membranes can be used as a means of sterilization for bio-products such as food, dairy and pharmaceutical products. Sterile filtration is used in the final step of product formulation as well as initial filtration of fermentation broth. Sterile filtration is typically performed by employing membranes with 0.1-0.2 μm average pore size in a dead-end configuration [110,111]. Also, MF is employed for both virus removal (e.g. virus-protein separation) [111–113] and virus purification (e.g. recovery of viral vectors for biotherapeutics production)

[114,115]. UF membranes are used in separation processes to purify and/or concentrate certain bio-molecules of interest such as proteins, DNA, enzymes and polysaccharides. Also, diafiltration is used as a tool for buffer exchange and desalting by washing the initial buffer and by replacing it with a new buffer with a different composition. Particularly, improvements in UF processes have led to development of more selective protein fractionation processes in food and pharmaceutical industries. The main advantages of UF compared to conventional protein fractionation techniques (e.g. electrophoresis and chromatography) are high throughput of the product, relative ease of sanitization, and ability to easily scale-up. UF processes are also helpful in antibiotic production process by removing the emulsifiers in the broth prior to solvent extraction to enhance the extraction efficiency [9]. Other techniques such as UF in the presence of electric field, UF using charged membranes, UF in the presence of ultrasonic field and UF by adjusting the experimental operating conditions are used for fractionation in non-size-based separations of proteins [90].

Another common application of membrane processes in bioprocessing is in development of membrane bioreactors (MBRs) where microorganisms, enzymes or antibodies are suspended in solution or immobilized within the membrane matrix. MBRs have been studied for a long time as a replacement for classic biological reactors with suspended biocatalysts. The membrane may be either combined with the reactor or be used as a support for enzyme immobilization in the reactor. MBRs have been studied over the last three decades, but have obtained very limited success in the biotechnology field due to scale-up difficulties and the potential for microbial contamination. Generally flat

sheet membranes are not very appropriate for bioreactor design due to the limited membrane surface area and fouling propensity [116,117]. HF membrane devices have been widely used in bioreactors, especially for cell culture. Depending on the membrane structure and module design, the cells can be grown either on inside or outside of the HFs. In practice, it is less challenging to use the outside of the HF for cell culture purposes and the membrane plays a role both as a cell support and a transport barrier for the media and nutrients. The nutrients are flown through the opposite side of the fibers. Generally the cell media is aerated to supply the required oxygen for the cell culture. Depending on the design, the HF bioreactor may be in dead-end format or have a recycle stream. There are several steps involved with running a HF membrane bioreactor for cell culture including sterilization, seeding, transport, cell attachment, cell expansion, differentiation and product removal (for more information see [118]). Cell immobilization in HFs has been widely studied as a beneficial technique for protecting cells from shear damage and to obtain higher productivity [119]. One of the common cell culture studies using HF bioreactor devices is testing bioartificial kidneys (BAKs) containing human primary renal proximal tubule cells, a recent study developed a single HF membrane bioreactor and reported that the HF with a skin layer on its outer surface was the preferred configuration [120].

1.4.2. Water and Wastewater Treatment

In the field of water and wastewater treatment, it is important to develop advanced processes to remove microorganisms, disinfection by-product precursors[5], synthetic organic chemicals, suspended and colloidal particles, NOM and salts from water supplies. MF and UF are low-pressure membrane processes that can be applied to remove microorganisms, suspended colloidal particles and macromolecules. One of the main drivers for the increased use of low-pressure filtration systems in the water industry was the Giardia and Cryptosporidium removal guidelines stressed by Safe Drinking Water Act and the US Environmental Protection Agency (EPA) in the disinfection processes used for water treatment. Furthermore, the increased need for drinking water supplies has led to the expanded use of RO systems to desalinate sea and brackish water, a process where MF and UF are usually used as a pre-treatment step. The quality of pre-treated water using MF/UF systems is usually higher than the water treated with conventional pre-treatment systems such as coagulation/sedimentation/filtration which can result in a higher efficiency in the RO system.

Another useful application of membrane technology is the use of MBR systems for water and wastewater systems. The MBR technology is based on the conventional activated sludge (CAS) process with biomass separation by membrane filtration. In the first step, the removal of organics, nitrification, and denitrification is achieved using microbial processes. Next, the suspended solids, colloidal solids and microorganisms are removed using a membrane system. An MBR system can produce a permeate stream with

[5] By-products formed due to the interaction between the disinfecting agents and water impurities.

a relatively high quality and a retentate stream containing the biomass and the return sludge. Also, this system requires a smaller footprint since there is no need for a secondary sedimentation tank and higher mixed-liquor suspended solid (MLSS) concentrations can be used. Ease of installation, replacement and cleaning, minimizing the number of dead-zones and introduction of turbulence by aeration are among the important factors to successfully design an MBR [5]. HF (typically outside-in), tubular (typically inside-out) and plate-and-frame membrane modules are the most commonly used membrane geometries used in MBRs.

Membrane technology has also been used for virus recovery and concentration from water. Considering the growing interest in water reuse, there is a crucial need for the rapid, sensitive and reproducible detection of viruses from different water streams. Proper virus concentration and recovery from water is one of the important challenges in regards to virus detection. Because of the low concentration and high volume of the samples used for virus detection, virus adsorption–elution (VIRADEL) and crossflow ultrafiltration (CFUF) are the only practical membrane-based methods for virus recovery [121,122]. The VIRADEL method consists of adsorption and elution steps and is usually performed by using electronegative or electropositive membranes. CFUF has been growing and becoming more popular as an alternative to VIRADEL and is performed by maintaining the recirculated retentate by a UF membrane typically with MWCO between 10-100 kDa. The filtration process performance can significantly change considering the virus properties, virus geometry, solution conditions (e.g. pH and solution composition), membrane properties (pore size, hydrophobicity, charge and structure) and operating

conditions. The main challenges related to VIRADEL and CFUF processes are elution of the adsorbed virus and virus adsorption respectively. An excellent review is published by Shi et al. [122] summarizing different aspects of virus recovery from different water sources which provides future guidance in this regard.

Different innovations in creating novel membrane materials have been reported recently in the literature including the modification of membrane surface with different nanomaterials for enhanced properties. For example, membranes containing carbon nanotubes (CNTs) have been employed as a promising tool for water purification considering the unique characteristics of CNTs including high conductivity, high adsorption capacity and disinfecting properties [123–127]. Vecitis et al. and Gao and Vecitis have reported that electrically conducting CNTs on a PTFE support can inactivate bacteria (*Escherichia coli*) and viruses (MS2) [128] and degrade organics to different degrees depending on the experimental conditions [129] in a dead-end configuration by using an electric bias. Gunawan et al. [130] have used PAN HF membranes as a support for silver nanoparticles and CNTs which were covalently coated on the external surface of the membrane as a disinfection barrier. The modified membranes showed antimicrobial properties against *E. coli* as well as enhanced antifouling properties. Yang et al. [131] have reported deposition of plasma treated CNTs onto a mixed cellulose ester support. Because of the ultra-high salt adsorption capacity of the treated CNTs the desalination and water purification processes were performed at significantly lower operating TMPs compared with RO membranes. de Lannoy et al. [126] have fabricated electrically conductive UF polymeric membranes by using a thin layer of polyvinyl alcohol (PVA)

cross-linked with carboxylated multiwalled CNTs and succinic acid onto a support CN MF membrane. Membranes displayed high permeability with good separation performance, high conductivity, and high hydrophilicity. Later a similar approach was used [127] by reacting CNTs with polyamides and depositing them onto a PES MF support membrane for enhanced salt rejection, biofilm prevention and water permeability.

1.5. High-throughput Process Development

1.5.1. Biological Processes

There is a growing interest in the use of high-throughput (HT) systems to speed-up the development and the optimization of biological processes. These techniques are generally defined as miniaturized version of unit operations that are scalable to real production settings. There are three main advantages with the use of these techniques. First, the material cost is reduced by running experiments using a small amount of sample. Second, it uses a parallel approach, ideally suited for statistical methodologies, for process development and optimization. Using the miniaturized format, the high resources needed for the conventional development of a product in a lab- or pilot-scale system can be reduced which also results in a reduced time for a product to be successfully introduced or the financial damages for the products which fail to enter the market. Also, these techniques can speed up the process understanding in the initial stages of a process development, improving the performance and reducing the potential risks [132]. The third advantage of using HT platforms is that these methods can be combined with automated systems and instrumentation for real-time monitoring of processes.

Recent developments in automation, microfluidic devices, and computational fluid dynamics (CFD) analysis offers a unique opportunity for further development of HT techniques. For example, automation can be used to minimize the human interference and CFD can be used to evaluate the scalability of the miniaturized processes although larger-scale studies will still be necessary to verify if the fluid flow and mass transport characteristics require any adjustments.

Multi-well plates have become a common tool in bioprocessing research and several studies have used HT techniques for the development of upstream processes such as fermentation [133–136], mammalian cell culture [137,138], tissue engineering applications [139], and bioreactors [140,141]. Further details and discussion regarding the use of HT techniques for upstream processes and the effect of various process parameters such as fill volume, well geometry, solution conditions, and mixing conditions on process performance can be found in excellent reviews published in this field [133,140,142–144].

Although downstream processes account for over 80% of overall production costs [145] very few HT studies were published in this regard until mid2000s. The development and optimization of downstream processes using conventional strategies can be very demanding due to the large number of factors that affect the performance or the nature of the process. Hence, increasing attention is needed for the development of HT techniques for downstream unit operations in order to profit from the progresses made in the field of upstream micro-scale processing.

1.5.1.1. Adsorption

Early HT downstream processing works were devoted to the optimization of adsorption experiments for removing process impurities such as metal ions from pharmaceutical products [146,147]. Welch and colleagues [146] used a microplate based approach combined with liquid chromatography–mass spectrometry (LC-MS) and colorimetric indicators to screen all of the possible adsorbents in terms of metal removal. Later, they extended this technique by using micro-tubes along with high-performance LC-MS for the selective removal of metal impurities [147].

1.5.1.2. Aqueous two-phase system (ATPS)

Other researchers have worked on development of HT techniques for aqueous two-phase system (ATPS). Bensch et al. [148] screened up to six hundred samples per day by combining a robotic instrument with a HT screening approach using deep well plates to quantify the protein partitioning behaviour in a polymer-salt ATPS. Oelmeier et al. [149] have evaluated the separation of mAbs from host cell protein mixtures by combining a HT ATPS technique with statistical methodologies and screening the effect of pH, sodium chloride concentration and the tie line length in a model system. Wiendahl et al. [150] have combined response surface modeling (RSM) and genetic algorithm (GA) with an automated HT ATPS approach for the separation of plasmid DNA (pDNA) and RNA. In all three studies the results were observed to be reproducible.

1.5.1.3. Chromatography

Chromatography is considered the workhorse of the downstream processing and thus several groups have developed HT methods for chromatography. HT format is ideal for chromatography processes since a wide variety of media and operating conditions need to be selected including the screening of ligands, resins and columns. Unlike conventional chromatography processes such as high-performance liquid chromatography (HPLC), which are conducted using commercially-available[6] lab-scale columns, HT chromatography techniques are developed using miniature packed bed columns, micropipette chromatography tips, and filter plates. Packed micro columns can be used with automated systems to evaluate the effect of flow rate on the chromatography performance in a HT format. Britsch [151] have reported the successful use of such columns (~200 µL of resin) along with a robotic system for protein separation. Micropipette tips, with resins sealed inside, can be used by repeated aspiration and dispensing of the feed and buffer samples in a micro-plate considering the required residence time. Wenger et al. [152] have used these tips for the purification of virus-like particles. Filter plates (membrane-bottom micro-plates) are used to remove the liquid phase of the mixture of the feed and the resin. Coffman et al. [153] have compared the results from a filter-plate based chromatography for feeds containing mAb and Fc fusion protein with a conventional chromatography system where reasonable predictions were observed on recoveries and purities using the microscale system.

[6] Conventional columns have an internal diameter of 1-5 mm and a height of 3-25 cm.

1.5.1.4. Filtration

Previous studies have presented the idea of HT testing for membrane filtration processes. The first study on the use of HT testing concept for membrane filtration was reported by Chandler and Zydney [154] where vacuum- and pressure-driven MF were used via 96-well filter plates, syringe filters and unstirred cells to study the harvesting of yeast cells. Overall, the results across different formats were quite consistent especially with PVDF and mixed cellulose ester membranes while a few inconsistencies were observed among different formats and within a plate when using other membranes presumably due to the sealing problems.

A number of studies have exclusively focused on using commercially available vacuum manifolds and vacuum-driven filtration setups because of the ease of operation. Jackson et al. [155] have studied the effects of broth harvest time, buffer composition, and growth media composition on the filtration performance of fermentation broth by using 96-well filter plates and a custom-designed plate in an automated vacuum-driven microfiltration platform. Kong et al. [156] have used a modified version of this platform to study DNA filtration behaviour in a HT format (eight parallel experiments) by analyzing the effects of TMP, plasmid size, and membrane type using small DNA volumes. Zhou and colleagues have employed a HT vacuum-driven filtration platform for surface modification and fouling studies of PES membranes [157]. Using this platform along with a photo-induced graft polymerization technique, they were able to assess the fouling propensity of proteins [157] and develop new fouling-resistant flat-sheet

membranes [158,159]. All of the mentioned studies were performed using flat-sheet membranes in dead-end filtration mode without stirring.

Solute accumulation is well-known to have a significant effect on the performance of dead-end filtration processes. As discussed in section 1.3.2, different methods can be used to control the effect of solute accumulation near the membrane. Introduction of mixing near the membrane surface is one of the simplest and most common approaches to limit these effects in conventional dead-end flat-sheet filtration modules [47–52,72,160]. Thus, the stirred well filtration (SWF) module was designed by combining the pressure-driven stirred conditions of a conventional stirred-cell filtration module with a 96-well filter plate [73]. The schematic summary of this design is shown in Fig. 1.8. This design allowed for running up to eight parallel constant flux filtration experiments in flat sheet format with or without stirring by using a magnetic lateral tumble stirrer. Preliminary experiments were performed by measuring the hydraulic permeability of PES UF membranes in HT format, parallel monitoring of TMP profiles during BSA filtration and analyzing the effect of stirring and flux on the filtration performance, permeate quality and fouling behaviour. This module was the first-ever HT filtration platform that used commercial filter plates and incorporated mixing of the feed solution above the membrane surface similar to the conventional stirred-cell filtration.

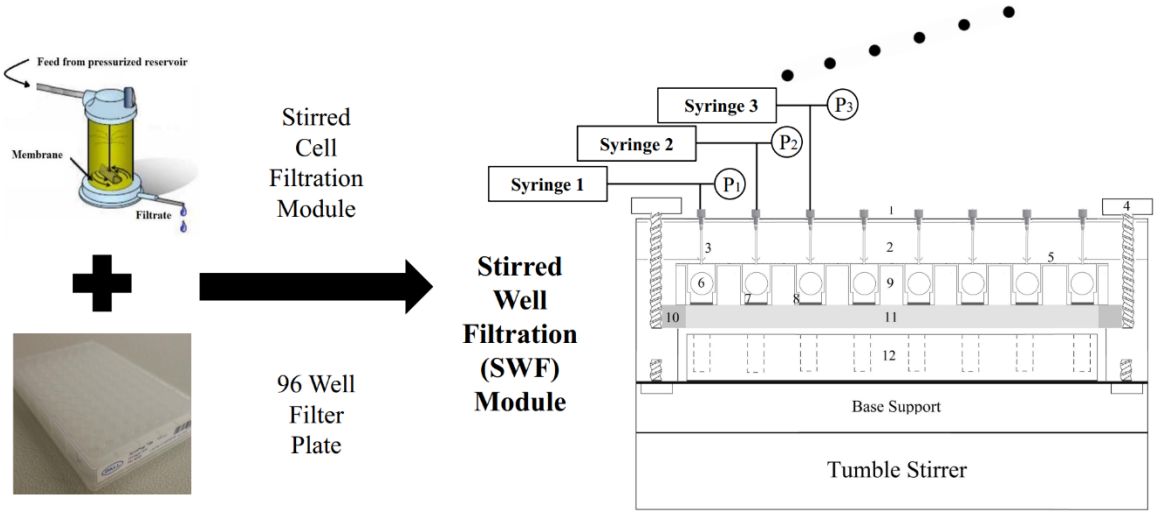

Fig. 1.8. Graphical demonstration of the stirred well filtration technique (Reproduced with permission from [73]).

The concept of HT testing of membrane filtration processes has also been considered by other bioprocessing researchers. Noyes et al. [161] have developed a HT platform for the parallel testing of the depth filtration process, which has a widespread application in biological separations. This platform was employed in order to conduct eight parallel constant flux single- or multi-layer depth filtration experiments using minimal sample. The performance was investigated with HT particle characterization of the permeate and it was shown that the results from the HT system can reasonably predict the results from a lab-scale system. Rayat et al. [162] have introduced a HT technique for cross-flow filtration evaluation using flat-sheet membranes. This method was integrated with a Tecan robotic system and was used for the evaluation of baker's yeast/BSA filtration as a model biological process feed. The reported results showed high levels of

reproducibility and scalability in terms of hydrodynamics and permeate flux measurements.

1.5.2. Environmental Processes

Despite the considerable advantages of HT testing in the field of bioprocessing, only a limited number of studies have focused on development of such technologies for environmental engineering processes. One of the earliest HT studies focused on using granular activated carbon to remove organic pollutants under different conditions was performed by Crittenden et al. [163]. This approach was reported to be effective for adsorption capacity and kinetics assessment with low capital and operational costs. Later similar approaches were used by Ying et al. [164] and Chang et al. [165] respectively for improved ranking of activated carbons for pollutant removal and conducting adsorption breakthrough experiments. Call and Logan [166] have developed a small-scale membrane-free microbial electrolysis cell (MEC) system for running twenty parallel reactors. The design was successfully run using a single power supply with pure and mixed cultures and it was suggested that similar approach can be used for running up to six thousand reactors in parallel. Ren et al. [167] have successfully used this MEC design to conduct treatability studies on refinery wastewater samples with different characteristics. They observed that the most successful strategy for starting up MECs was using domestic wastewater for pre-acclimation and improving electricity production, treatability, and reactor start-up. The results from these two studies showed the practicality of employing MECs as a treatment (or pre-treatment) of refinery wastewaters. Mohler et al. [168] have developed a HT platform in order to evaluate the performance of

different flocculants on the settling behaviour of oil sands tailings using a sophisticated robotic equipment with automated digital image analysis. LaRue et al. [169] designed a new microscale flocculation test (MFT) to identify the flocculation condition in which the optimal separation of water from suspended solid material in different wastewater samples occurs; the MFT approach can be used as a replacement for jar test which is conventionally used in flocculation studies. Cobbledick et al. [170] have developed a HT treatability study for testing of ten coagulants and seven flocculants in parallel for the treatment of reclaimed water from a palladium mine which was shown to be much more efficient than the conventional jar test. Also, a two-stage process using the best three coagulants (stage 1) along with the best three polymer flocculants (stage 2) was successfully screened yielding a good starting point for scale-up.

A few previous studies have focused on the development of HT membrane filtration techniques for environmental separation applications. Vandezande [171] demonstrated the use of stirred filtration in a HT format where the performance of flat-sheet membranes was evaluated by developing a module that featured sixteen individual stirred cells. This module was also used for the HT testing of phase inversion parameters for polyimide-based SRNF membranes [172]. Although HT stirred filtration experiments can be performed with this module, a number of costly equipment pieces need to be dedicated exclusively to this custom-made design which might restrict its applications in laboratory testing. Also, this module can only handle constant TMP filtration which is not always useful for large-scale filtration operations. Bilad et al. [173] developed a HT prototype for membrane bioreactors (HT-MBR) consisting six parallel filtration modules.

The scalability, reproducibility and reliability of the platform was evaluated by studying the critical flux and the filtration index using PS and PVDF membranes. Later Marbelia et al. [174] used the same module to study the effect of phase inversion parameters on the performance of asymmetric PVDF membranes. Optimum performance was observed at increased evaporation time and additive concentration along with decreased polymer concentration which results in higher porosities. Vanysacker et al. [175] have developed a HT cross flow filtration module suited for biofouling study of flat sheet membranes. Six parallel filtrations were performed in each test with in situ and real-time visualization of fouling layer testing the fouling behaviour of PVDF MF membrane. As a proof of concept, it was demonstrated that this method allows for the detailed study of *Pseudomonas aeruginosa* as a model microorganism involved in the biofouling phenomenon. Similar HT approach was employed to investigate the biofouling of RO membranes when running tap-water filtration experiments since retention of nutrients provides a rich environment that can possibly stimulate microbial growth [175]. Zhou et al. [60] have developed a novel HT method for synthesis, screening and optimization of NOM-resistant membranes. PES membranes were modified in microplate format using a UV-induced graft polymerization method [176,177] with a vacuum-driven filtration manifold. A library of sixty six monomers which were categorized into nine groups based on chemical functionality were tested for fouling propensity against Elliot Soil HA.

Recently the application of HT filtration modules have been extended to different formats and applications. In 2010 Khan et al. [178] introduced a HT gas separation module for assessing the permeability and selectivity of up to 16 membranes in parallel at

different feed pressures and temperatures. This concept was later employed for H_2/CO_2 separation using polysulfone acrylate–zeolite mixed matrix membranes [179].

1.6. Motivations, Objectives and Thesis Structure

This work was mainly inspired by the concept of HT testing and the development of microscale processing techniques in the biotechnology industry to speed up process development. There has been a growing interest in the use of efficient parallel processing techniques in the area of membrane filtration performance evaluation including the study of separation performance, fouling phenomena and surface modification. As explained in section 1.5, the usefulness of different HT membrane filtration platforms which utilize flat sheet membranes has been investigated during the past 10-15 years. These techniques have been used in both flat-sheet [60,154–157,159,171] and cross-flow configurations [162,175]. The majority of these works have focused on evaluating the filtration capacity in unstirred dead-end filtration and not the separation performance [60,154–157,159]. Therefore, it is key to develop new HT techniques to address the limitations of the earlier reported HT membrane filtration platforms. As mentioned in section 1.3.2, considering the importance of mixing and its effect on concentration polarization and membrane fouling, SWF was introduced as a HT filtration technique that integrates mixing above the membrane surface akin to the conventional stirred cell filtration device [73]. In that work, the importance of the stirring conditions for HT filtration experiments for single protein solutions was demonstrated. Also, considering the parallel nature of these methods, there

is an exceptional potential for combining statistical methodologies with the new developed HT membrane filtration techniques.

Although flat sheet membranes are widely used in laboratory experiments, especially related to bio-separations, other membrane geometries and module configurations are of great interest for other applications. For example, HF membranes are an ideal format for environmental separations because of the high packing density, self-supporting design, and the inherent ability to backwash the membrane. However, unlike the evaluation of flat sheet membranes using HT techniques, the majority of the previous studies using HF membranes have focused on process evaluation and optimization using a conventional lab- or pilot-scale module in a sequential manner. These modules are designed to represent the large commercial units and each module contains tens to thousands of fibers. The main limitation of this approach is the number of tests that can be conducted in a cost-effective manner because of the sequential fashion and the large volume of sample needed. Alternatively, a few studies have reported use of a single fiber module instead of a full module [12–16]. However, even this approach relies on a sequential style and is limited to the use of a dedicated experimental module for each membrane [97,101,104,105,180]. Hence, there exists a clear need for development of HT techniques for the testing of membranes with different geometries and module configurations such as HF membranes.

The main objective of this work is to address the limitations of the existing HT membrane filtration modules by using new membrane filtration platforms in flat sheet format along with statistical methodologies to evaluate the bioseparation performance,

combining HT filtration with a multi-channel microfluidic flow controller for enhanced hydrodynamic control as well as development of novel HT testing platforms for parallel evaluation and optimization of filtration performance and surface modification of HF membranes. Chapters 2 to 5 report four full projects introducing new HT approaches for the evaluation of flat sheet and HF membranes with applications in biological and environmental separations.

Chapter 2 reports the combination of the SWF technique [73] with design-of-experiment (DOE) methods for the optimization of the separation performance of three binary mixtures containing biomolecules: protein-protein, protein-polysaccharide and protein-DNA. Using this platform eight parallel constant flux UF experiments were conducted to study the influences of solution conditions (pH and ionic strength), stirring and permeate flux. By performing each experiment in quadruplicates over 100 separate filtration tests were performed using a small amount of sample. The main objectives of this chapter were: (1) to demonstrate the usefulness of the SWF technique as a HT platform to evaluate the performance of biomolecule separation in UF and (2) to show the utility of using statistical methodologies along with HT membrane filtration techniques by performing DOE analysis and displaying the sieving coefficient and selectivity results in a new arrangement matching the DOE format which enables a greater understanding of the effects of different process variables.

Chapter 3 introduces a new microscale filtration technique to conduct HT testing of membrane filtration performance by combining a multi-channel microfluidic flow control (MMFC) system with the SWF module. Using this platform, up to eight parallel

constant flux or constant TMP filtration experiments can be performed with stirring and direct real-time measurement of flux and TMP. A set of proof-of- principle experiments were performed to prove the utility of this method in order to investigate the filtration behaviour of single protein solutions and separation performance of binary mixture solutions. The objective of this chapter was mainly to introduce the first-ever stirred HT membrane filtration setup that operates in both constant flux and TMP since the majority of the earlier studies have used either pressure-driven (constant flux) or vacuum driven filtration (constant TMP) modes. This new platform can benefit biotechnology researchers by enabling them to run constant TMP and constant flux experiments, especially when they are planning to scale-up their systems and preliminary microscale tests are needed.

Chapter 4 reports the design and development of the first-ever high-throughput hollow-fiber (HT-HF) membrane platform that can perform multiple filtration tests in parallel with each test using a short length of a single HF membrane to minimize the hold-up volume. The main objective of this chapter was to show the usefulness of such module for running rapid parallel filtration tests of HF membranes in dead-end mode with applications in water and wastewater treatment. Proof-of-concept experiments were performed by investigating the effects of HA type and concentration, solution conditions, permeate flux, and backwashing conditions on the constant flux filtration performance of HF membranes by running over 60 filtration experiments and 190 hydraulic permeability tests.

While the HT-HF platform introduced in chapter 4 is extremely useful for quickly screening operating conditions, it has two main limitations: firstly, because of the setup configuration and the dead-end operation, the filtration test can only be conducted for a short period of time. Secondly, the HT-HF system cannot be operated in a recycle mode, the alternative to the dead-end mode in sequential lab- and pilot-scale setups. The main objectives of the study described in chapter 5 were: (1) to introduce the microscale, parallel-structured, cross-flow filtration (MS-PS-CFF) system that was designed with operational flexibility in mind; the MS-PS-CFF system can be employed for both dead-end filtration experiments as well as filtration experiments with recycle streams; (2) to exhibit the usefulness of the MS-PS-CFF system by running filtration experiments for extended periods of time and elucidation of the effect of buffer composition, solute properties and filtration time on filtration performance; (3) to demonstrate the usefulness of this HT platform for testing and optimization of surface modification strategies for HF membranes.

1.7. References

[1] R.W. Baker, Membrane Technology and Applications, McGraw-Hill, New York, NY, 2000.

[2] A.B. Koltuniewicz, E. Drioli, Membranes in Clean Technologies, John Wiley & Sons, 2008.

[3] L.J. Zeman, A.L. Zydney, Microfiltration and Ultrafiltration: Principles and Applications, CRC Press, 1996.

[4] M.M. Benjamin, D.F. Lawler, Water Quality Engineering: Physical / Chemical Treatment Processes, John Wiley & Sons, 2013.

[5] N.N. Li, A.G. Fane, W.S.W. Ho, T. Matsuura, eds., Advanced membrane technology and applications, John Wiley & Sons, 2011.

[6] T. Hirasaki, T. Sato, T. Tsuboi, H. Nakano, T. Noda, A. Kono, et al., Permeation mechanism of DNA molecules in solution through cuprammonium regenerated cellulose hollow fiber (BMMtm), J. Membr. Sci. 106 (1995) 123–129.

[7] D.R. Latulippe, K. Ager, A.L. Zydney, Flux-dependent transmission of supercoiled plasmid DNA through ultrafiltration membranes, J. Membr. Sci. 294 (2007) 169–177.

[8] H. de Balmann, R. Nobrega, The deformation of dextran molecules. Causes and consequences in ultrafiltration, J. Membr. Sci. 40 (1989) 311–327.

[9] R.J. LaRue, A.S. Kazemi, D.R. Latulippe, Microscale stirred-cell filtration for high-throughput evaluation of separation performance, Biochem. Eng. J. 130 (2018) 34–38.

[10] J. Johnson, M. Busch, Engineering Aspects of Reverse Osmosis Module Design, Desalin. Water Treat. 15 (2010) 236–248.

[11] H. Hyung, J.H. Kim, A mechanistic study on boron rejection by sea water reverse osmosis membranes, J. Membr. Sci. 286 (2006) 269–278.

[12] A. Matin, Z. Khan, S.M.J. Zaidi, M.C. Boyce, Biofouling in reverse osmosis membranes for seawater desalination: Phenomena and prevention, Desalination. 281 (2011) 1–16.

[13] J. Glater, S. kwan Hong, M. Elimelech, The search for a chlorine-resistant reverse osmosis membrane, Desalination. 95 (1994) 325–345.

[14] W.H.O. (WHO), Guidelines for drinking-water quality: fourth edition incorporating the first addendum, 2017. http://apps.who.int/iris/bitstream/handle/10665/254637/9789241549950-eng.pdf;jsessionid=544995D3EACA958B3CA6A2700DF993F1?sequence=1.

[15] DOW, Water & Process Solutions, FILMTEC ™ Reverse Osmosis Membranes: Technical Manual, Dow Chem. Co. (2013) 181. http://www.dow.com/en-us/water-and-process-solutions/products/reverse-osmosis#/accordion/F36C1D89-9385-480A-9242-575D600E6F81.

[16] S. Chellam, Effects of nanofiltration on trihalomethane and haloacetic acid precursors removal and speciation in waters containing low concentrations of bromide ion, Environ. Sci. Technol. 34 (2000) 1813–1820.

[17] J. Cho, G. Amy, J. Pellegrino, Membrane filtration of natural organic matter: Initial comparison of rejection and flux decline characteristics with ultrafiltration and nanofiltration membranes, Water Res. 33 (1999) 2517–2526.

[18] H.H. Yeh, I.C. Tseng, S.J. Kao, W.L. Lai, J.J. Chen, G.T. Wang, et al., Comparison of the finished water quality among an integrated membrane process, conventional and other advanced treatment processes, Desalination. 131 (2000) 237–244.

[19] A.W. Mohammad, Y.H. Teow, W.L. Ang, Y.T. Chung, D.L. Oatley-Radcliffe, N. Hilal, Nanofiltration membranes review: Recent advances and future prospects, Desalination. 356 (2015) 226–254.

[20] K. Hendrix, I.F.J. Vankelecom, Solvent-Resistant Nanofiltration Membranes, in: Encycl. Membr. Sci. Technol., John Wiley & Sons, Inc., Hoboken, NJ, USA, 2013: pp. 1–33.

[21] K.S. Ashaghi, M. Ebrahimi, P. Czermak, Ceramic ultra-and nanofiltration membranes for oilfield produced water treatment: a mini review, Open Environ. J. (2007) 1–8.

[22] G. Pearce, Introduction to membranes: Filtration for water and wastewater treatment, Filtr. Sep. 44 (2007) 24–27.

[23] W. Blatt, A. Darvid, A. Michaels, L. Nelsen, Solute Polarization and Cake Formation in Membrane Ultrafiltration: Causes, Consequences, and Control Techniques, Membr. Sci. Technol. (1970) 47–97.

[24] A.S. Kazemi, Development of stirred well filtration as a high-throughput technique for downstream bioprocessing, M.A.Sc. Thesis, McMaster University, Hamilton, ON, 2014.

[25] A. Saxena, B.P. Tripathi, M. Kumar, V.K. Shahi, Membrane-based techniques for the separation and purification of proteins: An overview, Adv. Colloid Interface Sci. 145 (2009) 1–22.

[26] P. Cote, Z. Alam, J. Penny, Hollow fiber membrane life in membrane bioreactors (MBR), Desalination. 288 (2012) 145–151.

[27] H. Verweij, Inorganic membranes, Curr. Opin. Chem. Eng. 1 (2012) 156–162.

[28] C.E. Carraher Jr, Seymour/Carraher's Polymer Chemistry, Sixth Edit, CRC Press, 2003.

[29] G. Kang, Y. Cao, Application and modification of poly(vinylidene fluoride) (PVDF) membranes – A review, J. Membr. Sci. 463 (2014) 145–165.

[30] G. dong Kang, Y. ming Cao, Application and modification of poly(vinylidene fluoride) (PVDF) membranes - A review, J. Membr. Sci. 463 (2014) 145–165.

[31] F. Liu, N.A. Hashim, Y. Liu, M.R.M. Abed, K. Li, Progress in the production and modification of PVDF membranes, J. Membr. Sci. 375 (2011) 1–27.

[32] S. Adnan, M. Hoang, H. Wang, Z. Xie, Commercial PTFE membranes for

membrane distillation application: Effect of microstructure and support material, Desalination. 284 (2012) 297–308.

[33] H. Tang, Y. Zhang, F. Wang, H. Zhang, Y. Guo, Long-Term Stability of Polytetrafluoroethylene (PTFE) Hollow Fiber Membranes for CO_2 Capture, Energy & Fuels. 30 (2016) 492–503.

[34] B. Van Der Bruggen, Chemical modification of polyethersulfone nanofiltration membranes: A review, J. Appl. Polym. Sci. 114 (2009) 630–642.

[35] C. Zhao, J. Xue, F. Ran, S. Sun, Modification of polyethersulfone membranes – A review of methods, Prog. Mater. Sci. 58 (2013) 76–150.

[36] A.L. Ahmad, A.A. Abdulkarim, B.S. Ooi, S. Ismail, Recent development in additives modifications of polyethersulfone membrane for flux enhancement, Chem. Eng. J. 223 (2013) 246–267.

[37] N. Nady, M.C.R. Franssen, H. Zuilhof, M.S.M. Eldin, R. Boom, K. Schroën, Modification methods for poly(arylsulfone) membranes: A mini-review focusing on surface modification, Desalination. 275 (2011) 1–9.

[38] R. Field, Fundamentals of Fouling, in Membrane Technology: Membranes for Water Treatment, Volume 4, Wiley, Weinheim, Germany, 2010.

[39] W. Sun, J. Nan, J. Xing, J. Tian, Identifying the major fluorescent components responsible for ultrafiltration membrane fouling in different water sources, J. Environ. Sci. (China). 45 (2015) 215–223.

[40] D.M. Kanani, X. Sun, R. Ghosh, Reversible and irreversible membrane fouling during in-line microfiltration of concentrated protein solutions, J. Membr. Sci. 315 (2008) 1–10.

[41] C. Cabassud, S. Laborie, L. Durand-Bourlier, J.M. Lainé, Air sparging in ultrafiltration hollow fibers: Relationship between flux enhancement, cake characteristics and hydrodynamic parameters, J. Membr. Sci. 181 (2001) 57–69.

[42] R. Ghosh, Q. Li, Z. Cui, Fractionation of BSA and lysozyme using ultrafiltration: Effect of gas sparging, AIChE J. 44 (1998) 61–67.

[43] Q. Li, R. Ghosh, S. Bellara, Z. Cui, D. Pepper, Enhancement of ultrafiltration by gas sparging with flat sheet membrane modules, Sep. Purif. Technol. 14 (1998) 79–83.

[44] Z. Cui, T. Taha, Enhancement of ultrafiltration using gas sparging: A comparison of different membrane modules, J. Chem. Technol. Biotechnol. 78 (2003) 249–253.

[45] R. Ghosh, Z.F. Cui, Mass transfer in gas-sparged ultrafiltration: Upward slug flow in tubular membranes, J. Membr. Sci. 162 (1999) 91–102.

[46] Z.F. Cui, K.I.T. Wright, Flux enhancements with gas sparging in downwards crossflow ultrafiltration: Performance and mechanism, J. Membr. Sci. 117 (1996) 109–116.

[47] C.K. Colton, S. Friedman, D.E. Wilson, R.S. Lfes, Ultrafiltration of Lipoproteins through a Synthetic Membrane, J. Clin. Invest. 51 (1972) 2472–2481.

[48] A.G. Fane, Ultrafiltration of suspensions, J. Membr. Sci. 20 (1984) 249–259.

[49] M. Chudacek, A.G. Fane, The dynamics of polarisation in unstirred and stirred ultrafiltration, J. Membr. Sci. 21 (1984) 145–160.

[50] K. Katsoufidou, S.G. Yiantsios, A.J. Karabelas, Experimental study of ultrafiltration membrane fouling by sodium alginate and flux recovery by backwashing, J. Membr. Sci. 300 (2007) 137–146.

[51] Chhaya, C. Sharma, S. Mondal, G.C. Majumdar, S. De, Clarification of Stevia extract by ultrafiltration: Selection criteria of the membrane and effects of operating conditions, Food Bioprod. Process. 90 (2012) 525–532.

[52] Y. Li, D. Currie, A.L. Zydney, Enhanced purification of plasmid DNA isoforms by exploiting ionic strength effects during ultrafiltration, Biotechnol. Bioeng. 113 (2016) 783–789.

[53] R. Amar, B.B. Gupta, M.Y. Jaffrin, Apple Juice Clarification using Mineral Membranes: Fouling Control by Backwashing and Pulsating Flow, J. Food Sci. 55 (1990) 1620–1625.

[54] B.B. Gupta, P. Blanpain, M.Y. Jaffrin, Permeate flux enhancement by pressure and flow pulsations in microfiltation with mineral membranes, J. Membr. Sci. 70 (1992) 257–266.

[55] B.J. Bellhouse, G. Costigan, K. Abhinava, a. Merry, The performance of helical screw-thread inserts in tubular membranes, Sep. Purif. Technol. 22–23 (2001) 89–113.

[56] S.X. Liu, J.-T. Kim, S. Kim, M. Singh, The effect of polymer surface modification via interfacial polymerization on polymer-protein interaction, J. Appl. Polym. Sci. 112 (2009) 1704–1715.

[57] D. Rana, T. Matsuura, Surface modifications for antifouling membranes., Chem. Rev. 110 (2010) 2448–71.

[58] D.B. Mosqueda-Jimenez, R.M. Narbaitz, T. Matsuura, Effects of preparation conditions on the surface modification and performance of polyethersulfone ultrafiltration membranes, J. Appl. Polym. Sci. 99 (2006) 2978–2988.

[59] D. Rana, T. Matsuura, Surface modifications for antifouling membranes., Chem. Rev. 110 (2010) 2448–71.

[60] M. Zhou, H. Liu, J.E. Kilduff, R. Langer, D.G. Anderson, G. Belfort, High-throughput membrane surface modification to control NOM fouling., Environ. Sci. Technol. 43 (2009) 3865–71.

[61] N. Nady, Enzyme-Catalyzed Modification of Poly(ethersulfone) Membranes, Ph.D. Dissertation, Wageningen University, Wageningen, GE, Netherlands, 2012.

[62] G. Trägårdh, Membrane cleaning, Desalination. 71 (1989) 325–335.

[63] S. Ebrahim, Cleaning and regeneration of membranes in desalination and wastewater applications: State-of-the-art, Desalination. 96 (1994) 225–238.

[64] A. Lim, Membrane fouling and cleaning in microfiltration of activated sludge wastewater, J. Membr. Sci. 216 (2003) 279–290.

[65] N. Porcelli, S. Judd, Chemical cleaning of potable water membranes: A review, Sep. Purif. Technol. 71 (2010) 137–143.

[66] S. Siavash Madaeni, T. Mohamamdi, M. Kazemi Moghadam, Chemical cleaning of reverse osmosis membranes, Desalination. 134 (2001) 77–82.

[67] J. Jurado, B.J. Bellhouse, Application of electric fields and vortex mixing for enhanced ultrafiltration, Filtr. Sep. 31 (1994) 273–268.

[68] H.M. Huotari, G. Trägårdh, I.H. Huisman, Crossflow Membrane Filtration Enhanced by an External DC Electric Field: A Review, Chem. Eng. Res. Des. 77 (1999) 461–468.

[69] O.A. Akoum, M.Y. Jaffrin, L. Ding, P. Paullier, C. Vanhoutte, An hydrodynamic investigation of microfiltration and ultrafiltration in a vibrating membrane module, J. Membr. Sci. 197 (2002) 37–52.

[70] J. Postlethwaite, S.R. Lamping, G.C. Leach, M.F. Hurwitz, G.J. Lye, Flux and transmission characteristics of a vibrating microfiltration system operated at high biomass loading, J. Membr. Sci. 228 (2004) 89–101.

[71] G. Genkin, T.D. Waite, A.G. Fane, S. Chang, The effect of vibration and coagulant addition on the filtration performance of submerged hollow fibre membranes, J. Membr. Sci. 281 (2006) 726–734.

[72] S.T. Johnston, K. a. Smith, W.M. Deen, Concentration polarization in stirred ultrafiltration cells, AIChE J. 47 (2001) 1115–1125.

[73] A.S. Kazemi, D.R. Latulippe, Stirred well filtration (SWF) – A high-throughput technique for downstream bio-processing, J. Membr. Sci. 470 (2014) 30–39.

[74] K. Smith, C. Colton, E. Merrill, L. Evans, Convective transport in a batch dialyzer: determination of true membrane permeability from a single measurement, Chem. Eng. Prog. Symp. Ser. 64 (1968) 45–58.

[75] W.S. Opong, A.L. Zydney, Diffusive and convective protein transport through asymmetric membranes, AIChE J. 37 (1991) 1497–1510.

[76] R. Ghosh, Protein Bioseparation Using Ultrafiltration: Theory, Applications and New Developments, Imperial College Press, 2003.

[77] A.S. Bhadouria, M. Sorci, M. Gu, G. Belfort, J. Hahn, Optimization of Membrane Separation Processes for Protein Fractionation, Ind. Eng. Chem. Res. 53 (2014) 5103–5109.

[78] R. Ghosh, Study of membrane fouling by BSA using pulsed injection technique, J. Membr. Sci. 195 (2002) 115–123.

[79] R. Ghosh, Z.. Cui, Protein purification by ultrafiltration with pre-treated membrane, J. Membr. Sci. 167 (2000) 47–53.

[80] A.G. Fane, C.J.D. Fell, A. Suki, The effect of ph and ionic environment on the ultrafiltration of protein solutions with retentive membranes, J. Membr. Sci. 16 (1983) 195–210.

[81] R. Ghosh, Z.. Cui, Fractionation of BSA and lysozyme using ultrafiltration: effect of pH and membrane pretreatment, J. Membr. Sci. 139 (1998) 17–28.

[82] Y. Wan, R. Ghosh, Z. Cui, High-resolution plasma protein fractionation using ultrafiltration, Desalination. 144 (2002) 301–306.

[83] S. Saksena, A.L. Zydney, Effect of solution pH and ionic strength on the separation of albumin from immunoglobulins (IgG) by selective filtration., Biotechnol. Bioeng. 43 (1994) 960–8.

[84] B. Cheang, A.L. Zydney, Separation of α-lactalbumin and β-lactoglobulin using membrane ultrafiltration, Biotechnol. Bioeng. 83 (2003) 201–209.

[85] R.H.C.M. van Eijndhoven, S. Saksena, A.L. Zydney, Protein fractionation using electrostatic interactions in membranel filtration, Biotechnol. Bioeng. 48 (1995) 406–414.

[86] Y. Baek, N. Singh, A. Arunkumar, A. Zydney, Ultrafiltration behavior of an Fc-fusion protein: Filtrate flux data and modeling, J. Membr. Sci. 528 (2017) 171–177.

[87] Y. Baek, N. Singh, A. Arunkumar, M. Borys, Z.J. Li, A.L. Zydney, Ultrafiltration behavior of monoclonal antibodies and Fc-fusion proteins: Effects of physical properties, Biotechnol. Bioeng. 114 (2017) 2057–2065.

[88] W.R. Bowen, F. Jenner, Theoretical descriptions of membrane filtration of colloids and fine particles: An assessment and review, Adv. Colloid Interface Sci. 56 (1995) 141–200.

[89] Z. Cui, Protein separation using ultrafiltration — an example of multi-scale

complex systems, China Particuology. 3 (2005) 343–348.

[90] A. Saxena, B.P. Tripathi, M. Kumar, V.K. Shahi, Membrane-based techniques for the separation and purification of proteins: An overview, Adv. Colloid Interface Sci. 145 (2009) 1–22.

[91] I. Manzano, A.L. Zydney, Quantitative study of RNA transmission through ultrafiltration membranes, J. Membr. Sci. 544 (2017) 272–277.

[92] M. Hadidi, J.J. Buckley, A.L. Zydney, Ultrafiltration behavior of bacterial polysaccharides used in vaccines, J. Membr. Sci. 490 (2015) 294–300.

[93] E. Arkhangelsky, V. Gitis, Effect of transmembrane pressure on rejection of viruses by ultrafiltration membranes, Sep. Purif. Technol. 62 (2008) 619–628.

[94] E. Arkhangelsky, B. Steubing, E. Ben-Dov, A. Kushmaro, V. Gitis, Influence of pH and ionic strength on transmission of plasmid DNA through ultrafiltration membranes, Desalination. 227 (2008) 111–119.

[95] Y. Li, K. Zhu, A.L. Zydney, Effect of ionic strength on membrane fouling during ultrafiltration of plasmid DNA, Sep. Purif. Technol. 176 (2017) 287–293.

[96] S. Hong, M. Elimelech, Chemical and physical aspects of natural organic matter (NOM) fouling of nanofiltration membranes, J. Membr. Sci. 132 (1997) 159–181.

[97] C.F. Lin, Y.J. Huang, O.J. Hao, Ultrafiltration processes for removing humic substances: Effect of molecular weight fractions and PAC treatment, Water Res. 33 (1999) 1252–1264.

[98] R.C. Kuhn, K.H. Oshima, Evaluation and optimization of a reusable hollow fiber ultrafilter as a first step in concentrating Cryptosporidium parvum oocysts from water, Water Res. 35 (2001) 2779–2783.

[99] H.A. Morales-Morales, G. Vidal, J. Olszewski, C.M. Rock, D. Dasgupta, K.H. Oshima, et al., Optimization of a reusable hollow-fiber ultrafilter for simultaneous concentration of enteric bacteria, protozoa, and viruses from water, Appl. Environ. Microbiol. 69 (2003) 4098–4102.

[100] J. Decarolis, S. Hong, J. Taylor, Fouling behavior of a pilot scale inside-out hollow fiber UF membrane during dead-end filtration of tertiary wastewater, J. Membr. Sci. 191 (2001) 165–178.

[101] X.E. Lei, Impact of hydrodynamic conditions and membrane configuration on the permeate flux in submerged membrane systems for drinking water treatment, Ph.D. Dissertation, The University of British Columbia, Vancouver, BC, 2005.

[102] J. Hermia, Constant Pressure Blocking Filtration Laws-Application to Power-law Non- Newtonian Fluid, Chem. Eng. Res. Des. 60 (1982) 183–187.

[103] R.W. Field, D. Wu, J. a. Howell, B.B. Gupta, Critical flux concept for

microfiltration fouling, J. Membr. Sci. 100 (1995) 259–272.

[104] K. Katsoufidou, S.G. Yiantsios, A.J. Karabelas, A study of ultrafiltration membrane fouling by humic acids and flux recovery by backwashing: Experiments and modeling, J. Membr. Sci. 266 (2005) 40–50.

[105] K.S. Katsoufidou, D.C. Sioutopoulos, S.G. Yiantsios, A.J. Karabelas, UF membrane fouling by mixtures of humic acids and sodium alginate: Fouling mechanisms and reversibility, Desalination. 264 (2010) 220–227.

[106] H. Huang, N. Lee, T. Young, A. Gary, J.C. Lozier, J.G. Jacangelo, Natural organic matter fouling of low-pressure, hollow-fiber membranes: Effects of NOM source and hydrodynamic conditions, Water Res. 41 (2007) 3823–3832.

[107] H.C. Kim, B.A. Dempsey, Membrane fouling due to alginate, SMP, EfOM, humic acid, and NOM, J. Membr. Sci. 428 (2013) 190–197.

[108] H. Yamamura, K. Okimoto, K. Kimura, Y. Watanabe, Hydrophilic fraction of natural organic matter causing irreversible fouling of microfiltration and ultrafiltration membranes, Water Res. 54 (2014) 123–136.

[109] F. Qu, H. Liang, J. Zhou, J. Nan, S. Shao, J. Zhang, et al., Ultrafiltration membrane fouling caused by extracellular organic matter (EOM) from Microcystis aeruginosa: Effects of membrane pore size and surface hydrophobicity, J. Membr. Sci. 449 (2014) 58–66.

[110] R. van Reis, A. Zydney, Membrane separations in biotechnology, Curr. Opin. Biotechnol. 12 (2001) 208–211.

[111] C. Charcosset, Membrane processes in biotechnology: An overview, Biotechnol. Adv. 24 (2006) 482–492.

[112] S.M. Cramer, M.A. Holstein, Downstream bioprocessing: recent advances and future promise, Curr. Opin. Chem. Eng. 1 (2011) 27–37.

[113] S.R. Wickramasinghe, E.D. Stump, D.L. Grzenia, S.M. Husson, J. Pellegrino, Understanding virus filtration membrane performance, J. Membr. Sci. 365 (2010) 160–169.

[114] D. Kenneth, J.R. Kostenbader, C. D.O., Membrane filter evaluations using poliovirus, J. Virol. Methods. 7 (1983) 253–257.

[115] S. Shoaebargh, I. Gough, M. Fe Medina, A. Smith, J. van der Heijden, B.D. Lichty, et al., Sterile filtration of oncolytic viruses: An analysis of effects of membrane morphology on fouling and product recovery, J. Membr. Sci. 548 (2018) 239–246.

[116] M. Nemati, C. Webb, Immobilized Cell Bioreactors, Compr. Biotechnol. 2 (2011) 331–346.

[117] J.J. Zhong, Bioreactor Engineering, Compr. Biotechnol. 2 (2011) 1739–1748.

[118] N. Wung, S.M. Acott, D. Tosh, M.J. Ellis, Hollow fibre membrane bioreactors for tissue engineering applications, Biotechnol. Lett. (2014) 2357–2366.

[119] S.-T. Yang, J. Luo, C. Chen, A fibrous-bed bioreactor for continuous production of monoclonal antibody by hybridoma., Adv. Biochem. Eng. Biotechnol. 87 (2004) 61–96.

[120] Z.Y. Oo, R. Deng, M. Hu, M. Ni, K. Kandasamy, M.S. bin Ibrahim, et al., The performance of primary human renal cells in hollow fiber bioreactors for bioartificial kidneys, Biomaterials. 32 (2011) 8806–8815.

[121] J. Jansons, M.R. Bucens, Virus detection in water by ultrafiltration, Water Res. 20 (1986) 1603–1606.

[122] H. Shi, E. V. Pasco, V. V. Tarabara, Membrane-based methods of virus concentration from water: a review of process parameters and their effects on virus recovery, Environ. Sci. Water Res. Technol. 3 (2017) 778–792.

[123] J.G. Yu, X.H. Zhao, H. Yang, X.H. Chen, Q. Yang, L.Y. Yu, et al., Aqueous adsorption and removal of organic contaminants by carbon nanotubes, Sci. Total Environ. 482–483 (2014) 241–251.

[124] R. Das, S.B. Abd Hamid, M.E. Ali, A.F. Ismail, M.S.M. Annuar, S. Ramakrishna, Multifunctional carbon nanotubes in water treatment: The present, past and future, Desalination. 354 (2014) 160–179.

[125] X. Liu, M. Wang, S. Zhang, B. Pan, Application potential of carbon nanotubes in water treatment: A review, J. Environ. Sci. (China). 25 (2013) 1263–1280.

[126] C.F. de Lannoy, D. Jassby, D.D. Davis, M.R. Wiesner, A highly electrically conductive polymer-multiwalled carbon nanotube nanocomposite membrane, J. Membr. Sci. 415–416 (2012) 718–724.

[127] C.F. de Lannoy, D. Jassby, K. Gloe, A.D. Gordon, M.R. Wiesner, Aquatic biofouling prevention by electrically charged nanocomposite polymer thin film membranes, Environ. Sci. Technol. 47 (2013) 2760–2768.

[128] C.D. Vecitis, M.H. Schnoor, M.S. Rahaman, J.D. Schiffman, M. Elimelech, Electrochemical multiwalled carbon nanotube filter for viral and bacterial removal and inactivation, Environ. Sci. Technol. 45 (2011) 3672–3679.

[129] G. Gao, C.D. Vecitis, Electrochemical carbon nanotube filter oxidative performance as a function of surface chemistry, Environ. Sci. Technol. 45 (2011) 9726–9734.

[130] P. Gunawan, C. Guan, X. Song, Q. Zhang, S.S.J. Leong, C. Tang, et al., Hollow fiber membrane decorated with Ag/MWNTs: Toward effective water disinfection and biofouling control, ACS Nano. 5 (2011) 10033–10040.

[131] H.Y. Yang, Z.J. Han, S.F. Yu, K.L. Pey, K. Ostrikov, R. Karnik, Carbon nanotube membranes with ultrahigh specific adsorption capacity for water desalination and purification, Nat. Commun. 4 (2013).

[132] S. Chhatre, N.J. Titchener-hooker, Micro-Biochemical Engineering: Using Small-Scale Devices to Predict Industry-Scale Downstream Performance, Compr. Biotechnol. 2 (2011) 891–903.

[133] M. Micheletti, G.J. Lye, Microscale bioprocess optimisation., Curr. Opin. Biotechnol. 17 (2006) 611–8.

[134] A. Zanzotto, N. Szita, P. Boccazzi, P. Lessard, A.J. Sinskey, K.F. Jensen, Membrane-aerated microbioreactor for high-throughput bioprocessing., Biotechnol. Bioeng. 87 (2004) 243–54.

[135] Z. Zhang, P. Boccazzi, H.-G. Choi, G. Perozziello, A.J. Sinskey, K.F. Jensen, Microchemostat-microbial continuous culture in a polymer-based, instrumented microbioreactor., Lab Chip. 6 (2006) 906–13.

[136] N. Szita, P. Boccazzi, Z. Zhang, P. Boyle, A.J. Sinskey, K.F. Jensen, Development of a multiplexed microbioreactor system for high-throughput bioprocessing., Lab Chip. 5 (2005) 819–26.

[137] A.S. Tait, J.P. Aucamp, A. Bugeon, M. Hoare, Ultra scale-down prediction using microwell technology of the industrial scale clarification characteristics by centrifugation of mammalian cell broths., Biotechnol. Bioeng. 104 (2009) 321–31.

[138] T.A. Barrett, A. Wu, H. Zhang, M.S. Levy, G.J. Lye, Microwell engineering characterization for mammalian cell culture process development., Biotechnol. Bioeng. 105 (2010) 260–75.

[139] A. Khademhosseini, R. Langer, J. Borenstein, J.P. Vacanti, Microscale technologies for tissue engineering and biology., Proc. Natl. Acad. Sci. U. S. A. 103 (2006) 2480–7.

[140] P. Fernandes, J.M.S. Cabral, Microlitre/millilitre shaken bioreactors in fermentative and biotransformation processes - A review, Biocatal. Biotransformation. 24 (2006) 237–252.

[141] W.-T. Hsu, R.P.S. Aulakh, D.L. Traul, I.H. Yuk, Advanced microscale bioreactor system: a representative scale-down model for bench-top bioreactors., Cytotechnology. 64 (2012) 667–78.

[142] J.I. Betts, F. Baganz, Miniature bioreactors: Current practices and future opportunities, Microb. Cell Fact. 5 (2006) 1–14.

[143] D. Schäpper, M.N.H.Z. Alam, N. Szita, A. Eliasson Lantz, K. V. Gernaey, Application of microbioreactors in fermentation process development: A review, Anal. Bioanal. Chem. 395 (2009) 679–695.

[144] G.J. Lye, P. Ayazi-Shamlou, F. Baganz, P.A. Dalby, J.M. Woodley, Accelerated design of bioconversion processes using automated microscale processing techniques, Trends Biotechnol. 21 (2003) 29–37.

[145] G. Lye, J. Hubbuch, T. Schroeder, E. Willimann, Shrinking the Costs of Bioprocess Development - Case Study - BioProcess International, Bioprocess Int. (2009) 18–22.

[146] C.J. Welch, M. Shaimi, M. Biba, J.R. Chilenski, R.H. Szumigala Jr, U. Dolling, et al., Microplate evaluation of process adsorbents Short Communication, J. Sep. Sci. (2002) 847–850.

[147] C.J. Welch, J. Albaneze-Walker, W.R. Leonard, M. Biba, J. DaSilva, D. Henderson, et al., Adsorbent Screening for Metal Impurity Removal in Pharmaceutical Process Research, Org. Process Res. Dev. 9 (2005) 198–205.

[148] M. Bensch, B. Selbach, J. Hubbuch, High throughput screening techniques in downstream processing: Preparation, characterization and optimization of aqueous two-phase systems, Chem. Eng. Sci. 62 (2007) 2011–2021.

[149] S.A. Oelmeier, F. Dismer, J. Hubbuch, Application of an aqueous two-phase systems high-throughput screening method to evaluate mAb HCP separation., Biotechnol. Bioeng. 108 (2011) 69–81.

[150] M. Wiendahl, S.A. Oelmeier, F. Dismer, J. Hubbuch, High-throughput screening-based selection and scale-up of aqueous two-phase systems for pDNA purification., J. Sep. Sci. 35 (2012) 3197–207.

[151] L. Britsch, T. Schroeder, J. Friedle, Automated, high-throughput chromatographic separation of biological compounds, Am Biotechnol Lab. 26:20–23 (2008).

[152] M.D. Wenger, P. Dephillips, C.E. Price, D.G. Bracewell, An automated microscale chromatographic purification of virus-like particles as a strategy for process development., Biotechnol. Appl. Biochem. 47 (2007) 131–9.

[153] J.L. Coffman, J.F. Kramarczyk, B.D. Kelley, High-throughput screening of chromatographic separations: I. Method development and column modeling., Biotechnol. Bioeng. 100 (2008) 605–18.

[154] M. Chandler, A.L. Zydney, High throughput screening for membrane process development, J. Membr. Sci. 237 (2004) 181–188.

[155] N. Jackson, J. Liddell, G. Lye, An automated microscale technique for the quantitative and parallel analysis of microfiltration operations, J. Membr. Sci. 276 (2006) 31–41.

[156] S. Kong, J. Aucamp, N.J. Titchener-Hooker, Studies on membrane sterile filtration of plasmid DNA using an automated multiwell technique, J. Membr. Sci. 353 (2010) 144–150.

[157] M. Zhou, H. Liu, J.E. Kilduff, R. Langer, D.G. Anderson, G. Belfort, High Throughput Synthesis and Screening of New Protein Resistant Surfaces for Membrane Filtration, AIChE J. 56 (2010) 1932–1945.

[158] P.S. Yune, J.E. Kilduff, G. Belfort, Fouling-resistant properties of a surface-modified poly(ether sulfone) ultrafiltration membrane grafted with poly(ethylene glycol)-amide binary monomers, J. Membr. Sci. 377 (2011) 159–166.

[159] M. Zhou, H. Liu, A. Venkiteshwaran, J. Kilduff, D.G. Anderson, R. Langer, et al., High throughput discovery of new fouling-resistant surfaces, J. Mater. Chem. (2011) 693–704.

[160] L. Earnest-Silveira, D. Christiansen, S. Herrmann, S.A. Ralph, S. Das, E.J. Gowans, et al., Large scale production of a mammalian cell derived quadrivalent hepatitis C virus like particle vaccine, J. Virol. Methods. 236 (2016) 87–92.

[161] A. Noyes, J. Basha, J. Frostad, S. Cook, D. Millard, J. Mullin, et al., A modular approach for the ultra-scale-down of depth filtration, J. Membr. Sci. 496 (2015) 199–210.

[162] A.C.M.E. Rayat, G.J. Lye, M. Micheletti, A novel microscale crossflow device for the rapid evaluation of microfiltration processes, J. Membr. Sci. 452 (2014) 284–293.

[163] J.C. Crittenden, P.S. Reddy, H. Arora, J. Trynoski, W. Hand, D.L. Perram, et al., Rapid Small-Scale Column Tests, Am. Water Work. Assoc. 83 (1991) 77–87.

[164] W.C. Ying, W. Zhang, Q.G. Chang, W.X. Jiang, G.H. Li, Improved methods for carbon adsorption studies for water and wastewater treatment, Environ. Prog. 25 (2006) 110–120.

[165] Q.-G. Chang, W. Zhang, W.-X. Jiang, B.-J. Li, W.-C. Ying, W. Lin, Degradation of Alizarin Yellow R using UV / H 2 O 2 Advanced Oxidation Process, Environ. Sci. Technol. 33 (2014) 482–489.

[166] D.F. Call, B.E. Logan, A method for high throughput bioelectrochemical research based on small scale microbial electrolysis cells, Biosens. Bioelectron. 26 (2011) 4526–4531.

[167] L. Ren, M. Siegert, I. Ivanov, J.M. Pisciotta, B.E. Logan, Treatability studies on different refinery wastewater samples using high-throughput microbial electrolysis cells (MECs), Bioresour. Technol. 136 (2013) 322–328.

[168] C. Mohler, M. Poindexter, M.J. Atias, W. Chen, C. Witham, Development of flocculants for oil sands techniques using high-throughput techniques, in: Proc. Third Int. Oil Sands Tailings Conf., Edmonton, 2012: pp. 113–120.

[169] R.J. LaRue, J. Cobbledick, N. Aubry, E.D. Cranston, D.R. Latulippe, The microscale flocculation test (MFT)-A high-throughput technique for optimizing

separation performance, Chem. Eng. Res. Des. 105 (2016) 85–93.

[170] J. Cobbledick, A. Kasza, C. Biederman, D. Moore, D.R. Latulippe, Demonstration of a high-throughput treatability study (HTTS) for reclaim water from palladium mine tailings, in: Proc. Tailings Mine Waste ’16 Conf., 2016.

[171] P. Vandezande, L. Gevers, J. Paul, I. Vankelecom, P. Jacobs, High throughput screening for rapid development of membranes and membrane processes, J. Membr. Sci. 250 (2005) 305–310.

[172] P. Vandezande, X. Li, L.E.M. Gevers, I.F.J. Vankelecom, High throughput study of phase inversion parameters for polyimide-based SRNF membranes, J. Membr. Sci. 330 (2009) 307–318.

[173] M.R. Bilad, P. Declerck, A. Piasecka, L. Vanysacker, X. Yan, I.F.J. Vankelecom, Development and validation of a high-throughput membrane bioreactor (HT-MBR), J. Membr. Sci. 379 (2011) 146–153.

[174] L. Marbelia, M.R. Bilad, A. Piassecka, P.S. Jishna, P. V. Naik, I.F.J. Vankelecom, Study of PVDF asymmetric membranes in a high-throughput membrane bioreactor (HT-MBR): Influence of phase inversion parameters and filtration performance, Sep. Purif. Technol. 162 (2016) 6–13.

[175] L. Vanysacker, P. Declerck, I. Vankelecom, Development of a high throughput cross-flow filtration system for detailed investigation of fouling processes, J. Membr. Sci. 442 (2013) 168–176.

[176] H. Yamagishi, J. V. Crivello, G. Belfort, Development of a novel photochemical technique for modifying poly (arylsulfone) ultrafiltration membranes, J. Membr. Sci. 105 (1995) 237–247.

[177] M. Taniguchi, J. Pieracci, W.A. Samsonoff, G. Belfort, UV-Assisted Graft Polymerization of Synthetic Membranes : Mechanistic Studies, Chem. Mater. (2003) 3805–3812.

[178] A.L. Khan, S. Basu, A. Cano-Odena, I.F.J. Vankelecom, Novel high throughput equipment for membrane-based gas separations, J. Membr. Sci. 354 (2010) 32–39.

[179] A.L. Khan, A. Cano-Odena, B. Gutierrez, C. Minguillon, I.F.J. Vankelecom, Hydrogen separation and purification using polysulfone acrylate-zeolite mixed matrix membranes, J. Membr. Sci. 350 (2010) 340–346.

[180] K. Katsoufidou, S.G. Yiantsios, a. J. Karabelas, Experimental study of ultrafiltration membrane fouling by sodium alginate and flux recovery by backwashing, J. Membr. Sci. 300 (2007) 137–146.

Chapter 2 - Optimization of Biomolecule Separation by Combining Microscale Filtration and Design-of-Experiment Methods

Authors: Amir S. Kazemi, Karina Kawka, David R. Latulippe

Published in Biotechnology and Bioengineering, 2016, Vol. 113, No. 10, 2131-2139.

2.1. Preface

This chapter presents the application of HT membrane filtration techniques for the optimization of biomolecule separation. As described in chapter 1, conventional membrane filtration techniques (e.g. stirred cell filtration) are widely used for lab-scale biological separations. However, when considering the numerous different factors that affect the performance of membrane filtration including the hydrodynamic and physicochemical conditions, application of the conventional filtration modules in a sequential manner is not an effective optimization approach. Therefore, it is important to employ HT techniques where multiple parallel experiments can be performed simultaneously using a small amount of sample to screen the effect of different factors. Herein, we have employed the SWF module, as a stirred HT membrane filtration platform in which up to eight parallel microscale filtration experiments can be performed simultaneously, and have studied the optimization of different model biomolecule separations including protein-protein, protein-DNA and protein-polysaccharide separations. Using this approach, a set of factorial designs were conducted for each separation in which the permeate flux and solution conditions (pH or ionic strength) were

selected as process variables. The rationale behind the selection of permeate fluxes and solution conditions for each separation performed in this study was to observe a substantial difference in the outcome variables (sieving coefficients, selectivity and transmembrane pressure profile) based on previous studies. Four individual sieving experiments in constant flux mode were conducted for each permeate flux-solution condition combination. The results were presented using a unique format that showcases the statistical analyses and matches the factorial design of the used DOE method. Overall, more than 100 individual filtration experiments were performed studying the effects of different operating conditions on biomolecule separation performance using UF. The results presented in this chapter evidently show: (1) the importance of studying the effect of different physicochemical and hydrodynamic conditions on the performance of biomolecule separation using UF, (2) the usefulness of a HT approach to screen the effect of different operating factors and (3) the effectiveness of using statistical methodologies along with HT membrane filtration techniques by performing DOE analysis and displaying the sieving coefficient and selectivity results.

2.2. Introduction

It is well known in the field of separation sciences that the performance of a membrane filtration process is determined by a multitude of factors including the membrane properties (e.g., material of construction, pore size/shape, surface charge density, specific surface functional groups), the solute(s) physico-chemical properties (e.g., size, shape, charge, flexibility), the solution conditions (e.g., pH, ionic strength,

presence of specific ions), the hydrodynamic conditions (e.g., cross flow versus dead-end mode, stirring speed), and the experimental operating conditions (e.g., permeate flux). There are numerous interaction effects between these factors; for example, the zeta potential of polyethersulfone membranes has been shown to be strongly affected by the adsorption of specific ions in solution [1]. A major challenge in any membrane process is determining the optimum combination of conditions that give the best separation performance. Depending on the specific application, the exact performance goal could be an increase in membrane selectivity, an increase in membrane throughput, a decrease in fouling propensity, or perhaps some combination of these goals.

Ultrafiltration (UF) membranes have pore sizes in the range of 2–20 nm and are widely used in separation processes to concentrate or purify a variety of bio-molecules such as recombinant proteins, plasmid DNA, industrial enzymes, and various types of polysaccharides. The conventional approach towards UF process development is to run an extensive number of lab-scale tests in sequential fashion to determine the effect of the different factors on process performance. Although they are available in a number of different membrane geometries, for lab-scale UF tests the flat sheet membrane is the most common; it can be tested in either a stirred-cell device with the flow oriented normal to the membrane surface or in a tangential flow filter (or cross-flow cell) with the flow oriented tangential to the membrane surface. Typically for bio-molecule separation applications there are very strong interactions between factors [2] and thus the extensive amount of testing that is required becomes a laborious and time-consuming task.

For a binary mixture of solutes, the separation performance of a membrane is quantified by the selectivity, the ratio of the percent transmission of one solute to the percent transmission of the other solute. The sieving behavior of a single component solution can be significantly different than a mixture due to solute interaction effects [3] and thus the recommended strategy is to conduct filtration tests with feed solutions that contain both solutes of interest. The current literature on UF-based biomolecule separation processes includes an extensive number of studies covering a wide variety of mixtures. Perhaps the most widely studied field is protein–protein separations; a number of reviews of this topic that outline the effects of different process factors have been published [4–6]. The effect of permeate flux on protein separation is well described via concentration polarization effects [7,8]. Also, the effect of solution conditions on selectivity has been well studied [9]. A common misconception is that UF is a simple "size-based" separation process with smaller solutes always being transmitted through the membrane while larger solutes are retained in the feed. Numerous studies have proven that the separation process is much more complex and elegant. For example, using charged UF membranes and careful adjustment of the solution conditions (e.g., pH, ionic strength) in order to exploit the electrostatic interaction effects, it is possible to achieve "reverse selectivity" conditions where the larger protein is transmitted through the membrane while the smaller protein is retained in the feed [7,10–12]. As well, a number of recent studies have studied the transmission of large flexible macromolecules through UF membranes with smaller pores. Hadidi et al. [13] reported that large polysaccharide molecules can be transmitted through UF membranes despite the fact that the molecular

weight of the polysaccharide was two times higher than the nominal molecular weight cut off (MWCO) of the membrane. Similar behavior has been reported in studies that investigated the filtration behavior of large DNA molecules [14–16]. Whereas the extent of polysaccharide transmission was explained according to concentration polarization effects, the DNA transmission was found to be due elongation/deformation effects at the entrance of the membrane pore.

The collective knowledge in the field of bio-molecule separations is the result of many studies conducted by various research groups. The development of filtration processes for the bio-molecule separation applications is a challenge given the need to run a large number of lab-scale tests to determine the optimal combination of factors that give the best separation performance. Various statistical methods have been employed in this process including artificial neural networks [17] and design-of-experiment (DOE) methods such as factorial designs, fractional-factorial designs, Taguchi method [18], and Box-Behnken designs [19,20]. It is well known that these techniques are much better than the conventional “one factor at a time” approach which does not consider interactions between factors and thus is not at all appropriate for testing multiple factors [21].

Within the biotechnology industry there is strong interest in developing microscale processes, miniaturized versions of separation modules that enable experiments to be run in parallel with smaller amounts of materials [22,23]. Previous studies have demonstrated the potential of using microscale membrane-based processes. For example, the fouling propensity of surface-modified UF membranes has been studied for natural organic matter [24] and protein solutions [25]. Also, the performance of

various microfiltration (MF) membranes with different feed materials such as yeast cell suspensions [26], fermentation broths [27], and DNA solutions [28] have been studied. However, all of these studies focused on evaluating the membrane filtration capacity for the given feed material and not on membrane separation performance. Vandezande et al. [29] developed a custom module for evaluating the performance of nanofiltration membranes in terms of the rejection of a small molecule.

In this work, we demonstrate the considerable advantage to using microscale filtration methods and DOE techniques in a synergistic way to solve the performance optimization challenge related to membrane-based bio-molecule separation. Recently, we developed the stirred-well filtration (SWF) method that uses 96-well filter plates and incorporates mixing of the feed solution directly above the membrane surface akin to the stirred-cell filtration device [30]. In that work, we demonstrated the importance of the stirring conditions for high-throughput filtration tests for single protein solutions. In this work, we demonstrate the extreme usefulness of combining the SWF method with DOE techniques to optimize the selectivity in terms of the permeate flux and solution conditions (pH or ionic strength) for three binary mixtures of bio-molecules: protein–protein, protein–polysaccharide, and protein–DNA. These mixtures were selected to demonstrate the "proof-of-concept," but the method described herein can be used to optimize the separation performance for any membrane-based process.

2.3. Experimental

2.3.1. Materials

The filtration experiments were performed using AcroPrep™ 96-well filter plates (Pall Corporation, Port Washington, NY) containing Omega™ UF membranes; the nominal MWCO of the two filter plates used for this work were 30 and 100 kDa. According to the manufacturer, this modified polyethersulfone membrane has the advantage of decreased protein binding, high permeate fluxes, high selectivity and high stability against biological and physical degradation. As per our previous study [30] there was no significant variation in the hydraulic permeability values for the individual wells across the entire filter plates.

Bovine serum albumin (BSA) and human immunoglobulin G (IgG) were purchased from Sigma–Aldrich (Oakville, ON, Canada). Green fluorescent protein (GFP) was purified from an Escherichia coli lysate using the HisPur™ Ni-NTA resin (Thermo Fisher Scientific, Ottawa, ON, Canada) according to the manufacturer's instructions; additional details about the GFP production can be found in [31]. The GFP was subjected to a dialysis step using 3500 Da Spectrum™ Spectra/Por™ 3 RC Dialysis Membrane Tubing (Thermo Fisher Scientific) and dialysis solution containing 71 mM Tris-HCl and 10 mM NaCl (pH 7.5). A 4 kDa dextran labelled with fluorescein isothiocyanate (FITC) was purchased from Sigma-Aldrich and used as received. A supercoiled 5.1 kilobase pair (kbp) plasmid was purchased from Aldevron and linearized by digestion with the Xho I restriction enzyme (Invitrogen™, Burlington, ON, Canada) according to the manufacturer's instructions. The effectiveness of the digestion reaction was confirmed

using agarose gel electrophoresis in that only a single DNA "band" was seen in the lane corresponding to the digestion reaction and it was in the correct position relative to the "bands" for the accompanying 1 kbp Plus DNA Ladder (Invitrogen™).

A variety of buffer solutions were used to investigate the effect of the ionic strength and pH conditions on separation performance. The feed solutions for the protein–polysaccharide tests were prepared using a phosphate buffered saline (PBS) solution, made by diluting a 10× concentrated buffer solution (Sigma–Aldrich) with distilled, deionized water from a Millipore Milli-Q system, with the pH adjusted to 4.9 or 7.0 via the addition of concentrated hydrochloric acid (LabChem, Zelienople, PA) or sodium hydroxide solutions (Thermo Fisher Scientific). The 1× PBS solution contained 137 mM NaCl and 2.7 mM KCl. The concentrations in the feed solution were 125 and 62.5 μg/mL for the proteins and FITC-dextrans respectively. A select number of experiments for protein–protein tests were performed with feed solutions prepared in 10× PBS solution diluted with deionized water to obtain a NaCl concentration of 900mM; the concentrations were 48 and 120 μg/mL of GFP and IgG, respectively. The feed solutions for the protein–DNA tests were prepared in 1× Tris/EDTA (TE) buffer (Thermo Fisher Scientific) at pH 8.0 and in the same buffer solution containing 150mM NaCl; the concentrations were 125 μg/mL and 250 ng/mL of BSA and DNA, respectively.

2.3.2. Filtration Experiments

The filtration experiments were conducted using the SWF module as previously described in extensive detail [30]; a brief description is given below. The feed reservoir for each UF test was a 3 mL Luer-Lok™ syringe. A programmable multi-rack syringe pump was used to run eight filtration tests at once in constant flux mode and individual pressure transducers were used to monitor the pressure in each well. The transducer signals were processed by a data acquisition board and the pressure profiles were monitored and recorded by LabVIEW software. Before an experiment, approximately 400 µL of each feed solution in the syringe was used to load the connecting tubing and displace any air bubbles that were present. Another 350 µL of each feed solution was used to fill the corresponding well on the filter plate. The stirring elements were placed into the wells, the filter plate was placed on the support plate, and the entire module was assembled to ensure a tight leak-free seal was obtained. A lateral tumble stirrer (V&P Scientific, San Diego, CA) was used to simultaneously rotate the stirring elements in each well at 300 rpm. The unstirred experiment were performed with no stirring elements and the tumble stirrer off. For each experiment, two 300 µL permeate samples were collected in different wells in two adjacent columns of a 96-well "collection" plate (Corning® Costar® 3596) located under the filter plate. At the end of each experiment, the SWF module was disassembled and retentate samples were taken from each filtration well. The tubing and connectors for each channels were rinsed repeatedly using both Milli-Q water and air (via the multi-rack syringe pump) to prepare the SWF module for the next filtration experiment. Then the initial feed, final feed (i.e., the retentate sample) and the

two permeate samples were analyzed as described below to determine the apparent sieving coefficient values at the various filtration conditions.

2.3.3. Sample Analysis

The concentrations of GFP and FITC-dextrans were determined using an Infinite® M1000 plate reader (Tecan, Morrisville, NC) with the excitation and emission wavelengths set to 490 and 520 nm, respectively. A 75 μL sample of each sample to be analyzed was transferred into 96-well half area black plates (Corning® NBS® 3993). The presence of BSA had no significant effect on the fluorescence intensity values for the FITC-dextran. Also, the presence of IgG had no significant effect on the fluorescence intensity values for the GFP molecules. The FITC-dextran fluorescence intensity signal is fairly sensitive to the buffer solution pH and thus different calibration curves were prepared for each test condition.

The concentration of BSA was determined using the BCA protein assay kit (Pierce™). The assay was performed in 96-well transparent plates (Corning® Costar® 3695) that were pre-filled with 200 μL of BCA reagent. A 25 μL sample of each sample to be analyzed was mixed with the BCA reagent via repeated aspiration. The plate was incubated at 37 °C for 30 min, then allowed to sit at room temperature on a shaker plate for 5 min, and then analyzed using the same Infinite® M1000 plate reader with the wavelength set to 562 nm. A standard calibration curve was used to convert the absorbance reading into protein concentration; the presence of the FITC-dextran in the

protein sample had no significant effect on the BCA assay. The same BCA protein assay kit was used to determine the concentration of IgG; however, only a 10 μL sample was mixed with the 200 μL of BCA reagent. It was found that the presence of GFP affected the BCA assay absorbance signal for a given amount of IgG. Thus, standard calibration curves were prepared over a range of GFP concentrations with the IgG concentration evaluated by appropriate interpolation.

The concentration of DNA was determined using the Quant-iT™ PicoGreen® dsDNA assay kit (Invitrogen™). A 50 μL sample of each sample to be analyzed was transferred into 96-well half area black plates (Corning® NBS® 3993) and mixed with 50 μL of the PicoGreen® working reagent via repeated aspiration. The plate was incubated at room temperature for 5 min and then analyzed using the same Infinite® M1000 plate reader with the excitation and emission wavelengths set to 480 and 520 nm, respectively. The PicoGreen fluorescence intensity signal is mildly sensitive to the presence of BSA and sodium chloride [32] and thus a similar approach to that used for the IgG determination was used with standard calibration curves were prepared over a range of BSA and salt concentrations.

2.4. Results and Discussion

2.4.1. Separation of a Protein–Polysaccharide Mixture

The experimental results for the separation of BSA (66 kDa) and 4 kDa FITC-dextran using a 30 kDa Omega™ membrane are shown in Figure 2.1. This particular

combination of biomolecules and membrane were chosen as a model system for separations application; the BSA was expected to be retained by the membrane while the dextran would be transmitted through the membrane. A 2^3 full-factorial DOE (i.e., three factors at two different levels) was conducted with the permeate flux (36 and 60 LMH), solution pH (4.9 and 7.0), and stirring conditions as process variables. The top half of the figure (i.e., panels a, b, c, g, h) is for the filtration tests that were done with stirring directly above the UF membrane; the bottom half of the figure (i.e., panels d, e, f, i, j) is for the unstirred filtration tests. For each "permeate flux-pH-stirring condition" combination, four separate filtration tests were conducted; thus, a total of 32 individual filtration tests were conducted for just this one separations application. The eight experiments for a given flux at a particular "pH-stirring condition" combination were done in the eight wells of one column of the 96-well filter plate; the exact positions in the column were assigned randomly to eliminate any potential effects associated with tests done in the wells at the perimeter of the filter plate. For each filtration test, the apparent sieving coefficient (S_a) of each biomolecule was determined according to equation (2.1):

$$S_a = \frac{C_p}{C_b} \times 100 \qquad (2.1)$$

where C_p is the solute concentration in the permeate sample and C_b is the solute concentration in the bulk solution. The permeate samples for each experimental condition were collected in two adjacent wells of the 96-well collection plate and C_p is the average concentration of the two samples. The four panels on the left hand side of Figure 2.1 display the S_a values for the 4 kDa FITC-dextran (panels a and d) and BSA (panels b and

e). The results are presented to match the inherent design of the DOE method. Within each panel, the top and bottom rows correspond to the high level (60 LMH) and low level (36 LMH) values of the permeate flux respectively, while the left and right columns correspond to the low level (4.9) and high level (7.0) values of the solution pH respectively. For each block corresponding to a particular permeate flux-pH combination, the S_a values from the four separation filtration tests are shown in the corners and the average S_a value is shown in the middle. Overall, the results from the separate tests were quite consistent—for example, the dextran Sa values for the 36 LMH, pH 7.0, stirred experiment (bottom right block of panel a) were 87.9%, 97.6%, 92.5%, and 92.0%; the corresponding coefficient of variation (CV) is 4.3%. For the 16 blocks of the sieving coefficient values shown in Figure 2.1, 10 had a CV less than 15%, 3 had a CV between 15% and 25%, and just 3 had a CV greater than 25%. The variability in our study is similar to that reported in previous studies that used the traditional stirred cell setup and the tedious "one factor at a time" approach [16,33,34]. The significance of each process variable on the S_a values was evaluated using statistical t-tests with the results displayed according to the line style that connects any two blocks; a solid line indicates a significant difference (P-value ≤ 0.05) while a dashed line indicates an insignificant difference (P-value > 0.05). For the stirred condition, the sieving coefficient for the dextran (panel a) was unaffected by both the permeate flux and solution pH at least over the range of conditions tested in this study. The sieving coefficient for BSA (panel b) was also unaffected by the change in permeate flux (from 36 to 60 LMH) but increased significantly (as indicated by the solid connecting lines) when the solution pH was

decreased from 7.0 to 4.9. The latter pH value corresponds to the isoelectric point of BSA and because the Omega^{TM} UF membrane is negatively charged over the range of pH values used for the filtration tests [1], it was expected that the isoelectric point condition would result in the higher sieving coefficient [10,35]. As expected the sieving coefficients for the dextran were larger than those for BSA at all the conditions tests.

The membrane selectivity (ψ) was calculated from the sieving coefficient results according to equation (2.2):

$$\psi = \frac{S_{a,\text{smaller molecule}}}{S_{a,\text{larger molecule}}} \qquad (2.2)$$

with the results displayed in panels c and f for the stirred and unstirred conditions respectively. For Figure 2.1, the "smaller" biomolecule is the dextran and the "larger" one is the BSA; the hydrodynamic radii of the 4 kDa FITC-dextran and BSA are estimated as 1.4 and 3.5 nm, respectively [36]. Note that the average selectivity value was calculated as the average of the ratios of the sieving coefficients from the four separation filtration tests. The selectivity was significantly higher at pH 7.0 due to the decrease in the BSA sieving coefficient, but again the effects of permeate flux changes were insignificant over the range of conditions tested in this study. To compare the effect of stirring, we chose to focus on the selectivity results, although a comparison of the sieving coefficient results could also be made. The membrane selectivity was higher for the unstirred tests except at the high flux (60 LMH), low pH (4.9) condition where there was no significant difference between the two. The biggest difference was found at the low flux (36 LMH), high pH (7.0) condition, where the selectivity for the unstirred test was over five times higher than

that for the stirred test. This is most likely due to concentration polarization effects, that is the greater accumulation of solutes at the membrane surface, in the absence of stirring. This hypothesis is supported by the transmembrane pressure (TMP) profiles shown in the four panels on the right hand side of Figure 2.1 (i.e., panels g, h, i, j); the eight TMP profiles in each panel correspond to the four filtration tests conducted at both the low pH and high pH condition. Each profile starts at zero TMP for zero filtrate volume because the LabVIEW program records the TMP immediately after the syringe pump is turned on to achieve the desired permeate flux value. The uniformity and reproducibility is quite good across the different wells that were used for each individual filtration test. At all four permeate flux-stirring condition combinations, the final TMP values were higher for the experiments conducted at pH 4.9, the isoelectric point for BSA. Previous studies have reported similar behavior due to the enhanced protein adsorption on membranes due to the more hydrophobic nature at their isoelectric point [37,38]. The TMP profiles for the stirred condition at pH 7.0 are relatively flat for both permeate flux conditions, whereas the profiles increase slightly at pH 4.9; for example, the average TMP (±CV) at 60 LMH increased from 12.7 (±9.5%) to 16.7 (±18.7%) kPa as the permeate volume increased from 200 to 600 μL. The TMP profiles for the unstirred condition were quite different from those for the stirred condition across all the permeate flux-pH combinations tested in this study. For example, at pH 4.9 the average final TMP (±CV) at 60 LMH was 49.6 (±14.9%) kPa. The results reported herein are in good agreement with our previous work that evaluated the filtration of single protein solutions using the SWF module [30] as well as previous studies that used the traditional stirred-cell membrane device [39,40].

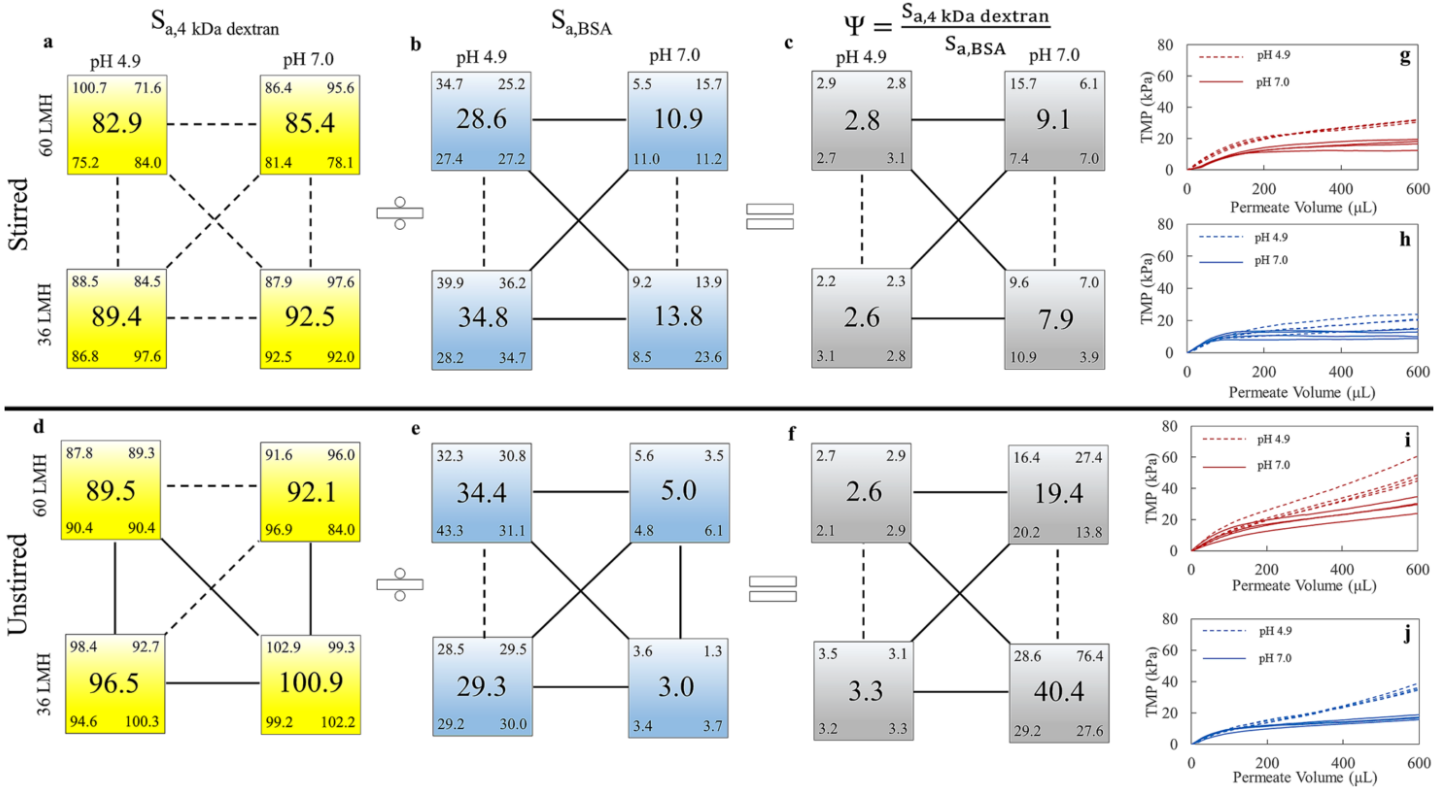

Fig 2.1. Filtration test results for BSA–4 kDa dextran mixture in PBS buffer and 30 kDa Omega^{TM} membrane: (a) 4 kDa dextran apparent sieving coefficient (stirred); (b) BSA apparent sieving coefficient (stirred); (c) Selectivity (stirred); (d) 4 kDa dextran apparent sieving coefficient (unstirred); (e) BSA apparent sieving coefficient (unstirred); (f) Selectivity (unstirred); (g) TMP profile for permeate flux of 60 LMH (stirred); (h) TMP profile for permeate flux of 36 LMH (stirred); (i) TMP profile for permeate flux of 60 LMH (unstirred); (j) TMP profile for permeate flux of 36 LMH (unstirred). On panels a–f, the data blocks are connected to each other using either solid lines (significant difference; *P*-value ≤ 0.05) or dashed lines (insignificant difference; *P*-value > 0.05) according to statistical t-test results. On panels g–j, the dashed and solid lines indicate the TMP profiles at pH 4.9 and 7.0, respectively.

In order to obtain additional insights into the effects of these process variables, another set of filtration tests were performed exactly as described above but at two other permeate flux values of 24 and 48 LMH. The sieving coefficient results are shown in Figure 2.2 (along with the results from Fig. 2.1 for 36 and 60 LMH) according to the more conventional format of plotting the sieving coefficient versus permeate flux. For the filtration tests that were conducted with stirring (panel a), the sieving coefficients for both biomolecules were independent of permeate flux at both pH conditions; the average S_a values between the 24 and 60 LMH varied by less than 5.5% and 8.4% for dextran at pH 4.9 and pH 7.0, and 5.2% and 0.5% for BSA at pH 4.9 and 7.0. For BSA, the sieving coefficients at pH 4.9 (open triangles) were significantly higher than those at pH 7.0 (filled triangles) over the entire range of permeate flux values tested. Previous studies have analyzed in great detail the effect of permeate flux on sieving behavior and described the phenomena using theoretical models [7,41]. In brief, at very low permeate fluxes, the sieving behavior is dominated by molecular diffusion while at moderate permeate fluxes the behavior is dominated by convective transport. Given that the change in permeate flux had an effect on the sieving behavior for the unstirred condition, our hypothesis about the effects of concentration polarization effect are confirmed. It is important to note that the results in panel a alone represent a total of 32 individual filtration tests (quadruplicate tests of eight different permeate flux-pH combinations). This level of testing is quite manageable using the parallel test format offered by the SWF module. For the same tests conducted without stirring (panel b), the BSA sieving coefficient at pH 4.9 (open triangles) was found to depend on the permeate flux. Based on

the combined set of results in Figures 2.1 and 2.2, we decided to focus on the permeate flux and solution condition effects for the sections below.

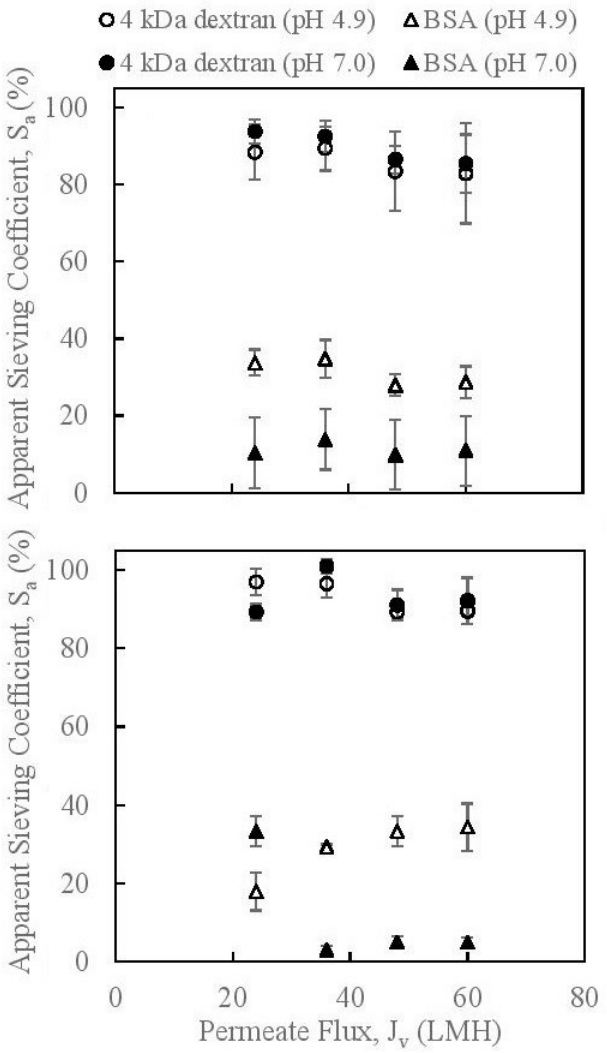

Fig 2.2. Effect of permeate flux on apparent sieving coefficient of 4 kDa dextran (circles) and BSA (triangles) at pH 4.9 (open symbols) and pH 7.0 (filled symbols): (a) Filtration tests conducted with stirring above the 30 kDa Omega^{TM} membrane surface; (b) Filtration tests conducted with no stirring above the 30 kDa Omega^{TM} membrane surface. Each experiment was repeated four times and the error bars are the standard deviation calculated according to the repeats.

2.4.2. Separation of a Protein–DNA Mixture

In order to demonstrate the usefulness of our approach of combining microscale filtration techniques with DOE methods, the separation of a binary protein–DNA mixture was studied. The experimental results for the separation of the linearized 5.1 kbp plasmid DNA molecule and BSA using a 100 kDa Omega^{TM} membrane and stirring conditions are shown in Figure 2.3. A 2^2 full-factorial DOE (i.e., two factors at two different levels) was conducted with the permeate flux (60 and 120 LMH), and NaCl concentration in the TE buffer solution (0 and 150 mM) as the process variables; the layout of the results is the same as that described in the section 'Separation of a Protein–Polysaccharide Mixture'. We used a linearized plasmid instead of a genomic DNA sample in order to rule out any sieving effects associated with a distribution of molecule sizes. Again, the results from each of the four filtration tests were consistent—for example, the DNA S_a values for the 60 LMH, 150 mM NaCl experiment (bottom right block of panel a) were 12.3%, 12.4%, 18.4%, and 22.1% (CV=29.5%). We hypothesize that the reported variability is principally due to variations in membrane properties because the four experiments for each "permeate flux-NaCl concentration" combination were performed in one column of the 96-well filter plate and a previous study has reported the greatest variation in membrane performance occurs within a column [27]. The same variation in membrane performance is also inherent in studies that use a multiple number of membrane discs in traditional stirred cell setup. It is interesting to note that although the molecular weight of the linear DNA molecule (~3366 kDa) is over 30 times greater than the membrane MWCO, the DNA sieving coefficients (panel b) were significantly greater than zero at all

the conditions tested. The largest DNA sieving coefficient was obtained at the high flux (120 LMH), high salt (150 mM) condition; those results were found to be significantly different (as indicated by the solid line) than the low flux, low salt condition. These results are consistent with previous studies that reported significant transmission of large DNA molecules through UF membranes due to elongation/deformation effects at the pore entrance [14,16] and the effects of solution ionic strength on DNA transmission [42,43]. The BSA sieving coefficients (panel a) were found to be significantly different at all four permeate flux-salt concentration combinations. The BSA sieving coefficient increased over fourfold as the permeate flux and NaCl concentration increased from 60 to 120 LMH and 0 to 150 mM respectively. Note that it is impossible to compare the BSA results with those shown in Figure 2.1 as the tests were done with a different solute pair (dextran vs. DNA) in a different solution (PBS vs. TE buffer) and with a different membrane.

The selectivity results in Figure 2.3c were calculated according to equation (2.2) with the “smaller” biomolecule being BSA and the “larger” molecule being the linearized plasmid DNA. The highest value of the selectivity (4.5) was obtained at the low flux (60 LMH), high salt (150 mM) condition. However, according to the statistical tests employed in this work, that condition was not significantly different than the results obtained at either salt concentration at the higher flux. The ability to conduct multiple filtration tests in a manageable way and run the appropriate statistical tests to make informed conclusions about the effects of different process factors is a key outcome of using the SWF module in combination with DOE studies. As shown in panels d and e of

Figure 2.3, the salt concentration had no effect on the TMP profiles for the BSA-DNA filtration tests.

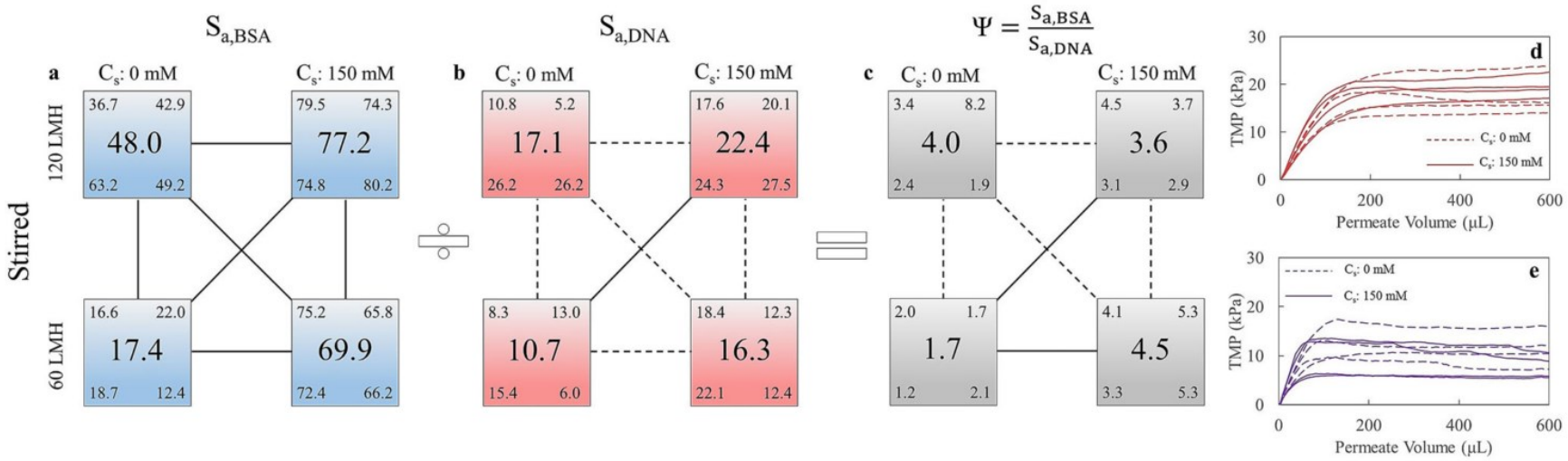

Fig 2.3. Filtration test results for BSA-DNA mixture in TE buffer and 100 kDa Omega^{TM} membrane conducted with stirring: (a) BSA apparent sieving coefficient; (b) Linearized 5.1 kbp plasmid DNA apparent sieving coefficient; (c) Selectivity; (d) TMP profile for permeate flux of 120 LMH; (e) TMP profile for permeate flux of 60 LMH. On panels a–c, the data blocks are connected to each other using either solid lines (significant difference; *P*-value ≤ 0.05) or dashed lines (insignificant difference; *P*-value > 0.05) according to statistical t-test results. On panels d and e, the dashed lines and solid lines indicate the TMP profiles at NaCl concentrations of 0 and 150mM, respectively.

2.4.3. Separation of a Protein–Protein Mixture

The final model system that was studied was a binary mixture of proteins. The experimental results for the separation of GFP and human IgG using a 100 kDa Omega^{TM} membrane and stirring conditions are shown in Figure 2.4; the corresponding results for the unstirred condition are in Figure 2.S1 in the supplementary material. A 2^3 full-factorial DOE was conducted with the permeate flux (36 and 60 LMH), NaCl concentration in the PBS solution (0 and 900 mM), and stirring conditions as process variables; the layout of the results is the same as that described in the section 'Separation of a Protein–Polysaccharide Mixture'. The sieving coefficient for GFP (panel a) was not significantly affected by the permeate flux, at least over the range of conditions tested in this study. However, the buffer solution NaCl concentration had a significant effect on GFP transmission through the 100 kDa Omega^{TM} membrane; at the high flux condition (60 LMH), the apparent sieving coefficient of GFP increased from 16.9 to 67.8 as the NaCl concentration increased from 0 to 900 mM. This is likely due to increase in electrostatic shielding provided by the salt [44]. We observed a statistically significant increase in transmission of both proteins at the high salt concentration condition. Although the hydrodynamic radius of GFP (2.3 nm) is nearly two times smaller than that for IgG (4.8–5.2 nm) [36,45], the sieving coefficients for these two biomolecules were nearly identical at the low salt condition.

The selectivity results (Fig. 2.4c) for the stirred condition showed that the permeate flux had no significant effect on IgG-GFP separation performance at the conditions tested in this study. However, we hypothesize that the increase in selectivity at the high salt

concentration condition is principally due to the higher GFP sieving coefficients because of the increased hydrophobic interactions [10,37,46]. In a similar fashion to the results in Figure 2.1, the unstirred selectivity values (Fig. 2.S1) are higher than stirred selectivity values due to the greater accumulation of solutes near the membrane surface. As shown in panels d and e of Figure 2.4, the salt concentration was found to have no effect on the TMP profiles for the GFP-IgG filtration tests as was reported above the BSA-DNA filtration tests.

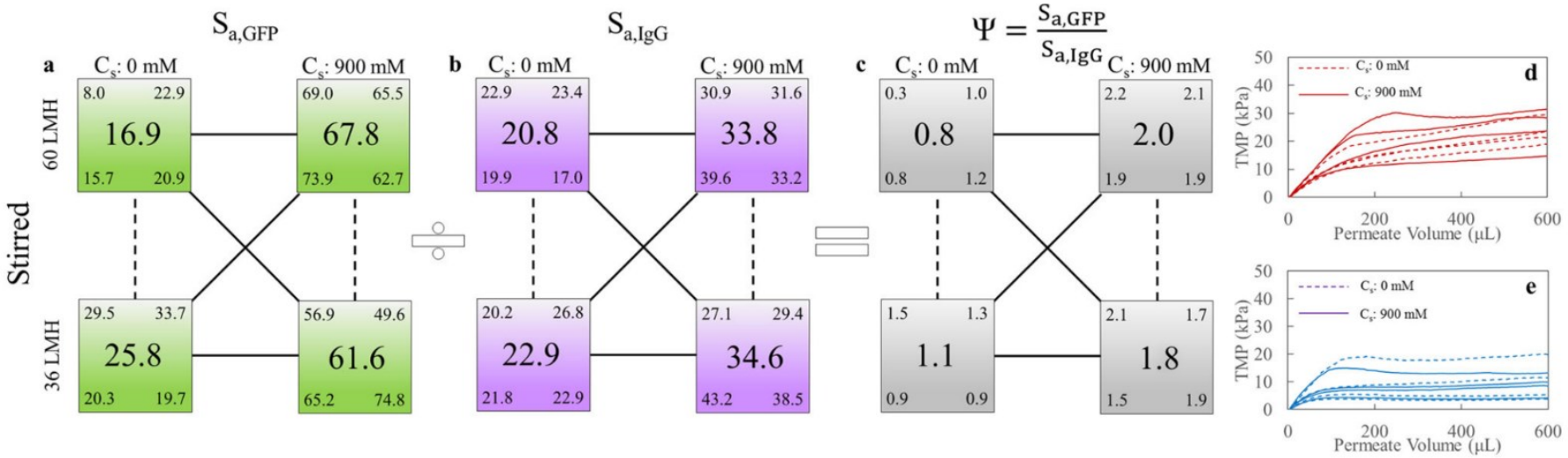

Fig 2.4. Filtration test results for IgG-GFP mixture in PBS buffer and 100 kDa Omega^{TM} membrane conducted with stirring: (a) GFP apparent sieving coefficient; (b) IgG apparent sieving coefficient; (c) Selectivity; (d) TMP profile for permeate flux of 60 LMH; (e) TMP profiles for permeate flux of 36 LMH. On panels a–c, the data blocks are connected to each other using either solid lines (significant difference; *P*-value ≤ 0.05) or dashed lines (insignificant difference; *P*-value > 0.05) according to statistical t-test results. On panels d and e, the dashed and solid lines indicate the TMP profiles at NaCl concentrations of 0 and 900mM, respectively.

2.5. Conclusions

In this work, the considerable advantage that is realized by combining the SWF technique, a HT method for process optimization, with DOE methods for optimizing the separation of biomolecules was demonstrated. The usefulness of this approach was shown for three different model solutions of biomolecules: a protein–protein mixture, a protein–polysaccharide mixture, and a protein–DNA mixture. For each mixture, a 2^2 factorial design was conducted with the permeate flux and solution conditions (pH or ionic strength) as process variables. For each permeate flux-solution condition combination, four individual sieving experiments were conducted. A unique way was used to present the statistical analysis that matches the factorial design of the DOE method. More than 100 individual filtration experiments were conducted and combined with appropriate tests in a manageable way to make informed conclusions about the effects of different operating conditions on biomolecule separation performance using UF process. A review of the key conclusions from these results are outlined below:

- For a mixture of 4 kDa dextran and bovine serum albumin, the selectivity obtained with an Omega^{TM} 30 kDa membrane was found to depend significantly on the solution pH. The selectivity was the highest at the pH 4.9 condition which corresponds to the net zero charge of BSA at its isoelectric point. Overall, unstirred selectivities were observed to be higher most likely due to the high wall concentration of the protein when performing unstirred experiments. The effect of permeate flux on sieving coefficient was found to be insignificant.

- The separation of DNA and BSA using an Omega™ 100 kDa membrane was observed to be highly dependent on combined effect of permeate flux and salt concentration in the mixture which is in agreement with the previous studies. The largest DNA sieving coefficient was obtained at the high flux (120 LMH), high salt (150 mM) condition. Furthermore, the BSA sieving coefficient increased over fourfold as the permeate flux and salt concentration increased from 60 to 120 LMH and 0 to 150 mM, respectively.
- It was found that salt concentration can be a significant factor in separation of GFP and IgG with an Omega™ 100 kDa membrane. There were significant difference in transmission of the two proteins at the high salt concentration condition. However, the sieving coefficients for these two biomolecules were nearly identical at the low salt condition although the molecular weight and hydrodynamic radius of GFP are significantly smaller than those for IgG.

2.6. Acknowledgements

The funding for this work was provided by NSERC Discovery Grant 435646-2013. Karina Kawka received a Canada-Brazil Ciência sem Fronteiras (CsF) scholarship to study at McMaster. We are especially grateful to Mr. Kevin Dunn (Department of Chemical Engineering, McMaster University) for his helpful suggestions in presenting the filtration test results in the DOE format. We acknowledge Pall Corporation for providing the Omega™ filter plates and Prof. Harald Stöver (Department of Chemistry, McMaster University) for providing the FITC-dextrans. Finally, we thank the

Biointerfaces Institute at McMaster for providing access to the microplate reader and gel imaging system.

2.7. References

[1] D.B. Burns, A.L. Zydney, Buffer effects on the zeta potential of ultrafiltration membranes, J. Membr. Sci. 172 (2000) 39–48.

[2] A.S. Bhadouria, M. Sorci, M. Gu, G. Belfort, J. Hahn, Optimization of Membrane Separation Processes for Protein Fractionation, Ind. Eng. Chem. Res. 53 (2014) 5103–5109.

[3] H. Susanto, H. Arafat, E.M.L. Janssen, M. Ulbricht, Ultrafiltration of polysaccharide–protein mixtures: Elucidation of fouling mechanisms and fouling control by membrane surface modification, Sep. Purif. Technol. 63 (2008) 558–565.

[4] W.R. Bowen, F. Jenner, Theoretical descriptions of membrane filtration of colloids and fine particles: An assessment and review, Adv. Colloid Interface Sci. 56 (1995) 141–200.

[5] Z. Cui, Protein separation using ultrafiltration — an example of multi-scale complex systems, China Particuology. 3 (2005) 343–348.

[6] A. Saxena, B.P. Tripathi, M. Kumar, V.K. Shahi, Membrane-based techniques for the separation and purification of proteins: An overview, Adv. Colloid Interface Sci. 145 (2009) 1–22.

[7] R. Ghosh, Protein Bioseparation Using Ultrafiltration: Theory, Applications and New Developments, Imperial College Press, 2003.

[8] G.B. van den Berg, I.G. Rácz, C.A. Smolders, Mass transfer coefficients in cross-flow ultrafiltration, J. Membr. Sci. 47 (1989) 25–51.

[9] B. Cheang, A.L. Zydney, Separation of α-lactalbumin and β-lactoglobulin using membrane ultrafiltration, Biotechnol. Bioeng. 83 (2003) 201–209.

[10] S. Saksena, A.L. Zydney, Effect of solution pH and ionic strength on the separation of albumin from immunoglobulins (IgG) by selective filtration., Biotechnol. Bioeng. 43 (1994) 960–8.

[11] R.H.C.M. van Eijndhoven, S. Saksena, A.L. Zydney, Protein fractionation using electrostatic interactions in membranel filtration, Biotechnol. Bioeng. 48 (1995)

406–414.

[12] Y. Wan, R. Ghosh, Z. Cui, High-resolution plasma protein fractionation using ultrafiltration, Desalination. 144 (2002) 301–306.

[13] M. Hadidi, J.J. Buckley, A.L. Zydney, Ultrafiltration behavior of bacterial polysaccharides used in vaccines, J. Membr. Sci. 490 (2015) 294–300.

[14] T. Hirasaki, T. Sato, T. Tsuboi, H. Nakano, T. Noda, A. Kono, et al., Permeation mechanism of DNA molecules in solution through cuprammonium regenerated cellulose hollow fiber (BMMtm), J. Membr. Sci. 106 (1995) 123–129.

[15] E. Arkhangelsky, Y. Sefi, B. Hajaj, G. Rothenberg, V. Gitis, Kinetics and mechanism of plasmid DNA penetration through nanopores, J. Membr. Sci. 371 (2011) 45–51.

[16] D.R. Latulippe, K. Ager, A.L. Zydney, Flux-dependent transmission of supercoiled plasmid DNA through ultrafiltration membranes, J. Membr. Sci. 294 (2007) 169–177.

[17] W.R. Bowen, M.G. Jones, H.N.S. Yousef, Dynamic ultrafiltration of proteins – A neural network approach, J. Membr. Sci. 146 (1998) 225–235.

[18] K. Yasotha, M.K. Aroua, K.B. Ramachandran, I.K.P. Tan, Recovery of medium-chain-length polyhydroxyalkanoates (PHAs) through enzymatic digestion treatments and ultrafiltration, Biochem. Eng. J. 30 (2006) 260–268.

[19] M. Sivakumar, G. Annadurai, D. Mohan, Studies on Box-Behnken design experiments: cellulose acetate-polyurethane ultrafiltration membranes for BSA separation, Bioprocess Eng. 21 (1999) 65.

[20] S.-H. Lin, C.-L. Hung, R.-S. Juang, Effect of operating parameters on the separation of proteins in aqueous solutions by dead-end ultrafiltration, Desalination. 234 (2008) 116–125.

[21] G.E.P. Box, J.S. Hunter, W.G. Hunter, Wiley: Statistics for Experimenters: Design, Innovation, and Discovery, 2nd ed., Wiley, 2005.

[22] M. Micheletti, G.J. Lye, Microscale bioprocess optimisation., Curr. Opin. Biotechnol. 17 (2006) 611–8.

[23] S. Chhatre, N.J. Titchener-Hooker, Micro-Biochemical Engineering: Using Small-Scale Devices to Predict Industry-Scale Downstream Performance, Elsevier, 2011.

[24] M. Zhou, H. Liu, J.E. Kilduff, R. Langer, D.G. Anderson, G. Belfort, High-throughput membrane surface modification to control NOM fouling., Environ. Sci. Technol. 43 (2009) 3865–71.

[25] M. Zhou, H. Liu, J.E. Kilduff, R. Langer, D.G. Anderson, G. Belfort, High Throughput Synthesis and Screening of New Protein Resistant Surfaces for

Membrane Filtration, AIChE J. 56 (2010) 1932–1945.

[26] M. Chandler, A. Zydney, High throughput screening for membrane process development, J. Membr. Sci. 237 (2004) 181–188.

[27] N. Jackson, J. Liddell, G. Lye, An automated microscale technique for the quantitative and parallel analysis of microfiltration operations, J. Membr. Sci. 276 (2006) 31–41.

[28] S. Kong, J. Aucamp, N.J. Titchener-Hooker, Studies on membrane sterile filtration of plasmid DNA using an automated multiwell technique, J. Membr. Sci. 353 (2010) 144–150.

[29] P. Vandezande, L. Gevers, J. Paul, I. Vankelecom, P. Jacobs, High throughput screening for rapid development of membranes and membrane processes, J. Membr. Sci. 250 (2005) 305–310.

[30] A.S. Kazemi, D.R. Latulippe, Stirred well filtration (SWF) – A high-throughput technique for downstream bio-processing, J. Membr. Sci. 470 (2014) 30–39.

[31] D.R. Latulippe, K. Szeto, A. Ozer, F.M. Duarte, C. V Kelly, J.M. Pagano, et al., Multiplexed microcolumn-based process for efficient selection of RNA aptamers., Anal. Chem. 85 (2013) 3417–24.

[32] V.L. Singer, L.J. Jones, S.T. Yue, R.P. Haugland, Characterization of PicoGreen reagent and development of a fluorescence-based solution assay for double-stranded DNA quantitation., Anal. Biochem. 249 (1997) 228–38.

[33] J.R. Molek, A.L. Zydney, Separation of PEGylated alpha-lactalbumin from unreacted precursors and byproducts using ultrafiltration., Biotechnol. Prog. 23 (2007) 1417–24.

[34] A. Arunkumar, M.R. Etzel, Fractionation of lactalbumin and lactoglobulin from bovine milk serum using staged, positively charged, tangential flow ultrafiltration membranes, J. Membr. Sci. 454 (2014) 488–495.

[35] R. Ghosh, Z.. Cui, Fractionation of BSA and lysozyme using ultrafiltration: effect of pH and membrane pretreatment, J. Membr. Sci. 139 (1998) 17–28.

[36] D. Venturoli, B. Rippe, Ficoll and dextran vs. globular proteins as probes for testing glomerular permselectivity: effects of molecular size, shape, charge, and deformability., Am. J. Physiol. Renal Physiol. 288 (2005) F605-13.

[37] I.H. Huisman, P. Prádanos, A. Hernández, The effect of protein–protein and protein–membrane interactions on membrane fouling in ultrafiltration, J. Membr. Sci. 179 (2000) 79–90.

[38] S. Salgın, S. Takaç, T.H. Özdamar, Adsorption of bovine serum albumin on polyether sulfone ultrafiltration membranes: Determination of interfacial

interaction energy and effective diffusion coefficient, J. Membr. Sci. 278 (2006) 251–260.

[39] M. Chudacek, A.G. Fane, The dynamics of polarisation in unstirred and stirred ultrafiltration, J. Membr. Sci. 21 (1984) 145–160.

[40] R. Ghosh, Study of membrane fouling by BSA using pulsed injection technique, J. Membr. Sci. 195 (2002) 115–123.

[41] W.S. Opong, A.L. Zydney, Diffusive and convective protein transport through asymmetric membranes, AIChE J. 37 (1991) 1497–1510.

[42] A. Higuchi, T. Yoshimura, K. Kato, M. Hara, M. Higuchi, N. Minoura, et al., Sieving study of chromatin and histone-DNA complex by porous hollow fiber membranes, J. Membr. Sci. 126 (1997) 7–17.

[43] D.R. Latulippe, A.L. Zydney, Salt-induced changes in plasmid DNA transmission through ultrafiltration membranes., Biotechnol. Bioeng. 99 (2008) 390–8.

[44] A. Mehta, A.L. Zydney, Effect of membrane charge on flow and protein transport during ultrafiltration., Biotechnol. Prog. 22 (2006) 484–92.

[45] J.K. Armstrong, R.B. Wenby, H.J. Meiselman, T.C. Fisher, The Hydrodynamic Radii of Macromolecules and Their Effect on Red Blood Cell Aggregation, Biophys. J. 87 (2004) 4259–4270.

[46] R. Chan, V. Chen, The effects of electrolyte concentration and pH on protein aggregation and deposition: critical flux and constant flux membrane filtration, J. Membr. Sci. 185 (2001) 177–192.

2.8.Supporting Information

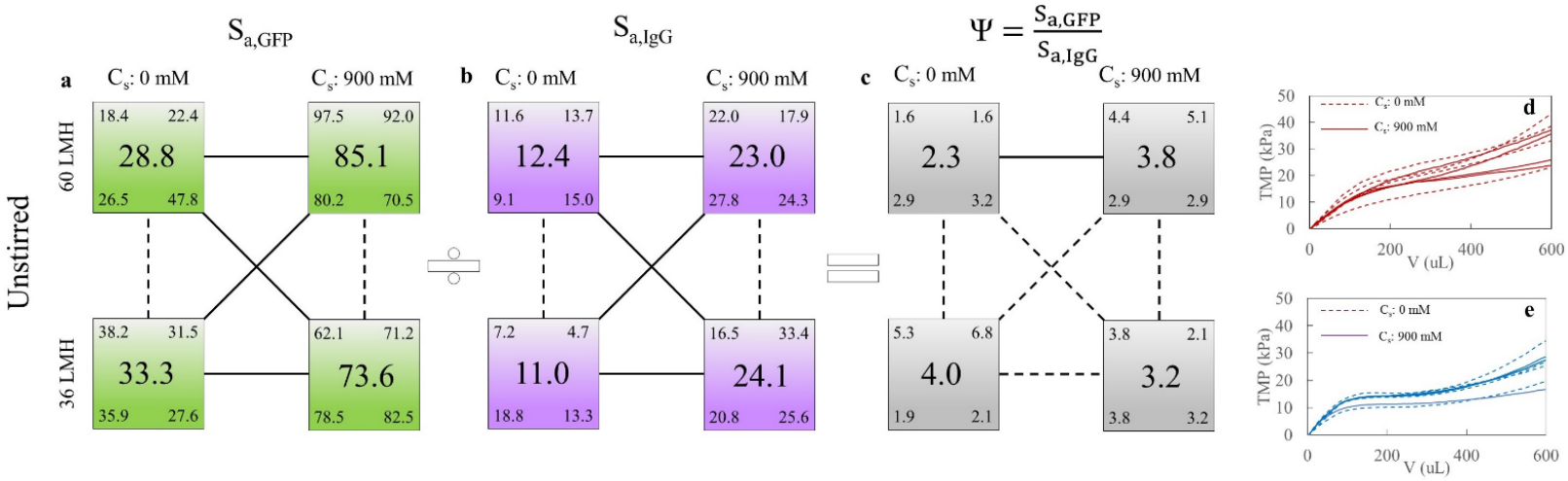

Fig 2.S1. Filtration test results for IgG-GFP mixture in PBS buffer and 100 kDa Omega^{TM} membrane conducted without stirring.

Chapter 3 - Microscale Filtration via a Multi-modal Microfluidic Flow Control System

Authors: Amir S. Kazemi, Melissa J. Larocque, David R. Latulippe

Accepted for Publication, Separation Science and Technology,
doi.org/10.1080/01496395.2018.1483949

3.1. Preface

This chapter highlights the importance of operating high-throughput (HT) membrane filtration tests in constant flux and constant transmembrane pressure (TMP) modes. As explained in chapter 2, there is a growing interest in developing HT techniques that enable multiple membrane filtration experiments to be performed simultaneously with smaller sample amounts which results in the reduction of the overall required time and cost to conduct tests. To date, the majority of HT techniques developed for membrane filtration processes are designed to be used in either constant flux or constant TMP mode. However, the effect of the mode of operation (constant flux vs. constant TMP) of a membrane process has been studied for different membranes using conventional lab- and pilot-scale filtration modules. Herein, we introduced a HT filtration system that integrated a multi-channel microfluidic flow control (MMFC) system with the stirred well filtration (SWF) module [1][1]. The MMFC system consists of an array of eight pressure controllers and flow sensors that can run up to eight filtration experiments in parallel in either a constant permeate flux or constant TMP mode of operation. Using this system, a range of

[1] For more information regarding the SWF module refer to chapters 1 and 2.

different TMP and/or different flux settings can be used in parallel for each well of the 96-well filter plate allowing for a rapid testing of the filtration performance. Also, the changes in the permeate fluxes are directly monitored and recorded in real-time when operating in constant TMP. The mode of operation can be switched from constant TMP to constant flux (and vice-versa) during a filtration experiment. Among the previous HT studies only Chandler and Zydney [2] have tested constant flux and constant TMP. However, their study was performed in the dead-end unstirred format which may adversely affect the filtration performance[2]. Additionally, the constant flux and constant TMP experiments performed in that study were run separately using two separate apparatuses and fluid handling setups.

As a proof-of-principle, the usefulness of this technique was demonstrated by performing HT hydraulic permeability measurements of UF membranes as well as studying the filtration performance of single protein solutions and separation of two binary mixtures (polymer-polymer and protein-polymer) in constant flux and constant TMP mode.

3.2. Introduction

Membrane filtration processes are used in a wide range of separation applications due to their availability in various configurations (flat sheet, tubular, hollow-fiber) and in specific processes across the filtration spectrum. Membrane technologies are a key

[2] Refer to section 1.3.2.

separation technique in downstream bio-processing applications; the production of a standard bio-therapeutic product can involve between 10 and 20 membrane-based separation processes [3]. For example, microfiltration (MF) membranes can be used for sterilization and removal of microorganisms, ultrafiltration (UF) membranes can be used for concentration and purification of recombinant proteins and nanofiltration (NF) membranes are used for virus removal at the end of downstream processing. Membrane technologies also play a key role in a variety of environmental applications including the removal of suspended solids using MF membranes, the removal of colloidal material using UF membranes, and the removal of heavy metals and dissolved organic matter using NF membranes.

Given the number of process and operating factors that are known to affect the membrane filtration performance (including solution conditions, hydrodynamic conditions, and membrane properties), it is a considerable challenge to fully optimize a specified separation process. Thus, there is considerable interest in the development of microscale filtration technologies to enable a high-throughput (HT) evaluation of membrane separation performance. HT studies have most commonly been run in a vacuum manifold format, in combination with commercially available 96-well filter plates [4–6] or custom-made multi-well filtration plates [7,8]. With this design, a single transmembrane pressure (TMP) difference is applied across all the filtration wells. The effects of different operating factors on the filtration of fermentation broth [7], and the filtration of large DNA vectors through MF membranes [8] have been thoroughly studied using this approach. In a selected number of these studies, HT approach was used to study

the fouling of surface modified membranes during the filtration of protein [4], natural organic matter [5], and other typical feed solutions from the biotechnology industry [6]. While each of these studies reported valuable findings, there are two key limitations with this approach. First, because there was no feed reservoir, the duration of the filtration experiment was limited by the amount of feed solution in the well above the membrane. Second, there was no real-time measurement of the permeate flux as an indicator of membrane performance. In an alternative format, a multi-rack syringe pump (or other suitable fluid delivery device) is used to set the same constant permeate flux across all the filtration wells [1,2,9]; this approach allows for typically 8 to 12 experiments to be conducted in parallel, with the amount of feed solution determined by the volume of the syringe barrel. Our recent work in this area demonstrated the importance of incorporating mixing above the membrane surface in these microscale studies to minimize the accumulation of solutes at the membrane surface [1,9]; all of the previous studies had operated in an unstirred, dead-end filtration regime [2,4–8].

The effect of the mode of operation of a membrane process has been studied for a variety of membrane types and configurations using conventional lab-scale and pilot-scale filtration apparatuses. For example, Marshall et al. [10,11] compared membrane fouling mechanisms in constant flux and constant TMP filtration of proteins through MF and UF membranes. Miller et al. [12] have studied the fouling of polysulfone UF membranes with emulsified oil in constant flux and constant TMP mode, and compared the mass transfer resistance changes. Also, Decloux and Tatoud [13] studied the effect of filtration mode during processing of raw cane remelts with tubular UF and MF

membranes. Sim et al. [14] have compared the modified fouling UF indices in constant flux and constant TMP filtration and found that the crossflow sampler-modified fouling index was sensitive to the applied flux. Sioutopoulos and Karabelas [15] studied the fouling resistance during constant flux and constant TMP filtration of a sodium alginate-humic acid mixture. Kanani and Ghosh [16] compared the modelling aspects of constant flux and constant TMP protein UF.

To the best of our knowledge, only one previous study of microscale filtration has used both constant flux and constant TMP operating modes - Chandler and Zydney [2] evaluated the performance of MF membranes for yeast cell harvesting under both constant flux and constant TMP. However, that study was also performed in the dead-end unstirred format. In this work, we developed a HT filtration system that integrated a multi-channel microfluidic flow control (MMFC) system with the 'stirred well filtration' (SWF) module that was previously developed by our group [1]. The MMFC system consists of a bank of eight pressure controllers and flow sensors that can run up to eight filtration experiments in parallel in either a constant permeate flux or constant TMP mode of operation. The advantages of this approach include the following:

- A range of different TMP and/or different permeate flux settings can be used simultaneously for each individual filtration well allowing for a rapid screening of filtration performance
- A direct real-time measurement of the change in permeate flux is obtained when operating in the constant TMP mode.

- The microscale format enables multiple filtration experiments to be conducted with small amounts of feed stock material.
- At anytime during a filtration experiment, the mode of operation can be switched from constant TMP to constant flux and vice-versa.

We demonstrated the usefulness of combining the MMFC system with the SWF module to study the filtration behaviour of single protein solutions and separation of two binary mixture solutions: polymer-polymer and protein-polymer. These conditions were chosen simply to demonstrate the "proof-of-concept," but the method described herein can be used to optimize the performance for any membrane-based process.

3.3. Experimental

3.3.1. Materials

All of the filtration experiments were performed with AcroPrep Advance 96-well filter plates (Pall) containing Omega^{TM} modified polyethersulfone (PES) UF membranes with a nominal molecular weight cut-off (MWCO) of 30 kDa. According to the manufacturer, these particular membranes demonstrate low protein binding, high permeate fluxes, high selectivity, and high stability against biological and physical degradation. Bovine serum albumin (BSA), α-lactalbumin, polyethylene glycol (PEG) with a molecular weight (MW) of 4 kDa, dextran (DEX) with a MW of 200 kDa, and fluorescein isothiocyanate–dextran (FITC-DEX) with a MW of 250 kDa were all purchased from Sigma. The BSA was diluted to a final concentration of 0.25 mg/mL by

diluting a 2 mg/mL BSA solution with Phosphate Buffered Saline (PBS) solution. A binary solution of PEG (2.5 mg/mL) and DEX (2.5 mg/mL) was prepared using 0.5 M $NaNO_3$ solution in 2-(Cyclohexylamino)ethanesulfonic acid (CHES) buffer at pH 10; the same solution was used as the mobile phase for the gel permeation chromatography (GPC) system that was used to analyze the samples from this experiment (see Section 3.3.3). A binary solution of FITC-DEX (0.1 mg/mL) and α-lactalbumin (0.1 mg/mL) was prepared in the same PBS buffer used for the BSA experiments. All of the prepared solutions were pre-filtered with 0.2 μm Supor® membrane syringe filters (Pall) before they were used for the filtration experiments.

3.3.2. Microscale Filtration Experiments

As shown in Figure 3.1, microscale filtration experiments were conducted by integrating a MMFC system (Elveflow) with the SWF module that uses 96-well filter plates and incorporates mixing of the feed solution directly above the membrane surface; the development of the SWF module is described in detail in our previous work [1]. Briefly, the manifold plate used in the SWF module consists of eight inlets where the microfluidic tubings (1/16" OD) are attached using microfluidic connectors (f-332nx from IDEX Health & Science). A custom gasket (made from Parafilm and o-rings) is used to provide sealing between each individual well and the manifold. Furthermore, a support plate (including an outlet channel which allows for sample collection) is used to hold the filter plate in place. The stirring was achieved using a tumble stirrer (V&P

Scientific) that uses one rotating cylindrical magnet to simultaneously stir multiple vessels. The MMFC system consists of a pair of four-channel OB1 MK3 pressure controllers (range of 0 to 800 kPa); each channel also contains a MFS4 thermal flow sensor (range of 0 to 1000 μL/min). According to the manufacturer, the pressure controllers and flow sensors are accurate to 0.006% and 5% of the measured value respectively. The reservoir for each filtration experiment was a 15 mL Falcon™ centrifuge tube. The MMFC system software was used to set, monitor and record the individual TMP or flow rate in each well of the SWF module. Thus, the system can facilitate up to eight filtration experiments in parallel, with the ability to independently set the conditions (constant flux or constant TMP) in each well. Note that with a reasonable amount of modifications to the SWF module and the addition of another four-channel OB1 MK3 pressure controller, twelve filtration experiments could be run simultaneously in the twelve wells that make up a single row on a 96-well filter plate.

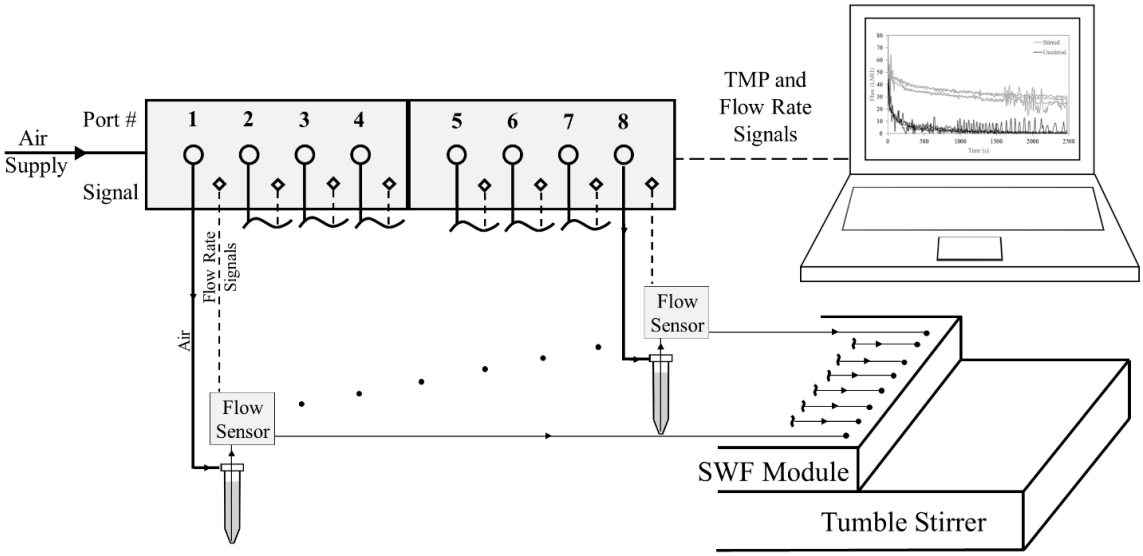

Fig 3.1. Schematic demonstration of the integration of the multichannel microfluidic flow control (MMFC) system and the stirred well filtration (SWF) module. This setup allows for up to eight filtration experiments to be run in parallel with each individual experiment conducted at either a constant flux or a constant TMP condition.

In this study, each filtration experiment was conducted on an unused well from the 96-well filter plate. Prior to each filtration experiment, the hydraulic permeability (L_p) of each membrane disc in the individual well of the 96-well filter plate was measured according to Equation 3.1:

$$L_p = \frac{J}{\Delta P}\,\mu \qquad (3.1)$$

where J is the permeate flux (calculated as flow rate divided by the membrane area in $L/m^2/h$ (LMH) unit), ΔP is the transmembrane pressure (kPa) and μ is the solution viscosity (Pa.s). The MMFC system allows for the hydraulic permeability to be determined in either constant flux mode (by setting the flow rate and recording the TMP) or constant TMP mode (by setting the TMP and recording the flow rate). Solute free

buffer solution was used for the hydraulic permeability measurements. All of the permeability experiments were conducted at room temperature with the solution viscosity evaluated using literature data.

At the onset of each filtration experiment, the microfluidic tubing that connects the MMFC system to the SWF module was pre-filled with the appropriate feed solution. Next, the appropriate number of wells in the filter plate were filled with approximately 350 μL of the feed solution. If required, magnetic stir elements (VP 772DP-N42-5-2 from V&P Scientific) were added to the wells and then the SWF module was sealed to prevent leakage. Finally, the SWF module was placed on a lateral tumble stirrer that would simultaneously rotate the stir elements at approximately 350 rpm. Permeate samples were normally collected in a standard 96-well microplate; however, for certain experiments a custom acrylic plate with eight long grooves (well capacity of 1.5 mL) that matched the spacing of wells on the filter plate was used. After the filtration experiment was complete, the SWF module was disassembled and retentate samples were collected from the filter plate. The entire system was extensively flushed with deionized, distilled water after each experiment. According to the protocol provided by the manufacturer, the tubing and the flow sensors were flushed using 5 mL of deionized water, 5 mL of 10% sodium dodecyl sulfate in 1 M acetic acid, 1 mL of acetone, 1 mL of isopropyl alcohol, and compressed air after each experiment.

3.3.3. Sample Analysis

A gel permeation chromatography (GPC) system was used to analyze samples from the filtration experiment with the binary mixture of PEG and DEX. The GPC system consisted of three columns (each one 30 cm length × 7.8 mm internal diameter) in series: Waters Ultrahydrogel-120, -250 and -500. The nominal fractionation range of the system is between 100 and 400,000 Da. The sample injection volume was 80 μL and detection was performed using a refractive index detector. The flow rate of the mobile phase (0.5 M $NaNO_3$ solution in CHES buffer at pH 10) was 0.8 mL/min. Each sample was pre-filtered using a 0.2 μm Supor® membrane syringe filter (Pall) immediately before the GPC analysis.

A Spark 10 M microplate reader (Tecan) was used to analyze samples from the filtration experiment with the binary mixture of FITC-DEX and α-lactalbumin. The concentration of FITC-DEX was determined by pipetting 75 μL of each sample into the wells of a 'half area' 96-well black microplate (Corning® 3993) and measuring the fluorescence intensity at 518 nm (excitation at 492 nm); actual concentrations were determined by comparison with a standard calibration curve. The concentration of α-lactalbumin was determined by pipetting 25 μL of each sample into the wells of a 96-well transparent microplate (Corning® 3695) that were pre-filled with 200 μL of BCA reagent from the BCA protein assay kit (Pierce). The plate was then incubated at 37 °C for 30 min, cooled to room temperature, and the absorbance reading was measured at 562 nm;

again, actual concentrations were determined by comparison with a standard calibration curve.

The membrane filtration performance was evaluated by calculating the apparent sieving coefficient (S_a) for each component according to Equation 32:

$$S_a = \frac{C_p}{C_b} \times 100 \qquad (3.2)$$

where C_p is the concentration in the permeate sample and C_b is the concentration in the bulk solution on the feed side; the latter concentration was estimated by interpolation with respect to the cumulative filtered volume between the initial concentration in the feed sample and the final concentration in the collected retentate sample.

3.4. Results and Discussion

3.4.1. Multi-modal Measurement of Hydraulic Permeability in Microscale Format

In order to demonstrate the extreme utility of using the MMFC system in microscale filtration experiments, a simple filtration experiment was run where the operating mode was toggled between constant flux and constant TMP. Figure 3.2a displays the resulting TMP and permeate flux profiles for the filtration of PBS buffer through the 30 kDa Omega^{TM} membrane using the SWF module. The experiment was initially run under a constant TMP (set point = 45 kPa) and the average flux value was 159 LMH (66.3 µL/min). At the 12 minute mark, the mode of operation was switched to constant flux (set point = 90 LMH) and the MMFC system adjusted the TMP to approximately 26 kPa to achieve the desired setting. As shown in Figure 3.2a, the time

required for the pressure and flux profiles to stabilize is slightly longer for the constant flux condition. At the 27 minute mark, the mode of operation was switched back to constant TMP (set point = 45 kPa) and then it was switched to constant flux (at 41 minute mark) and back again to constant TMP (at 61 minute mark). It is interesting to note that across the three constant TMP conditions, there was a gradual decrease in the flux that was achieved from 159 to 153 to 148 LMH, which we hypothesize is likely due to membrane compaction effects. Since native (i.e. brand new) membranes were used in this study, further experiments are needed to be performed with fully compacted membranes to verify our hypothesis. Also, further experiments are required to distinguish compaction from fouling due to the presence of trace particulates and impurities in the feed solution since these two effects are often confounded [17,18].

After successfully demonstrating the concept of alternating between constant flux and constant TMP filtration, two sets of hydraulic permeability measurements were run for both operating modes using two adjacent columns of wells on the 96 well Omega^{TM} filter plate. Eight wells (i.e. eight independent measurements) were used for each set of permeability measurements. For the constant flux hydraulic permeability measurement, the TMPs were recorded for five distinct flux settings (72, 132, 192, 252 and 312 LMH, which correspond to flow rates of 30, 55, 80, 105 and 130 μL/min). The hydraulic permeability results are shown as the hatched bars in Figure 3.2b; the average hydraulic permeability (± standard deviation) was calculated as 1.1 (±0.2) $\times 10^{-12}$ m. For the constant TMP hydraulic permeability measurements, the flux values were recorded for five distinct TMP values (25, 35, 45, 55 and 65 kPa). The hydraulic permeability results

are shown as the solid bars in Figures 3.2b; the average hydraulic permeability (± coefficient of variation) was calculated as 1.2 (±0.2) $\times 10^{-12}$ m. The measured hydraulic permeabilities in the two operating were not statistically different (P-value > 0.05 in student's t-test); also the calculated hydraulic permeabilities are in good agreement with previous studies [1,19]. The error bar reported for each permeability measurement in Fig. 3.2b corresponds to the 95% confidence interval from the regression analysis of flux versus TMP profiles. The size of the error bars reported for wells B and D (constant TMP) and wells F-H (constant flux) was relatively large which can be due to the observed fluctuations in the flow rate readings. The observed well-to-well variations are comparable with those reported in the literature using similar setups [1,2,7] and are presumably due to the inherent differences between the membranes. In general, the variabilities observed in this study are quite reasonable compared to conventional filtration platforms.

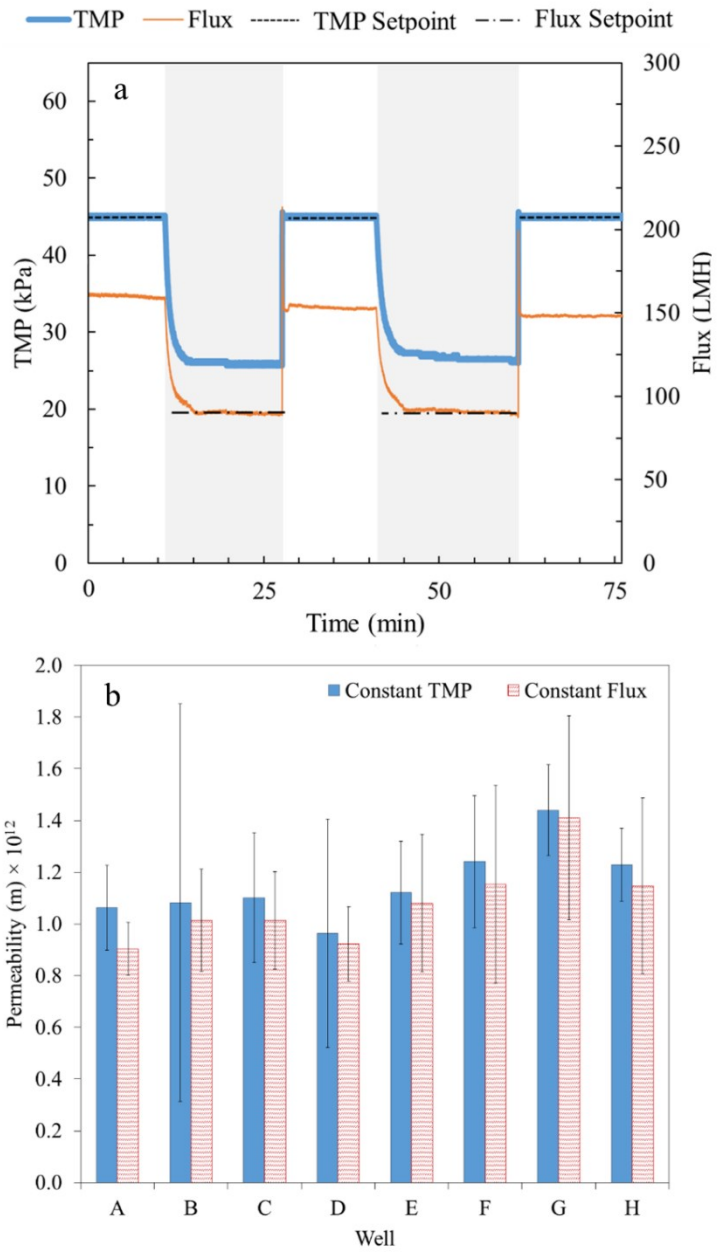

Fig 3.2. Typical TMP and flux profiles when alternating between constant flux and constant TMP modes of operation are shown in panel a; the unshaded and shaded sections correspond to the constant TMP and constant flux conditions respectively. Hydraulic permeability measurements for 30 kDa Omega™ membranes using the SWF module in the constant flux and constant TMP modes are shown in panel b; the error bars correspond to the 95% confidence interval from the regression analysis of flux versus TMP profiles.

3.4.2. Microscale Filtration Studies of Protein Solution at Constant TMP Mode

Further filtration experiments were performed with a single solute solution (0.25 mg/mL BSA solution) at two constant TMP conditions (25 kPa and 30 kPa) both with and without the stirring condition that is generated above the membrane surface by the lateral tumble stirrer. In general, the effect of stirring was found to be significant on the permeate flux profile especially at higher TMP values. Eight parallel experiments (four stirred and four unstirred) were performed at 25 kPa. The permeate flux significantly dropped in the unstirred experiments with a flux decline between 68 to 77%. However, the stirred flux profiles were not significantly affected during the filtration; two of the stirred fluxes remained constant while one flux increased around 8% and another flux, which had the lowest initial permeate flux, decreased around 22%. The results were quite stable and consistent except for one stirred channel which had the lowest initial flux. This could be due to the membrane pore size distribution of the well used for this experiment. A similar approach was used by running a constant TMP experiment at 30 kPa where the stirred flux profile was significantly different from the unstirred flux profile. For stirred experiments, the flux declined between 8 to 16%. However, a significant flux decline of 40 to 80% was observed for unstirred filtration experiments. The reason for the flux profile differences between stirred and unstirred experiments at constant TMP is typically attributed to the concentration polarization phenomena [16,20,21]. The initial rapid decrease in flux for unstirred filtration is known to be due to the rapid initial fouling of the membrane followed by a linear and slower decrease in flux in the next part of filtration. A similar phenomenon was reported for constant flux microscale filtration in

our previous work [1] where the TMP increase was a function of stirring conditions and operating flux. In that work, the maximum TMP in the unstirred wells were on average 7.5, 3.8, and 2.6 times higher than those in the stirred wells at fluxes of 12, 36, and 60 LMH respectively for BSA filtration through the Omega™ 30 kDa membrane. The differences between each condition studied was evaluated using a student's t-test. It was found that at 25 kPa, the final flux for the stirred condition (76.3±19.7 LMH) was significantly higher than the final flux for the unstirred condition (25.6 ± 9.0 LMH) with *P*-values ≤ 0.05. A similar trend was observed when comparing the final flux at 30 kPa where the final flux for the stirred condition (87.0 ± 9.8 LMH) was significantly higher than that of the unstirred condition (36.0 ± 11.5 LMH). This clearly shows the importance of stirring when performing experiments at different TMPs. All the errors were calculated based on the standard deviation. Furthermore, the final fluxes with the same stirring condition were compared to each other at different TMPs. For the stirred condition, it was found that the final fluxes from 25 and 30 kPa were not significantly different with a *P*-value > 0.05. A similar trend was observed for the unstirred condition, where no significant difference was observed between the final fluxes from 25 and 30 kPa (*P*-value > 0.05). Although a significant difference was not observed in the final flux by increasing the TMP for 5 kPa, further changes in the TMP may result in more significant changes in the final flux at other conditions which are not tested in this study.

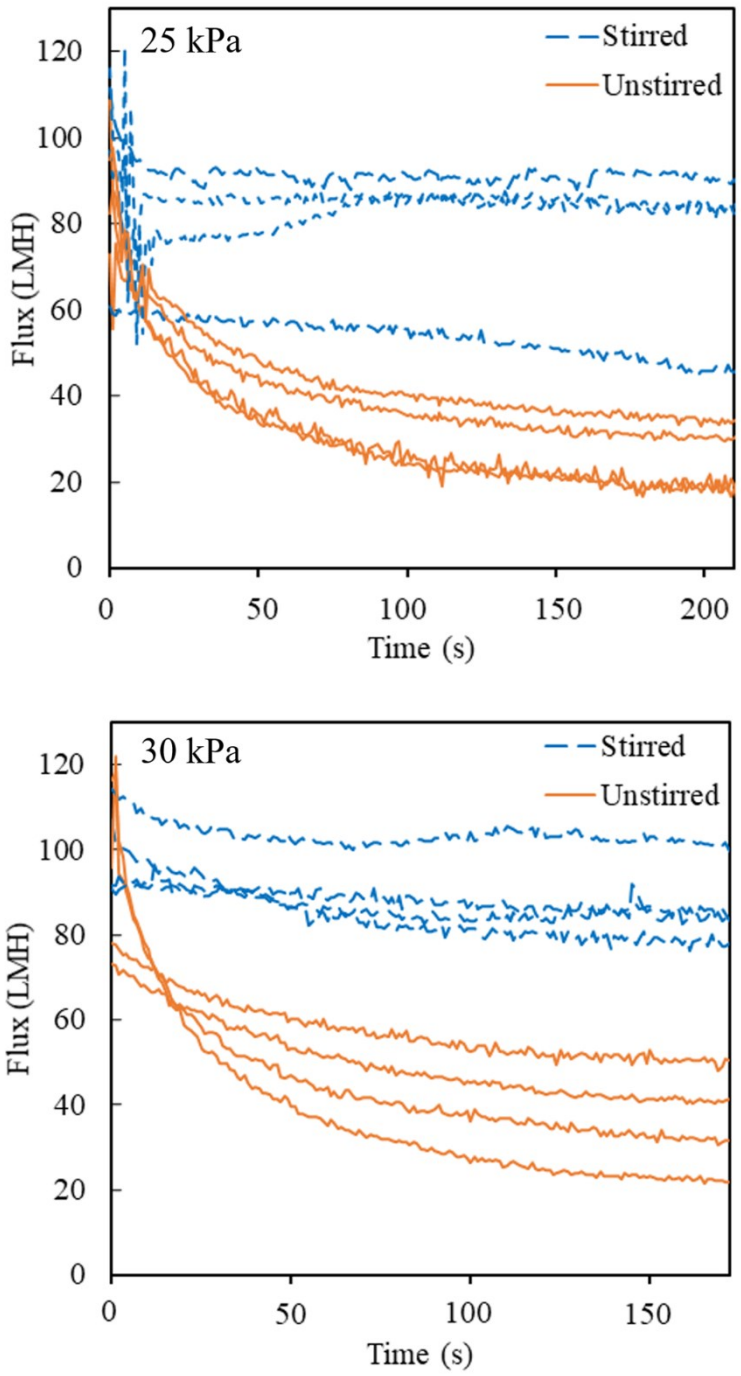

Fig 3.3. Permeate flux profiles during constant TMP filtration experiments (25 and 30 kPa) with BSA solution (0.25 mg/mL) and 30 kDa Omega™ membrane for both stirred (dashed line) and unstirred (solid line) conditions.

3.4.3. Microscale Bio-separation Studies at Constant TMP Mode

Eight parallel experiments (four with stirring and four without stirring) were performed in constant TMP mode (25 kPa) to demonstrate the usefulness of combining the SWF module with the MMFC system for bio-separations. The resulting flux profiles for stirred and unstirred filtration of the PEG-DEX mixture using the 30 kDa MWCO membrane are shown in Figure 3.4a. For the unstirred filtration condition, the flux rapidly declined to less than 10 LMH in a relatively short period of time (approximately 200 seconds) due most likely to concentration polarization effects. As such, it was impossible to collect a sufficient amount of the permeate sample at these conditions for GPC analysis. However, for the stirred filtration condition, the flux decline was more gradual over the entire duration of the experiment (1500 seconds) and thus the permeate, initial feed and retentate samples from each stirred well were subsequently analyzed by the GPC system; a typical set of the GPC chromatograms is shown in Figure 3.4c. The chromatogram for the initial feed sample displayed two distinct peaks; the broad first peak corresponds to the larger dextran molecule (MW = 200 kDa) and the sharp second peak corresponds to the smaller PEG molecule (MW = 4 kDa). The chromatogram for the permeate sample clearly showed that it contained only a small amount of dextran and nearly the full amount of PEG in the permeate sample. The chromatogram for the retentate sample showed much higher amounts of both molecules compared to the feed sample. An estimate of the apparent sieving coefficients for each molecule was made based on the resulting peak areas gave values of 3.3 (±0.8) % and 63.0 (±5.3) % for the dextran and PEG molecules respectively where the errors are calculated based on the

standard deviation. It is worth mentioning that the presence of PEG can affect the fouling behavior of PES membrane as reported in some of the previous studies [22–24]. However, detailed discussion in this regard is beyond the scope of this work. Similar separation experiments were performed using constant flux (30 LMH) mode (Figure 3.4b) to demonstrate the usefulness of the integration of the MMFC system in this case. It was observed that the system can maintain a constant flux during the binary separation with stirring and the set-point flux is maintained after 1500 seconds although fluctuations due to measurement errors of the flow sensors were observed due to the low flow rates used in this experiment.

Another model bio-separation was performed using α-lactalbumin and 250 kDa FITC-DEX. Six filtration experiments were performed in parallel using the MMFC system at a low (25 kPa) and high (35 kPa) constant TMP condition. Given the results shown in Figure 3.4a for the PEG-DEX mixture, all of the experiments were performed with stirring. The six individual flux profiles are shown in the top panels of Figure 3.5; the consistency across the triplicate testing for each TMP was quite good. The final value of the filtrate flux in the 35 kPa TMP experiments (71 ± 8 LMH) was significantly higher (P-value ≤ 0.05) than that for the 25 kPa TMP experiments (38 ± 10 LMH). The permeate and retentate samples were analyzed to quantify the apparent sieving coefficient (S_a) for the α-lactalbumin and FITC-DEX (Figure 3.5 g-l). For all samples, the S_a values for α-lactalbumin (82 (±21) % and 88 (±16) % for 25 and 35 kPa respectively) were significantly higher than those for the 250 kDa FITC-DEX (11 (±6) % and 14 (±5) % for 25 and 35 kPa respectively) which shows that the separation was quite successful. A

student's t-test was performed to determine the effect of TMP on the S_a values and concluded that there were no significant differences due to the change in TMP (all *P*-values > 0.05). All the errors were calculated based on the standard deviation.

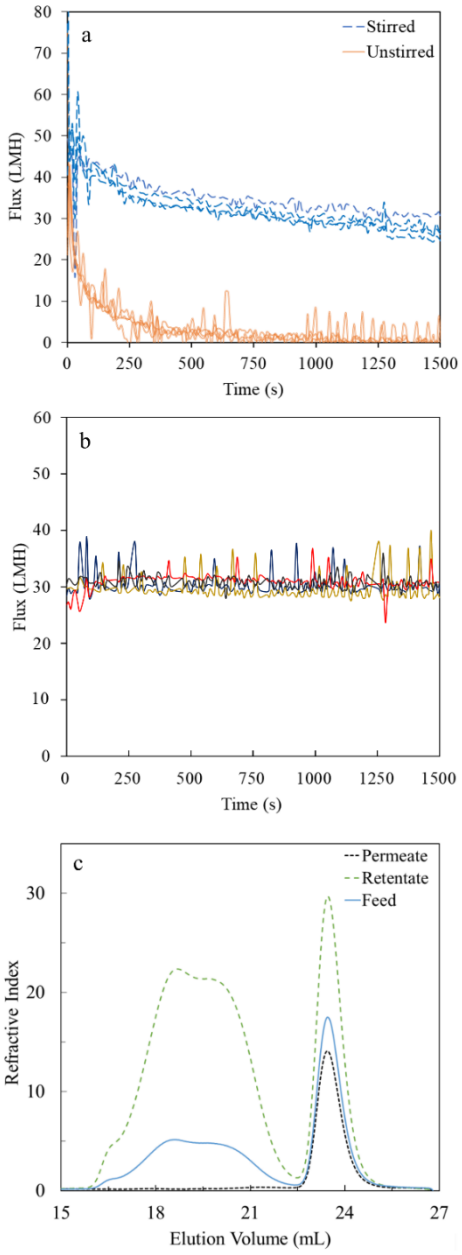

Fig 3.4. Filtration results for separation of mixture of PEG (2.5 mg/mL) and DEX (2.5 mg/mL) in 0.5 M $NaNO_3$ solution in CHES buffer using the 30 kDa Omega™ membrane and constant TMP (25 kPa) mode of operation. The permeate flux profiles for stirred (dashed line) and unstirred (solid line) experiments are shown in panel a. The flux profiles for the same binary separation experiment conducted with stirring in a constant flux (30 LMH) mode are shown in panel b. A sample set of GPC chromatograms for the feed, permeate and retentate samples from one of the stirred filtration tests (from panel a) is shown in panel c.

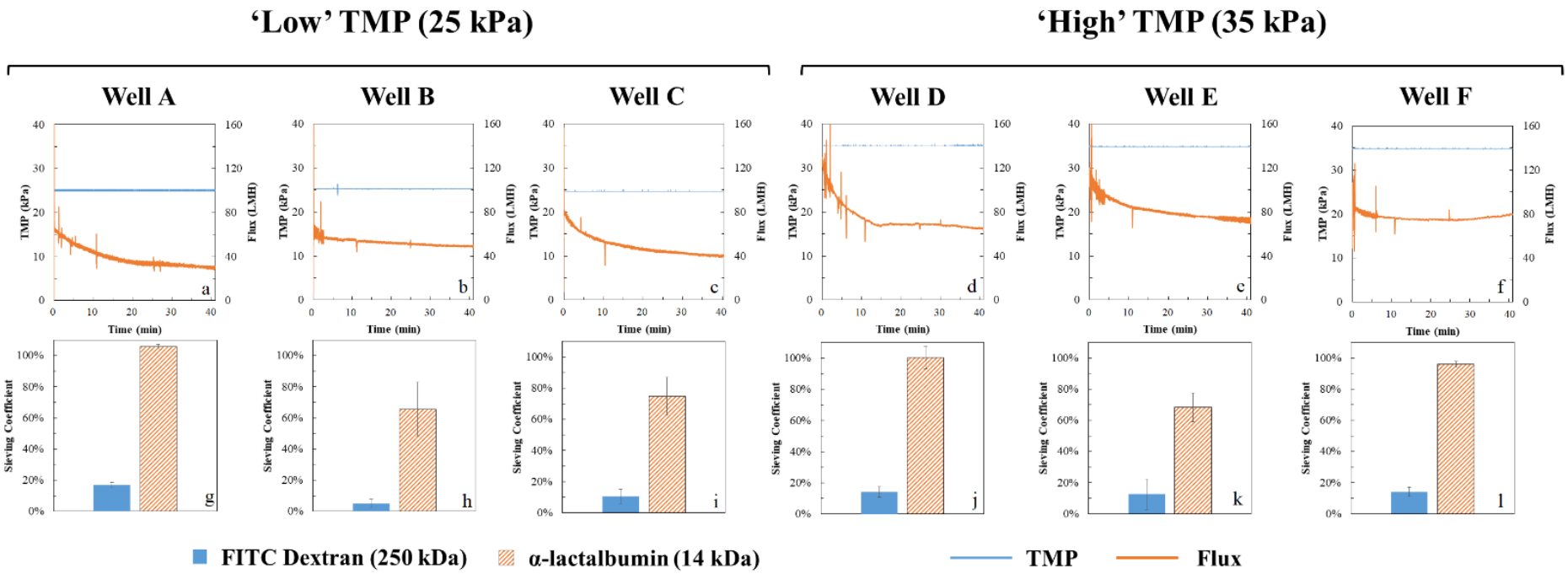

Fig 3.5. Filtration results for separation of mixture of FITC-DEX (0.1 mg/mL) and α-lactalbumin (0.1 mg/mL) in PBS buffer using a 30 kDa Omega™ membrane. The six panels on the left (a-c,g-i) correspond to constant TMP experiments at 25 kPa and the six panels on the right (d-f,j-l) correspond to constant TMP experiments at 35 kPa. The top six panels (a-f) display the TMP and permeate flux profiles. The bottom six panels (g-l) display the sieving coefficient results; the corresponding error bars were calculated from the collection of three permeate samples during each filtration experiment.

3.5. Conclusions

In this study, a multi-modal HT microscale filtration approach was developed by combining the MMFC system with the SWF technique. This strategy allows for up to eight microscale filtration experiments to be conducted in parallel in either constant TMP or constant flux and at different settings for each mode of operation. A summary of the key findings from this work are listed below:

- It was demonstrated that the operating mode can be switched from constant TMP to constant flux and vice versa in the middle of an experiment. The measurement of hydraulic permeability of the membrane was not affected by the mode of operation.
- As a proof of usefulness of the HT approach, single solute filtration and model binary separations were successfully performed in constant TMP mode. It was shown that stirring plays an important role in preventing flux decline and sample collection in constant TMP mode in HT format. A mixture of PEG (MW = 4 kDa) and dextran (MW = 200 kDa) was filtered under stirred and unstirred conditions at constant TMP. GPC analysis suggests a relatively successful separation for the samples collected with stirring. However, adequate sample volume for GPC analysis was not available due to the extensive flux decline under the unstirred conditions.
- A mixture of α-lactalbumin (MW = 14 kDa) and FITC-dextran (MW = 250 kDa) was separated at constant TMP. The S_a results demonstrated relatively successful separations under two different operating TMPs.

3.6. Acknowledgements

The funding for this work was provided by the Natural Sciences and Engineering Research Council of Canada (NSERC) in the form of a Discovery Grant (435646-2013 to DRL), a Research Tools and Instruments Grant (458744-2014 to DRL), and an Undergraduate Student Research Award (to MJL). We thank Dr. Nick Burke and Dr. Harald Stöver (Department of Chemistry at McMaster University) for their assistance with the GPC analysis of the samples.

3.7. References

[1] A.S. Kazemi, D.R. Latulippe, Stirred well filtration (SWF) – A high-throughput technique for downstream bio-processing, J. Membr. Sci. 470 (2014) 30–39.

[2] M. Chandler, A.L. Zydney, High throughput screening for membrane process development, J. Membr. Sci. 237 (2004) 181–188.

[3] A.S. Rathore, A. Shirke, Recent developments in membrane-based separations in biotechnology processes: review, Prep. Biochem. Biotechnol. 41 (2011) 398–421.

[4] M. Zhou, H. Liu, J.E. Kilduff, R. Langer, D.G. Anderson, G. Belfort, High Throughput Synthesis and Screening of New Protein Resistant Surfaces for Membrane Filtration, AIChE J. 56 (2010) 1932–1945.

[5] M. Zhou, H. Liu, J.E. Kilduff, R. Langer, D.G. Anderson, G. Belfort, High-throughput membrane surface modification to control NOM fouling., Environ. Sci. Technol. 43 (2009) 3865–71.

[6] M. Zhou, H. Liu, A. Venkiteshwaran, J. Kilduff, D.G. Anderson, R. Langer, et al., High throughput discovery of new fouling-resistant surfaces, J. Mater. Chem. (2011) 693–704.

[7] N. Jackson, J. Liddell, G. Lye, An automated microscale technique for the quantitative and parallel analysis of microfiltration operations, J. Membr. Sci. 276 (2006) 31–41.

[8] S. Kong, J. Aucamp, N.J. Titchener-Hooker, Studies on membrane sterile filtration

of plasmid DNA using an automated multiwell technique, J. Membr. Sci. 353 (2010) 144–150.

[9] A.S. Kazemi, K. Kawka, D.R. Latulippe, Optimization of biomolecule separation by combining microscale filtration and design-of-experiment methods, Biotechnol. Bioeng. 113 (2016) 2131–2139.

[10] A.D. Marshall, P.A. Munro, G. Trägårdh, The effect of protein fouling in microfiltration and ultrafiltration on permeate flux , protein retention and selectivity : A literature review, Desalination. 91 (1993) 65–108.

[11] A.D. Marshall, P.A. Munro, G. Trägårdh, Influence of permeate flux on fouling during the microfiltration of β-lactoglobulin solutions under cross-flow conditions, J. Membr. Sci. 130 (1997) 23–30.

[12] D.J. Miller, S. Kasemset, D.R. Paul, B.D. Freeman, Comparison of membrane fouling at constant fl ux and constant transmembrane pressure conditions, J. Membr. Sci. 454 (2014) 505–515.

[13] M. Decloux, L. Tatoud, Importance of the control mode in ultrafiltration: case of raw cane sugar remelt, J. Food Eng. 44 (2000) 119–126.

[14] L.N. Sim, Y. Ye, V. Chen, A.G. Fane, Comparison of MFI-UF constant pressure , MFI-UF constant flux and Crossflow Sampler-Modified Fouling Index, Water Res. 45 (2010) 1639–1650.

[15] D.C. Sioutopoulos, A.J. Karabelas, Correlation of organic fouling resistances in RO and UF membrane filtration under constant flux and constant pressure, J. Membr. Sci. 407–408 (2012) 34–46.

[16] D.M. Kanani, R. Ghosh, A constant flux based mathematical model for predicting permeate flux decline in constant pressure protein ultrafiltration, J. Membr. Sci. 290 (2007) 207–215.

[17] D.M. Bohonak, A.L. Zydney, Compaction and permeability effects with virus filtration membranes, J. Membr. Sci. 254 (2005) 71–79.

[18] E.K. Lee, V. Chen, A.G. Fane, Natural organic matter (NOM) fouling in low pressure membrane filtration - effect of membranes and operation modes, Desalination. 218 (2008) 257–270.

[19] W. Yuan, A.L. Zydney, Humic Acid Fouling during Ultrafiltration, Environ. Sci. Technol. 34 (2000) 5043–5050.

[20] R. Ghosh, Protein separation using membrane chromatography : opportunities and challenges, J. Chromatogr. A. 952 (2002) 13–27.

[21] M. Chudacek, A.G. Fane, The dynamics of polarisation in unstirred and stirred ultrafiltration, J. Membr. Sci. 21 (1984) 145–160.

[22] Z.L. Xu, F.A. Qusay, Effect of polyethylene glycol molecular weights and concentrations on polyethersulfone hollow fiber ultrafiltration membranes, J. Appl. Polym. Sci. 91 (2004) 3398–3407.

[23] B. Chakrabarty, A.K. Ghoshal, M.K. Purkait, Effect of molecular weight of PEG on membrane morphology and transport properties, J. Membr. Sci. 309 (2008) 209–221.

[24] A. Idris, N. Mat Zain, M.Y. Noordin, Synthesis, characterization and performance of asymmetric polyethersulfone (PES) ultrafiltration membranes with polyethylene glycol of different molecular weights as additives, Desalination. 207 (2007) 324–339.

Chapter 4 - Elucidation of Filtration Performance of Hollow-fiber Membranes via High-throughput Screening Platform

Authors: Amir S. Kazemi, Luke Boivin, Seung Mi Yoo, Raja Ghosh and David R. Latulippe

Published in Journal of Membrane Science 533 (2017) 241–249.

4.1. Preface

The work presented in this chapter introduces the development and application of the first ever high-throughput (HT) module for testing and optimization of the filtration performance of hollow-fiber (HF) membranes. As mentioned in chapters 1-3, a number of previous studies (including the works presented in chapters 2 and 3) have focused on the development of HT techniques that allow for performing multiple membrane filtration experiments in parallel using minimal amounts of sample. However, all of these studies have used flat sheet membranes in their HT module which is not be the most practical test format for many of filtration applications such as environmental separations[1]. In contrast to flat sheet membranes, HF membranes are widely used in the field of water and wastewater treatment, yet the fouling of HF membranes is a complex and ongoing challenge in the field. Therefore, the high-throughput hollow-fiber (HT-HF) module was developed for screening the effect of different factors on the filtration performance of HF

[1] For more information regarding different membrane configurations and test formats refer to section 1.2.2 of chapter 1.

membrane modules. This device can run up to six constant flux dead-end filtration tests simultaneously by using a small piece of HF membrane for each test. The usefulness of the HT-HF module platform was demonstrated by performing proof-of-concept experiments and evaluating the filtration performance and fouling behavior of polyvinylidenefluoride (PVDF) ultrafiltration (UF) membranes under different operating conditions using a range of HA solutions; each test condition was evaluated in triplicate. Overall, over 60 filtration experiments and 190 hydraulic permeability measurements were successfully performed in a manageable manner using this platform. This technique allows for a rapid and efficient screening of the fouling behavior of HF membranes and can be employed for the investigation of a wide variety of separation challenges involving HF membranes in the water and wastewater treatment field.

4.2. Introduction

Hollow-fiber (HF) membranes are the preferred configuration for various membrane-based water and wastewater treatment applications including pre-treatment for reverse osmosis processes, tertiary treatment of wastewater, and drinking water treatment. The advantages of HF membranes include the high packing density, self-supporting design (i.e. resistant to wall collapse), and the inherent ability to backwash the membrane. The fouling of HF membrane is a ubiquitous, but quite complex phenomenon that depends on various factors including the feed solution conditions, pre-treatment conditions, membrane material properties, and hydrodynamic conditions. Fouling has a severe effect

on membrane filtration performance as evident by either a reduction in membrane permeability (ratio of filtrate flux to applied pressure) and/or a decrease in filtrate quality.

Given the significance of membrane fouling, a wide variety of strategies have been proposed to mitigate its effects. Variations in membrane materials have been tested via either blending certain additives (e.g. copolymer [1], inorganic nanoparticles [2]) into the membrane during the manufacturing process or performing surface modification strategies on pre-formed membranes [3]. These strategies have been evaluated for a wide range of foulant materials including microorganisms [4–7], proteins [8–10], and natural organic matter [6,11,12]. Alternatively, a number of studies have proposed to control membrane fouling by adjusting the hydrodynamic conditions at the membrane surface via gas sparging [13,14], the creation of pulsatile flow conditions [15–17] , or adjusting the HF membrane geometry[18]; other less-conventional methods for fouling mitigation include the use of electrical [19] and magnetic fields [20]. Similarly, a significant level of work has been done to model membrane fouling in order to better understand the fouling mechanism with the most commonly used models based on pore blockage [21–23], pore constriction [22–24], or cake formation [25–27]; a combination of those mechanisms have been used to describe specific fouling events (Katsoufido et al. [23,25,28]). Despite all these efforts, membrane fouling control and mitigation is an ongoing challenge. Therefore, the study and optimization of HF membrane fouling is a major challenge in membrane-based water treatment systems.

The conventional approach to study HF membrane fouling is to use a single ‘pilot-scale’ or ‘lab-scale’ membrane module and run an extensive number of experiments in a

sequential fashion to determine the effect of various factors on membrane fouling and to elucidate the fouling mechanisms [4,5,29]. However, this approach limits the ability to run multiple experiments, to evaluate process reproducibility, and to optimize the process conditions in a cost-effective manner. For example, Decarolis et al. [30] studied the effect of operating flux, membrane cleaning and coagulant addition on the fouling behavior of 'pilot scale' membrane modules (each one containing approximately 2000 HF membranes for a total membrane surface area of 1.9 m^2) for tertiary wastewater filtration.

Thus, there exists a clear need for an advanced method to screen new HF membranes and fouling mitigation strategies for various water and wastewater treatment applications. Previous studies have demonstrated the usefulness of using a single HF membrane instead of a full membrane module [25,31–34]; however those studies required a dedicated experimental setup (e.g. pump, vessels, and tubing) for each membrane and thus still rely on a sequential test approach. In this work, we have developed the first ever high-throughput hollow-fiber (HT-HF) membrane module that uses a single experimental setup to run multiple HF tests in parallel. This platform was principally inspired by the development of microscale processing techniques in the biotechnology industry to accelerate process development work [35–37]. The method presented herein is adaptable to any HF membrane (both 'outside-in' or 'inside-out' configurations) and gives reproducible results to rapidly determine the membrane fouling propensity at a wide range of conditions and the effects of different flux recovery strategies (e.g. chemical cleaning/backwashing). The usefulness of such a HT approach has been proven for flat sheet membranes in dead-end [38–42] and cross-flow [43] formats with applications in

downstream bioprocessing [9,38–40,44] and environmental engineering processes [11,45]. A 'proof-of-concept' demonstration of the HT-HF module platform was made by evaluating the filtration performance and fouling behavior of polyvinylidenefluoride (PVDF) ultrafiltration membranes (nominal pore size of 0.04 μm) at various conditions using a range of humic acid (HA) solutions; each test condition was evaluated in triplicate to allow for statistical comparison of the results. In total, over 60 filtration experiments and 190 hydraulic permeability measurements are reported herein. The technique described in this work is shown to be superior to conventional strategies as it allows for a rapid and efficient way to screen the fouling properties of HF membranes for various applications.

4.3. Experimental

4.3.1. Materials

The HA solutions were prepared by dissolving either the HA sodium salt (from Sigma Aldrich) or the Suwannee River HA Standard II (from International Humic Substances Society) at concentrations from 100 to 300 ppm in deionized water from a Milli-Q system (MQ-water) or diluted phosphate buffered saline (PBS) solutions (from Corning). The average molecular weight of the Sigma and Suwannee HAs were determined to be 2.4 and 3.9 kDa respectively via gel permeation chromatography – refer to Fig. 4.S1 and the accompanying details in the Supporting Information section. The pH and conductivity of each HA solution was measured using an HI5522 pH/conductivity

meter (from Hanna Instruments). All the HA solutions were prepared, pre-filtered with a 0.2 μm Supor® syringe filter, and used for testing on the same day. Hydrophilic HF PVDF membranes from GE Power –Water and Process Technologies (0.04 μm nominal pore size) were used in all the filtration experiments. As per the manufacturer's suggestion, the membranes were pre-treated to remove the chemical agents used to preserve the membrane during storage and delivery by submerging them first in MQ-water at 40 °C for 3 hours, then in a 1:9 dilution of household bleach and MQ-water at 50 °C for 3 hours, and then finally again in MQ-water at ambient temperature for 18 hours.

4.3.2. High-throughput Hollow-fiber (HT-HF) Filtration Module

The HT-HF filtration module shown in Fig. 4.1 was designed to allow for six filtration sub-modules (designated as A through F in Fig. 4.1b), with each one using a single HF membrane, to be run in parallel. Each sub-module includes two compartments (identified as 3 and 6 in Fig. 4.1a) which are connected to each other via a short length of Tygon tubing (1/8" ID, 3/16" OD) and appropriate fluidic connectors. The exterior dimensions of the compartments were designed such that when six sub-modules are 'sandwiched' together, the outlet positions of both the filtrate line (via the three-way stopcock valve identified as 8 in Fig. 4.1a) and retentate line (via one-way stopcock valve identified as 7 in Fig. 4.1a) are perfectly aligned with the 6 wells in one row of a standard 24-well microplate (see Fig. 4.1b). This arrangement was the primary reason for choosing to run six experiments in parallel. It is possible to run more than six

experiments at once. For example, if an alternative sample collection method was used then ten experiments could be run at once using the same multi-rack syringe pump used in this study (see below for details); also, the use of a multi-channel peristaltic pump could allow for twenty to thirty different experiments to be conducted at once. In order to accommodate the valves for each sub-module, the assembly is arranged in a staggered configuration (see Fig. 4.1c) and thus both the filtrate and retentate samples are collected in a staggered pattern in the standard 24-well microplate.

Three-way stopcock valves (Nordson Medical) are used at both ends of the sub-module to be able to run in both 'outside-in' and 'inside-out' formats to perform filtration and backwashing of the membrane respectively; the HF PVDF membranes from GE Power –Water and Process Technologies operate via an 'outside-in' flow path. Any length of HF membrane can be used, however for this work the total available length of the PVDF membrane was 9 cm. The HF is sealed inside each sub-module using a specific combination of multiple washers and o-rings. Two multi-rack PHD Ultra (Harvard Apparatus) syringe pumps are used to perform the permeability tests, constant flux filtration tests, and backwashing steps. The following procedure was performed to eliminate air bubbles from each sub-module. First, MQ-water was loaded into 10 mL plastic syringes and connected to compartment A via a short length of Tygon tubing. Then 3 mL of MQ-water was flushed through each sub-module at 0.45 mL/min with the retentate valves (identified as 7 in Fig. 4.1a) in the open position. The retentate valves were then closed and an additional 3 mL of MQ-water passed through the HF membrane and collected via the filtrate lines. Finally, 3 mL of MQ-water was back-flushed through

the HF membrane at 0.2 mL/min. The transmembrane pressure (TMP) for each sub-module was monitored using individual pressure transducers (Omega Engineering PX26-030GV). The TMP signals were monitored using LabVIEW and recorded using a C series analog input data acquisition (DAQ) board (National Instruments) for post-processing.

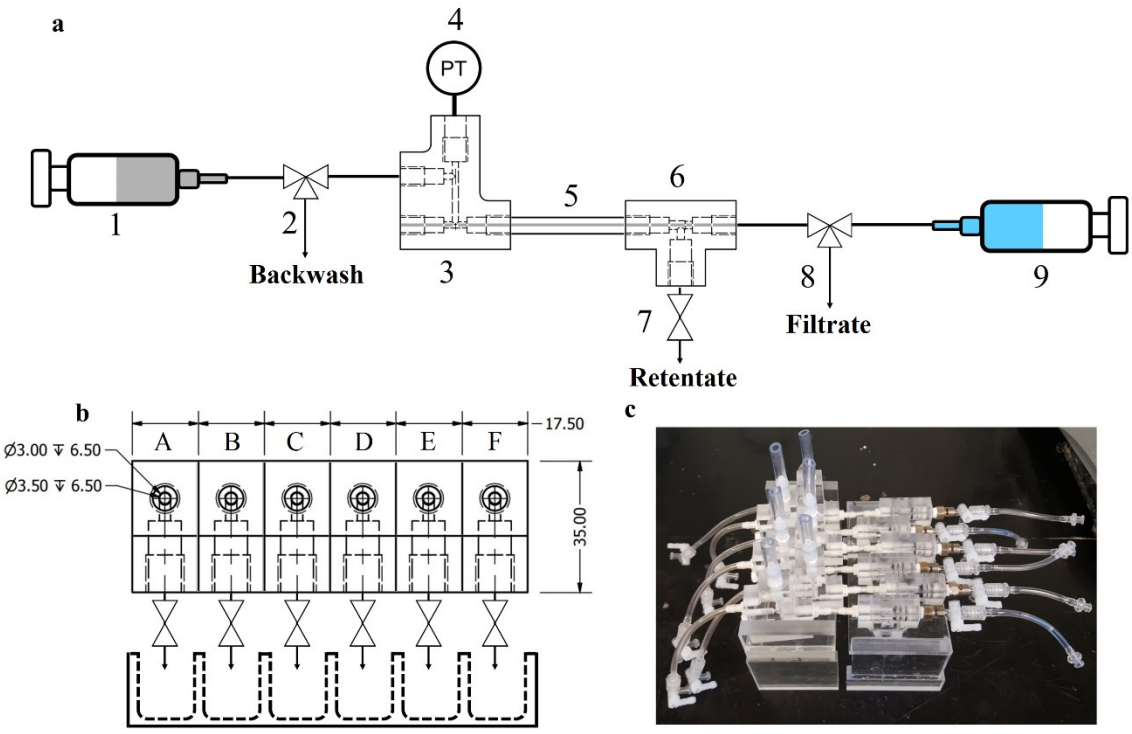

Fig. 4.1. Overview of the high-throughput hollow-fiber (HT-HF) module. a. Schematic of a single filtration sub-module with the following parts: 1) Standard syringe filled with appropriate solution for permeability or HA filtration tests. 2) Three way stopcock valve. 3) Compartment A. 4) Pressure transducer. 5) Tygon tubing with hollow-fiber membrane inside. 6) Compartment B. 7) One-way stopcock valve. 8) Three way stopcock valve. 9) Standard syringe filled with appropriate solution for the backwashing procedure. b. Overview of parallel filtration in six sub-modules (A-F) with sample collection in a 24-well plate; the listed dimensions are in mm units. c. Picture view of the experimental setup. Note that, the pressure transducers, the DAQ board, and the syringe pumps are not shown.

4.3.3. Humic Acid Filtration Experiments

All of the filtration tests were conducted at room temperature. The hydraulic permeability of the HF membrane was measured three times within the course of each filtration test; once before the filtration test (designated as L_{p0}), once after the filtration test (designated as L_p), and once after the backwash step (designated as $L_{p\text{-}BW}$). The same aqueous solution that was used to prepare the HA solution was used for the permeability measurement with the result calculated according to equation (4.1):

$$L_p = \frac{J}{\Delta P} \qquad (4.1)$$

where J is the filtrate flux (set via the multi-rack syringe pump) and ΔP is the transmembrane pressure (recorded by the pressure transducer).

The prepared HA solutions were loaded into 10 mL plastic syringes and connected to compartment A as described above. Initially, the retentate valves (identified as 7 in Fig. 4.1a) were opened and 3 mL of HA solution was purged through each sub-module to account for the dead volume (estimated as approximately 2 mL) from the syringe connection points. The set of six filtration experiments were conducted at filtrate fluxes of 20, 30 and 40 gallons/ft^2/day (GFD; note that 1 GFD corresponds to approximately 1.7 liters/m^2/h (LMH)) which correspond to flow rate values of 0.30, 0.45, and 0.60 mL/min. In order to compare TMP profiles for experiments done with different sections of the entire membrane, the recorded TMP values for each filtration test were multiplied by the ratio of the native hydraulic permeability measured for that particular membrane section to a reference hydraulic permeability (being the average L_{p0} of six experiments performed

with MQ-water). The retentate sample for each experiment was collected through the retentate valve by attaching an empty syringe to the first three-way stopcock valve (identified as 2 in Fig. 4.1a) and pushing in air to displace the bulk solution contents that were present on the feed side of the membrane. The 24-well microplates containing the filtrate and retentate samples were temporarily stored at 4 °C. The absorbance reading at 310 nm was measured for 150 µL aliquots of each filtrate and retentate sample using a UV-transparent 96-well plate and Tecan M1000 plate reader. Actual concentrations were determined by comparison with a ten-point calibration curve.

After each HA filtration test, a backwash step was performed by opening the first three-way stopcock valve and using a set of syringes on the second syringe pump to push the desired solution in an 'inside-out' configuration through each membrane at a flow rate of 0.2 mL/min for 15 minutes. For the majority of experiments, the solution used for this step was the exact same one as that used to prepare the HA solution. However, a subset of experiments were performed with sodium hypochlorite and citric acid solutions.

4.4. Results and Discussion

4.4.1. Parallel-based Evaluation of HF Membrane Filtration Performance

The reproducibility of the hydraulic permeability and HA sieving results obtained in the six sub-modules of the HT-HF system was very good. For example, as shown in Fig. 4.S2, the native hydraulic permeability (L_{p0}) for the six HF membranes ranged from 39.7 to 49.9 GFD/psi (equivalent to 0.00978 to 0.0123 LMH/Pa); the average permeability was

43.8 GFD/psi (0.0108 LMH/Pa) with a coefficient of variation of 10.6%. Note that the six membranes for this test were all taken from one specific section (approximately 0.8 m in length) of the entire membrane (approximately 40 m in length) that was provided by the manufacturer. The fouling behavior of the PVDF membrane is shown in the TMP profiles (Fig. 4.2a) that were obtained during the filtration of a technical grade HA solution (concentration of 100 ppm in PBS solution) at a filtrate flux of 30 GFD (flow rate of 0.45 mL/min). Each TMP profile starts at zero for zero filtrate volume because the LabVIEW program records the TMP immediately after the syringe pump is turned on to achieve the desired filtrate flux value. The TMP increases during the course of each filtration experiment. The slope of the TMP profile is considerably higher in all six runs in the initial part of the experiment (i.e. at cumulative filtration volumes less than 1 mL) than the final part of the experiment where the TMP increase is quite slow. Previous studies have reported a similar fouling behavior for protein [46] and HA [47] solutions, presumably due to the rapid initial fouling of the membrane. The reproducibility is quite good across the six filtration sub-modules that were run in parallel; the coefficient of variation (CV) was 7.2% at the maximum TMP. The filtration behavior of the membrane at those same conditions is represented by the apparent sieving coefficient (S_a):

$$S_a = \frac{C_f}{C_b} \times 100\% \qquad (4.2)$$

where C_f is the solute concentration in the filtrate (or alternatively known as C_p; solute concentration in the permeate) sample and C_b is the solute concentration in the bulk solution on the feed side; the apparent rejection coefficient (%) can be determined simply

as 100 - S_a. As shown in Fig. 4.2b, the apparent sieving coefficient results are plotted for the four consecutive filtrate samples (the volume for each one being 1.8 mL) that were collected in the 24-well microplate; the bulk solution concentration on the feed side for each filtrate sample was estimated by interpolation with respect to the cumulative filtered volume between the initial concentration and the final concentration in the collected retentate sample. The sieving coefficient results are quite consistent with the CV being less than 10% over the entire experiment. There is a dramatic increase in the apparent sieving coefficient between the first and second filtrate sample followed by a gradual increase with subsequent filtrate samples. This effect is primarily due to the 'dead volume' of approximately 0.5 mL between the retentate and filtrate valves in each sub-module. The sieving coefficient results for the 3rd and 4th filtrate samples are indistinguishable and thus will be used to compare the membrane performance at different filtration conditions. Although the filtration results within a short section of the entire HF membrane were quite consistent, there was a noticeable difference along the length of the entire membrane provided by the manufacturer. A total of 63 individual sections were tested in this study; hydraulic permeability measurements of the native (i.e. unfouled) membranes are shown in Fig. 4.S3. The average was 27.8 GFD/psi; the minimum and maximum values were 16.1 and 52.1 GFD/psi respectively – the exact cause for this variation is not currently known but it could be due to many different

factors including membrane pore size distribution, membrane pretreatment variations, and post-treatment of the membrane after the manufacturing process.

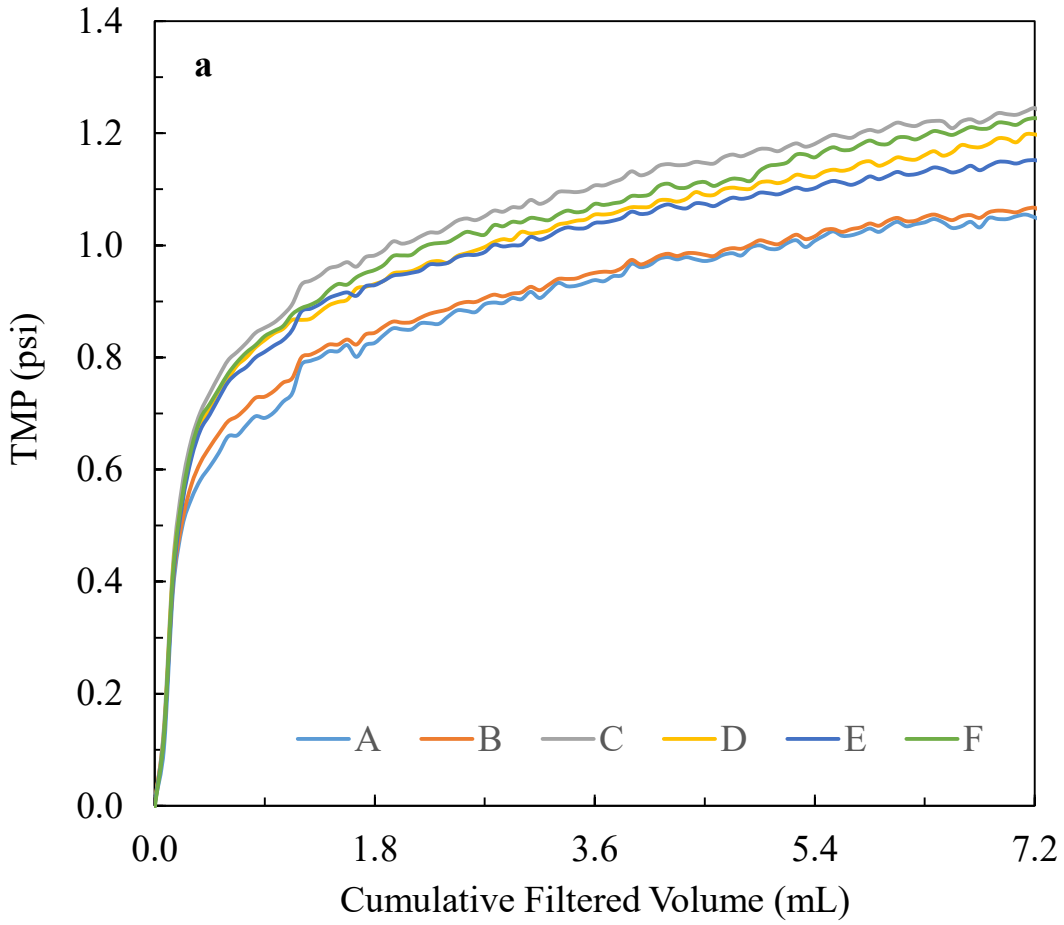

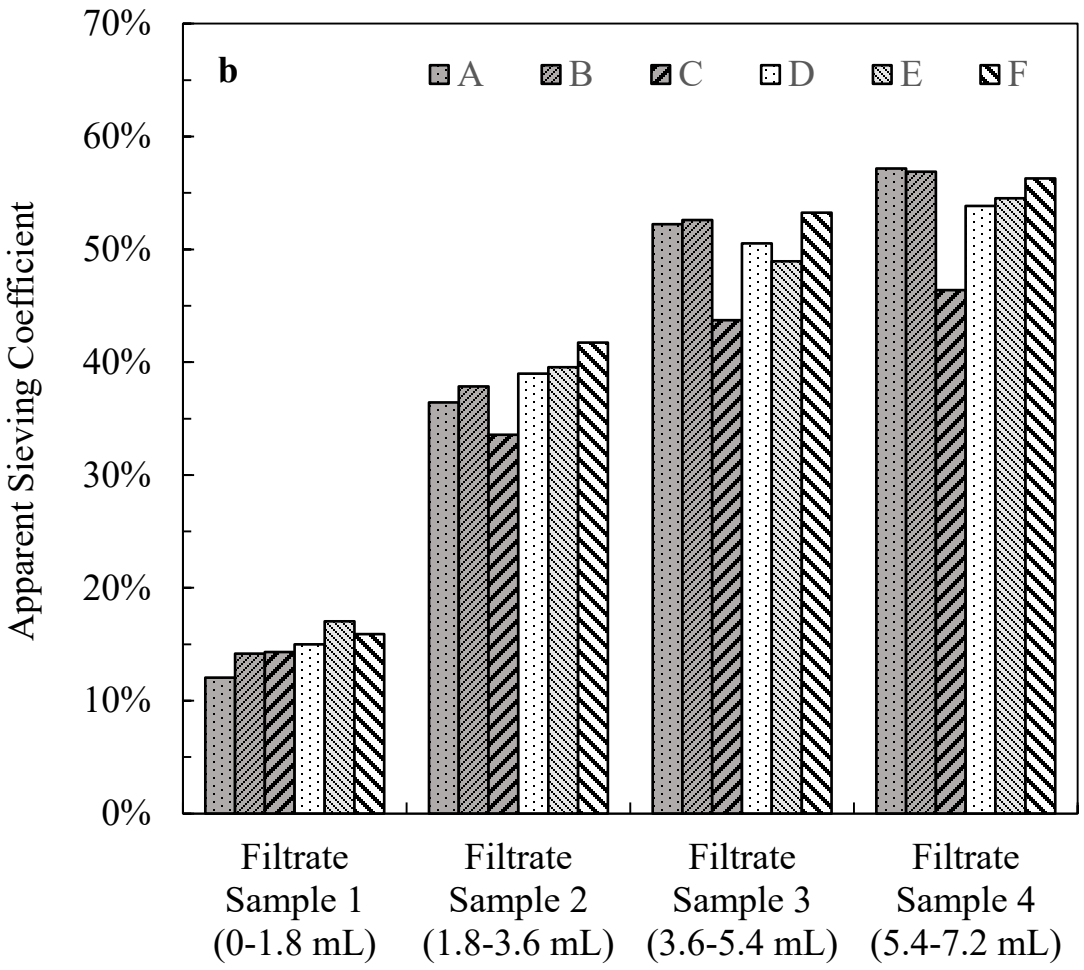

Fig. 4.2. Technical grade Sigma humic acid filtration (100 ppm in PBS) using HT-HF setup (in the six different sub-modules identified as A through F as per Fig. 4.1b) at a filtrate flux of 30 GFD (flow rate of 0.45 mL/min): a. Transmembrane pressure (TMP) profiles; b. Apparent sieving coefficient results.

4.4.2. Effect of Solution Conditions and Filtrate Flux on HF Membrane Filtration Performance

The design of the HT-HF system with the ability to run six separate filtration experiments in parallel is ideal for elucidating the effects of various process conditions on filtration performance. The effect of the solution conditions on HF membrane performance is shown in Fig. 4.3 for experiments conducted with the technical grade HA (concentration of 100 ppm) at a filtrate flux of 30 GFD. Each of the five different solution conditions (MQ-water, PBS solution, and three mixtures) were evaluated at a minimum in triplicate; the exact solution properties (pH and conductivity measurements) are listed in Table 4.1. All of those tests can be conducted in just four separate runs of the HT-HF system with each test requiring approximately 10 mL of solution. It was found that the solution conditions had a very significant effect on filtration performance both in terms of the filtrate quality and TMP profile. As shown in Fig. 4.3a, the apparent sieving coefficient for the fourth filtrate sample increased from 20% (± 2%) to 54% (± 5%) as the solution conditions changed from 5% PBS to 100% PBS. This is likely due to a change in extent of adsorption of HA on the membrane based on the solution condition[48] and not due to changes in size and shape of the HA at different solution conditions since the reported radius of gyration for HA (1 to 3 nm) [49] is much lower than the reported pore size (40 nm) for the membrane used in this study. There was a significant difference in the appearance of the post-filtration PVDF fibers from experiments conducted at different solution conditions; the membranes exposed to the HA solutions of higher conductivity and lower pH were observed to have a darker color (Fig. 4.3b). It is likely that this effect

is due to a lower extent of adsorption for solutions at the higher pH and lower conductivity condition [48] and hydrophobic interactions [26], however further experiments are needed to verify this hypothesis.

As shown by the TMP profiles in Fig. 4.3c, the fouling behavior of the PVDF membranes is significantly affected by the solution conditions. Each profile shown is the average TMP from at least 3 separate experiments that were run in parallel on the HT-HF system. The final TMP value increased from 1.3 to 2.2 psi as the HA solution conditions were changed from 100% PBS to 5% PBS; it is hypothesized that this is due to the higher extent of solute-membrane repulsions at the higher pHs and lower conductivities. Lastly, it is interesting to note that a strong correlation was found between the apparent sieving coefficient values and the recorded TMP values; as shown in Fig 4.S4, this correlation was found for the data corresponding to both the 3rd and 4th filtrate samples that were collected in each experiment. The three hydraulic permeability measurements that were made during each filtration test were used as an additional measure of the degree of membrane fouling at the various experimental conditions. Due to the variation in the hydraulic permeability of the native membrane before it was used in the filtration experiment (L_{p0}), the results shown in Fig. 4.3d are reported in terms of the relative hydraulic permeability after the filtration experiment (i.e. L_p/L_{p0}) and the relative hydraulic permeability after the backwash step (i.e. $L_{p\text{-}BW}/L_{p0}$). It is interesting to note the percent decrease in permeability after the filtration experiment was lowest for those performed with the HA in MQ-water; also at these conditions there was no evidence of fouling after the backwash step as the value of $L_{p\text{-}BW}/L_{p0}$ was 103% (± 8%). However,

this was not the case for the solutions containing even small amounts of PBS solution; the relative hydraulic permeability after backwashing ranged from 71% (for 10% PBS) to 85% (for 25% PBS). The entire collection of results that are provided by the HT-HF technique (including sieving coefficient data, TMP profiles, and hydraulic permeability results) clearly indicate the importance of the HA solution conditions on the fouling behavior of the PVDF membranes.

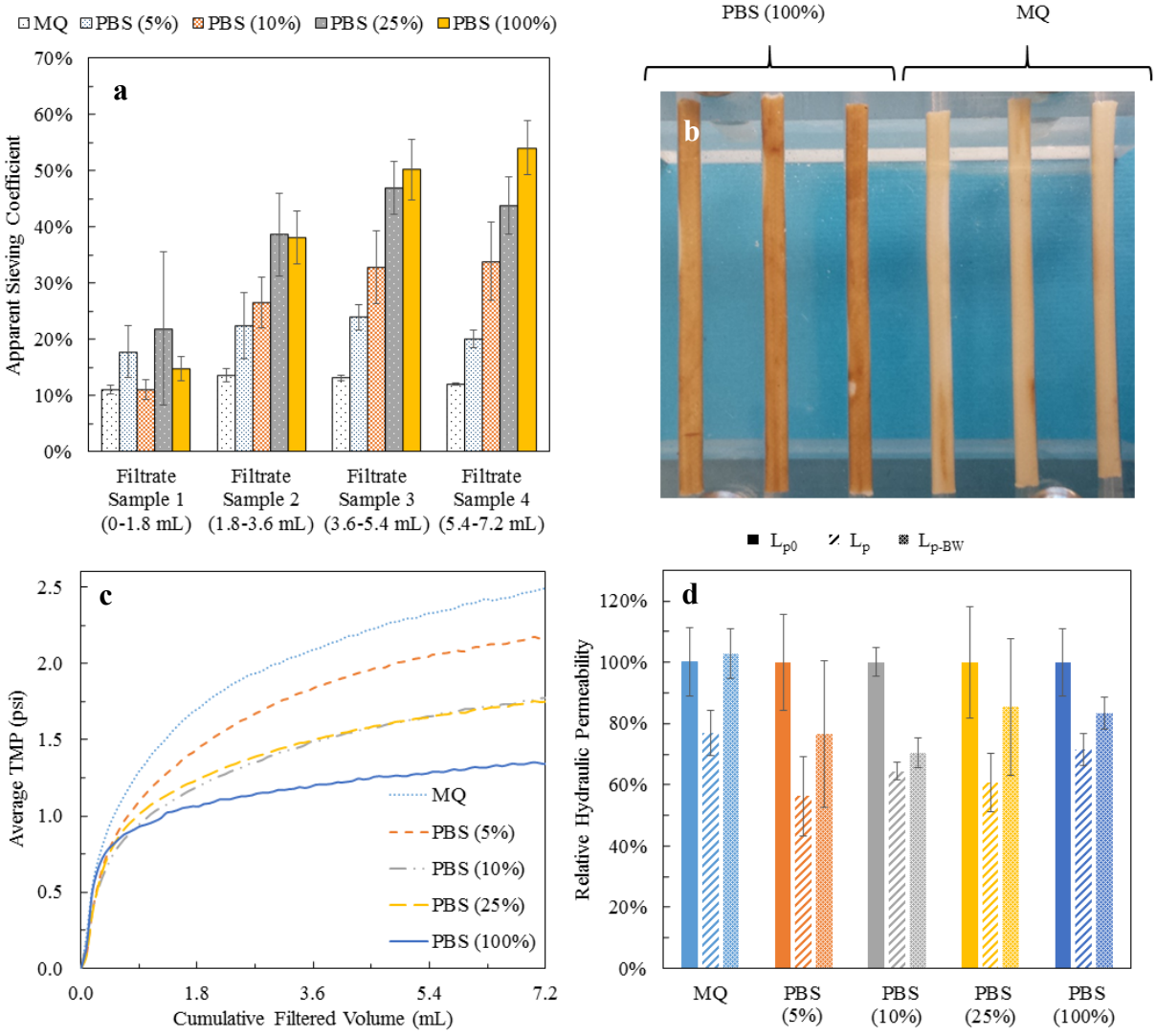

Fig. 4.3. Effect of solution condition (PBS ratio in MQ-water) on technical grade Sigma humic acid (100 ppm) filtration performance at a filtrate flux of 30 GFD (flow rate of 0.45 mL/min): a. Apparent sieving coefficient results with error bars corresponding to the standard deviation for the triplicate measurement at each experimental condition; b. Post-experimental image of six PVDF HF membranes that were used to study the effect of different solution conditions; c. Average transmembrane pressure (TMP) profiles, d. Comparison of changes in hydraulic permeability following the HA filtration experiments. The results were normalized by the hydraulic permeability of the native membrane (L_{p0}). The error bars were determined from the triplicate measurement at each experimental condition using standard propagation analysis.

Table 4.1. pH and conductivity measurements of technical grade Sigma humic acid solutions (100 ppm) with different ratios of PBS in MQ-water.

Solution Condition	Conductivity (mS/cm)	pH
MQ-water	0.12 ± 0.04	8.81 ± 0.11
PBS (5%)	0.98 ± 0.07	8.08 ± 0.03
PBS (10%)	1.89 ± 0.09	7.89 ± 0.04
PBS (25%)	4.51 ± 0.2	7.65 ± 0.05
PBS (100%)	16.8 ± 0.5	7.37 ± 0.05

The effect of the filtrate flux on the HF membrane performance was studied by running triplicate experiments at 20, 30, and 40 GFD (corresponding to flow rates of 0.30, 0.45 and 0.60 mL/min) with the technical grade HA solutions (concentration of 100 ppm) prepared in either MQ-water or PBS. As shown in Fig. 4.4a, the apparent sieving coefficient decreased with increasing filtrate flux at all the conditions tested. Similar behavior has been reported in the literature [50,51] however it is not possible to make a direct comparison to those results since the experiments were not performed under the same conditions. At all the fluxes, the same trend of significantly higher sieving coefficients was found for the experiments conducted with PBS. The fouling behavior of the PVDF membrane is shown via the TMP profiles in Fig. 4.4b. The greatest increase in TMP with filtrate volume was seen at the highest filtrate flux (40 GFD); the average final TMP values were 1.7 and 3.9 psi for the MQ-water and PBS solutions respectively. These results highlight the importance of optimization of the HF filtration experiments

considering the interactions between different factors, which can be performed rapidly using the HT-HF module.

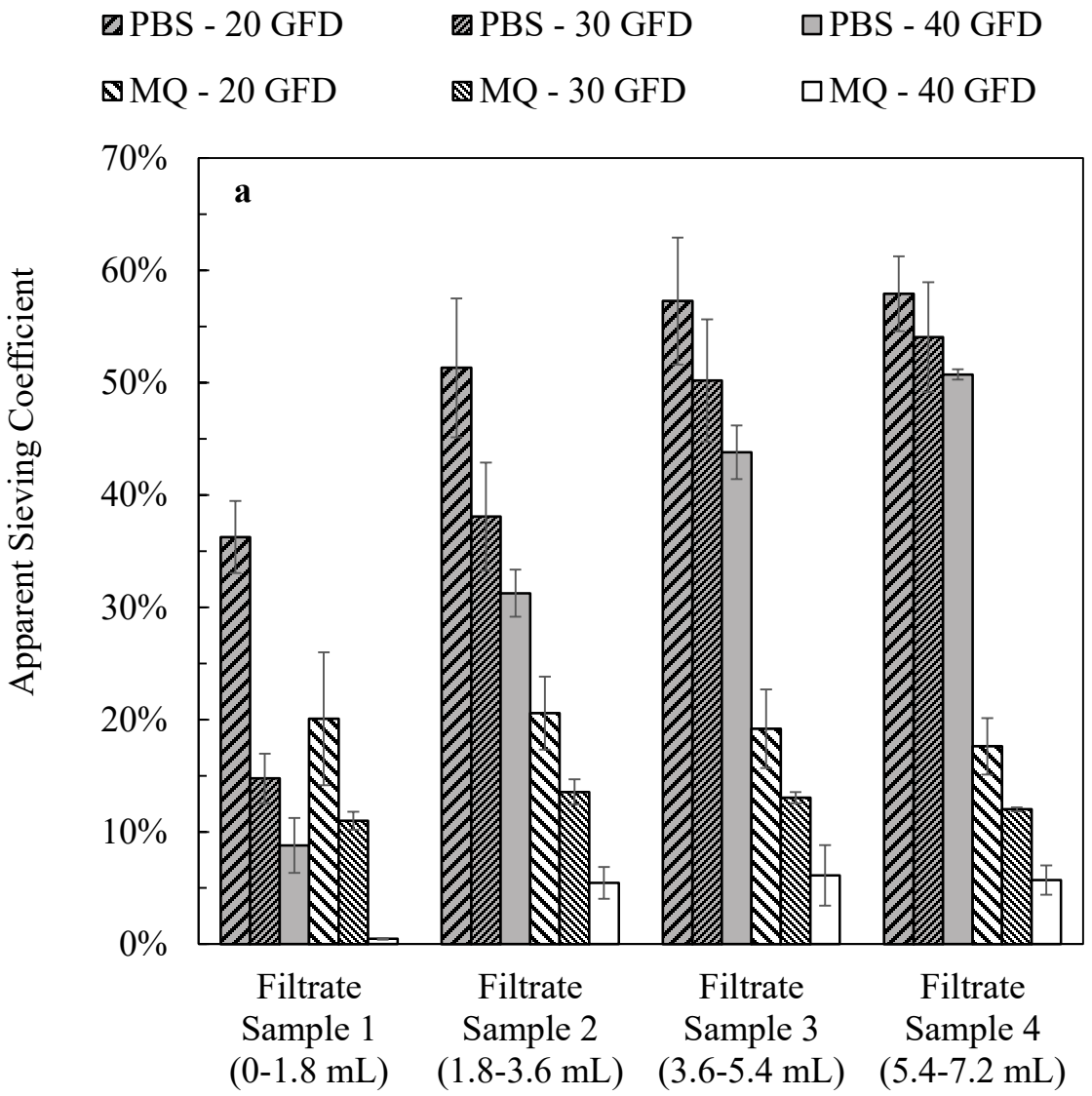

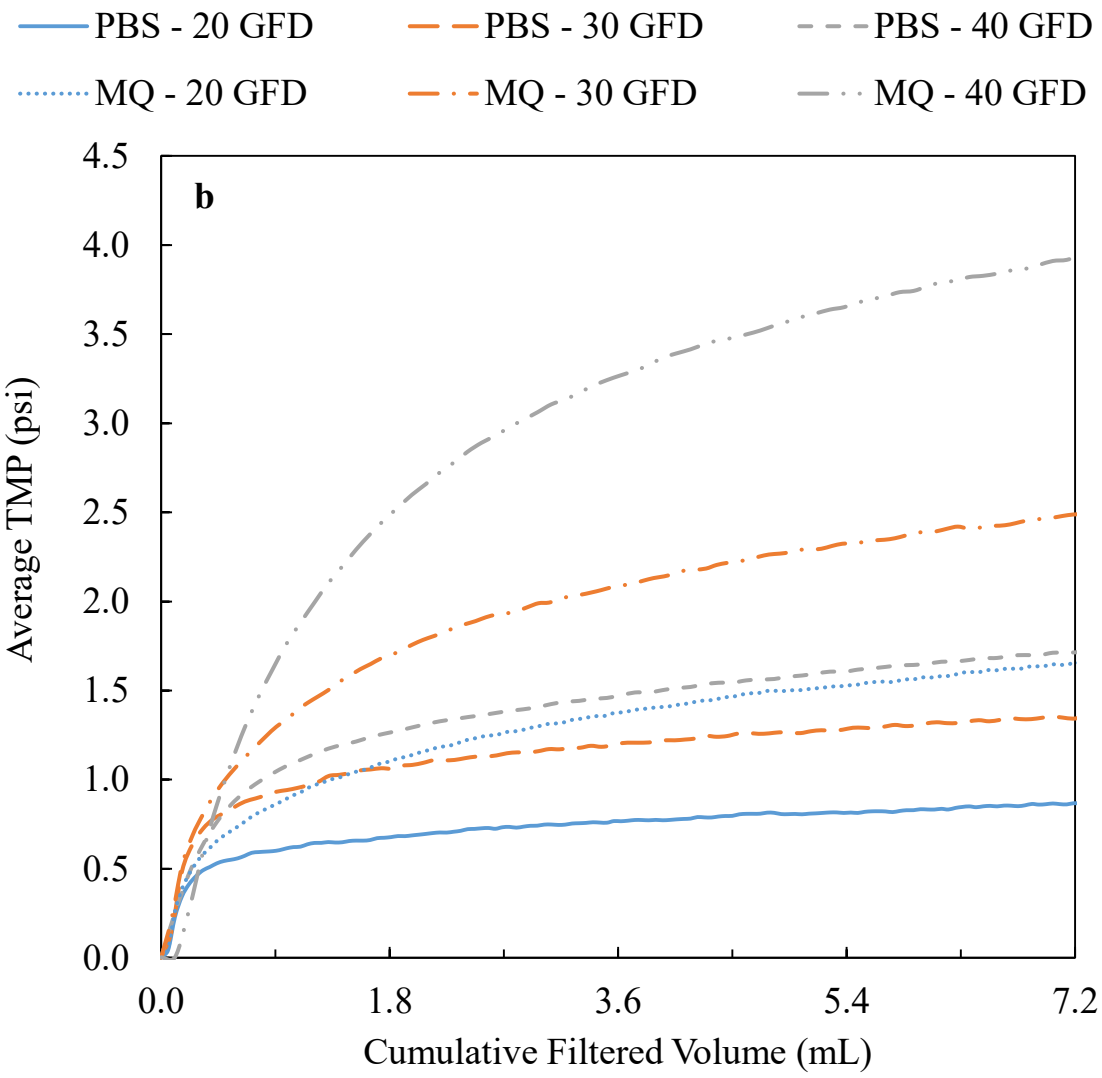

Fig. 4.4. Effect of filtrate flux on technical grade Sigma humic acid (100 ppm in PBS or MQ-water) filtration performance: a. Apparent sieving coefficient results with error bars corresponding to the standard deviation for the triplicate measurement at each experimental condition; b. Average transmembrane pressure (TMP) profiles.

4.4.3. Effect of HA Type and Concentration on HF Membrane Filtration Performance

In order to demonstrate the great potential of the HT-HF system for screening a variety of WW sources in membrane treatment processes, a comparison of the filtration behavior of two HA types (technical grade HA from Sigma and Suwannee River HA from the International Humic Substances Society) in different solution conditions was made. As shown in Fig. 4.5a, and as per the previous results, the reproducibility is excellent across the triplicate experiments that were conducted for each combination of HA type and solution condition. The S_a values for the tests performed with Suwannee River HA were significantly higher than those performed with technical grade HA. For example, for the fourth filtrate sample, S_a increases from 54% (± 5%) to 76% (± 6%) and from 12% (± 0%) to 27% (± 1%) when using Suwannee River HA instead of technical grade HA in PBS and MQ-water solutions respectively. Although the GPC characterization results (Fig. 4.S1) show that higher average molecular weight species are present in the Suwannee River HA, it is not believed that the measured size difference is the main reason for the difference in filtration performance. As per previous studies, we believe the observed difference is most likely due to structural differences between the two HA types. For example, the technical grade HA has a higher hydrophobicity [52] and conductivity [50] while the Suwannee River HA has a higher fraction of functional groups [53]. It is interesting to note that the trend observed with the TMP and apparent sieving coefficient results is in good agreement with those reported by Yuan and Zydney [50] in their study of HA filtration through ultrafiltration and microfiltration flat sheet

membranes. However, it is not possible to make a direct comparison of the results because of the many differences between the two studies including the membrane geometry, module type, and experimental conditions (e.g. constant flux versus constant pressure). The tests performed with Suwanee River HA showed the same effect of solution conditions as that previously reported for the technical grade HA; the S_a values for the PBS solution were 2.5 to 3.1 times higher than those for MQ-water. The fouling behavior of the PVDF membrane is shown in the average TMP profiles for the triplicate analysis for each combination of HA type and solution condition. (Fig. 4.5b). There was no difference in the TMP profiles for the experiments conducted in PBS solution, however there was a noticeable difference caused by the HA type for those tests conducted in MQ-water.

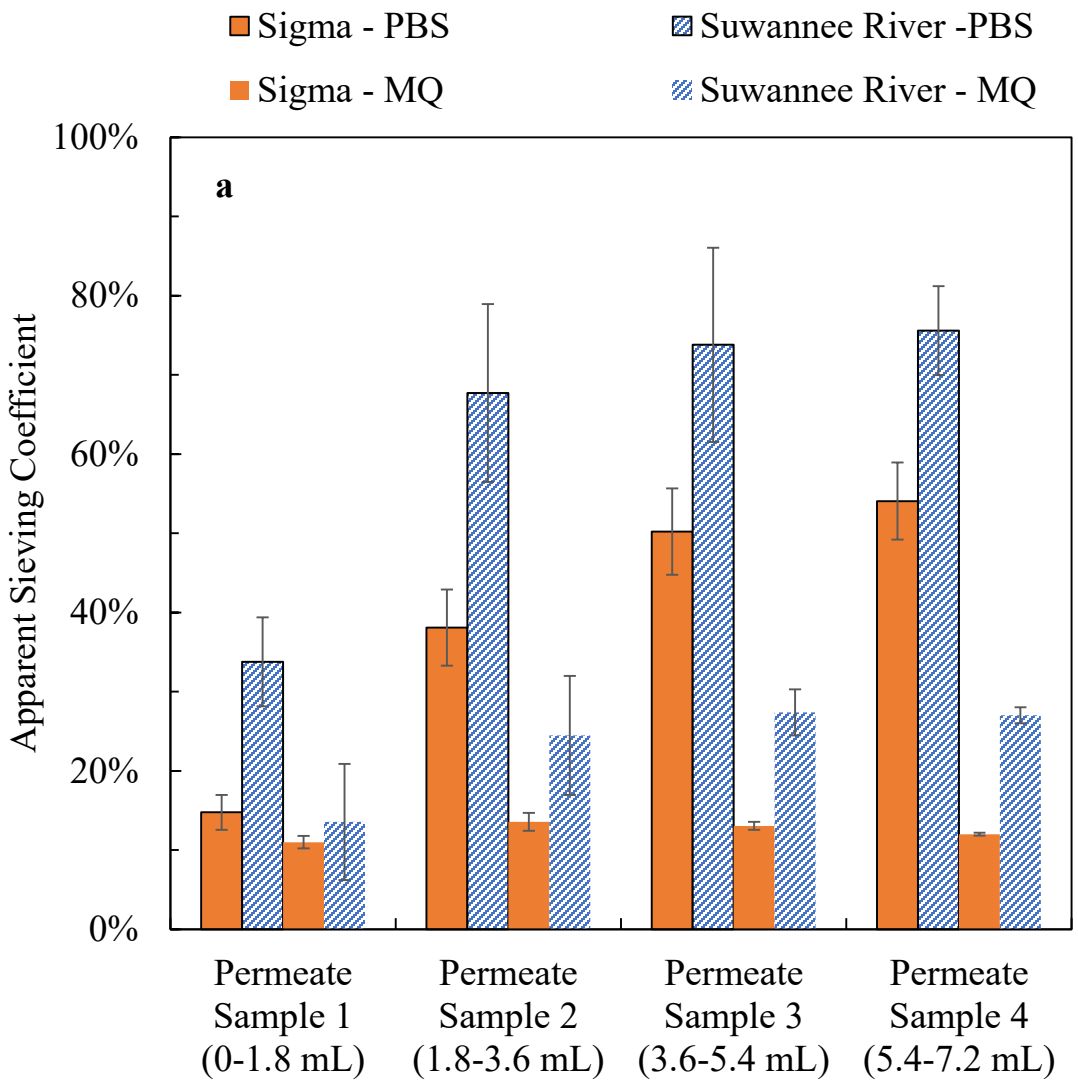
Sigma - PBS
Suwannee River -PBS
Sigma - MQ
Suwannee River - MQ
a
Apparent Sieving Coefficient
100%
80%
60%
40%
20%
0%
Permeate Sample 1 (0-1.8 mL)
Permeate Sample 2 (1.8-3.6 mL)
Permeate Sample 3 (3.6-5.4 mL)
Permeate Sample 4 (5.4-7.2 mL)

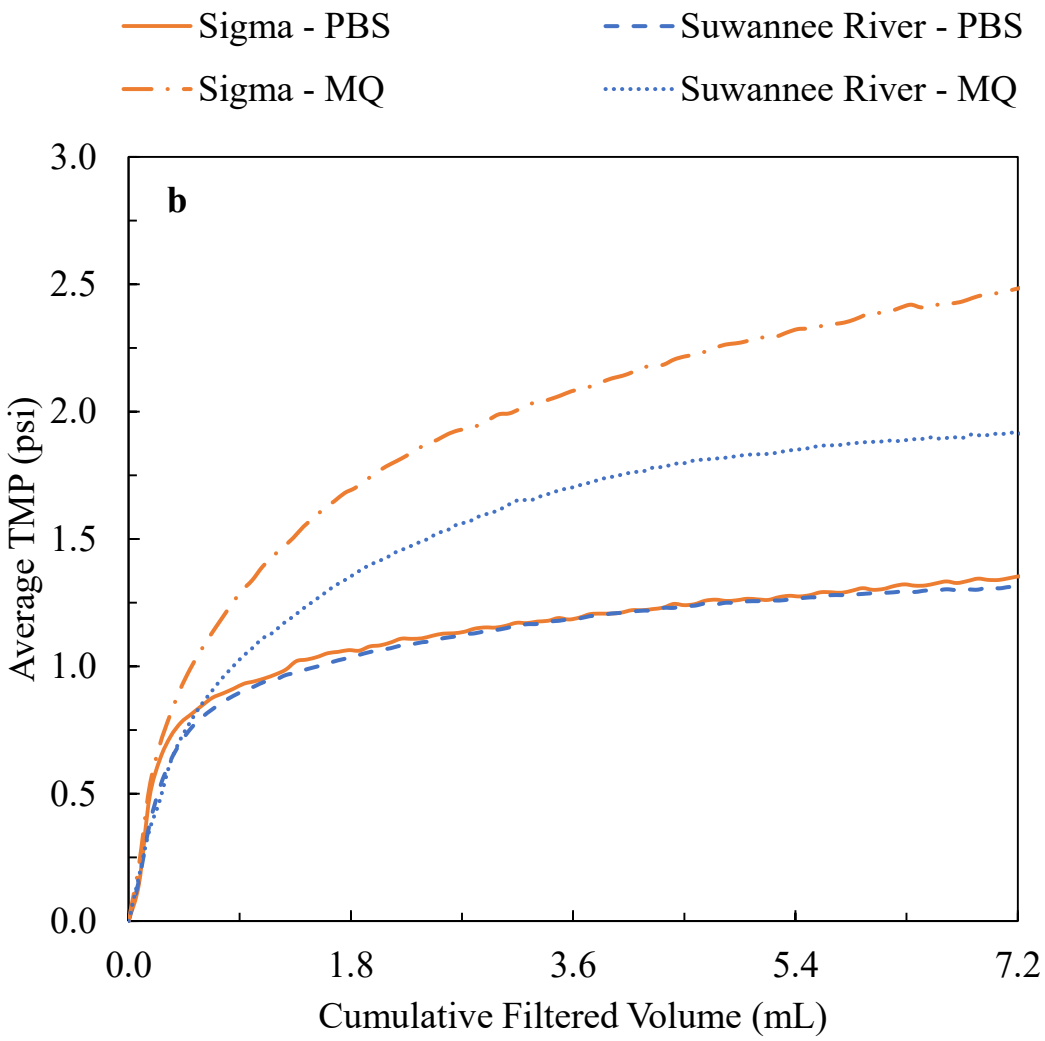

Fig. 4.5. Effect of humic acid type (technical grade Sigma humic acid and Suwannee River standard II humic acid) on filtration performance: a. Apparent sieving coefficient results with error bars corresponding to the standard deviation for the triplicate measurement at each experimental condition; b. Average transmembrane pressure (TMP) profiles. Each experiment was performed at a filtrate flux of 30 GFD (flow rate of 0.45 mL/min) using 100 ppm humic acid in water or PBS.

The effect of the concentration of the technical grade HA in both MQ-water and PBS on HF membrane performance is shown in Fig. 4.S5. The hydraulic permeability recovery results (Fig. 4.S5a) show that the change in HA concentration does not significantly affect the L_p recovery when HA is dissolved in PBS. However, for the experiments with HA solution in MQ-water, a lower L_p recovery (73 ± 5%) is observed at the highest feed concentration (300 ppm) possibly due to the higher extent of hydraulically irreversible adsorption. The TMP profiles shown in Fig. 4.S5b indicate that the concentration of HA significantly affects the TMP profile. The highest TMPs were observed when using 300 ppm of HA in MQ-water. Sieving coefficient results are in good agreement with previous observations; as shown in Fig. 4.S5, at each concentration, the values for tests performed with MQ-water are significantly lower than those for PBS solution.

4.4.4. Effect of Backwashing Solution Conditions on HF Membrane Filtration Performance

As the final demonstration of the capacity of the HT-HF system to optimize the filtration performance of HF membranes, solutions of different composition were used for the final backwashing step to evaluate the effect on hydraulic permeability recovery. For all of the previous results reported herein, the same solution used to dissolve the HA was also used for the backwash step but in this section each of the five different solutions (MW-water, bleach at two concentrations, citric acid at two concentrations) were

evaluated in triplicate for a total of fifteen experiments; conditions were recommended by the membrane supplier. According to Fig. 4.S5a, the experimental condition of 300 ppm HA solution in MQ-water at 30 GFD gave the lowest post-backwash relative hydraulic permeability (i.e. $L_{p\text{-}BW}/L_{p0}$). Therefore, this condition was used to evaluate the effect of each backwashing solution. It is worth noting that the relative hydraulic permeability after the filtration experiment (i.e. L_p/L_{p0}) was remarkably consistent across all fifteen experiments – the values ranged from 47.7% (± 1.3%) to 53.4% (± 1.8%). It was observed that the hydraulic permeability enhancement obtained by using 500 ppm bleach solution was not significantly different from the recovery obtained with MQ-water for backwashing (24% and 23% respectively). Increasing the bleach concentration to 1000 ppm resulted in a slight increase in the hydraulic permeability enhancement to 32%. However, a completely different behavior was observed by using citric acid as the backwashing solution. The hydraulic permeability enhancement was observed to be 85% and 92% for 2000 ppm and 5000 ppm citric acid respectively. For those cases, the hydraulic permeability of the post-backwashing membrane ($L_{p\text{-}BW}$) was higher than the hydraulic permeability of the native membrane (L_{p0}). While the exact reason for this behavior is not known, there are a number of possible reasons. First, as mentioned in the materials and methods section, all of the membranes were pretreated with a bleach solution to remove the chemical agents that preserve the membrane during storage. We believe that a pre-treatment step with citric acid will make the understanding of this phenomenon easier. Furthermore, the citric acid may have affected the properties of the

polymeric membrane considering that the concentration used here was higher than the bleach concentration. An expanded screening study is needed to confirm our hypothesis.

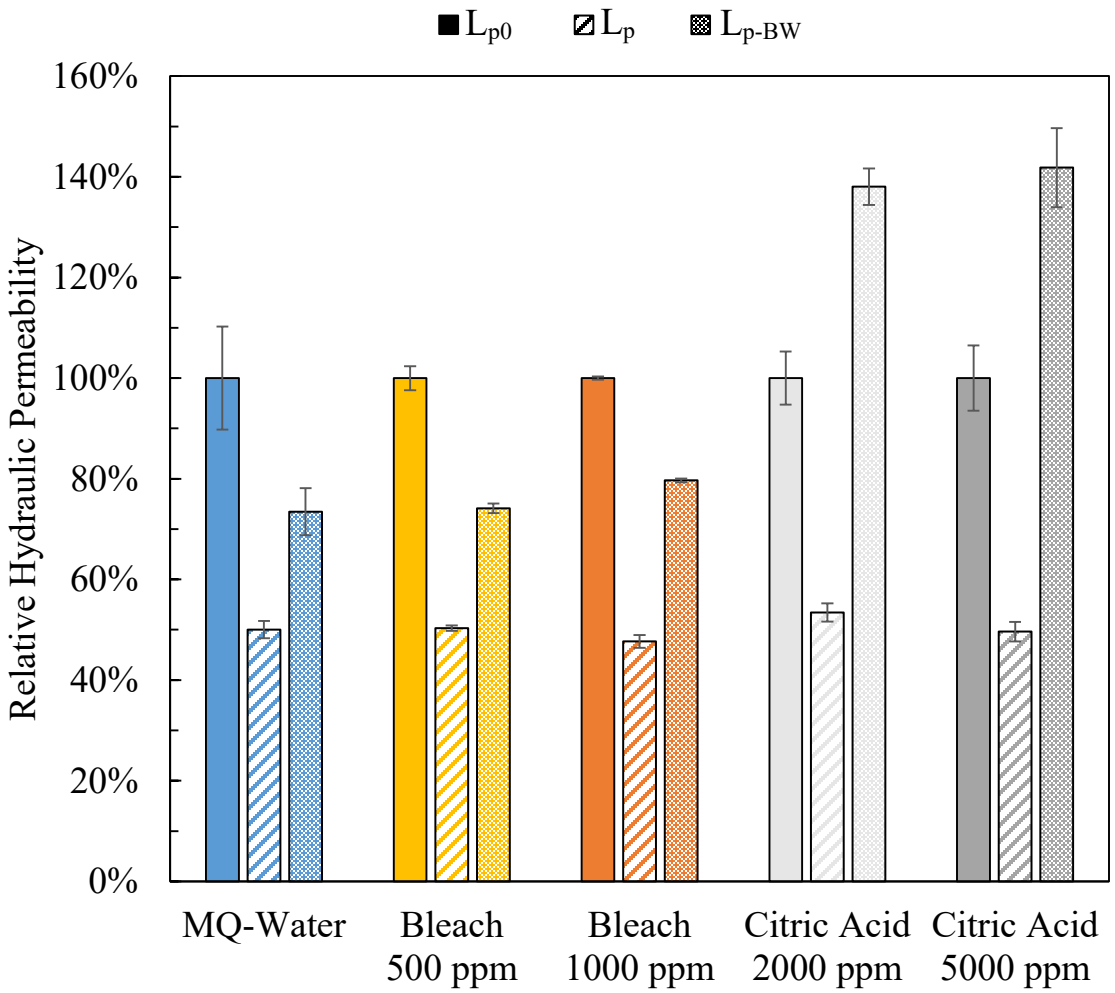

Fig. 4.6. Comparison of effect of backwashing solution properties on changes in hydraulic permeability following the HA filtration (300 ppm concentration of technical grade Sigma humic acid in MQ-water at a filtrate flux of 30 GFD (flow rate of 0.45 mL/min)). The results were normalized by the hydraulic permeability of the native membrane (L_{p0}). The error bars were determined from the triplicate measurement at each experimental condition using standard propagation analysis.

4.5. Conclusions

The HT-HF system described in this study is ideally suited for conducting an extensive amount of experimental work given its unique design that allows for six filtration experiments to be conducted in parallel. This parallel-processing approach can be applied to the investigation of a wide variety of environmental separations challenges including the testing and optimization of filtration process used in wastewater plants (e.g. effect of operating conditions and addition of different coagulants to wastewater on filtration performance [54,55]), the testing and fouling study of natural water filtration [29], and the screening of the fouling propensity in membrane bioreactors [56–59].

In order to demonstrate the utility of the HT-HF design, the effects of a wide range of operating factors on HA filtration through PVDF 'outside-in' HF membranes were studied in constant flux mode. The reproducibility of the results was studied by performing a number of hydraulic permeability measurement and sieving coefficient quantifications. It was clearly demonstrated that the solution conditions, foulant types, and backwashing conditions, both alone and in combination, can significantly affect the filtrate quality, the TMP and the hydraulic permeability recovery in HA filtration experiments. Overall, the entire collection of the data presented in this work give a detailed understanding of the role of processing conditions (filtrate flux, HA type/concentration, solution conditions) on the filtration performance of HF membranes.

4.6. Acknowledgements

The funding for this work was provided by NSERC Discovery Grant 435646-2013 (to DRL) and the Chambers Experiential Learning & Discovery Fund (to LB). We acknowledge Dr. Henk Koops and Dr. Nick Adams at GE Power & Water (Water & Process Technologies) for providing the HF PVDF membranes. We thank Paul Gatt and Dan Wright for their involvement in the manufacture and setup of the experimental system and the Biointerfaces Institute at McMaster University for access to equipment for sample analysis. We thank Dr. Nick Burke and Dr. Harald Stöver for GPC analysis of the different HA samples.

4.7. References

[1] F. Liu, Y.Y. Xu, B.K. Zhu, F. Zhang, L.P. Zhu, Preparation of hydrophilic and fouling resistant poly(vinylidene fluoride) hollow fiber membranes, J. Membr. Sci. 345 (2009) 331–339.

[2] L.Y. Yu, Z.L. Xu, H.M. Shen, H. Yang, Preparation and characterization of PVDF-SiO2 composite hollow fiber UF membrane by sol-gel method, J. Membr. Sci. 337 (2009) 257–265.

[3] S.S. Madaeni, S. Zinadini, V. Vatanpour, A new approach to improve antifouling property of PVDF membrane using in situ polymerization of PAA functionalized TiO2 nanoparticles, J. Membr. Sci. 380 (2011) 155–162.

[4] R.C. Kuhn, K.H. Oshima, Evaluation and optimization of a reusable hollow fiber ultrafilter as a first step in concentrating Cryptosporidium parvum oocysts from water, Water Res. 35 (2001) 2779–2783.

[5] H.A. Morales-Morales, G. Vidal, J. Olszewski, C.M. Rock, D. Dasgupta, K.H. Oshima, et al., Optimization of a reusable hollow-fiber ultrafilter for simultaneous concentration of enteric bacteria, protozoa, and viruses from water, Appl. Environ. Microbiol. 69 (2003) 4098–4102.

[6] F. Diagne, R. Malaisamy, V. Boddie, R.D. Holbrook, B. Eribo, K.L. Jones,

Polyelectrolyte and silver nanoparticle modification of microfiltration membranes to mitigate organic and bacterial fouling, Environ. Sci. Technol. 46 (2012) 4025–4033.

[7] A. Adout, S. Kang, A. Asatekin, A.M. Mayes, M. Elimelech, Ultrafiltration membranes incorporating amphiphilic comb copolymer additives prevent irreversible adhesion of bacteria, Environ. Sci. Technol. 44 (2010) 2406–2411.

[8] M. Taniguchi, G. Belfort, Low protein fouling synthetic membranes by UV-assisted surface grafting modification: varying monomer type, J. Membr. Sci. 231 (2004) 147–157.

[9] M. Zhou, H. Liu, J.E. Kilduff, R. Langer, D.G. Anderson, G. Belfort, High Throughput Synthesis and Screening of New Protein Resistant Surfaces for Membrane Filtration, AIChE J. 56 (2010) 1932–1945.

[10] B.D. McCloskey, H.B. Park, H. Ju, B.W. Rowe, D.J. Miller, B.J. Chun, et al., Influence of polydopamine deposition conditions on pure water flux and foulant adhesion resistance of reverse osmosis, ultrafiltration, and microfiltration membranes, Polymer. 51 (2010) 3472–3485.

[11] M. Zhou, H. Liu, J.E. Kilduff, R. Langer, D.G. Anderson, G. Belfort, High-throughput membrane surface modification to control NOM fouling., Environ. Sci. Technol. 43 (2009) 3865–71.

[12] H. Susanto, H. Arafat, E.M.L. Janssen, M. Ulbricht, Ultrafiltration of polysaccharide–protein mixtures: Elucidation of fouling mechanisms and fouling control by membrane surface modification, Sep. Purif. Technol. 63 (2008) 558–565.

[13] C. Cabassud, S. Laborie, L. Durand-Bourlier, J.M. Lainé, Air sparging in ultrafiltration hollow fibers: Relationship between flux enhancement, cake characteristics and hydrodynamic parameters, J. Membr. Sci. 181 (2001) 57–69.

[14] S.R. Bellara, Z.F. Cui, D.S. Pepper, Gas sparging to enhance permeate flux in ultrafiltration using hollow fibre membranes, J. Membr. Sci. 121 (1996) 175–184.

[15] R. Amar, B.B. Gupta, M.Y. Jaffrin, Apple Juice Clarification using Mineral Membranes: Fouling Control by Backwashing and Pulsating Flow, J. Food Sci. 55 (1990) 1620–1625.

[16] B.B. Gupta, P. Blanpain, M.Y. Jaffrin, Permeate flux enhancement by pressure and flow pulsations in microfiltation with mineral membranes, J. Membr. Sci. 70 (1992) 257–266.

[17] N. Hilal, O.O. Ogunbiyi, N.J. Miles, R. Nigmatullin, Methods Employed for Control of Fouling in MF and UF Membranes: A Comprehensive Review, Sep. Sci. Technol. 40 (2005) 1957–2005.

[18] S.P. Motevalian, A. Borhan, H. Zhou, A. Zydney, Twisted hollow fiber membranes

for enhanced mass transfer, J. Membr. Sci. 514 (2016) 586–594.

[19] C.-F. de Lannoy, D. Jassby, K. Gloe, A.D. Gordon, M.R. Wiesner, Aquatic Biofouling Prevention by Electrically Charged Nanocomposite Polymer Thin Film Membranes, Environ. Sci. Technol. 47 (2013) 2760–2768.

[20] G. Zin, F.M. Penha, K. Rezzadori, F.L. Silva, K. Guizoni, J.C.C. Petrus, et al., Fouling control in ultrafiltration of bovine serum albumin and milk by the use of permanent magnetic field, J. Food Eng. 168 (2016) 154–159.

[21] Z. Yang, Y.C. Juang, D.J. Lee, Y.Y. Duan, Pore blockage of organic fouling layer with highly heterogeneous structure in membrane filtration: Role of minor organic foulants, J. Membr. Sci. 411–412 (2012) 30–34.

[22] G. Bolton, D. LaCasse, R. Kuriyel, Combined models of membrane fouling: Development and application to microfiltration and ultrafiltration of biological fluids, J. Membr. Sci. 277 (2006) 75–84.

[23] Y.S. Polyakov, A.L. Zydney, Ultrafiltration membrane performance: Effects of pore blockage/constriction, J. Membr. Sci. 434 (2013) 106–120.

[24] Y.S. Polyakov, Pore constriction in ultrafiltration: A discrete multilayer deposition model with steric exclusion of solutes at the pore inlet, Theor. Found. Chem. Eng. 48 (2014) 382–396.

[25] K.S. Katsoufidou, D.C. Sioutopoulos, S.G. Yiantsios, A.J. Karabelas, UF membrane fouling by mixtures of humic acids and sodium alginate: Fouling mechanisms and reversibility, Desalination. 264 (2010) 220–227.

[26] D. Jermann, W. Pronk, S. Meylan, M. Boller, Interplay of different NOM fouling mechanisms during ultrafiltration for drinking water production, Water Res. 41 (2007) 1713–1722.

[27] Y.J. Choi, H. Oh, S. Lee, S.H. Nam, T.M. Hwang, Investigation of the filtration characteristics of pilot-scale hollow fiber submerged MF system using cake formation model and artificial neural networks model, Desalination. 297 (2012) 20–29.

[28] W. Yuan, A. Kocic, A.L. Zydney, Analysis of humic acid fouling during microfiltration using a pore blockage-cake filtration model, J. Membr. Sci. 198 (2002) 51–62.

[29] H. Huang, N. Lee, T. Young, A. Gary, J.C. Lozier, J.G. Jacangelo, Natural organic matter fouling of low-pressure, hollow-fiber membranes: Effects of NOM source and hydrodynamic conditions, Water Res. 41 (2007) 3823–3832.

[30] J. Decarolis, S. Hong, J. Taylor, Fouling behavior of a pilot scale inside-out hollow fiber UF membrane during dead-end filtration of tertiary wastewater, J. Membr. Sci. 191 (2001) 165–178.

[31] C.F. Lin, Y.J. Huang, O.J. Hao, Ultrafiltration processes for removing humic substances: Effect of molecular weight fractions and PAC treatment, Water Res. 33 (1999) 1252–1264.

[32] X.E. Lei, Impact of hydrodynamic conditions and membrane configuration on the permeate flux in submerged membrane systems for drinking water treatment, Ph.D. Dissertation, The University of British Columbia, Vancouver, BC, 2005.

[33] K. Katsoufidou, S.G. Yiantsios, A.J. Karabelas, A study of ultrafiltration membrane fouling by humic acids and flux recovery by backwashing: Experiments and modeling, J. Membr. Sci. 266 (2005) 40–50.

[34] K. Katsoufidou, S.G. Yiantsios, a. J. Karabelas, Experimental study of ultrafiltration membrane fouling by sodium alginate and flux recovery by backwashing, J. Membr. Sci. 300 (2007) 137–146.

[35] M. Bensch, B. Selbach, J. Hubbuch, High throughput screening techniques in downstream processing: Preparation, characterization and optimization of aqueous two-phase systems, Chem. Eng. Sci. 62 (2007) 2011–2021.

[36] M. Micheletti, G.J. Lye, Microscale bioprocess optimisation., Curr. Opin. Biotechnol. 17 (2006) 611–8.

[37] N.J. Titchener-Hooker, P. Dunnill, M. Hoare, Micro biochemical engineering to accelerate the design of industrial-scale downstream processes for biopharmaceutical proteins., Biotechnol. Bioeng. 100 (2008) 473–87.

[38] N. Jackson, J. Liddell, G. Lye, An automated microscale technique for the quantitative and parallel analysis of microfiltration operations, J. Membr. Sci. 276 (2006) 31–41.

[39] M. Chandler, A. Zydney, High throughput screening for membrane process development, J. Membr. Sci. 237 (2004) 181–188.

[40] A.S. Kazemi, D.R. Latulippe, Stirred well filtration (SWF) – A high-throughput technique for downstream bio-processing, J. Membr. Sci. 470 (2014) 30–39.

[41] P. Vandezande, L. Gevers, J. Paul, I. Vankelecom, P. Jacobs, High throughput screening for rapid development of membranes and membrane processes, J. Membr. Sci. 250 (2005) 305–310.

[42] S. Kong, J. Aucamp, N.J. Titchener-Hooker, Studies on membrane sterile filtration of plasmid DNA using an automated multiwell technique, J. Membr. Sci. 353 (2010) 144–150.

[43] A.C.M.E. Rayat, G.J. Lye, M. Micheletti, A novel microscale crossflow device for the rapid evaluation of microfiltration processes, J. Membr. Sci. 452 (2014) 284–293.

[44] A.S. Kazemi, K. Kawka, D.R. Latulippe, Optimization of biomolecule separation

by combining microscale filtration and design-of-experiment methods, Biotechnol. Bioeng. 113 (2016) 2131–2139.

[45] M.R. Bilad, P. Declerck, A. Piasecka, L. Vanysacker, X. Yan, I.F.J. Vankelecom, Development and validation of a high-throughput membrane bioreactor (HT-MBR), J. Membr. Sci. 379 (2011) 146–153.

[46] R. Ghosh, Study of membrane fouling by BSA using pulsed injection technique, J. Membr. Sci. 195 (2002) 115–123.

[47] W. Yuan, A.L. Zydney, Humic acid fouling during microfiltration, J. Membr. Sci. 157 (1999) 1–12.

[48] K.L. Jones, C.R. O'Melia, Protein and humic acid adsorption onto hydrophilic membrane surfaces: effects of pH and ionic strength, J. Membr. Sci. 165 (2000) 31–46.

[49] M. Kawahigashi, H. Sumida, K. Yamamoto, Size and shape of soil humic acids estimated by viscosity and molecular weight, J. Colloid Interface Sci. 284 (2005) 463–469.

[50] W. Yuan, A.L. Zydney, Humic Acid Fouling during Ultrafiltration, Environ. Sci. Technol. 34 (2000) 5043–5050.

[51] S. Saha, C. Das, Analysis of Fouling Characteristics and Flux Decline during Humic Acids Batch Ultrafiltration, J. Chem. Eng. Process Technol. 6 (2015).

[52] P. MacCarthy, R.L. Malcolm, I. The Nature of Commercial Humic Acids, in: Suffet, I. H., MacCarthy, P., Eds, Aquatic humic substances: influence on fate and treatment of pollutants, American Chemistry Society, Washington, DC, 1989.

[53] C.T. Chiou, D.E. Kile, T.I. Brinton, R.L. Malcolm, J.A. Leenheer, P. MacCarthy, A comparison of water solubility enhancements of organic solutes by aquatic humic materials and commercial humic acids, Environ. Sci. Technol. 21 (1987) 1231–1234.

[54] K. Konieczny, D. Sakol, M. Bodzek, Efficiency of the hybrid coagulation-ultrafiltration water treatment process with the use of immersed hollow-fiber membranes, Desalination. 198 (2006) 102–110.

[55] A.W. Zularisam, A.F. Ismail, M.R. Salim, M. Sakinah, T. Matsuura, Application of coagulation-ultrafiltration hybrid process for drinking water treatment: Optimization of operating conditions using experimental design, Sep. Purif. Technol. 65 (2009) 193–210.

[56] P. Le-Clech, V. Chen, T.A.G. Fane, Fouling in membrane bioreactors used in wastewater treatment, J. Membr. Sci. 284 (2006) 17–53.

[57] A. Drews, Membrane fouling in membrane bioreactors-Characterisation, contradictions, cause and cures, J. Membr. Sci. 363 (2010) 1–28.

[58] S. Chang, Application of submerged hollow fiber membrane in membrane bioreactors: Filtration principles, operation, and membrane fouling, Desalination. 283 (2011) 31–39.

[59] F. Meng, S.R. Chae, A. Drews, M. Kraume, H.S. Shin, F. Yang, Recent advances in membrane bioreactors (MBRs): Membrane fouling and membrane material, Water Res. 43 (2009) 1489–1512.

4.8. Supporting Information

Gel permeation chromatography (GPC)

Gel permeation chromatography (GPC) was used to estimate the average molecular weight of the humic acids (HAs). The GPC system consists of three columns in series: Waters Ultrahydrogel-120, -250 and -500; 30 cm length × 7.8 mm internal diameter. The nominal fractionation range of the columns is between 100 and 400,000 Da. The solvent phase used for the GPC system was a 0.5 M $NaNO_3$ solution in 2-(Cyclohexylamino)ethanesulfonic acid buffer with pH 10. The samples were prepared with a HA concentration of 1 mg/mL using the aforementioned solvent. All the HA solutions were pre-filtered with a 0.2 μm Supor® syringe filter prior to injection (injection volume of 80 μL). The average molecular weight was calculated based on refractive index (RI) intensity and the retention time. The calibration curve was made by using polyethylene glycol (PEG) standards. The average molecular weights were calculated as 2.4 and 3.9 kDa for the technical grade and the Suwannee River HAs respectively from Fig. 4.S1.

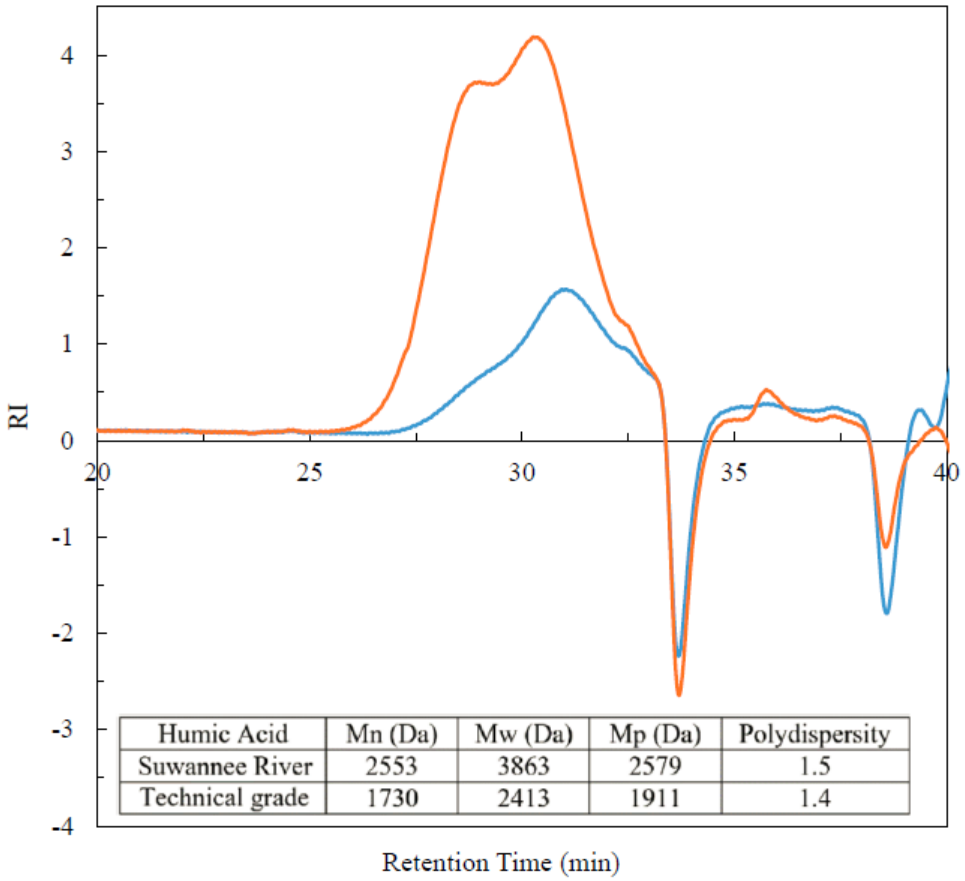

Humic Acid	Mn (Da)	Mw (Da)	Mp (Da)	Polydispersity
Suwannee River	2553	3863	2579	1.5
Technical grade	1730	2413	1911	1.4

Fig. 4.S1. GPC analysis for technical grade and Suwannee River humic acids. Number-average molecular weight, weight-average molecular weight and peak molecular weight are shown by Mn, Mw and Mp respectively.

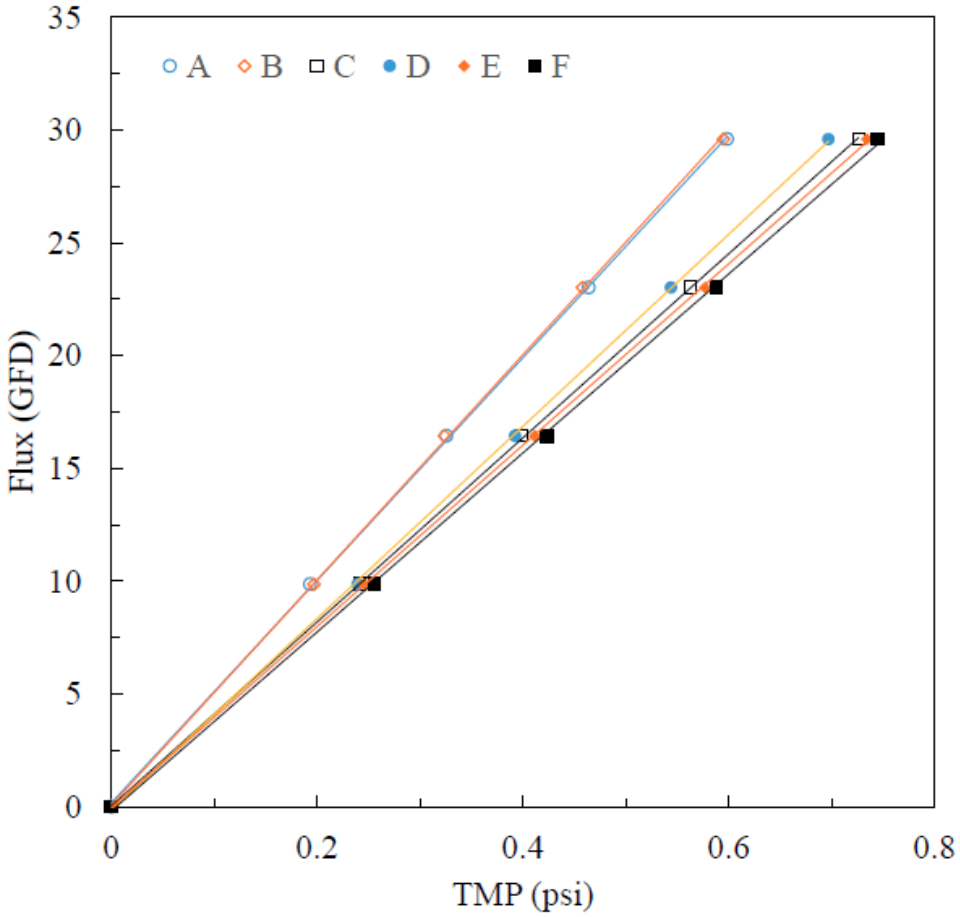

Fig. 4.S2. Flux vs transmembrane pressure (TMP) plotted for the six filtration experiments associated with the results shown in Figure 4.1; the best fit straight line for each data series gives the native membrane hydraulic permeability (L_{p0}) according to equation (4.1).

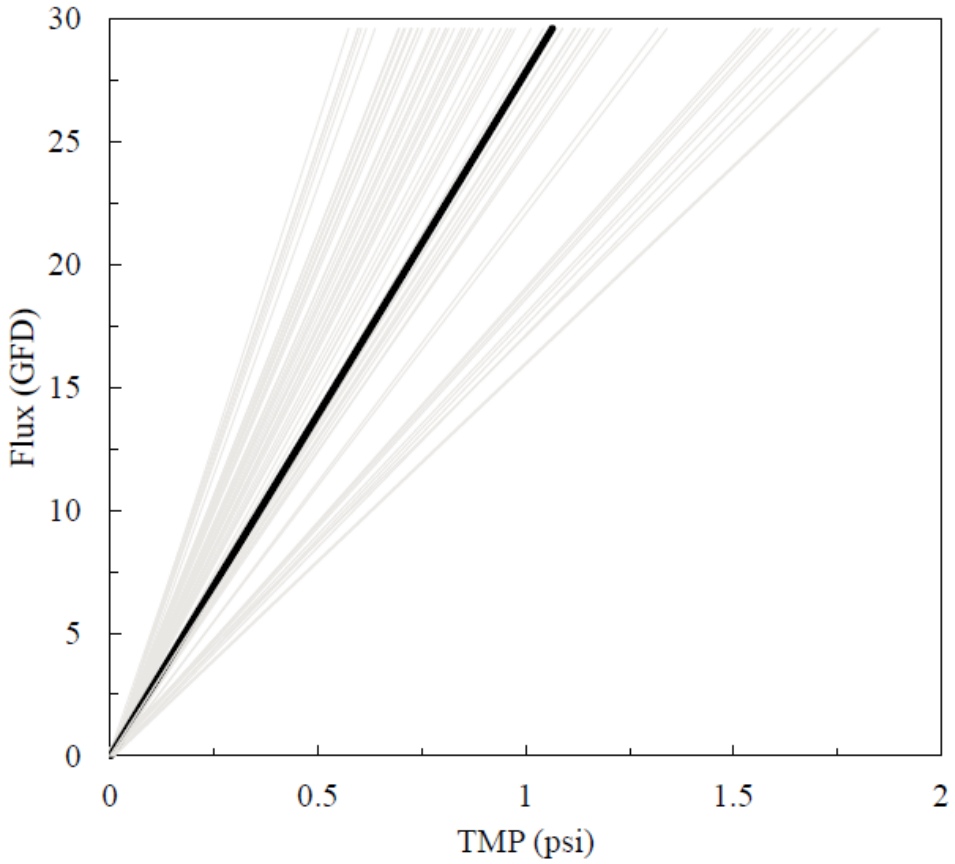

Fig. 4.S3. Collection of all 63 hydraulic permeability measurements that were made during the experimental study; the minimum and maximum values are 16.1 and 52.1 GFD/psi (equivalent to 0.00397 to 0.0128 LMH/Pa) respectively. The thick black line shows the average of the 63 results with a value of 27.8 GFD/psi

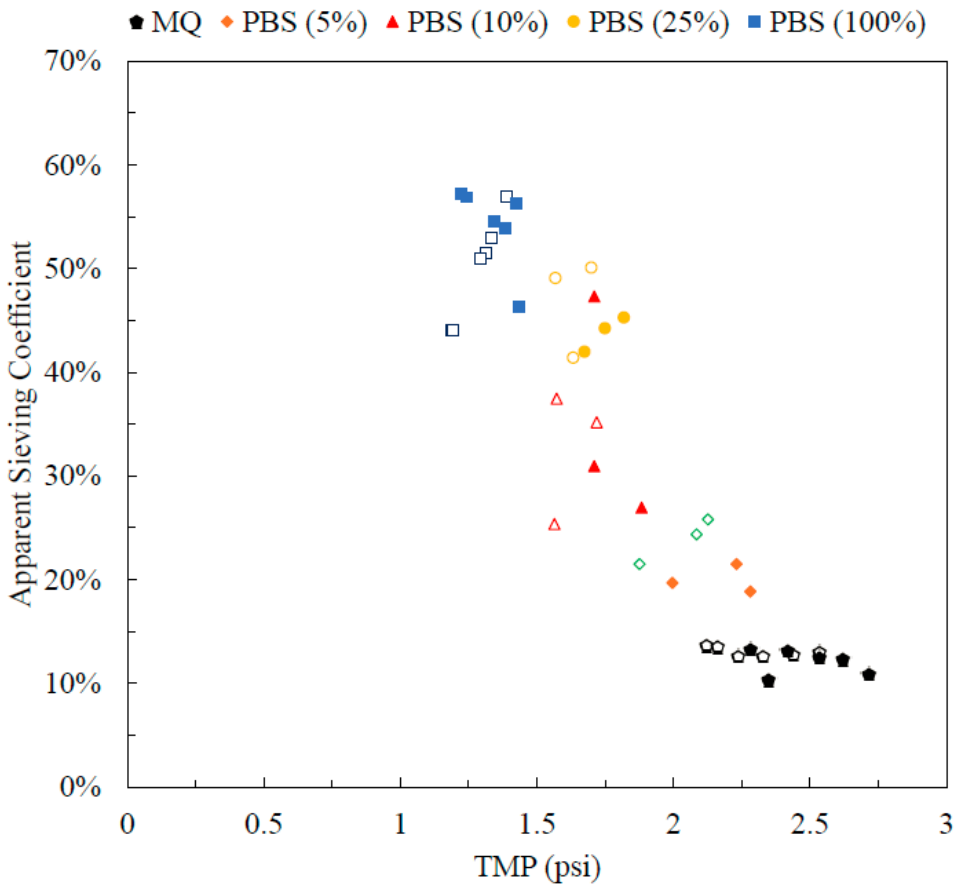

Fig. 4.S4. Correlation between the TMP and apparent sieving coefficient for the filtration experiments conducted in different solution conditions (corresponding to Figure 4.3). All the humic acid filtration experiments were performed in triplicates, with 100 ppm technical grade Sigma humic acid at a flux of 30 GFD (flow rate of 0.45 mL/min). Open symbols represent the 3rd filtrate sample; the calculated Spearman rank correlation and Pearson product-moment correlation coefficients are -0.848 and -0.890 respectively. Filled symbols represent the 4th filtrate sample; the calculated Spearman rank correlation and Pearson product-moment correlation coefficients are -0.961 and -0.951 respectively.

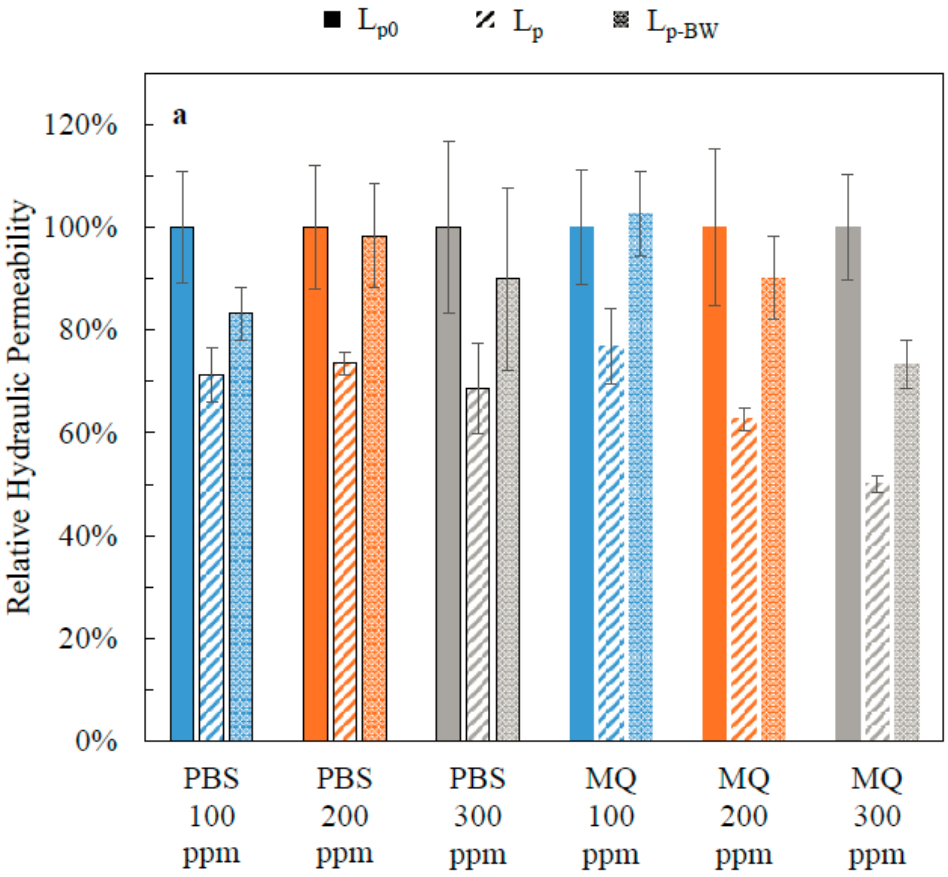

Fig. 4.S5. Effect of technical grade Sigma HA concentration (in PBS or MQ-water) on filtration performance at a flux of 30 GFD (flow rate of 0.45 mL/min): **a**. Comparison of changes in hydraulic permeability following the HA filtration experiments. The results were normalized by the hydraulic permeability of the native membrane (L_{p0}). The error bars were determined from the triplicate measurement at each experimental condition using standard propagation analysis;

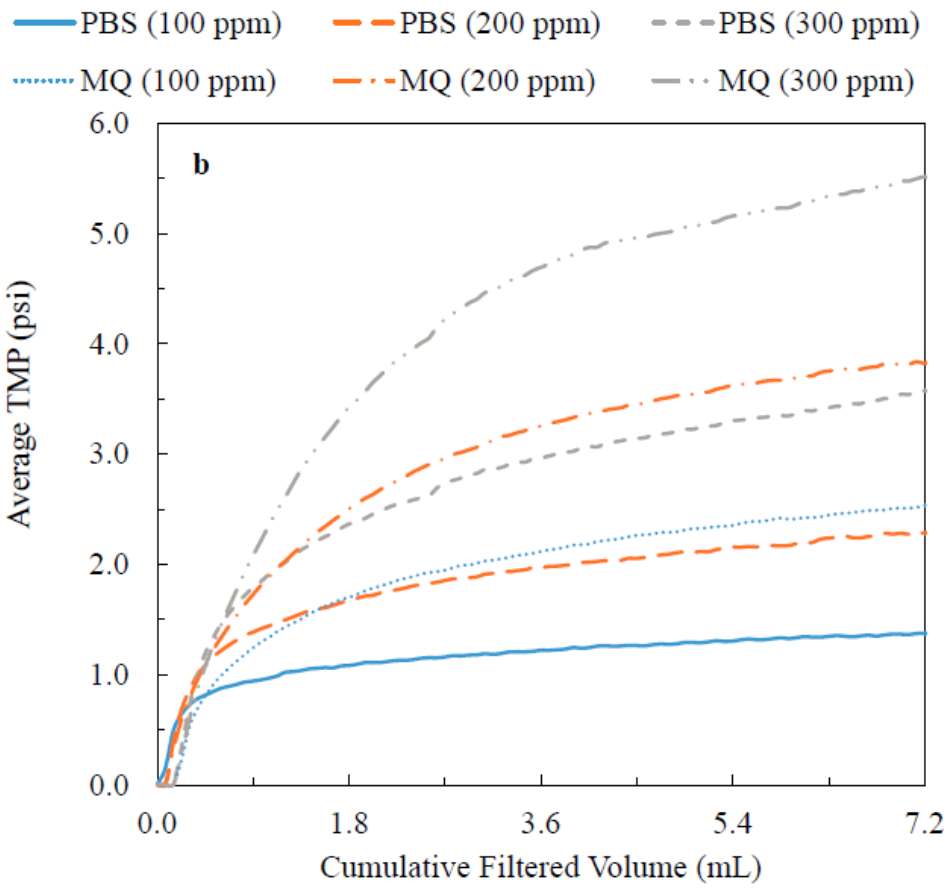

Fig. 4.S5. Effect of technical grade Sigma HA concentration (in PBS or MQ-water) on filtration performance at a flux of 30 GFD (flow rate of 0.45 mL/min): **b.** Average transmembrane pressure (TMP) profiles;

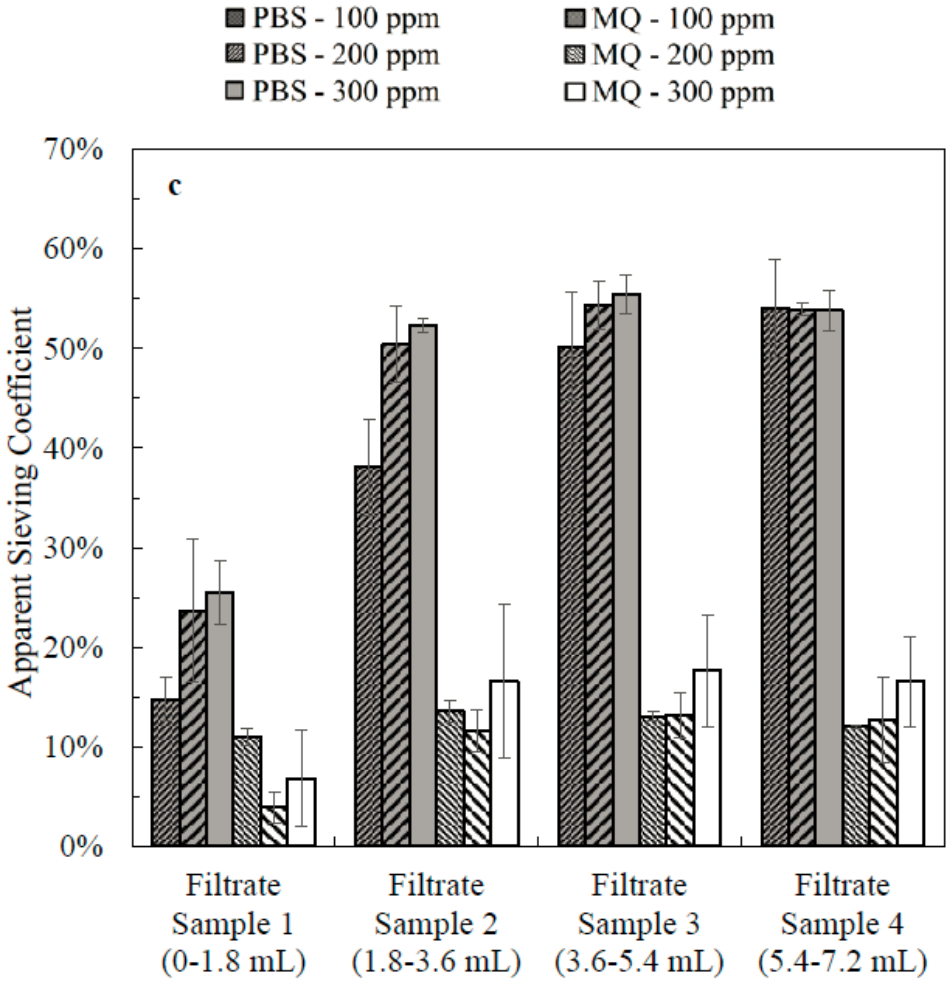

Fig. 4.S5. Effect of technical grade Sigma HA concentration (in PBS or MQ-water) on filtration performance at a flux of 30 GFD (flow rate of 0.45 mL/min): **c.** Apparent sieving coefficient results with error bars corresponding to the standard deviation for the triplicate measurement at each experimental condition;

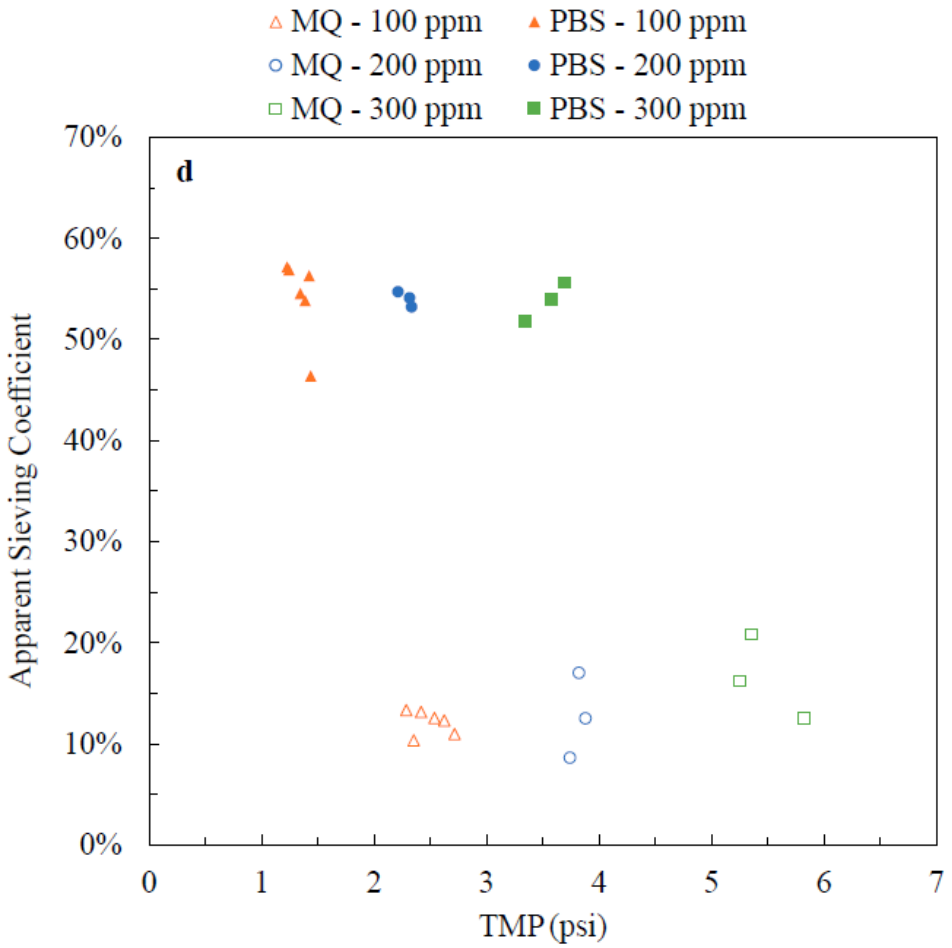

Fig. 4.S5. Effect of technical grade Sigma HA concentration (in PBS or MQ-water) on filtration performance at a flux of 30 GFD (flow rate of 0.45 mL/min): **d.** Correlation between the TMP and apparent sieving coefficient for the filtration experiments conducted at different HA concentrations. Open and filled symbols correspond to HA solutions prepared in MQ-water and PBS solution respectively. The x-axis shows the maximum TMP obtained in panel b for each solution condition while the y-axis shows the final apparent sieving coefficient for the same experiment (shown in panel c).

Chapter 5 - Microscale Parallel-structured, Cross-flow Filtration System for Evaluation and Optimization of the Filtration Performance of Hollow-fiber Membranes

Authors: Amir S. Kazemi, Blake Patterson, Ryan J. LaRue, Panagiotis Papangelakis, Seung Mi Yoo, Raja Ghosh, David R. Latulippe

Submitted to Separation and Purification Technology, June 2018

5.1. Preface

In chapter 4, by the development of the high-throughput hollow-fiber (HT-HF) module, the concept of high-throughput (HT) testing was expanded to the optimization of the filtration performance of hollow-fiber (HF) membranes, which are widely used in the water/wastewater sector. Although the HT-HF method proved to be valuable for the rapid testing of the operating conditions of HF membrane filtration processes, it can only be used for dead-end filtration. Additionally, filtration experiments can only be performed for a short period of time. Another shortcoming of the design was that it did not accommodate permeate and/or retentate recycle streams, which are very common in lab- and pilot-scale HF membrane filtration systems. The microscale, parallel-structured, cross-flow filtration (MS-PS-CFF) system is introduced in this chapter which is developed with operational flexibility in mind. The MS-PS-CFF platform can be used for running HT fouling tests in dead-end mode in a short period of time as well as for extended filtration tests where retentate and/or permeate streams can be recycled for a

prolonged period of time. Major design improvements were achieved by using a set of feed reservoirs, a multi-channel peristaltic pump as the fluid delivery system and an array of needle valves which enabled performing filtration experiments that included recycle streams. The design introduced herein was used to perform humic acid (HA) filtration experiments with different durations (0.5, 4, 24 and 72 hours) where it was shown that this systems allows for running parallel extended filtration experiments in a practical manner. The usefulness of this design was further demonstrated through running over 80 filtration experiments and 150 hydraulic permeability measurements with polyvinylidenefluoride (PVDF) HF membranes to investigate the effect of solute type (HA, sodium alginate, dextrans with different molecular weights and polyethylene oxides with different molecular weights) and solution conditions (i.e. phosphate, borate and carbonate). Furthermore, the importance of HT testing and optimization of surface modification techniques used for HF membranes was demonstrated by investigating and optimizing a surface modification technique reported in the literature, where dopamine hydrochloride and sodium periodate (as an strong oxidizer) were used to improve the hydrophilicity of the membrane. The surface modification results showed that a small change in membrane pore structure, geometry or modification conditions can significantly affect the hydraulic permeability, rejection and surface properties of the membrane. Thanks to the unique design of the MS-PS-CFF system, different lengths (~8 cm vs. ~16 cm) of HF membranes could be tested which led to more findings on the effects of membrane length on its hydraulic permeability and the filtration performance (results shown in Fig. 5.S7). Note that this section (i.e. the effect of membrane length)

was not included in the manuscript prepared for submission to the Separation and Purification Technology but is included in section 5.8 to provide future directions for the researchers in the field. Also, note that SI units are used in this section as per Journal guidelines. The following unit conversions can be used for comparison purposes: 1 LMH = 0.588 GFD; 1 kPa = 0.145 psi.

5.2. Introduction

Hollow-fiber (HF) membranes are an ideal separation technology for various environmental and biotechnology applications due to the high amounts of membrane surface area that are available in compact module configurations (i.e. high packing density). For example, a single ZeeWeed 500D module from SUEZ Water Technologies & Solutions (formerly GE Water & Process Technologies) can have up to 40 m^2 of membrane surface area in approximately 0.1 m^3 of space via the assembly of approximately 3000 individual fibers in a slender rectangular configuration. Also, HF membranes have the particular advantage over other membrane geometries of being able to be operated in a crossflow filtration regime and to be cleaned using automated backflushing strategies. HF membranes are widely used for different water and wastewater treatment applications including as a reverse osmosis pre-treatment step in desalination and as a tertiary treatment step in wastewater plants. HF membranes are also used in bioreactor systems for mammalian cell culture. In general, the performance of membrane technologies will depend on various operational factors including the membrane properties (e.g. base material, pore size distribution), the physico-chemical

properties of the feed solution (e.g. solute size, solution conditions), and the hydrodynamic conditions (e.g. crossflow versus 'dead-end' filtration).

HF membranes for environmental applications are designed to operate for a long period of time; for example, the expected life of a ZeeWeed HF module is estimated as 'more than 10 years' [1]. However, membrane fouling is ubiquitous process which causes significant operational challenges such as reduced throughput, permeate quality reduction, and flux decline which drive up separation costs due to maintenance shutdowns and addition of antifouling chemicals. Since membrane fouling is a complex phenomenon that is difficult to predict, experimental assessments are used to evaluate the fouling behaviour of different membranes. In order to study the effect of those various factors on the fouling of HF membranes, the majority of previous studies have focused on process evaluation and optimization using a single pilot-scale or full-scale membrane module at various experimental conditions but with each experimental condition tested in a sequential manner [2–4]. The disadvantage to this approach is that only a limited number of experiments can be performed in a reasonable amount of time and with reasonable amount of effort.

There is growing interest in the development of microscale versions of membrane filtration devices to facilitate the completion of high-throughput (HT) studies in order to rapidly evaluate the performance of membranes over a wide range of operating conditions. Zhou and colleagues demonstrated the extreme usefulness of this approach for flat-sheet polyethersulfone membranes in identifying the best surface modification strategies to hinder their propensity to foul by natural organic matter [5] and protein

solutions [6] and also to develop new fouling-resistant membranes [7]. Those studies, as well as others in the literature [8–12], used commercial 96-well filter plates that contain a small flat sheet membrane (on the order of 0.2 cm^2) at the base of each well; a similar approach for running HT screening studies used customized versions of the 96-well filter plate design [8,12] The flat-sheet membrane format is typically used for biotechnology applications, such as protein/DNA filtration, cell harvesting, and protein fractionation [6,8–12], rather than environmental applications.

Our team recently developed the first-ever microscale parallel-structured filtration system to evaluate the performance of HF polyvinylidenefluoride (PVDF) membranes with humic acid solutions [13]. While that system proved to be extremely useful for quickly screening operating conditions, it was limited to running 'dead-end' filtration tests with typical experiments lasting about 30 minutes. This is somewhat of a limitation because, as mentioned earlier, the anticipated 'life' of a HF membrane module is on the order of many years. Also, cross-flow (aka tangential-flow) filtration is the preferred mode of operation for HF membranes. Given these limitations, in this work we developed a 'next-generation' system to evaluate and optimize the performance of HF membranes; the primary outcomes are summarized below:

- We built a microscale, parallel-structured, cross-flow filtration (MS-PS-CFF) system that uses a multichannel peristaltic pump and an array of miniaturized feed reservoirs to run multiple HF filtration experiments at once with the permeate and retentate streams being continuously recycled back into the feed reservoir akin to typical lab-scale and pilot-scale systems. For this study, four microscale filtration

sub-modules were run in parallel with each one containing a single HF membrane. However, the system could be easily expanded to run more than four experiments at once by using a higher capacity multi-channel peristaltic pump (e.g. the 205CA peristaltic pump (Watson Marlow) can run up to 32-channels simultaneously) and making some simple modifications to the sample collection system.

- We performed several 'proof-of-principle' experiments in order to demonstrate the usefulness of our MS-PS-CFF system for evaluating the performance of HF PVDF ultrafiltration (UF) membranes. PVDF membranes are widely used in various separation applications including membrane distillation, membrane contactors, wastewater treatment, and bio-separations [14]. We studied the effects of filtration duration (between 0.5 and 72 hours), solution conditions, and solute properties (dextran, polyethylene oxide, humic acid, sodium alginate) on filtration performance. Also, we optimized a dopamine (DA)-based modification technique for PVDF UF membranes. DA has been shown to be a promising candidate as a hydrophilic surface coating for PVDF membranes [15–17] and other materials (e.g. polysulfone, polyethersulfone, polypropylene, polyethylene, copper, silver, glass and Metal–organic frameworks [16–19]). The DA modification step is typically performed at basic pH conditions [16–19], but this approach has been reported to suffer from poor homogeneity and stability [15,20]. Recently, an alternative DA modification method was developed using various oxidizing agents (e.g. sodium periodate) at acidic pH conditions [20]. Luo and Liu [15] adopted this method for the surface modification of flat-sheet PVDF

microfiltration membranes and showed a significant improvement in terms of both hydraulic permeability and hydrophilicity for an oil/water separation application. Given the experimental complexities and the need to evaluate many different factors of the surface modification strategy, it is impractical to complete such a task with a traditional HF membrane module, however the MS-PS-CFF system was ideally suited to conduct a HT evaluation of the surface modification strategy.

5.3. Experimental

5.3.1. Materials

Technical grade humic acid (HA) sodium salt, sodium alginate (SA), dextrans (reported molecular weights of 40, 100, 550 and 2000 kDa), and polyethylene oxides (reported molecular weights of 100 and 600 kDa) were purchased from Sigma-Aldrich. The molecular weight of each solute was measured using gel permeation chromatography (GPC) – the exact details are provided in the Supporting Information file. Single-solute feed solutions (concentration = 300 ppm) were mostly prepared in phosphate buffered saline (PBS) solution (Corning; 0.144 g/L KH_2PO_4, 9 g/L NaCl, 0.795 g/L Na_2HPO_4). However, a number of filtration tests were done with feed solutions prepared in 10 mM borate buffer (Thermo Fisher Scientific), 80 mM borate buffer, 10 mM carbonate buffer (Alfa Aesar), or 10 mM phosphate buffer (prepared by diluting Sorensen's PB solution [21]). The pH and conductivity of each solution were measured using an HI5522

pH/conductivity meter (Hanna Instruments). Each of the feed solutions was first pre-filtered with a 0.2 μm Supor® syringe filter (Pall) to remove any possible agglomerates.

The PVDF UF membranes (available commercially as ZeeWeed 500) with nominal pore size of 0.04 μm were provided by SUEZ Water Technologies & Solutions (formerly GE Water & Process Technologies). These HF membranes (OD = 1.9 mm, ID = 0.8 mm) have a 'supported' structure, with the PVDF membrane coated on top of a braided polyester support, and thus are normally operated in an 'outside-in' flow direction. Scanning electron microscopy images of the top surface and cross-section of the membrane are shown in Fig. 5.S1 in the Supporting Information file. In order to remove the preservative agents that are applied at the end of the manufacturing process, the membranes were immersed in deionized water (resistivity > 18 MΩ ·cm) at 40 °C for 3 hours, then transferred into a 10% bleach solution at 50°C for 3 hours, and finally transferred into deionized water at ambient temperature for 18 hours [13].

5.3.2. Membrane Modification Protocol

The HF membranes were modified following a protocol based on that previously reported in the literature [15,20] for superhydrophilic-superoleophobic coatings and flat sheet membranes. Short lengths of the HF membranes were first immersed in a 60% ethanol in water solution for 15 minutes in a sonicator bath. The membranes were thoroughly rinsed with deionized water and then immersed in deionized water for 15 minutes under sonication. A 4 mg/mL sodium periodate (SPI) solution in 50 mM acetate

buffer (pH 5) was prepared in an amber glass vial and then dopamine hydrochloride (DA-HCl; Alfa Aesar) was added to a final concentration of 0.4 or 2 mg/mL. The HF membranes were added to the solution and the bottle was gently agitated for between 24 and 120 min according to the experimental protocol. The modified membranes were gently rinsed with deionized water and dried at 40°C for one hour; in a limited number of experiments, the membranes were dried overnight at 40°C for approximately 14 hours. The unmodified and modified membranes were characterized in terms of water contact angle using a High Speed Contact Angle (Future Digital Scientific OCA 25) and chemical groups using a HYPERION 3000 Fourier transform infrared (FTIR) spectrometer (Bruker). For the contact angle measurements, the PVDF membrane was carefully peeled off of the braided support layer and then attached to a microscope slide using a piece of double-sided tape. The membrane samples were dried at 40°C for three hours prior to both contact angle measurement and FTIR analysis.

5.3.3. Microscale, Parallel-structured Cross-flow Filtration (MS-PS-CFF) System

As mentioned above, the MS-PS-CFF system developed in this study had four filtration sub-modules that were run in parallel (see Fig. 5.1b). Each sub-module includes an upstream and downstream compartment that are connected to each other using barbed hose connectors and flexible Tygon tubing (OD = 4.8 mm, ID = 3.2 mm); this feature allows for the system to be easily adapted to run tests with HF membranes of different lengths. In this study, the total length of the HF membrane was 12 cm but the ‘effective

length' (i.e. that which was available for filtration) was approximately 7.8 cm. The rest of the membrane was used to accommodate the series of alternating washers and silicon rubber o-rings that create a liquid-tight seal between the outside of the membrane and the threaded ports on the two compartments. A stainless-steel needle (length = 3 cm, OD = 0.9 mm) was used as an insert inside both ends of the fiber to prevent the HF membrane from getting crushed. The exterior dimensions of the compartments were designed such that when four sub-modules are 'sandwiched' together with acrylic spacers between each one, the positions of the permeate valves (identified as 7 in Fig. 5.1a) are perfectly aligned with every other column in a standard 48-well microplate (i.e. 8 columns by 6 rows). This arrangement was the primary reason for choosing to run four experiments in parallel, however as mentioned above it would be possible to modify the entire setup to accommodate more than four sub-modules and thus run more than four filtration experiments at once.

As per the manufacturer's recommendations, the HF membranes were operated in an 'outside-in' configuration (as shown in Fig. 5.1) for the filtration test; the alternative 'inside-out' configuration (details given below) was used initially to pre-wet the HF membrane and for the post-filtration backwashing step. The feed solution is delivered from an array of miniaturized feed reservoirs (each with 100 mL capacity) to the filtration sub-modules via a Masterflex L/S multi-channel peristaltic pump (Cole-Parmer). The transmembrane pressure (TMP) for each filtration sub-module is continuously monitored and recorded on a laptop using PX409 pressure transducers (Omega). A three-way stopcock valve on the permeate line (identified as 7 in Fig. 5.1a) is most often used to

recycle the permeate stream back to the feed reservoir (via a 55 cm length of Tygon tubing) and occasionally used to collect a permeate sample directly into the 48-well microplate. Feed samples are collected at the same time as the permeate samples using another three-way stopcock valve (identified as 3 in Fig. 5.1a) just downstream of the peristaltic pump. The retentate is also recycled back to the feed reservoir (via a 45 cm length of Tygon tubing). A needle valve on the retentate line (identified as 6 in Fig. 5.1a) is used to control the back-pressure on the HF membrane. Also, by fully closing the needle valve, the system can be run in a 'dead-end' filtration mode.

After each sub-module was assembled and connected to the system, deionized water was flushed through each one at a flow rate of 1.5 mL/min for 7 minutes with the retentate line needle valves in the fully-open position to displace any possible air bubbles. Then, the system was switched to the 'inside-out' flow configuration (as shown in Fig. 5.S2 in the Supporting Information file) and deionized water was passed through the membrane at flow rate of 0.2 mL/min for 15 minutes; briefly this configuration was achieved using an extra length of Tygon tubing that connected the three-way stopcock valve on the feed line to the three-way stopcock valve on permeate line which directs flow axially into the inside of HF membrane (via downstream compartment), radially out through the HF membrane, and axially along the annular space between the HF membrane and Tygon tubing towards the upstream compartment. Next, the system was switched back to the normal 'outside-in' flow configuration (as shown in Fig. 5.1a) and the retentate line needle valves were closed completely. The hydraulic permeability of the native membrane (L_{p0}) was calculated using equation 5.1:

$$L_p = \frac{J}{\Delta P} \quad (5.1)$$

where J is the permeate flux of deionized water and ($L/m^2/h$; LMH) and ΔP is the average TMP (kPa) that was recorded by the pressure transducer. The permeate flux was calculated as flowrate divided by the effective HF membrane area (4.66×10^{-4} m^2) with the flowrate determined from timed collection of permeate samples into a UV-transparent 48-well microplate (Greiner Bio-One); the volume of solution in each well was calculated from absorbance readings at a wavelength of 977 nm [6] using a Spark M10 microplate reader (Tecan). A typical set of TMP profiles for the five different flow rates that were used for each membrane permeability test is shown in Fig. 5.S3 in the Supporting Information file.

Next, the water was displayed from each sub-module, and was replaced with the desired feed solution for the membrane filtration/fouling test. These experiments were conducted in recycle mode with the retentate line needle valves opened one-eighth of one rotation to provide back pressure against the membranes. The experiments were performed with a feed solution flow rate of 1.5 mL/min. The total run time was varied from 0.5 hour to 72 hours with permeate samples collected at regular intervals. The sub-modules were then emptied of the feed solution, and the post-filtration permeability of the membrane (L_p) was measured using deionized water. The membranes were then backwashed using the same 'inside-out' configuration that was used to wet the membrane. Finally, the post-backwashing (BW) permeability of the membrane ($L_{p\text{-}BW}$)

was again measured using deionized water. Note that a brand new HF membrane was used for each filtration test.

An aliquot of each sample was transferred into a UV-transparent 96-well plate (Greiner Bio-One). The concentration of HA each sample was determined from absorbance measurements at a wavelength of 310 nm using the Spark M10 microplate reader and a ten point calibration curve for HA concentration versus absorbance. The concentration of all the other solutes used in this study (i.e. sodium alginate, dextran, polyethylene oxide) were determined via a TOC-L total organic carbon (TOC) analyzer (Shimadzu) using an eight point calibration curve based on TOC standard (potassium hydrogen phthalate).

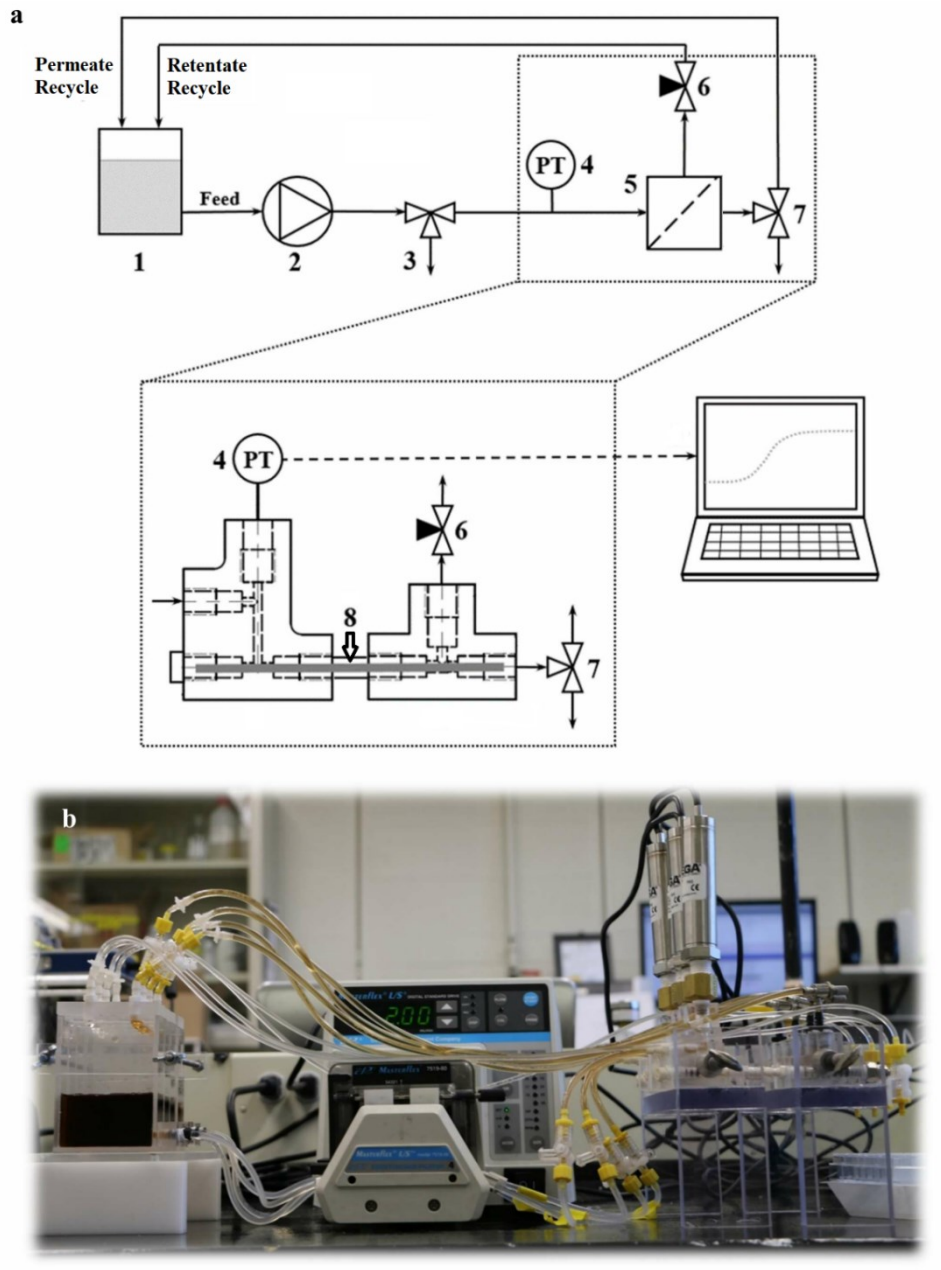

Fig. 5.1. Panel a: Schematic of the normal mode of operation for the MS-PS-CFF system. The identified components include: 1) Feed reservoir (nominal capacity of 100 mL); 2) Multi-channel peristaltic pump; 3) 3-way stopcock valve for collecting feed sample; 4) Pressure transducer; 5) filtration sub-module; 6) Retentate line needle valve; 7) 3-way stopcock valve for collecting permeate sample; 8) Tygon tubing with HF membrane inside. Panel b: Picture of the experimental setup with four filtration experiments running in parallel.

5.4. Results and Discussion

5.4.1. Effect of Run Time on HF Filtration Performance

The system developed for this study allowed for four filtration experiments to be conducted in parallel with the feed stream for each module being directed in a cross-flow direction across the HF membrane and both the retentate and permeate streams being continuously recycled back to the feed reservoir. In order to demonstrate the usefulness of the MS-PS-CFF system in running prolonged filtration runs, experiments with different run times were conducted using 300 ppm HA in PBS solution. The shortest time (0.5 hour) was chosen based on the typical run time in our previous study that exclusively used the 'dead-end' filtration mode [13]. The longest time (72 hours) was chosen as a reasonable value to demonstrate the ability to run multiple filtration experiments in parallel for an extended period of time; the TMP of each sub-module was very stable throughout the entire run (results not shown). It should be noted that in full-scale systems, HF membranes are not typically run in a continuous filtration mode for this long. However, this study was conducted in order to demonstrate the capability of the MS-PS-CFF system and how it could be used for atypical filtration test conditions.

The effect of the filtration run time on HF membrane performance is shown in Fig. 5.2 for experiments conducted with 300 ppm solution of HA in PBS. Due to the slight variation in the measured hydraulic permeability of the native membrane (i.e. L_{p0}), the results shown in Fig. 5.2a are reported in terms of the relative hydraulic permeability of the fouled membrane (i.e. L_p/L_{p0}) and the relative hydraulic permeability of the backwashed (BW) membrane (i.e. $L_{p\text{-}BW}/L_{p0}$). The measured value of L_{p0} for all the

membranes used in this study was 12.6 ± 2.7 LMH/kPa. Each experimental condition was tested in quadruplicate in order to assess the variations in the membrane properties and thus measure the true performance of the PVDF membrane. Thus, the results reported in Fig. 5.2 correspond to a total of 16 filtration experiments and 48 hydraulic permeability measurements. This level of detail would be challenging to complete with a traditional filtration setup, but it was quite manageable with the MS-PS-CFF system. For the shortest run time (0.5 hour), the accumulation of HA onto the PVDF membrane caused the relative hydraulic permeability to decrease to 44 ± 5% (where the ± value represents one standard deviation) of the pre-filtration value. After the BW step with deionized water, the relative hydraulic permeability increased to 60 ± 9% of the pre-filtration value. The difference in permeability values reflects the degree of irreversible and reversible fouling that occurs on the HF membrane at the given experimental conditions. There was a negligible change in both relative permeability values for the filtration tests operated for 0.5 and 4 hours. However, at the longer run times there was a significant impact on the permeability of the HF PVDF membranes. For example, the relative hydraulic permeability after BW decreased from 67 ± 3% to 50 ± 6% to 33 ± 6% as the run time increased from 4 to 24 to 72 hours. We also observed a noticeable darkening in the color of the HF PVDF membranes at the longer run times – see Fig. 5.S4 in the Supporting Information file. Both of these results suggest there is an increase in the degree of irreversible adsorption of the HA onto the membrane at the longer run times. Also, at the three lowest run times (0.5, 4, and 24 hours), the relative hydraulic permeability after the BW step was significantly higher than the relative hydraulic permeability after filtration

(all student's t-test P-values < 0.02) suggesting that some fraction of the membrane fouling was reversible. However, for the 72 hour run time, there was no statistical difference (student's t-test P-value = 0.05) between the two relative hydraulic permeability values.

The quality of the permeate produced by the HF PVDF membranes during the same set of experiments is shown in Fig. 5.2b. For each filtration test, a pair of permeate and feed samples were taken immediately before the set run time expired, also for the three longer run times a pair of samples were taken at any of the shorter run times. For example, for the 24 hour test three sets of samples (identified as P1, P2, and P3) were taken at the 0.5, 4 and 24 hour timepoint; an additional set of samples (identified as P4) was taken at the 48 hour mark for the 72 hour test. Each pair of samples was used to calculate the HA apparent rejection coefficient according to equation 5.2:

$$R_a = \left(1 - \frac{C_f}{C_b}\right) \times 100\% \qquad (5.2)$$

where C_f is the concentration in the permeate sample and C_b is the concentration in the corresponding feed sample. For the three longer run times (i.e. 4, 24, and 72 hours), there was no significant difference in the rejection values for the multiple samples collected within each run (all student's t-test P-values > 0.06). Also, there was no significant difference for five of the six possible comparisons between the rejection values for the P1 sample; the only significant difference (student's t-test P-vale = 0.025) was found for the 0.5 and 72 hour run times. It is not exactly known why this difference exists, but it could

be due to very slight differences in the properties of the HF membranes that were used for those two particular test conditions.

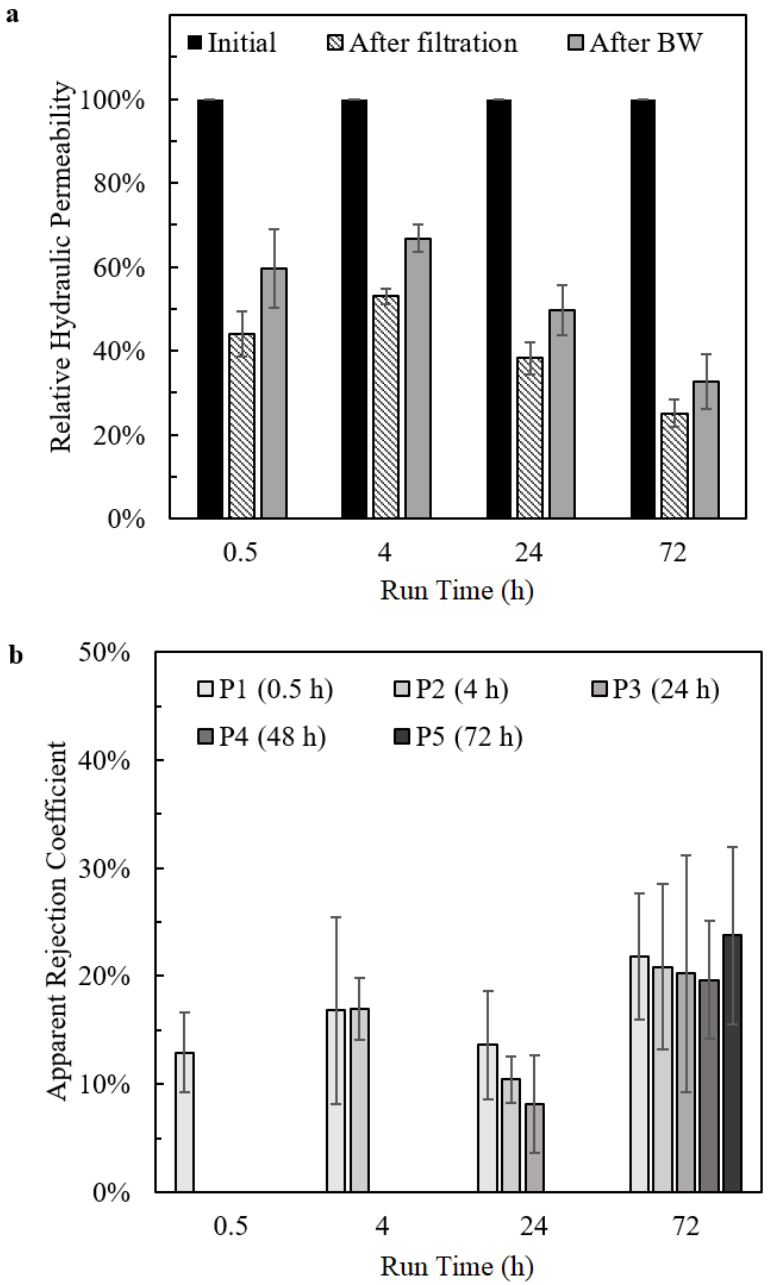

Fig. 5.2. Effect of filtration run time on the performance of the HF PVDF membrane for a 300 ppm HA solution in PBS operated at a cross flow rate of 1.5 mL/ min. Panel a: Relative hydraulic permeability before filtration, after filtration, and after BW; the error bars correspond to the standard deviation for the quadruplicate measurement at each condition. Panel b: Apparent rejection coefficients for the permeate samples; again, the error bars correspond to the standard deviation for the quadruplicate measurement at each condition.

5.4.2. Effect of Solution Conditions and Solute Type on HF Filtration Performance

The design of the MS-PS-CFF system with the ability to run four separate filtration experiments in parallel is ideal for elucidating the effects of various process conditions on filtration performance. In our initial experimental design, we had planned to evaluate only phosphate, borate, and carbonate buffers at a concentration of 10 mM, however after measuring the pH and conductivity values (as shown in Table 5.1) we realized the possible confounding effect of pH and conductivity changes. Thus, a fourth condition of borate buffer at a concentration of 80 mM was added to the study – this particular condition was chosen because it had a similar conductivity value as the 10 mM phosphate buffer.

Table 5.1. pH and conductivity values for the four buffer solutions used in the HA filtration experiments.

Buffer Solution	pH	Conductivity (μS/cm)
10 mM Phosphate	7.52 ± 0.02	1967 ± 37
10 mM Carbonate	9.52 ± 0.02	457 ± 1
10 mM Borate	9.03 ± 0.01	240 ± 3
80 mM Borate	9.04 ± 0.01	1652 ± 101

The effect of the buffer solution conditions on HF membrane performance is shown in Fig. 5.3 for a set of 4-hour filtration experiments conducted with the technical grade HA (concentration of 300 ppm). Again each experimental condition was tested in

quadruplicate. As shown in Fig. 5.3a, the relative hydraulic permeability after filtration was remarkably similar for the three 10 mM concentration buffers. Also, at each of these conditions the relative hydraulic permeability after the BW step was significantly higher than the relative hydraulic permeability after filtration (all student's t-test P-values ≤ 0.02) suggesting that some fraction of the membrane fouling was reversible. It is worthwhile to note that the relative hydraulic permeability after the BW step for the 10 mM borate buffer (87 ± 8%) is much greater than that shown in Fig. 5.2a for the 4-hour run with PBS buffer (67 ± 3%). For the 80 mM borate buffer, there was no statistical difference (student's t-test P-value = 0.04) between the two relative hydraulic permeability values. As shown in panels c through f of Fig. 5.2, the final color of the fouled PVDF HF membranes was noticeably darker for the 80 mM borate buffer. Thus, our results indicate that there is a strong effect of the buffer ion concentration on the degree of irreversible and reversible fouling that occurs on the HF membrane at the exact same operating conditions.

As shown in Fig. 5.3b, the quality of the permeate produced by the HF PVDF membranes was affected by the type and concentration of buffer that was used to prepare the HA solution. For the rejection values corresponding to the 0.5 hour (i.e. P1) samples, there was a clear difference across the four buffer conditions. However, it is interesting to note that there was no significant difference between the 10 mM carbonate and 10 mM borate buffers (student's t-test P-value = 0.145) and also between the 10 mM phosphate and 80 mM borate buffers (student's t-test P-value = 0.067). Thus, our results indicate that there is a strong effect of the specific buffer ion on the filtration quality at the exact

same operating conditions. Based on the values reported in Table 5.1, our results indicate the solution conductivity has a dominant effect on the HA rejection values. It is hypothesized that the solution conductivity affects the solute-membrane interactions; a similar phenomenon was reported by Burns and Zydney [22] in their study of flat-sheet polyethersulfone membranes. For the 4 hour (i.e. P2) samples, the rejection coefficient decreased from 90 ± 8% to 25 ± 6% as the concentration of borate buffer increased from 10 to 80 mM. A similar effect was observed in our previous HF membrane filtration study with the same HA in buffers of different phosphate concentrations [13].

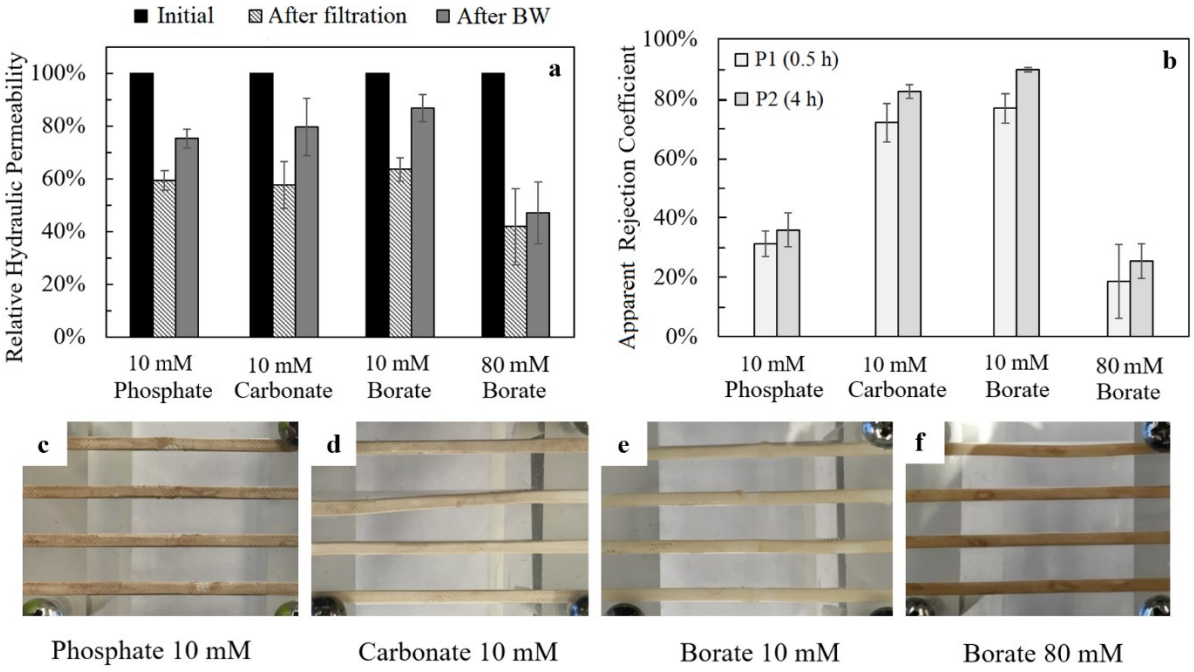

Fig. 5.3. Effect of buffer composition on filtration performance of HA solutions (300 ppm) during 4-hour test at a cross flow rate of 1.5 mL/min. Panel a: Relative hydraulic permeability before filtration, after filtration, and after BW; the error bars correspond to the standard deviation for the quadruplicate measurement at each condition. Panel b: Apparent rejection coefficients for the two sets of samples (P1 and P2) that were collected during the 4-hour filtration test; again, the error bars correspond to the standard deviation for the quadruplicate measurement at each condition. Panels c through f: Images of the four HF membranes at the end of the 4-hour filtration test for each of the four solution conditions.

In order to further demonstrate the potential of the MS-PS-CFF system for conducting a HT study of the performance of HF membranes, a set of filtration experiments were conducted with seven single solute solutions: sodium alginate, four dextrans (reported MW values of 40, 100, 550, and 2000 kDa), and two polyethylene oxides (reported MW values of 100 and 600 kDa). Dextrans and polyethylene oxides are commonly used solutes for characterizing the filtration performance of UF membranes

[23–30]. Additionally, sodium alginate has been used to evaluate the fouling propensity of UF membranes under different operating conditions [31–34]. Each solute was first characterized via GPC (as described in detail in the Supporting Information file) in order to allow for a better comparison of the corresponding filtration results. The measured mass-weighted MW varied from 2.4 kDa for the technical grade HA to 359.1 kDa for the largest polyethylene oxide; the complete set of GPC results is given in Table 5.S1 in the Supporting Information file. In order to enable a direct comparison with the HA results in Fig. 5.2, the feed solutions were prepared in PBS and the run time was fixed at 4 hours; each experimental condition was tested in quadruplicate using the MS-PS-CFF system. The apparent rejection coefficient values that were obtained for the final set of permeate and feed samples (i.e. the P2 samples according to Fig. 5.2) are shown in Fig. 5.4 as a function of the mass-weighted MW values from the GPC analysis; the high and low values associated with the width of the half-peak from the GPC chromatograms were used to approximate the polydispersity of the solute and were converted into the x-axis error bars. The rejection values varied considerably from 8 ± 4% for the smallest dextran (i.e. measured MW = 25.4 kDa; reported MW = 40 kDa) to 82 ± 9% for the largest polyethylene oxide (i.e. measured MW = 359.1 kDa; reported MW = 600 kDa). It is interesting to note that the rejection coefficient for the sodium alginate (59 ± 4%) was statistically the same as that for the largest dextran (56 ± 18%).

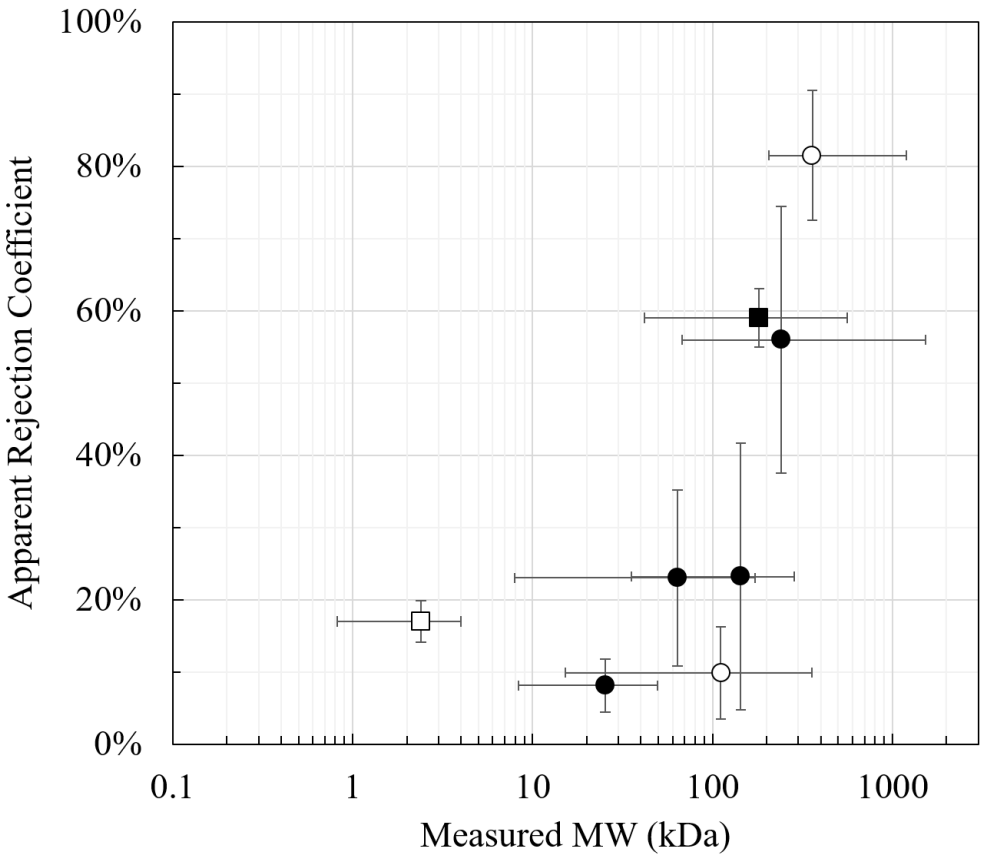

Fig. 5.4. Comparison of solute size and chemical structure on the apparent rejection coefficient of the HF PVDF membrane for a 300 ppm solution of polyethylene oxide (○), dextran (●), sodium alginate (■) and HA (□) in PBS operated at a cross flow rate of 1.5 mL/ min. The horizontal error bars denote the variation in solute MW based on the width of the half-peak from the GPC chromatograms; the vertical error bars denote the standard deviation of the rejection coefficient results from the quadruplicate filtration experiments that were conducted for each solute.

5.4.3. Optimization of Membrane Surface Modification Protocol for HF Membranes

As a final demonstration of the potential of the MS-PS-CFF system for conducting a HT study of HF membranes, we optimized a dopamine (DA)-based modification technique for the PVDF UF membranes. The modification protocol was a slight adaptation of that proposed by Luo and Liu [15]; specifically a 1-hour drying step was used instead of an overnight drying step because it was found the latter caused a severe drop in the hydraulic permeability (approximately 98%) for the unmodified PVDF membrane. It is believed that the overnight drying step caused an irreversible change in the porous structure of the HF membrane; previous studies have reported a similar effect [35]. We setup a 2^2 factorial design-of-experiments with the reaction time varied between 24 and 120 minutes and the DA-HCl concentration varied between 0.4 and 2 mg/mL. An additional control condition with only SPI was included in order to ensure that any observed changes in HF membrane properties were due to the dopamine. Each modification was done in triplicate while the control experiments were performed in quadruplicates and thus a total of 20 HF membranes were prepared and 60 hydraulic permeability measurements were made just for this part of the overall study. The completion of these experiments was particularly efficient with the MS-PS-CFF system since the experiments were performed in a parallel format using small amounts of material.

The effects of the surface modification conditions on the HF PVDF membrane properties are shown in Fig. 5.5. The four modified membranes were darker than the

unmodified and control membrane (see Fig. 5.5a); the color intensity was found to increase with both reaction time and DA-HCl concentration. The FTIR spectroscopy results for the modified and unmodified HF membranes are shown in Fig. 5.S5 (in the Supporting Information file); it was observed that an increase in the DA-HCl concentration resulted in visible peaks at wavenumbers of 3600-3000 cm^{-1}, 1735-1725 cm^{-1}, and 1670-1605 cm^{-1} which correspond to –OH, C=C and COOH groups respectively. The change in membrane surface hydrophilicity was assessed using dynamic water contact angle measurements. As shown in Fig. 5.5b, for all the membranes the contact angle decreased gradually over the course of the test. For example, the initial contact angle of the native-dried membrane was initially recorded as 96 ± 1° but that value decreased to 85 ± 1° after 100 seconds. The water contact angle decreased significantly for the highest DA-HCl concentration; at the highest reaction time condition (120 minutes) the value after 100 seconds of contact time was 21 ± 6°. The contact angle results for the modifications done at the lower DA-HCl concentration (0.4 mg/mL) were not significantly different than the control condition.

As shown in Fig. 5.5c, the hydraulic permeability of the HF membranes was strongly dependent on the surface modification conditions. It was found that the modified HF membranes for the 2 mg/mL DA-HCl and 120 minutes reaction time condition gave an initial hydraulic permeability (L_{p0}) value that was less than 0.5 LMH/kPa. This result is in sharp contrast to the significant increase in hydraulic permeability that was reported by Luo and Liu [15] for flat-sheet MF PVDF membranes. We believe this discrepancy is principally due to the difference between the average pore size of the UF PVDF

membrane used in this study (0.04 μm) versus that for the MF PVDF membrane (0.45 μm) as well as the difference in membrane resistance against drying after the removal of its preservatives. Thus, there is a critical need to optimize the surface modification conditions despite even for a fairly similar membrane material. Hence, multiple experiments were done to optimize the hydraulic permeability, hydrophilicity and separation properties of the HF PVDF membrane used in this study. As the reaction time was decreased from 120 minutes to 24 minutes, the initial hydraulic permeability only slightly increased to 1.7 ± 1.1 LMH/kPa. However, by decreasing the DA-HCl concentration from 2 mg/mL to 0.4 mg/mL, a significant improvement in the hydraulic permeability (to 13.2 ± 1.8 LMH/kPa for the 24 minute reaction time and 10.9 ± 0.8 LMH/kPa for the 120 minute reaction time) occurred. Thus it was found that by properly choosing the surface modification condition the negative effects of drying can be mitigated. The six types of membranes (i.e., unmodified, control, and modified) were tested with a 300 ppm solution of HA in PBS for 4 hours. It was found that at the one modification condition with the lower reaction time (24 minutes) and lower concentration (0.4 mg/mL), the post-BW permeability was the same as the initial permeability value which indicates that there was no irreversible fouling at the conditions tested in this study. As shown in Fig. 5.5d, the apparent rejection coefficient values for HA were also strongly affected by the surface modification conditions; for example, at a fixed reaction time of 24 minutes, the 4-hour rejection value decreased from 62 ± 10% to 3 ± 2% as the DA-HCl decreased from 2 mg/mL to 0.4 mg/mL. It was found that a strong correlation exists between the hydraulic permeability and rejection coefficient values – see Fig. 5.S6 in the

Supporting Information file. It is believed that the higher DA-HCl concentration creates a thick polydopamine layer on the surface that blocks the membrane pores; however further experiments are needed to confirm this hyphothesis. Although further experiments are required to find the true 'optimum', the results presented here demonstrate the true utility of the MS-PS-CFF system for conducting a HT study of the HF membrane surface modification conditions.

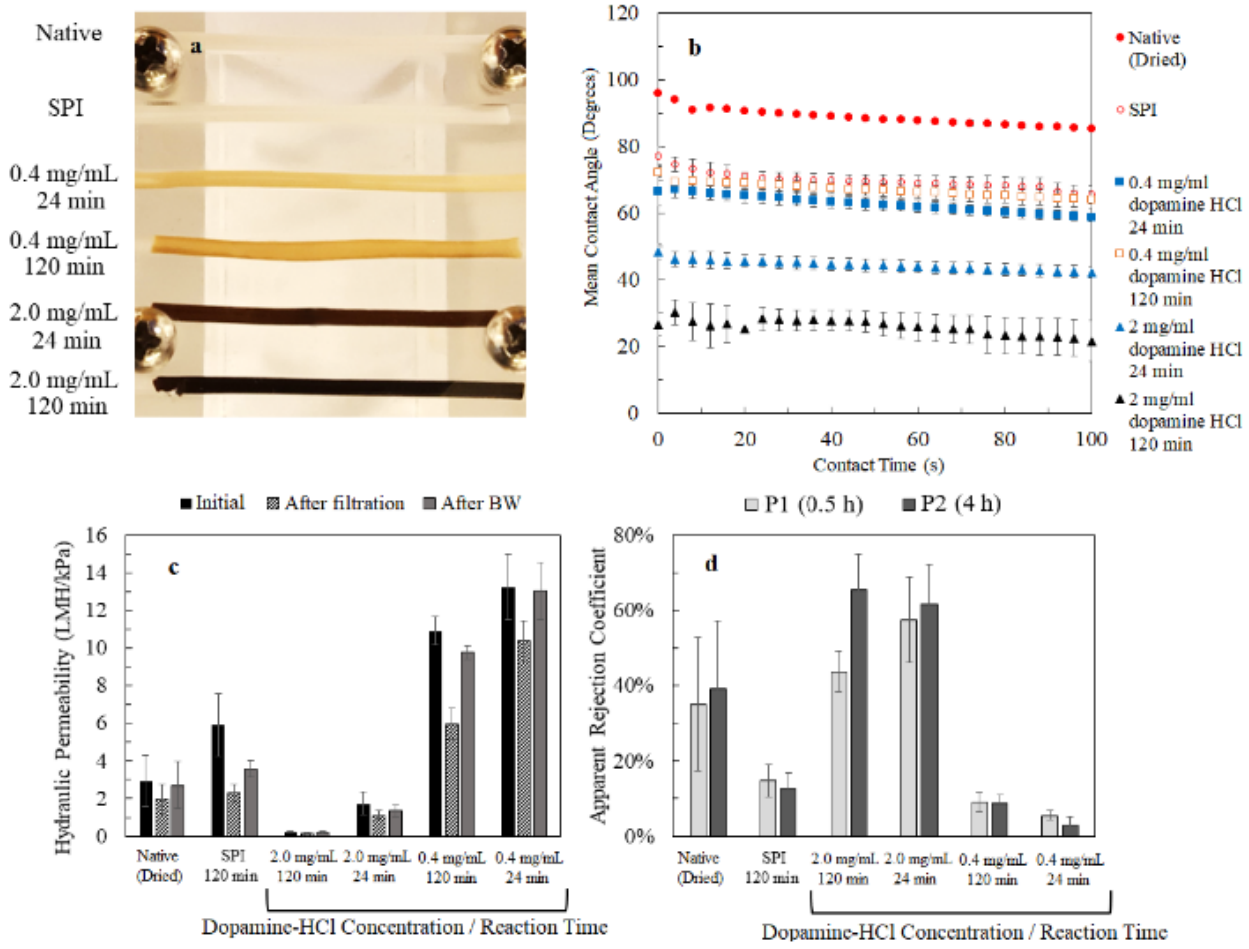

Fig. 5.5. Key performance results from the 2^2 design-of-experiments study on the dopamine-based modification of the HF PVDF membrane. Panel a: Representative images of the HF membranes after the dopamine-based modification technique described in the text. Panel b: Water contact angle measurements of the HF membranes; the error bars represent the standard deviation associated with the triplicate measurement for each modification condition. Panel c: Hydraulic permeability results for the unmodified and modified membranes before the filtration test, after the filtration test, and after the BW step; the error bars correspond to the standard deviation for the triplicate/quadruplicate measurement at each condition. Panel d: Apparent rejection coefficients for the two sets of samples (P1 and P2) that were collected during the 4-hour filtration test; again, the error bars correspond to the standard deviation for the triplicate/quadruplicate measurement at each condition.

5.5. Conclusions

The MS-PS-CFF system has been shown to be ideal for running HT studies of HF membrane performance as the cross-flow filtration pattern allows for continuous recycling of the permeate and retentate streams. Each sub-module of the filtration system requires just a small length of HF membrane, although it is possible to use longer lengths, and a small volume of feed solution. In order to demonstrate the usefulness of MS-PS-CFF module, parallel filtration experiments were run for up to three days with HA solutions in PBS. The effect of buffer type (i.e. solution conditions) on HF membrane fouling and separation performance was assessed using the MS-PS-CFF module by HA filtration. Also, the effect of solute type and size on filtration performance was studied using HA, sodium alginate, dextrans, and polyethylene oxides. It was clearly shown that the filtration time, solution conditions (i.e. buffer type), and solute type can dramatically affect the permeate quality as well as the extent of membrane fouling. Furthermore, a HT screen of a membrane surface modification process was performed using DA-HCl and SPI under acidic conditions. A 2^2 factorial design was conducted with the reaction time and DA-HCl concentration as process variables and the fouling propensity and solute rejection as the performance metrics. The membranes were also compared based on their colors after modification and were characterized using contact angle measurements and FTIR analysis. Overall, the results showed that optimizing the surface modification procedure was not a simple task, but instead required accounting for multiple factors including the modification solution concentration, reaction time, membrane geometry and pore size. Hence, an effective modification method may not be as effective at slightly

different conditions. In particular, a method that was previously found to improve the hydrophilicity and hydraulic permeability of a flat-sheet microfiltration PVDF membrane [15] was entirely unsuitable for the HF ultrafiltration membranes that were used in this sudy. Therefore, multiple experiments had to be conducted to optimize the hydraulic permeability, hydrophilicity and separation properties. Although further experiments are required to find the optimum, the results presented here demonstrate the utility of our MS-PS-CFF method which can be used for screening of different modification conditions. In total, over 80 filtration experiments and over 150 hydraulic permeability measurements were run in a short period of time in this study which shows that the MS-PS-CFF system can easily be used to speed up the screening of HF membranes performance in different ways. In terms of future work, the addition of additional process equipment to allow for automated cycling between the permeation and backwash modes would increase the speed of testing and better mimic how full-scale HF membrane systems are run.

5.6. Acknowledgements

This work was primarily supported by the Natural Sciences and Engineering Research Council of Canada (NSERC) in the form of a Discovery Grant (435646-2013) and an Undergraduate Student Research Award (to Blake Patterson); additional funding was provided the Faculty of Engineering at McMaster University in the form of Dean's Undergraduate Student Summer Research Award (to Panagiotis Papangelakis). We

acknowledge Juliane Kagansky and Henk Koops at SUEZ Water Technologies & Solutions for providing the HF PVDF membranes. We thank Paul Gatt for his involvement in the manufacture and setup of the experimental system. Finally, we thank the Biointerfaces Institute at McMaster for providing access to the contact angle and FTIR systems.

5.7. References

[1] P. Cote, Z. Alam, J. Penny, Hollow fiber membrane life in membrane bioreactors (MBR), Desalination. 288 (2012) 145–151.

[2] R.C. Kuhn, K.H. Oshima, Evaluation and optimization of a reusable hollow fiber ultrafilter as a first step in concentrating Cryptosporidium parvum oocysts from water, Water Res. 35 (2001) 2779–2783.

[3] H.A. Morales-Morales, G. Vidal, J. Olszewski, C.M. Rock, D. Dasgupta, K.H. Oshima, et al., Optimization of a reusable hollow-fiber ultrafilter for simultaneous concentration of enteric bacteria, protozoa, and viruses from water, Appl. Environ. Microbiol. 69 (2003) 4098–4102.

[4] H. Huang, N. Lee, T. Young, A. Gary, J.C. Lozier, J.G. Jacangelo, Natural organic matter fouling of low-pressure, hollow-fiber membranes: Effects of NOM source and hydrodynamic conditions, Water Res. 41 (2007) 3823–3832.

[5] M. Zhou, H. Liu, J.E. Kilduff, R. Langer, D.G. Anderson, G. Belfort, High-throughput membrane surface modification to control NOM fouling., Environ. Sci. Technol. 43 (2009) 3865–71.

[6] M. Zhou, H. Liu, J.E. Kilduff, R. Langer, D.G. Anderson, G. Belfort, High Throughput Synthesis and Screening of New Protein Resistant Surfaces for Membrane Filtration, AIChE J. 56 (2010) 1932–1945.

[7] M. Zhou, H. Liu, A. Venkiteshwaran, J. Kilduff, D.G. Anderson, R. Langer, et al., High throughput discovery of new fouling-resistant surfaces, J. Mater. Chem. (2011) 693–704.

[8] N. Jackson, J. Liddell, G. Lye, An automated microscale technique for the quantitative and parallel analysis of microfiltration operations, J. Membr. Sci. 276 (2006) 31–41.

[9] M. Chandler, A.L. Zydney, High throughput screening for membrane process development, J. Membr. Sci. 237 (2004) 181–188.

[10] A.S. Kazemi, K. Kawka, D.R. Latulippe, Optimization of biomolecule separation by combining microscale filtration and design-of-experiment methods, Biotechnol. Bioeng. 113 (2016) 2131–2139.

[11] A.S. Kazemi, D.R. Latulippe, Stirred well filtration (SWF) – A high-throughput technique for downstream bio-processing, J. Membr. Sci. 470 (2014) 30–39.

[12] S. Kong, J. Aucamp, N.J. Titchener-Hooker, Studies on membrane sterile filtration of plasmid DNA using an automated multiwell technique, J. Membr. Sci. 353 (2010) 144–150.

[13] A.S. Kazemi, L. Boivin, S. Mi Yoo, R. Ghosh, D.R. Latulippe, Elucidation of filtration performance of hollow-fiber membranes via a high-throughput screening platform, J. Membr. Sci. 533 (2017) 241–249.

[14] G. Kang, Y. Cao, Application and modification of poly(vinylidene fluoride) (PVDF) membranes – A review, J. Membr. Sci. 463 (2014) 145–165.

[15] C. Luo, Q. Liu, Oxidant-Induced High-Efficient Mussel-Inspired Modification on PVDF Membrane with Superhydrophilicity and Underwater Superoleophobicity Characteristics for Oil/Water Separation, ACS Appl. Mater. Interfaces. 9 (2017) 8297–8307.

[16] Z.Y. Xi, Y.Y. Xu, L.P. Zhu, Y. Wang, B.K. Zhu, A facile method of surface modification for hydrophobic polymer membranes based on the adhesive behavior of poly(DOPA) and poly(dopamine), J. Membr. Sci. 327 (2009) 244–253.

[17] B.D. McCloskey, H.B. Park, H. Ju, B.W. Rowe, D.J. Miller, B.D. Freeman, A bioinspired fouling-resistant surface modification for water purification membranes, J. Membr. Sci. 413–414 (2012) 82–90.

[18] H. Lee, S.M. Dellatore, W.M. Miller, P.B. Messersmith, Mussel-Inspired Surface Chemistry for Multifunctional Coatings, Science 318 (2007) 426–431.

[19] H. Zhu, S. Zhu, A versatile and facile surface modification route based on polydopamine for the growth of MOF films on different substrates, Can. J. Chem. Eng. 93 (2015) 63–67.

[20] F. Ponzio, J. Barthès, J. Bour, M. Michel, P. Bertani, J. Hemmerle, et al., Oxidant Control of Polydopamine Surface Chemistry in Acids: A Mechanism-Based Entry to Superhydrophilic-Superoleophobic Coatings, Chem. Mater. 28 (2016) 4697–4705.

[21] R.M.C. Dawson, W.H. Elliott, D.C. Elliott, K.M. Jones, Data for biochemical

research;, Oxford University Press, 1969.

[22] D.B. Burns, A.L. Zydney, Buffer effects on the zeta potential of ultrafiltration membranes, J. Membr. Sci. 172 (2000) 39–48.

[23] K.J. Lee, H.D. Park, The most densified vertically-aligned carbon nanotube membranes and their normalized water permeability and high pressure durability, J. Membr. Sci. 501 (2016) 144–151.

[24] M. Hossein Razzaghi, A. Safekordi, M. Tavakolmoghadam, F. Rekabdar, M. Hemmati, Morphological and separation performance study of PVDF/CA blend membranes, J. Membr. Sci. 470 (2014) 547–557.

[25] T. Urase, K. Yamamoto, S. Ohgaki, Effect of pore size distribution of ultrafiltration membranes on virus rejection in crossflow conditions, Water Sci. Technol. 30 (1994) 199–208.

[26] A. Xenopoulos, M. Blanchard, An improved mixed dextran rejection test for characterization of UF membranes in an R&D environment, Desalination. 199 (2006) 219.

[27] S.R. Wickramasinghe, S.E. Bower, Z. Chen, A. Mukherjee, S.M. Husson, Relating the pore size distribution of ultrafiltration membranes to dextran rejection, J. Membr. Sci. 340 (2009) 1–8.

[28] T. Urase, K. Yamamoto, S. Ohgaki, Effect of pore structure of membranes and module configuration on virus retention, J. Membr. Sci. 115 (1996) 21–29.

[29] S. Mochizuki, A.L. Zydney, Effect of Protein Adsorption on the Transport Characteristics of Asymmetric Ultrafiltration Membranes, Biotechnol. Prog. 8 (1992) 553–561.

[30] A.L. Zydney, A. Xenopoulos, Improving dextran tests for ultrafiltration membranes: Effect of device format, J. Membr. Sci. 291 (2007) 180–190.

[31] W. Yuan, A.L. Zydney, Humic Acid Fouling during Ultrafiltration, Environ. Sci. Technol. 34 (2000) 5043–5050.

[32] K. Katsoufidou, S.G. Yiantsios, A.J. Karabelas, A study of ultrafiltration membrane fouling by humic acids and flux recovery by backwashing: Experiments and modeling, J. Membr. Sci. 266 (2005) 40–50.

[33] K. Katsoufidou, S.G. Yiantsios, a. J. Karabelas, Experimental study of ultrafiltration membrane fouling by sodium alginate and flux recovery by backwashing, J. Membr. Sci. 300 (2007) 137–146.

[34] K.S. Katsoufidou, D.C. Sioutopoulos, S.G. Yiantsios, A.J. Karabelas, UF membrane fouling by mixtures of humic acids and sodium alginate: Fouling

mechanisms and reversibility, Desalination. 264 (2010) 220–227.

[35] D. Wang, K. Li, W.K. Teo, Porous PVDF asymmetric hollow fiber membranes prepared with the use of small molecular additives, J. Membr. Sci. 178 (2000) 13–23.

[36] M. Bakhshayeshi, A. Teella, H. Zhou, C. Olsen, W. Yuan, A.L. Zydney, Development of an optimized dextran retention test for large pore size hollow fiber ultrafiltration membranes, J. Membr. Sci. 421–422 (2012) 32–38.

5.8. Supporting Information

Gel permeation chromatography (GPC) analysis of test solutes

Gel permeation chromatography (GPC) was used to calculate the average molecular weight of the eight solutes that were used in this study: humic acid, sodium alginate, four dextrans, and two polyethylene oxides. Three columns (Waters Ultrahydrogel-120, -250 and -500; 30 cm length × 7.8 mm internal diameter) in series were used in this GPC system; polyethylene glycol and polyethylene oxide standards up to a molecular weight of 800 kDa were used to prepare the GPC calibration curve. The GPC analysis for the largest dextran (2000 kDa) was done to get an estimate of the polydispersity and thus the relative amount of smaller solutes. A 0.5 M $NaNO_3$ solution in 2-(Cyclohexylamino)ethanesulfonic acid buffer (pH 10) was used as the continuous phase. Each sample was at a concentration of 1 mg/mL in the same buffer solution and the pre-filtered through a 0.2 μm Supor® syringe filter immediately prior to injection (injection volume of 80 μL) onto the system. The mass-weighted molecular weight was calculated from the refractive index signal using the GPC system software. The polydispersity was

calculated from the ratio of mass-weighted molecular weight and number-weighted molecular weight.

Table 5.S1. Summary of GPC results obtained with different solutes used in section 5.4.2.

Solute	Reported MW (kDa)	Measured mass-weighted MW (kDa)	Polydispersity (-)
Technical grade humic acid	n/a	2.4	1.4
Sodium alginate	n/a	181.8	2.7
Polyethylene oxide (PEO)	100 [a]	111.2	3.6
	600 [a]	359.1	1.8
Dextran	35 – 45 [b]	25.4	1.4
	100 [c]	63.9	4.1
	450 – 650 [c]	143.5	2.2
	2000 [c]	241.2	2.3

[a] Viscosity average molecular weight
[b] Weight average molecular weight
[c] Relative molecular weight

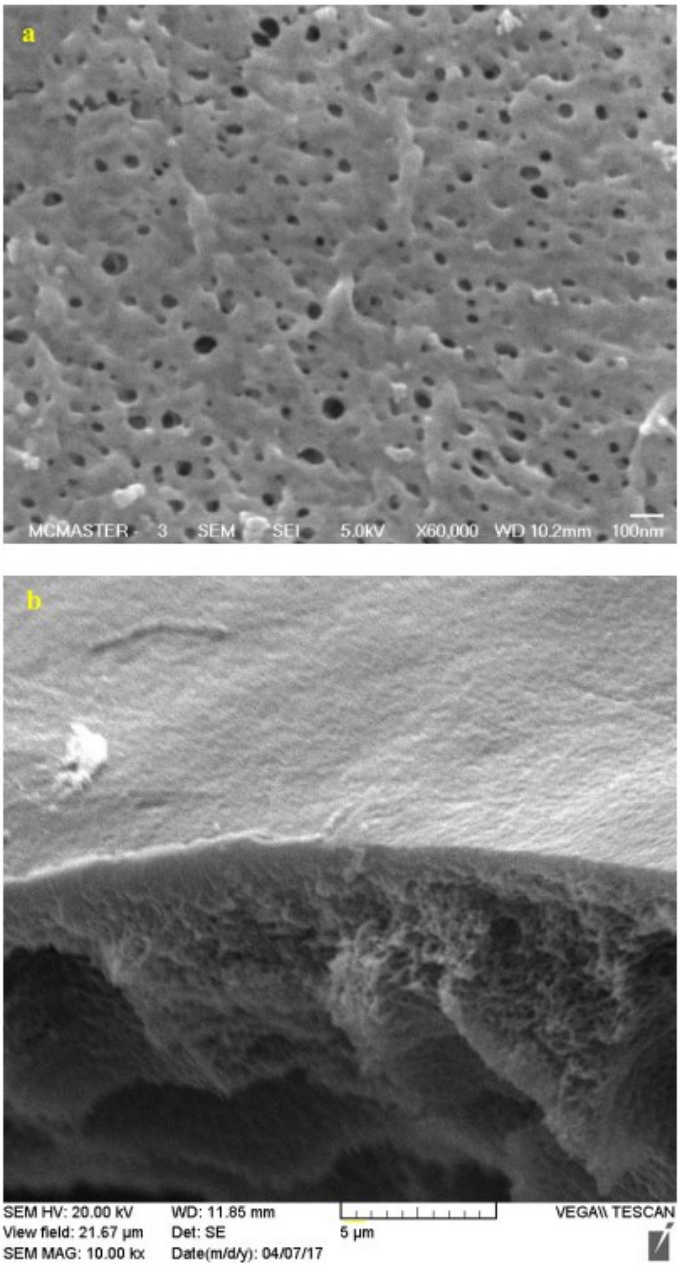

Fig. 5.S1. Panel a: Scanning electron microscopy image of the top surface of the PVDF HF membrane; the membrane was dried at 40 ºC for 45 minutes, attached to a mount, platinum sputtered under vacuum, and then imaged using a JEOL JSM-7000F instrument. Panel b: Scanning electron microscopy image of the cross section of the PVDF HF membrane; the membrane was freeze-fractured using liquid nitrogen, attached to a mount, gold sputtered under vacuum, and then imaged using a Tescan Vega II LSU instrument.

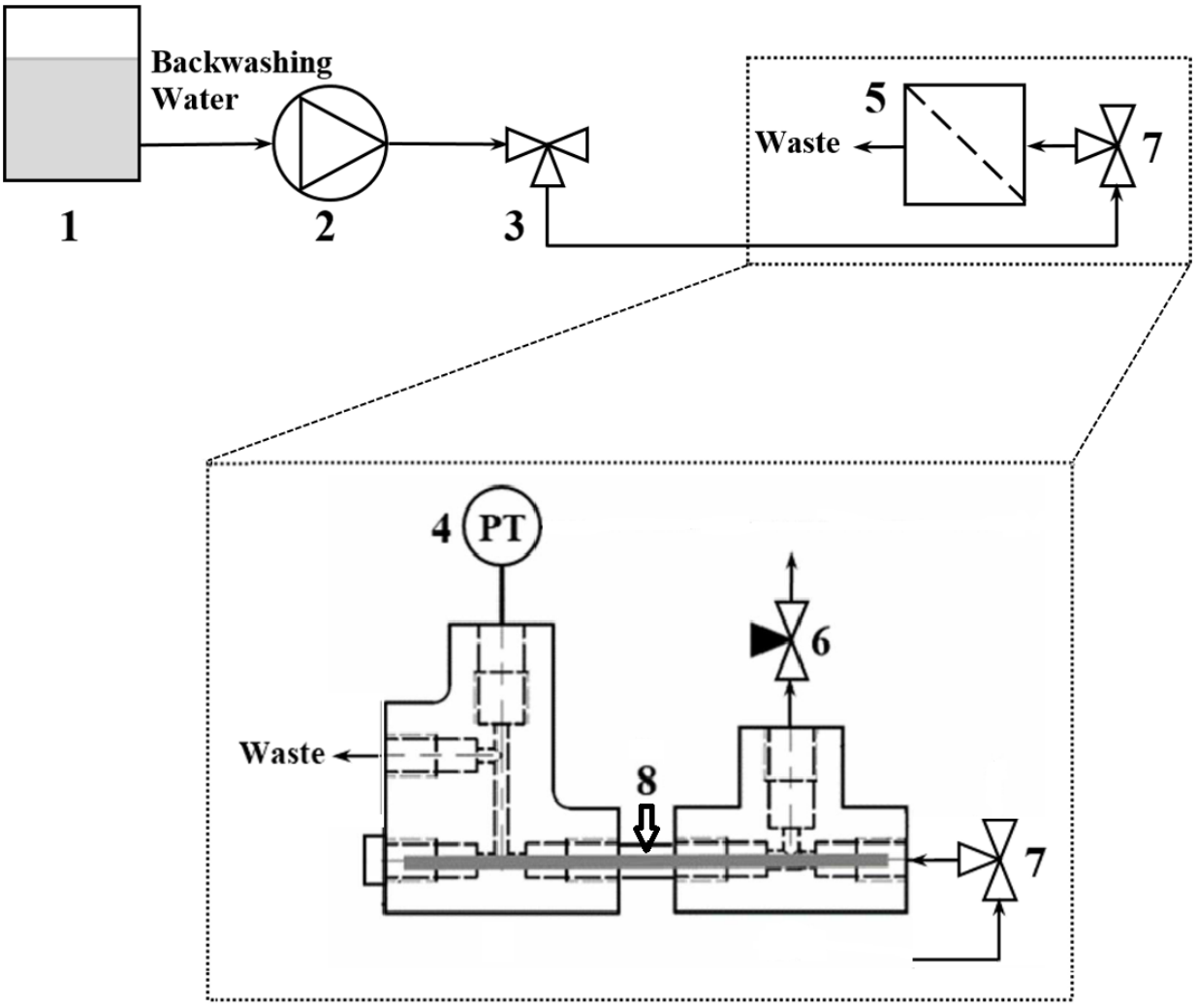

Fig. 5.S2. Schematic of the backwashing mode of operation for a single filtration sub-module of the MS-PS-CFF system. The identified components include: 1) Feed reservoir (nominal capacity of 100 mL); 2) Multi-channel peristaltic pump; 3) 3-way stopcock valve; 4) Pressure transducer; 5) filtration sub-module; 6) Retentate line needle valve (fully closed); 7) 3-way stopcock valve; 8) Tygon tubing with HF membrane inside. The same configuration was used to pre-wet the HF membrane prior to each filtration experiment.

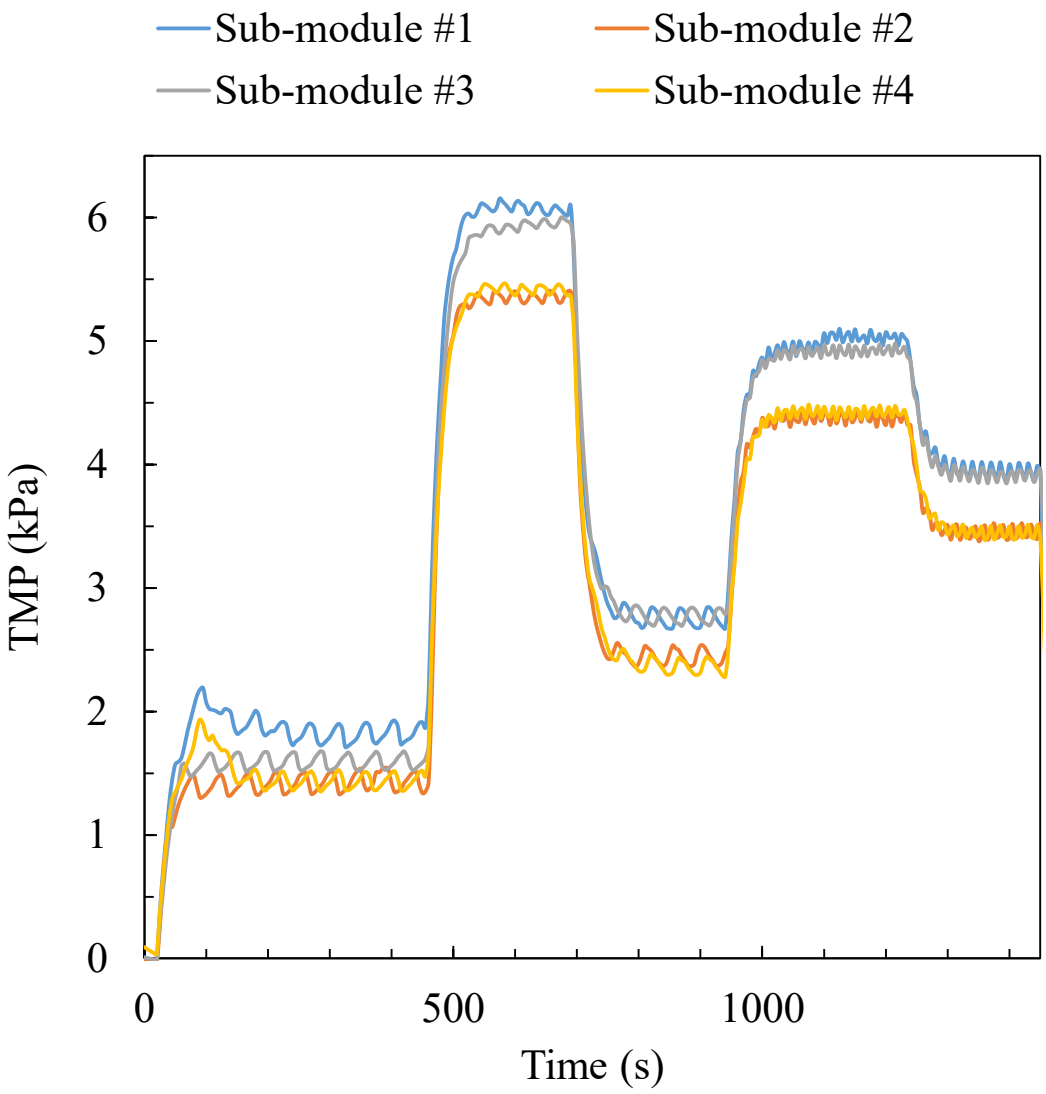

Fig. 5.S3. A typical TMP profile (for five different flow rates of 0.15, 0.55, 0.25, 0.45 and 0.35 mL/min) from the initial hydraulic permeability measurements of four PVDF HF membranes that were run in parallel on the MS-PS-CFF system.

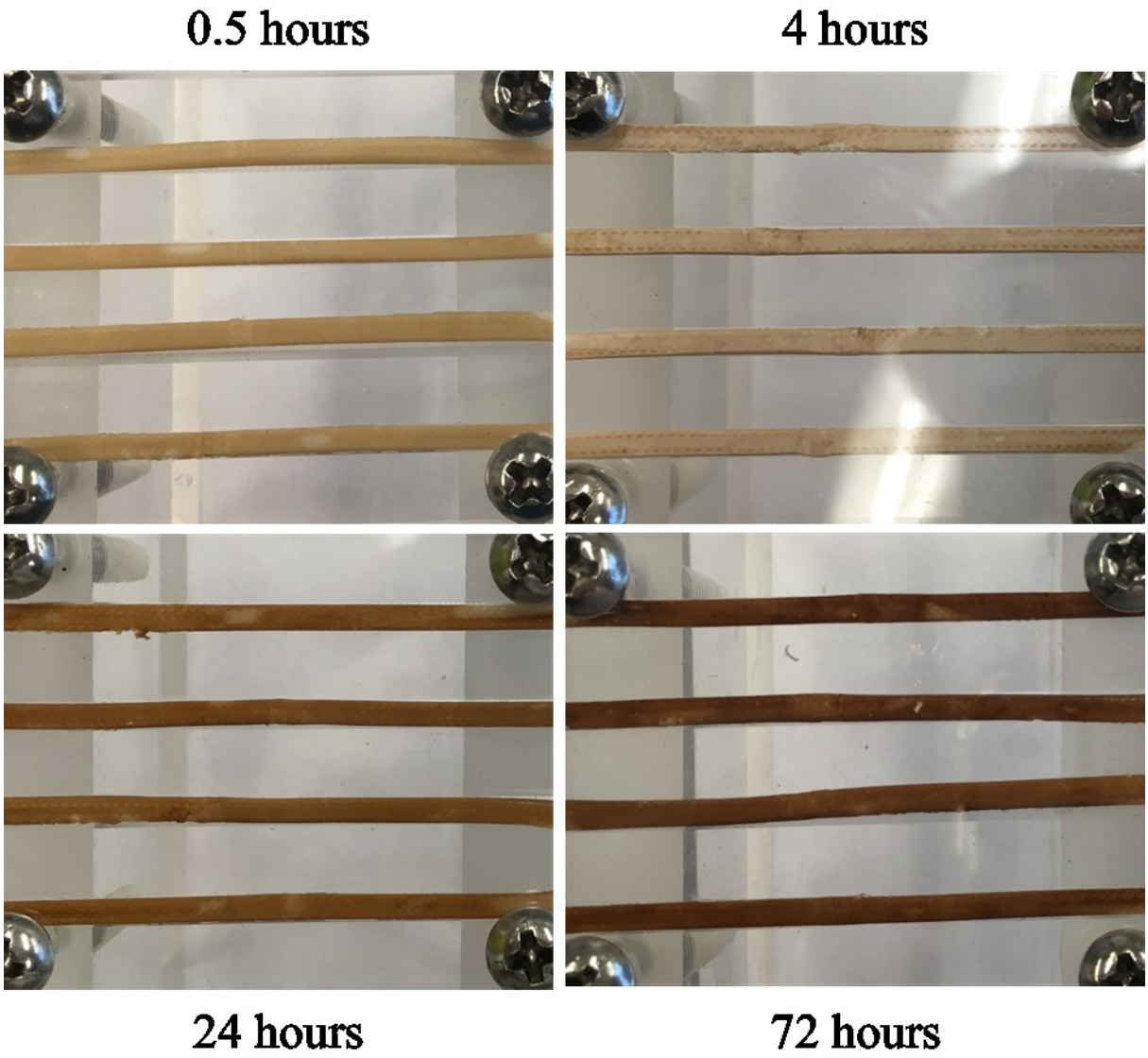

Fig. 5.S4. Images of the four PVDF HF membranes that were run in parallel on the MS-PS-CFF system after different total run times with a 300 ppm HA solution in PBS (as described in section 5.4.1).

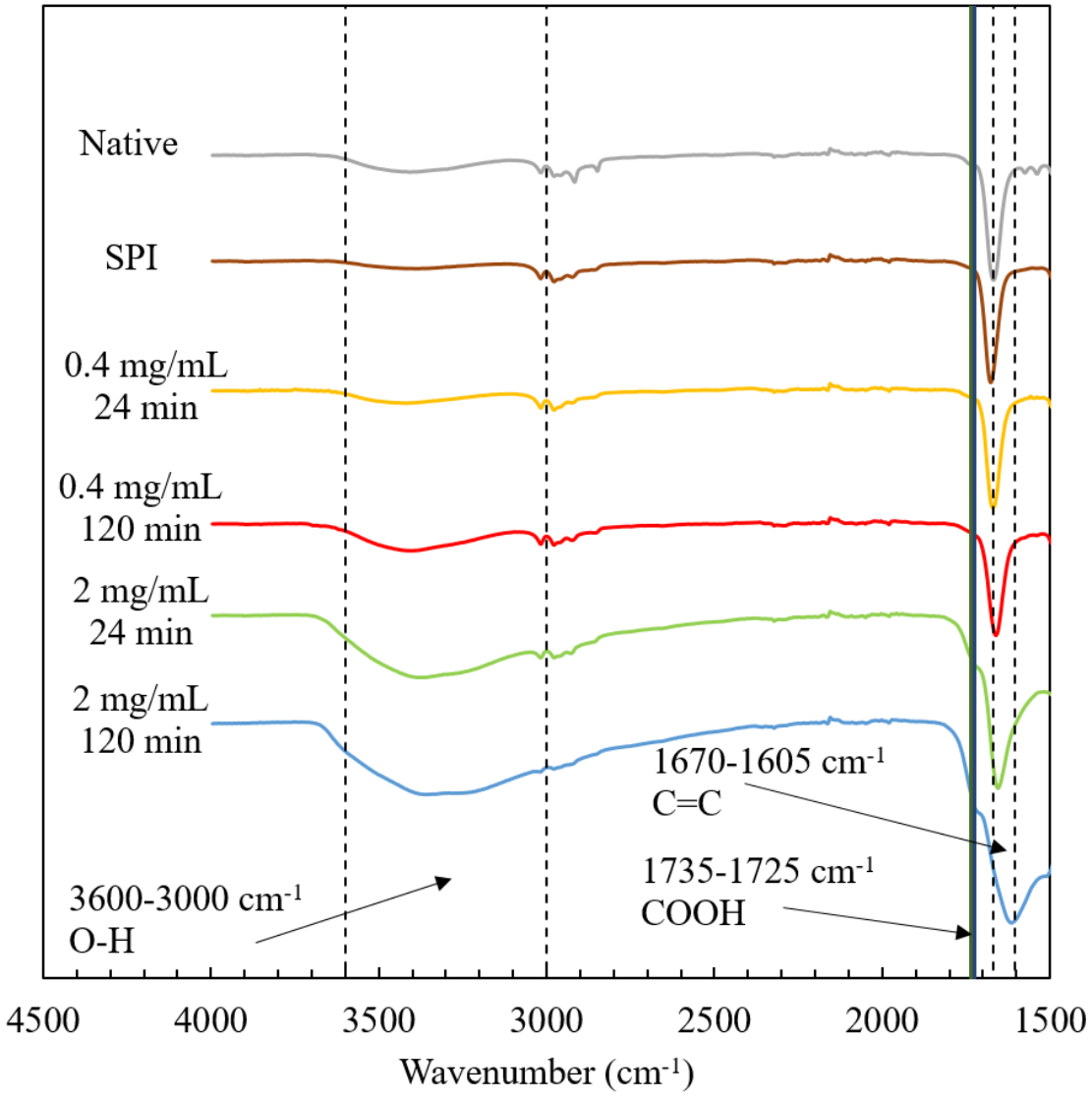

Fig. 5.S5. FTIR analysis of the native and modified HF PVDF membranes.

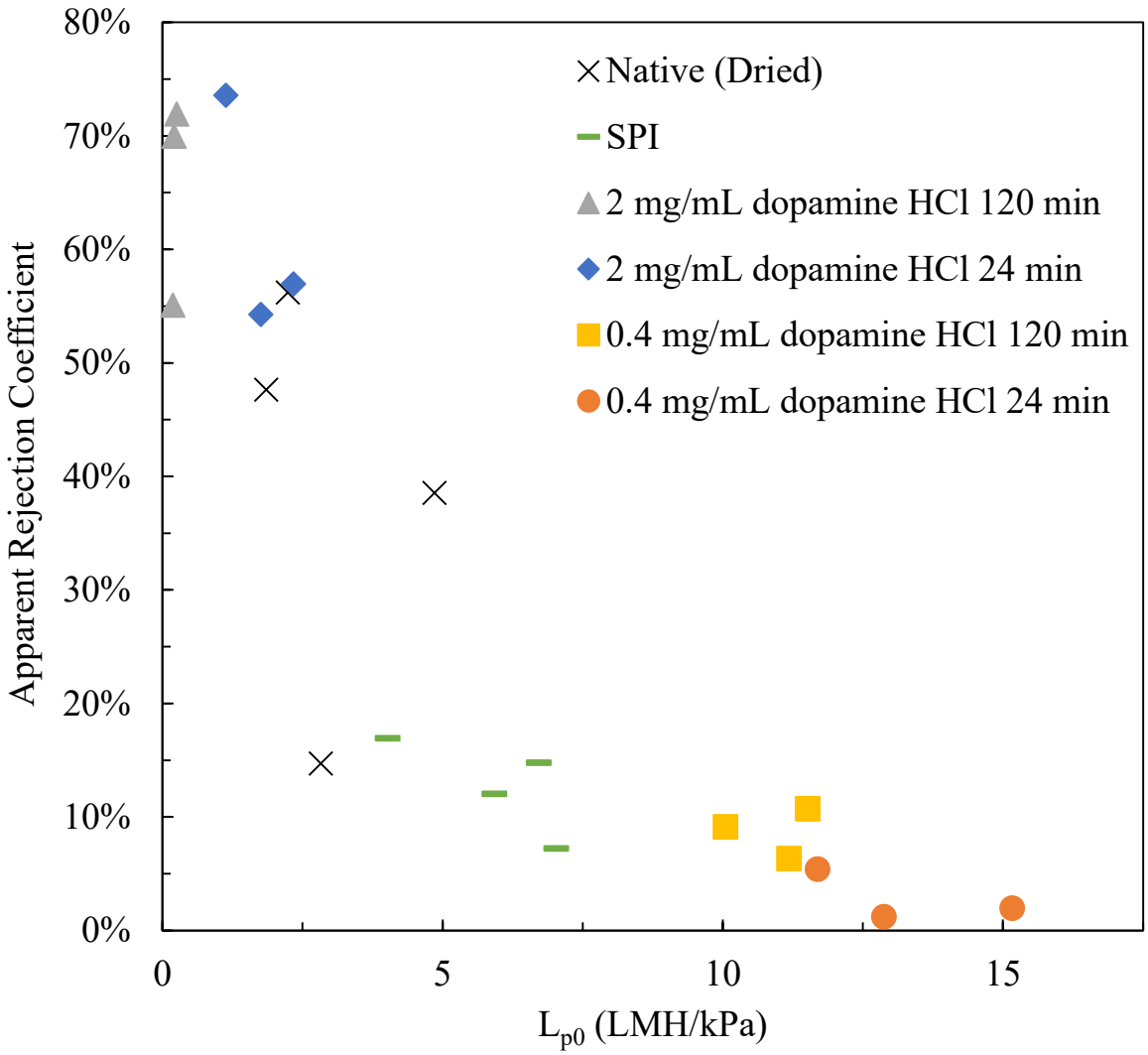

Fig. 5.S6. Correlation between initial permeability (L_{p0}) and apparent rejection coefficient (after 4 hours) for experiments corresponding to Figure 5. The HA filtration experiments (with 300 ppm technical grade HA in PBS) were performed in triplicate for the modified membranes and in quadruplicate for the control experiments. The Pearson product-moment correlation coefficient is -0.86. Note that the observed variations are believed to be mainly related to the variations in the membrane properties such as molecular weight distribution of different pieces of the membrane. However, slight variations due to the surface modification and drying of the membrane can potentially exist as well.

Effect of membrane length on the filtration performance

Two different membrane lengths (8 and 16 cm) were tested with the MS-PS-CFF system by running model filtration experiments with 300 ppm HA and performing hydraulic permeability measurements (Fig. 5.S4). The hydraulic permeability results were not statistically different for the native, fouled and backwashed membranes. However, the rejection coefficients for the first (after 30 minutes of filtration) and the second (after 4 hours of filtration) permeate samples were identical for the 8 cm modules. However, a significant difference was observed between the apparent rejection coefficient of the first and the second permeate samples for the 16 cm modules.

Bakhshayeshi et al. [36] have developed a theoretical platform that evaluates the effects of module geometry (number of fibers, fiber diameter, and fiber length) and operating conditions (feed and permeate flow rates) on the on the performance of dextran retention tests in HF modules. It was reported that factors such as cross flow rate, permeate flux and module length can significantly affect the filtration behavior, and specifically the back filtration near the exit of the module. This might explain the observations reported in this section where a lower permeate concentration (i.e. lower rejection) is observed for the second permeate sample for the 16 cm membrane although the results reported herein are preliminary and further experimental work and CFD simulations are required to evaluate the effect of module length on the filtration performance.

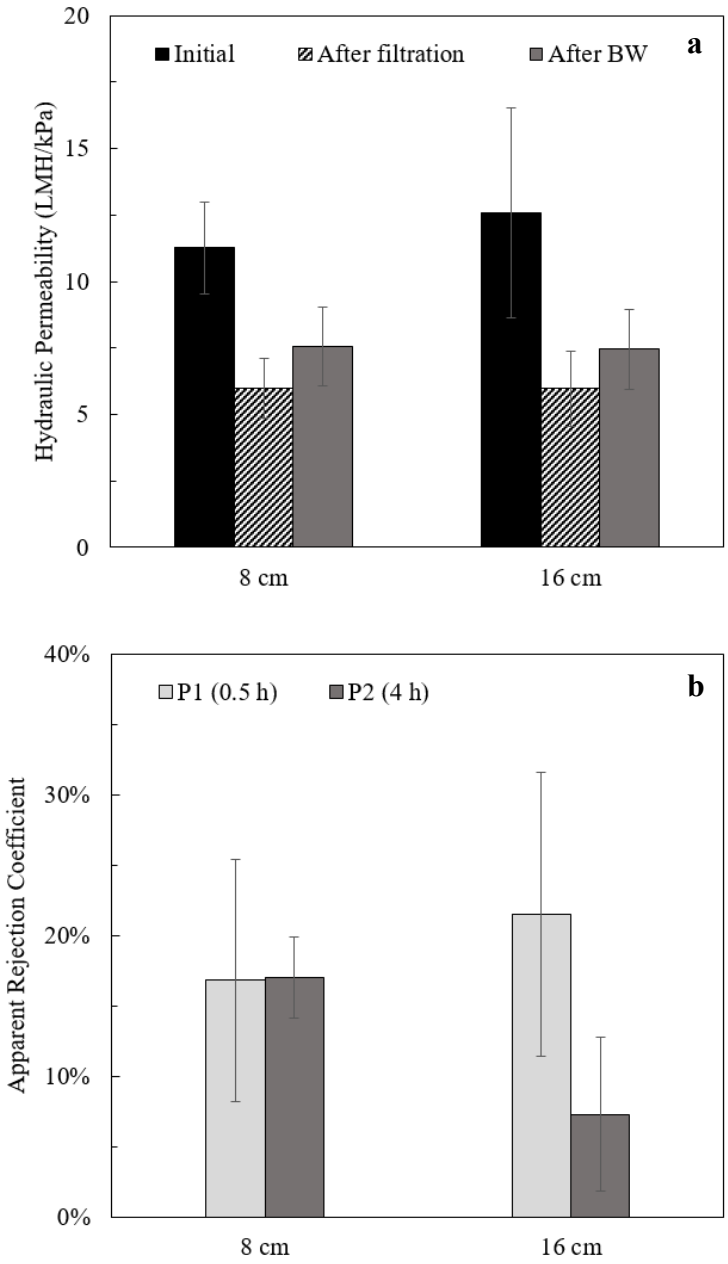

Fig. 5.S7. Effect of different HF membrane lengths on humic acid (300 ppm) filtration performance at a cross flow rate of 1.5 mL/min: a. Comparison of changes in hydraulic permeability after filtration and BW. The error bars were calculated using the standard deviation for the quadruplicate measurements at each experimental condition. b. Apparent rejection coefficient results with error bars corresponding to the standard deviation for the quadruplicate measurements at each experimental condition.

Chapter 6 – Conclusions and Recommendations

6.1. Concluding Remarks

In this work the development of different HT approaches for testing and optimization of filtration performance using flat sheet and HF membranes with applications in biological and environmental separations were reported. The unique design of each HT method allows for performing parallel filtration experiments using minimal amount of sample.

The work presented herein started with combining the SWF technique, as a HT membrane filtration method, with DOE methods to optimize the separation performance of different binary mixtures of biomolecules and to study the effects of solution conditions (pH and ionic strength) and hydrodynamics (permeate flux and stirring) by running over 100 membrane filtration tests in flat sheet format and reporting the sieving coefficients, selectivities and pressure profiles. A 2^2 factorial design was used for each bioseparation along with a unique statistical demonstration that matches the factorial design of DOE method. Considering the small amount of sample required for each experiment, each condition was tested in quadruplicates. Overall, it is concluded that these 100 individual filtration tests can be performed and analyzed in a practical manner to make informed conclusions about the effects of different operating conditions. For example, for a mixture of 4 kDa dextran and BSA the selectivity obtained with an 30 kDa PES (Omega^{TM}) membrane was the highest at pH 4.9 which is the pI of BSA. None of the

previous works in this area have studied separation performance in HT format using statistical methods thus the separations described in chapter 2 demonstrate "proof-of-concept" experiments and the method described here can be used to optimize the separation performance of other membrane filtration separation processes.

A multi-modal HT membrane filtration approach was developed subsequently in chapter 3 by combining the MMFC system with the SWF technique. By using this strategy, up to eight parallel membrane filtration tests (with or without stirring) can be conducted in either constant TMP or constant flux mode. None of the previously reported HT methods can be used to perform constant flux and constant pressure filtration experiments in parallel although both modes of operation have been widely studied using conventional membrane filtration modules. This approach was used to perform parallel hydraulic permeability measurements for UF membranes in constant TMP and constant flux mode and it was shown that the operating mode can be switched from constant TMP to constant flux and vice versa in the middle of an experiment. A set of filtration experiments were performed using single solute (BSA) and model binary solute (PEG/dextran and α-lactalbumin/FITC-dextran) solutions as a proof of usefulness of this approach. The results were analyzed with GPC analysis and sieving coefficient quantification showing the importance of stirring in separation performance and sample collection.

Chapter 4 describes a new approach in HT testing of membrane filtration processes by introducing the HT-HF module, the first ever HT unit that uses HF membranes to run parallel membrane filtration tests in constant flux mode using a

minimal amount of sample. As discussed earlier, all of the HT membrane filtration modules developed earlier have used flat sheet membranes. This chapter was principally inspired by the development of microscale processing techniques in biotechnology industry to speed-up process development. This HT method can be used to rapidly evaluate the membrane filtration performance at different experimental conditions. Furthermore, cleaning studies can be performed by backwashing HF membranes in HT format using this module. The main application of this approach is in the field of water and wastewater treatment where HF membranes are widely used and the filtration performance is generally affected by several operating factors. HAs were used as model foulants for running HT filtration experiments. It was observed that the effect of different operating conditions such as buffer concentration, operating flow rate (i.e. permeate flux), HA type, HA concentration and backwashing solution on HA filtration performance can easily be studied using the HT-HF module in a manageable manner. This parallel processing approach can potentially be employed to improve the investigation of environmental separations such as optimization of filtration processes used in wastewater plants, the testing and fouling study of natural water filtration and the HT fouling evaluation in membrane bioreactors.

Although the HT-HF system (introduced in chapter 4) demonstrated to be remarkably valuable for quickly screening the operating conditions of membrane filtration processes, development of a more advanced HT system with operational flexibility was required in order to perform extended filtration experiments with recycling. Therefore, the MS-PS-CFF system was designed and successfully used for

running extended filtration experiments using HF membranes in chapter 5. In addition to the extended filtration experiments, the effect of solute size and type on membrane rejection and the effect of solution conditions on the filtration performance and fouling propensity of HA were successfully studied in HT format. Furthermore, the usefulness and versatility of this module was further demonstrated by conducting a simple set of optimization experiments for surface modification of HF membranes in HT format using sodium periodate as a strong oxidizer and dopamine hydrochloride where the importance of factors such as modification time, dopamine hydrochloride concentration and membrane drying on surface properties of the membrane as well as the filtration performance were shown.

Overall, in this project different HT membrane filtration approaches for different applications were developed and tested. This work is intended to show the usefulness and potential applications of HT testing platforms for membrane filtration processes to inspire other researchers to employ such platforms in their work and develop similar innovations. The introduced techniques can reduce the amount of sample used in each test between 10-50 times and accelerate process development and optimization by running parallel tests. The presented modules can be used in current format for rapid testing of flat sheet and HF membranes for biological and environmental separations.

6.2. Future Work and Recommendations

The following areas are recommended for future studies related to this thesis and in general HT membrane filtration:

- As described earlier in this thesis (see section 1.3.3), the apparent sieving coefficient does not take the effect of concentration polarization into account while this effect can be considered by using the intrinsic sieving coefficient. To convert the apparent sieving coefficient to intrinsic sieving coefficient, the mass transfer coefficient (k) is used. However, the procedure and the equations proposed for the mass transfer coefficient calculations in previous works are based on the module hydrodynamics of a stirred cell filtration module when using an impermeable membrane [1–5]. Considering the unique mixing pattern (a stir element rotating around an axis that is parallel to the membrane surface) employed in the SWF module (used in chapters 2 and 3) compared to the traditional stirred cell filtration device, the module hydrodynamics of the SWF module should be investigated to find the proper equation for the mass transfer coefficient calculations of the SWF system. For further information on how this was done for the stirred cell filtration module refer to the previous studies in this area [1–5]. The assessment of the effect of module hydrodynamics on flow velocity profiles and mass transfer properties can also be performed using CFD simulations [6–8] where the scalability of the results obtained with the developed HT techniques can be evaluated .

- Experiments should be performed with more complex solutions for both biological and environmental processes. For example, protein purification from cell culture [9], egg white [10] or whey [11] solutions can be performed by using different membranes with the strategies introduced in chapters 2 and 3. For environmental applications, surface water samples as well as real and synthetic wastewater samples containing more than one component can be used to obtain a better understanding regarding the application of the HT-HF and the MS-PS-CFF systems.
- It is important to note that only the ZeeWeed 500 membrane from SUEZ Water & Process Technologies (formerly GE Water & Process Technologies) was used in chapters 4 and 5. There are several advantages to using the HT-HF and MS-PS-CFF systems to screen the performance of other HF membranes. Different materials and membrane chemistries can be compared with each other in parallel by using commercially available and modified HF membranes in the proposed HT systems for HF membranes. PVDF membranes are not suitable for many of surface modification strategies due to the membrane chemistry. This is especially the case for the modification strategies that are based on adsorption. For example, layer-by-layer polyelectrolyte adsorption on PVDF membrane was reported to be less effective than on PES membranes [12]. Therefore, using other membrane materials appropriate for different surface modification strategies can be considered in the future. Table 6.1 provides a summary of the specifications for some of the available HF membranes which can be considered for future work

using the HT-HF and MS-PS-CFF modules. Slight modifications in the sealing mechanism may be needed if using HF membranes with different diameters than the ZeeWeed 500 membranes from SUEZ. Furthermore, the pressure transducers' ports must be relocated if inside-out membranes are needed to be tested.

Table 6.1. Specifications of some of the commercially available HF membranes (ND: not disclosed). The term "supported" in this table is used to describe a relatively thick porous support layer which is used to increase the mechanical strength of a fiber during the module assembly and the filtration process.

Supplier	**Material**	**Flow Configuration**	**Supported?**	**Reported Pore Size (µm)**	**Inside Diameter (mm)**	**Outside Diameter (mm)**
SUEZ (formerly GE)	PVDF	Outside-in	Yes	0.04	0.8	1.9
Koch	PVDF	Outside-in	Yes	0.03	ND	2.6
LG-Hitachi	PVDF	Outside-in	No	0.1	0.7	1.15
Dow	PVDF	Outside-in	No	0.03	0.7	1.3
Arkema	PVDF	Outside-in	No	Pore size < 60 nm; MWCO 100 kDa	0.8	1.3
Spectrum Labs	Modified PES	Inside-out	No	Varying UF and MF sizes	0.5, 0.75 and 1.0	ND
WaterSep	Modified PES	Inside-out	ND	Varying UF and MF sizes	0.5, 1.0 and 2.0	0.75, 1.25 and 2.25

- A number of improvements can be made in the future designs of the HT platforms developed in this work. The HT-HF technique introduced in chapter 4 can be expanded to 10 parallel filtration experiments by slightly modifying the sample collection technique since the fluid handling system used in this study was a 10-rack syringe pump. The MS-PS-CFF system introduced in chapter 5 can be enhanced by installing flow adjustment and measurement devices (e.g. rotameter) instead of the needle valves used in the current design. Also, this method can be expanded by using a 24- or 32-channel peristaltic pump and by installing additional pressure transducers. However, the cost of changing the pump and adding the rotameters and the additional pressure transducers should be taken into account and alternative options should be considered to reduce the capital cost. For example, cheaper pressure measurement devices with less accuracy may be adequate for the majority of applications.
- Advanced strategies for characterizing membrane fouling can be combined with the modules introduced in chapters 4 and 5. For example, Unified Membrane Fouling Index (UMFI) was developed by Huang et al. [13] in order to quantify and assess the fouling of membranes observed at various scales of water treatment. The basis of UMFI is a modified Hermia model applied to both constant flux and constant pressure filtration. UMFI simplifies and standardizes the testing of membrane fouling propensity by directly using the membrane of interest. Excitation-emission matrix (EEM) fluorescence spectroscopy has been widely used to characterize dissolved organic matter (DOM) in water [14]. For

example, fluorescence spectroscopy can be employed to identify the relative abundance of organic fractions from different origins in water samples, namely humic substances and protein-like organics as identified by the emission intensities at different excitation/emission coordinates. A combination of these two methods along with the HT approaches introduced in this thesis for environmental applications can be considered as a valuable approach to study the fouling of HF membranes.

- The HT systems introduced in chapters 4 and 5 can be used to study the changes in the HF membranes structure and in their filtration behaviour when they are exposed to different chemicals during both the filtration and cleaning cycles. For example, exposure to sodium hypochlorite, which is commonly used as a cleaning agent has been studied in some of works reported in this area [15,16]. An excellent guideline in this regard was published in 2014 which can help in developing future studies [17].
- The flexibility of the design introduced in chapter 5 allows for combining HF membrane filtration processes with other processes used in water and wastewater treatment such as coagulation, flocculation [18,19] and advanced oxidation [20]. Two approaches can be used in this regard: first, the complementary process can be performed prior to filtration to enhance the filtration performance (e.g. coagulation/flocculation prior to filtration); second, membrane cleaning can be conducted with the help of other processes after running a filtration test, for example, advanced oxidation processes can be used in order to remove organic

foulants from fouled membranes and to regenerate membranes [20]. It is important to note that running any of these processes along with filtration in HT format is beneficial since the performance of these processes also depends on different factors.

- The HF membrane used in this work, and in general HF membranes, can potentially be used as a support for immobilization of different catalysts [21–24] to perform reactions integrated with membrane filtration in HT format. For example, by immobilizing enzymes, bio-reactions can be driven along with filtration using the HT design. One important challenge in this regard will be maintaining the hydraulic permeability and separation performance of the membrane after immobilization. Immobilization can decrease the membrane permeability significantly similar to the phenomena observed in chapter 5 after surface modification of HF membranes under certain conditions.

6.3. References

[1] K. Smith, C. Colton, E. Merrill, L. Evans, Convective transport in a batch dialyzer: determination of true membrane permeability from a single measurement, Chem. Eng. Prog. Symp. Ser. 64 (1968) 45–58.

[2] W.S. Opong, A.L. Zydney, Diffusive and convective protein transport through asymmetric membranes, AIChE J. 37 (1991) 1497–1510.

[3] B.D. Mitchell, W.M. Deen, Effect of concentration on the rejection coefficients of rigid macromolecules in track-etch membranes, J. Colloid Interface Sci. 113 (1986) 132–142.

[4] D.M. Malone, J.L. Anderson, Diffusional boundary-layer resistance for membranes with low porosity, AIChE J. 23 (1977) 177–184.

[5] B.D. Mitchell, W.M. Deen, Theoretical effects of macromolecule concentration and charge on membrane rejection coefficients, J. Membr. Sci. 19 (1984) 75–100.

[6] S. Darvishmanesh, J. Vanneste, J. Degrève, B. Van Der Bruggen, Computational fluid dynamic simulation of the membrane filtration module, in: Proc. 20th Eur. Symp. Comput. Aided Process Eng. – ESCAPE20, 2010.

[7] R. Ghidossi, D. Veyret, P. Moulin, Computational fluid dynamics applied to membranes: State of the art and opportunities, Chem. Eng. Process. Process Intensif. 45 (2006) 437–454.

[8] G. Keir, V. Jegatheesan, A review of computational fluid dynamics applications in pressure-driven membrane filtration, Rev. Environ. Sci. Biotechnol. 13 (2014) 183–201.

[9] K. Mohanty, R. Ghosh, Novel tangential-flow countercurrent cascade ultrafiltration configuration for continuous purification of humanized monoclonal antibody, J. Membr. Sci. 307 (2008) 117–125.

[10] R. Ghosh, Z. Cui, Protein purification by ultrafiltration with pre-treated membrane, J. Membr. Sci. 167 (2000) 47–53.

[11] A.L. Zydney, Protein Separations Using Membrane Filtration: New Opportunities for Whey Fractionation, Int. Dairy J. 8 (1998) 243–250.

[12] G. Liu, D.M. Dotzauer, M.L. Bruening, Ion-exchange membranes prepared using layer-by-layer polyelectrolyte deposition, J. Membr. Sci. 354 (2010) 198–205.

[13] H. Huang, T.A. Young, J.G. Jacangelo, Unified Membrane Fouling Index for Low Pressure Membrane Filtration of Natural Waters: Principles and Methodology, Environ. Sci. Technol. 42 (2008) 714–720.

[14] W. Chen, P. Westerhoff, J.A. Leenheer, K. Booksh, Fluorescence Excitation-Emission Matrix Regional Integration to Quantify Spectra for Dissolved Organic Matter, Environ. Sci. Technol. 37 (2003) 5701–5710.

[15] V. Puspitasari, A. Granville, P. Le-Clech, V. Chen, Cleaning and ageing effect of sodium hypochlorite on polyvinylidene fluoride (PVDF) membrane, Sep. Purif. Technol. 72 (2010) 301–308.

[16] S.Z. Abdullah, P.R. Bérubé, Assessing the effects of sodium hypochlorite exposure on the characteristics of PVDF based membranes, Water Res. 47 (2013) 5392–5399.

[17] P. LeClech, Development of Predictive Tools for Membrane Ageing, IWA Publishing, 2014.

[18] F. Harrelkas, A. Azizi, A. Yaacoubi, A. Benhammou, M.N. Pons, Treatment of textile dye effluents using coagulation-flocculation coupled with membrane

processes or adsorption on powdered activated carbon, Desalination. 235 (2009) 330–339.

[19] A.B. Şengül, G. Ersan, N. Tüfekçi, Removal of intra- and extracellular microcystin by submerged ultrafiltration (UF) membrane combined with coagulation/flocculation and powdered activated carbon (PAC) adsorption, J. Hazard. Mater. 343 (2018) 29–35.

[20] L. Yao, L. Zhang, R. Wang, S. Chou, Z.L. Dong, A new integrated approach for dye removal from wastewater by polyoxometalates functionalized membranes, J. Hazard. Mater. 301 (2016) 462–470.

[21] E. Fontananova, E. Drioli, Membrane reactors: Advanced systems for intensified chemical processes, Chemie-Ingenieur-Technik. 86 (2014) 2039–2050.

[22] H.S. Oh, K.M. Yeon, C.S. Yang, S.R. Kim, C.H. Lee, S.Y. Park, et al., Control of membrane biofouling in MBR for wastewater treatment by quorum quenching bacteria encapsulated in microporous membrane, Environ. Sci. Technol. 46 (2012) 4877–4884.

[23] S.R. Kim, H.S. Oh, S.J. Jo, K.M. Yeon, C.H. Lee, D.J. Lim, et al., Biofouling control with bead-entrapped quorum quenching bacteria in membrane bioreactors: Physical and biological effects, Environ. Sci. Technol. 47 (2013) 836–842.

[24] S. Kim, J.H. Kim, B.T. Yoon, C.H. Lee, H.H. Kwon, D.J. Lim, Removal of trace organic pollutants and removal mechanisms using catalyst-immobilized resin/ultrafiltration hybrid system, J. Water Supply Res. Technol. 59(2-3) (2010) 100–110.